Diversification of early cnidarians : exceptionally preserved microfossils from the Kuanchuanpu Formation (lower Cambrian; 535 Ma), Shaanxi Province, China

Xing Wang

N°d'ordre NNT : xxx

THESE de DOCTORAT DE L'UNIVERSITE DE LYON
opérée au sein de
l'Université Claude Bernard Lyon 1

Ecole Doctorale N° ED 341
(Evolution Ecosystèmes Microbiologie Modélisation)

Spécialité de doctorat : Sciences de la Terre
Discipline : Paléontologie

Soutenue publiquement le 18/12/2018, par :
Xing WANG

Diversification précoce des cnidaires: études des microfossiles à préservation exceptionnelle de la Formation de Kuanchuanpu (base du Cambrien; ~535 Ma), Province de Shaanxi, Chine.

Devant le jury composé de :

MATTIOLI Emanuela	Professeure	UCBL	Présidente
SKOVSTED Christian	Professeure	Swedish Museum of Natural History Stockholm	Rapporteur
CLAUSEN Sébastien	Maître de conférences	Université de Lille	Examinateur
SCHUCHERT Peter	Chargé de recherche	Muséum d'Histoire Naturelle Genève	Examinateur
VANNIER Jean	Directeur de recherche	CNRS/UCBL	Directeur de thèse
HAN Jian	Professeure	Northwest University Xi'an	Co-directeur de thèse

Acknowledgements

I am very grateful to those who kindly helped me during my 3-year stay in Lyon from 2016 to 2018 and especially through the successive steps of my PhD.

First and foremost my respectful thanks go to my two supervisors and also good friends, Jean Vannier from the Laboratoire de Géologie de Lyon (LGL-TPE) and Jian Han from Northwest University (Xi'an China) who gave me an interesting subject to explore, the remote ancestry of jellyfish, and provided me with constant help, constructive suggestions and patient guidance during the last three years. Jean became my close neighbor after I shared his office last year just after the Chinese New Year (the colourful decorations are still hanging around the door). His smile, good mood and friendly daily exchange always made me feel warm. Not so easy to communicate so directly with Jian but since the first time I met him over a nice meal of Chinese dumplings which are one my favorite food, he inspired me and encouraged me with new endeavors such a studying Small Shelly Fossils with microtomographic techniques. I realize how lucky I am to have met these two persons based on the opposite sides of the world but sharing the same passion for research. Merci Jean. 谢谢 Jian.

I appreciate the help of many of my Chinese colleagues, Hujun Gong, Jie Sun, Xiaoguang Yang, Juan Luo, Xi Liu, Xin Han, Meirong Cheng and Juanping Zhai for their assistance in both field and laboratory work in China. I thank Zongjun Yin and Tao Zhou for technical assistance with 3D-reconstructions.

Many thanks to the colleagues from the Laboratoire de géologie de Lyon who helped me since my first days in the Geode Building. Special thanks to Samuel Mailliot (Service Infographie de l'Observatoire de Lyon) and Xiqiang Liu (Institute of Geochemistry,Chinese Academy of Scien, Guiyang, China) for help and advice in the layout and printing of my thesis, and to Vincent Perrier for encouraging me to speak in English. I like his tattoo with climbing ants. I would also like to thank Fabrice Cordey, Gilles Escarguel, Vincent Perrier, Romain Amiot for their advice and guidance as members of my doctoral college (E2M2) committee and Emanuela Mattioli (Lyon), Christian Skovsted (Stockholm), Sébastien Clausen (Lille), Peter Schuchert (Genève) who kindly accepted to take part in my jury.

I thank Heyo Van Iten and Qiang Ou for correcting and improving my published work.

I enjoyed sharing very good times with my Chinese friends who like have chosen to study in Lyon, Xingjie Ma, Shishan Wang, Zhan Zhang, Lei Dong, Biwen Zhu, Shihua Wang, Li Zhong, Lu Pan, Li Fu, Yakun Luo, Yan Sun, Qiang Zhao, Shu Zhang, etc. and not

to forget the ‘table tennis group’ with Jihua Hao, Jiao He, Renbiao Tao, and Weidong Zhang, etc. I will remember all of you.

Evelyn Houliston, Lucas Leclere and Tsuyoshi Momose (l’Observatoire Océanologique de Villefranche sur Mer) help me a lot on the taphonomic experiment of extant marine tiny animals.

Thank you to the China Scholarship Council who supported financially my stay in France.

Last, but by no means least, I owe my family so much. When I left China to settle in Lyon, my wife was expecting a baby. I realize how difficult it was for my wife not to be able to share the very first months of my daughter’s childhood together and with the whole family. Luckily, my daughter grew up healthily and happily with the help of my mother, my father and my sister. Without their support this fruitful experience in France would not have been possible. I will spend the rest of my lifetime with them.

Diversification précoce des cnidaires: étude des microfossiles à preservation exceptionnelle de la Formation de Kuanchuanpu (base du Cambrien; ~535 Ma), Province de Shaanxi, Chine

Résumé

Le Cambrien basal (Étage Fortunien, env. 535 Ma) de la Formation de Kuanchuanpu dans la Province chinoise du Shaanxi, contient une grande variété de Small Shelly Fossils (SSF) préservés grâce à une phosphatisation secondaire. On y trouve les éléments exosquelettiques de groups animaux très variés mais également des embryons et stades larvaires conservés en trois dimensions et interprétés par les auteurs précédents comme de possible cnidaires. Cette faune dans son ensemble est une source d'informations exceptionnelle sur les toutes premières étapes de la diversification animal avant qu'elle n'atteigne son plein développement (ex : au cours du Cambrien inférieur, Série 2, Étage 3). Nous avons exploré ici la morphologie de ces organismes fossiles submillimétriques au moyen de la Microscopie Électronique à Balayage (SEM) et de techniques microtomographiques aux rayons X (Computed X-ray Microtomography, XTM et Synchrotron X-ray Microtomography, SRXTM), testé les hypothèses concernant leurs possibles affinités avec les cnidaires et analysé leur possible relations phylogénétiques avec les groups actuels de cnidaires. Parmi ces fossiles, certains (ex : *Olivooides* et formes apparentées) peuvent être raisonnablement considérées comme des cnidaires sur la base de leur anatomie interne, leur symétrie radiale et leurs caractères externes, et pourraient appartenir au groupes-souche des Scyphozoa, Cubozoa et Anthozoa. Des représentants des groupes-couronne Scyphozoa, Cubozoa, Anthozoa et Hydrozoa semblent apparaître plus tard dans l'évolution des cnidaires (pas avant le Cambrien inférieur Série 2, Étage 3) comme l'indiquent les méduses du gisement exceptionnel (Lagerstätte) de Chengjiang (env. 521 Ma) qui ressemblent en tout point aux méduses actuelles et possédaient déjà un système sensorial sophistiqué. Notre étude met en lumière une série de caractères atypiques chez les cnidaires ancestraux de Kuanchuanpu: 1) la coexistence de divers modes de symétrie, 2) la prédominance de la symétrie pentaradiale, 3) l'existence d'un mode de développement direct (apparemment sans larve planula) contrastant ainsi avec tous les cnidaires actuels et 4) une taille corporelle très petite compatible avec un mode de vie meiobenthique.

Mots-clé: Cambrien, biodiversification animale, Small Shelly Fossils, cnidaires, Formation de Kuanchuanpu, Chine.

Diversification of early cnidarians: Exceptionally preserved microfossils from the Kuanchuanpu Formation (lower Cambrian; 535 Ma), Shaanxi Province, China

Abstract

The lowermost Cambrian (Fortunian Stage; *ca.* 535 Ma) Kuanchuanpu Formation from China contains a great variety of secondarily phosphatized Small Shelly Fossils such as exoskeletal elements of various animal groups but also yields three-dimensionally preserved embryos and larval stages interpreted as cnidarians by previous authors. This biota is an exceptional source of information on the early steps of animal biodiversification before its full development (e.g. early Cambrian, Series 2, Stage 3). We explored the morphology of these sub-millimetric fossil organisms by means of Scanning Electron Microscopy (SEM), Computed X-ray Microtomography (XTM) and Synchrotron X-ray Microtomography (SRXTM), and tested their cnidarian affinities and analyzed their possible relation to modern cnidarian groups. Some of them (e.g. *Olivooides* and related forms) can be reasonably considered as cnidarians based on their internal anatomy, radial symmetry and external features, and may belong to the stem groups Scyphozoa, Cubozoa and Anthozoa. Crown-group scyphozoans, cubozoans, anthozoans and hydrozoans seem to appear later in the evolution of cnidarians, not before Stage 3, Series 2 of the early Cambrian as indicated by the jellyfish from the Chengjiang Lagerstätte (*ca.* 521 Ma) which closely resemble modern tetraradial medusae and possessed sophisticated sensory organs. Our study highlights some important “atypical” features of the ancestral cnidarians from the Kuanchuanpu biota such as 1) the co-existence of diverse symmetry patterns, 2) the prevalence of pentaradial symmetry, 3) a possible direct development (with no planula larva) contrasting with all modern cnidarians and 4) a small body size consistent with a meiobenthic lifestyle.

Keywords: Cambrian animal biodiversification, Small Shelly Fossils, cnidarians, Kuanchuanpu Formation, China.

Contents

Chapter 1: Emergence of animal life

Chapter 1: Emergence of animal life

1.1 Prebiotic stage and first prokaryotes

Our planet is about 4567 million years old according to isotopic datations of calcium aluminum–rich inclusions found in the Efremovka carbonaceous chondrite (Amelin et al. 2002). The chronology of appearance of the first cells or cell-like structures is still uncertain and follows a long period of prebiotic evolution before the Hadean when nucleobases and amino acids are assumed to have formed from simpler organic compounds. It has been hypothesized that the earliest life forms were based entirely on RNA and that RNA would later have been replaced by DNA, which is more stable and therefore can build longer genomes (Joyce 2002, Forterre 2005).

The oldest fossil evidence for microbial life are micron-scale haematite tubes come from the Nuvvuagittuq belt of Canada (Dodd et al. 2017). They are associated with *ca.* 3.7-4.2 Ga (Eo-archean to Hadean; Fig. 1) hydrothermal vent precipitates and are assumed to represent filamentous microbes similar to those found as fossils in younger rocks and in present-day environments.

The oldest stromatolites (layered bio-chemical accretionary structures formed in shallow water by the trapping, binding and cementation of sedimentary grains by biofilms microorganisms, especially cyanobacteria) can be traced back to at least 3.5 Ga (e.g. in the Cowles Lake Formation, northern Canada (Grotzinger and Rothman 1996)). Organic-walled microfossils were also discovered in 3.2 Ga-old rocks from the Moodies Group in South Africa (Javaux, Marshall and Bekker 2010). Biomarkers such as 2-Methylhopanoids were extracted from *ca.* 2.5 Ga-old sediments and are strong indicators of oxygenic photosynthesis (Summons et al. 1999, Planavsky et al. 2014).

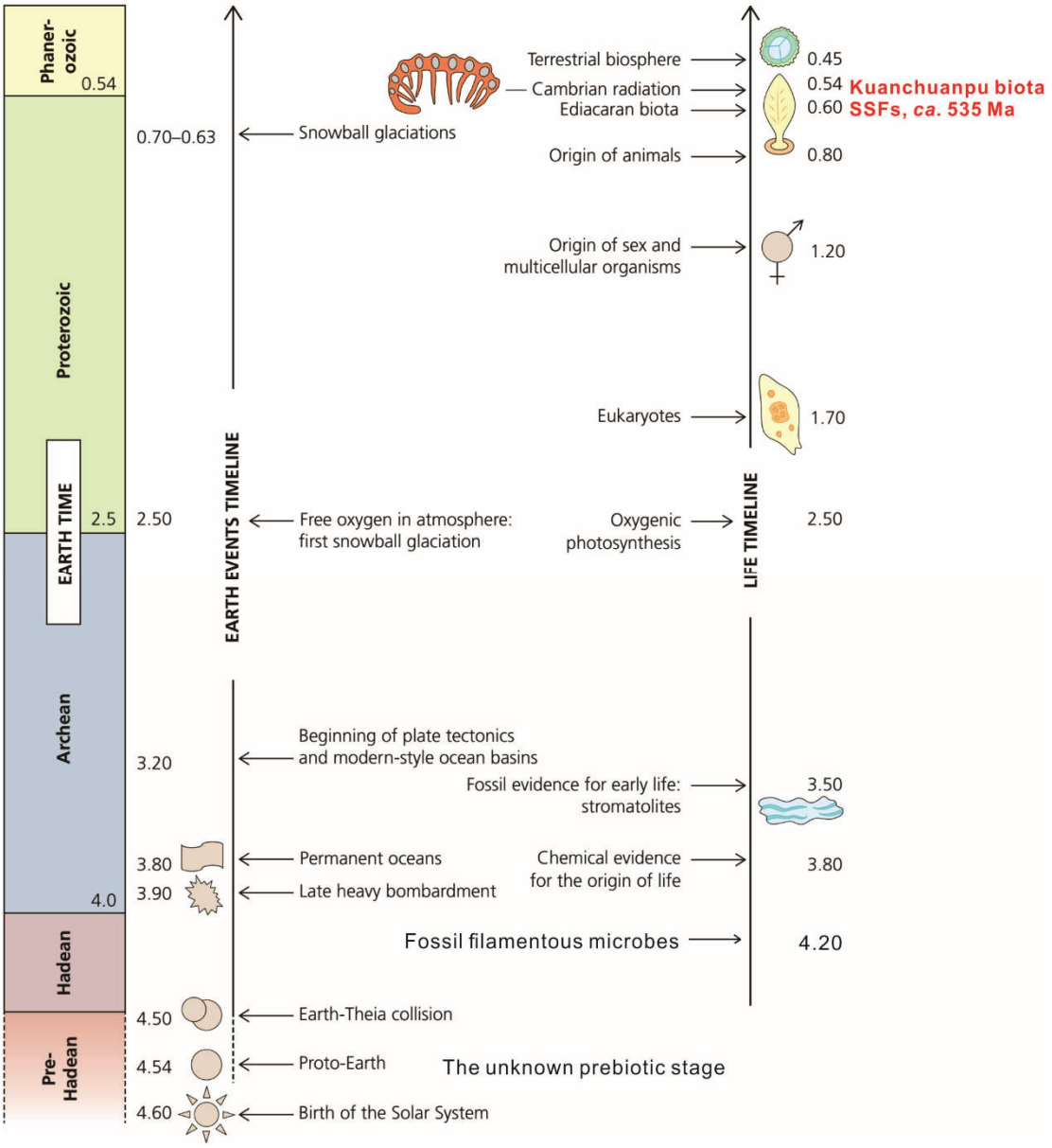

Fig. 1. Major events in the history of life on Earth, from pre-biotic stage to the early diversification of animal life. Modified from (Hou et al. 2017).

1.2 Rise of eukaryotic life

By definition, Eukaryotes are organisms whose cells have a nucleus enclosed within membranes, unlike prokaryotes (Bacteria and Archaea) (Fig. 2). Unlike unicellular archaea and bacteria, numerous eukaryotes are multicellular and include organisms consisting of many cell types forming different kinds of tissue. They form a distinct domain (Eukaryota) which appears to be monophyletic and have three important components: plants, fungi and animals (or Metazoa). The appearance of eucaryotes is a key event in the history of life that revolutionized the functioning if the Earth ecosystems.

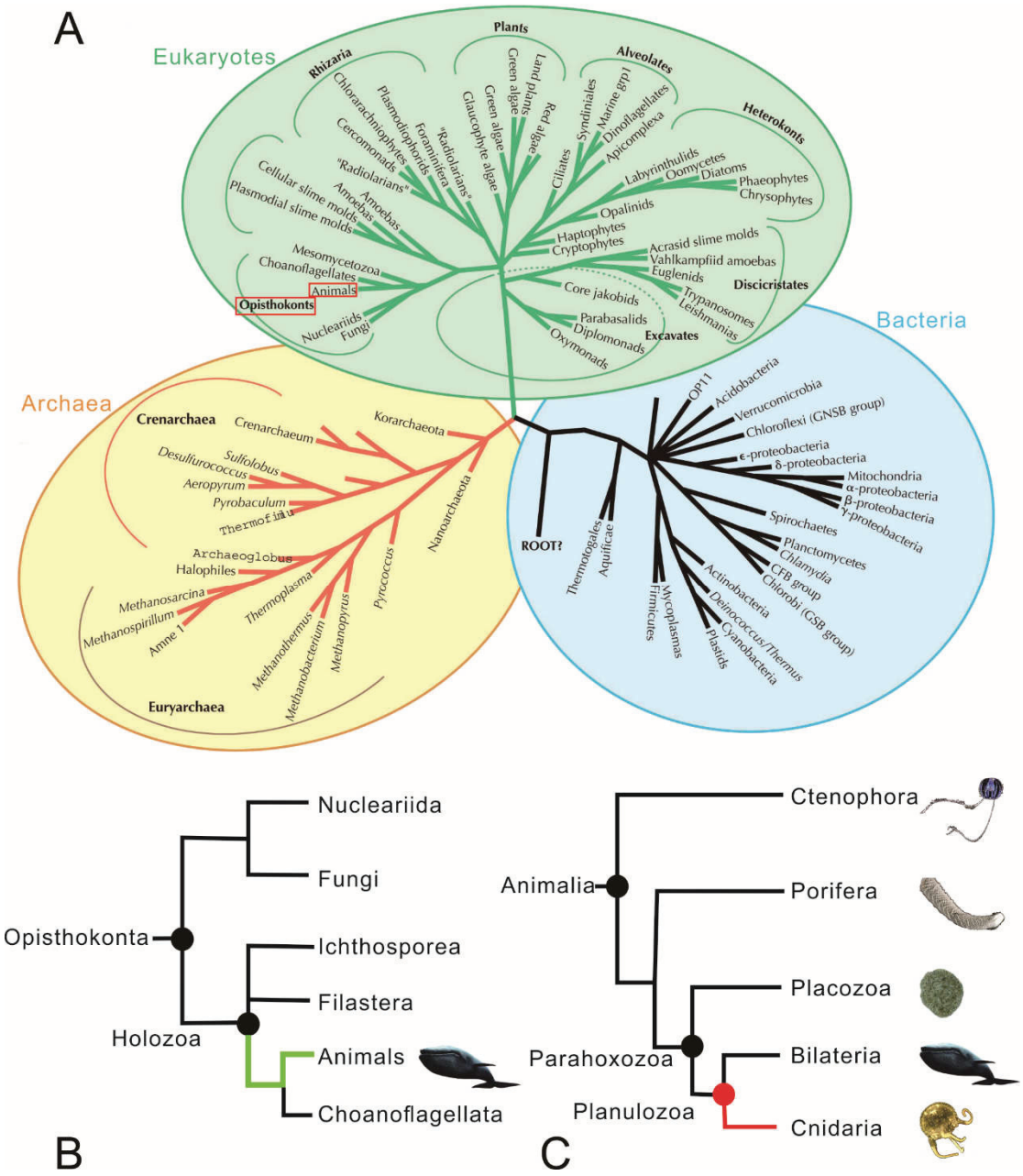

Fig. 2. Position of animals in the Tree of Life, among Opisthokonta and major animal clades. A. The Tree of Life, based on the most accepted opinion on classification of life and its inner relationship within each group (modified from (Martin 2016, Baldauf 2003). The solid bars in green, orange and black represent major lineages in Eukaryota, Archaea and Bacteria, respectively. Animals and Opisthokonta highlighted with red boxes. B. Hypothesized animal phylogeny (modified from (Martin 2016, Dunn et al. 2014)). Animals (green lines) belong to Opisthokonta (Cavalier-Smith 1987). Choanoflagellata appears as the sister group of animals (Carr et al. 2008). C. Cladogram showing major animal clades and the position of bilaterains and radial animals (cnidarians in red lines) (Ryan et al. 2013).

The appearance of eukaryotes around 1.7 Ga (Brasier and Lindsay 1998) also attested by specific biomarkers, including eukaryotic steranes and productive *in situ*

hydrocarbons (Logan et al. 1995). Microfossil colonies from the Hunting Formation (*ca.* 1.2 Ga), Somerset Island, Canada, indicate that sexual reproduction occurred among Proterozoic eukaryotes (Butterfield 2000). Eucaryotes with intracellular structures (possible nuclei) occur in the *ca.* 850 Ma-old Bitter Spring Formation of central Australia and suggest a more remote origin before the Tonian in the Mesoproterozoic (Schopf and Kudryavtsev 2005). The centimetre-sized structures from the 2.1-Gyr-old black shales of the Paleoproterozoic of Gabon purportedly interpreted as the oldest large colonial macro-organisms (El Albani et al. 2010) remain highly controversial in the absence of strong evidence for cellular features, eukaryotic markers and consistent shape and growth pattern (Donoghue and Antcliffe 2010).

1.3 Ediacaran life: evidence from macro- and microfossils

More complex eukaryotic organisms appear during the Ediacaran period (635-541 Ma), among them macro-organisms with very distinctive and unfamiliar morphologies, lifestyles and ecologies that are uneasy to compare with those of modern animal groups, except a few forms with a bilaterian symmetry (e.g. *Kimberella* (Ivantsov 2009, Ivantsov 2010, Ivantsov 2013) Fig. 3 B). They are often characterized by modular body plans and fractal growth (Narbonne 2004, Narbonne 2005, Narbonne et al. 2009, Seilacher 2007, Cuthill and Conway Morris 2014). Their construction and symmetry modes (e.g. glide plane of symmetry) has no equivalent among modern animals. Recent studies show that the high taxonomic diversity and relatively complex shapes of rangeomorphs, a major group of frond-like sessile Ediacaran organisms (Fig. 3 G), may have arisen from relatively simple branching and fractal processes that have been modelled by using mathematical calculations (Cuthill and Conway Morris 2014). These macrofossils formed diverse epibenthic communities (Fig. 4) and were associated with microbial mats. Recently, the fossil *Dickinsonia* (Fig. 3 A) (a macro-organism with the plate-like appearance) from Ediacaran (*ca.* 558 Ma), White Sea biota, Lyamtsa locality, Russia, is tested to close to animals based on the extracted hydrocarbon biomarkers (fossil animal fat) which gives a new clue on further attempting to the early evolution of animals (Bobrovskiy et al. 2018a).

Ediacaran fossil macro-organisms occurred worldwide (e.g. Newfoundland, Russia, Namibia, England and Australia). Three distinct assemblages through time are recognized (Avalon, White Sea and Nama; see (Laflamme and Narbonne 2008, Droser, Tarhan and Gehling 2017)). The diversity of body plans found among Ediacaran organisms suggest a great phylogenetic diversity (Fig. 5) with possible crown-group and stem-group bilaterians and other representatives lying in a much more basal postion (e.g. rangeomorphs as possible stem-group Metazoa) (Xiao and Laflamme 2009).

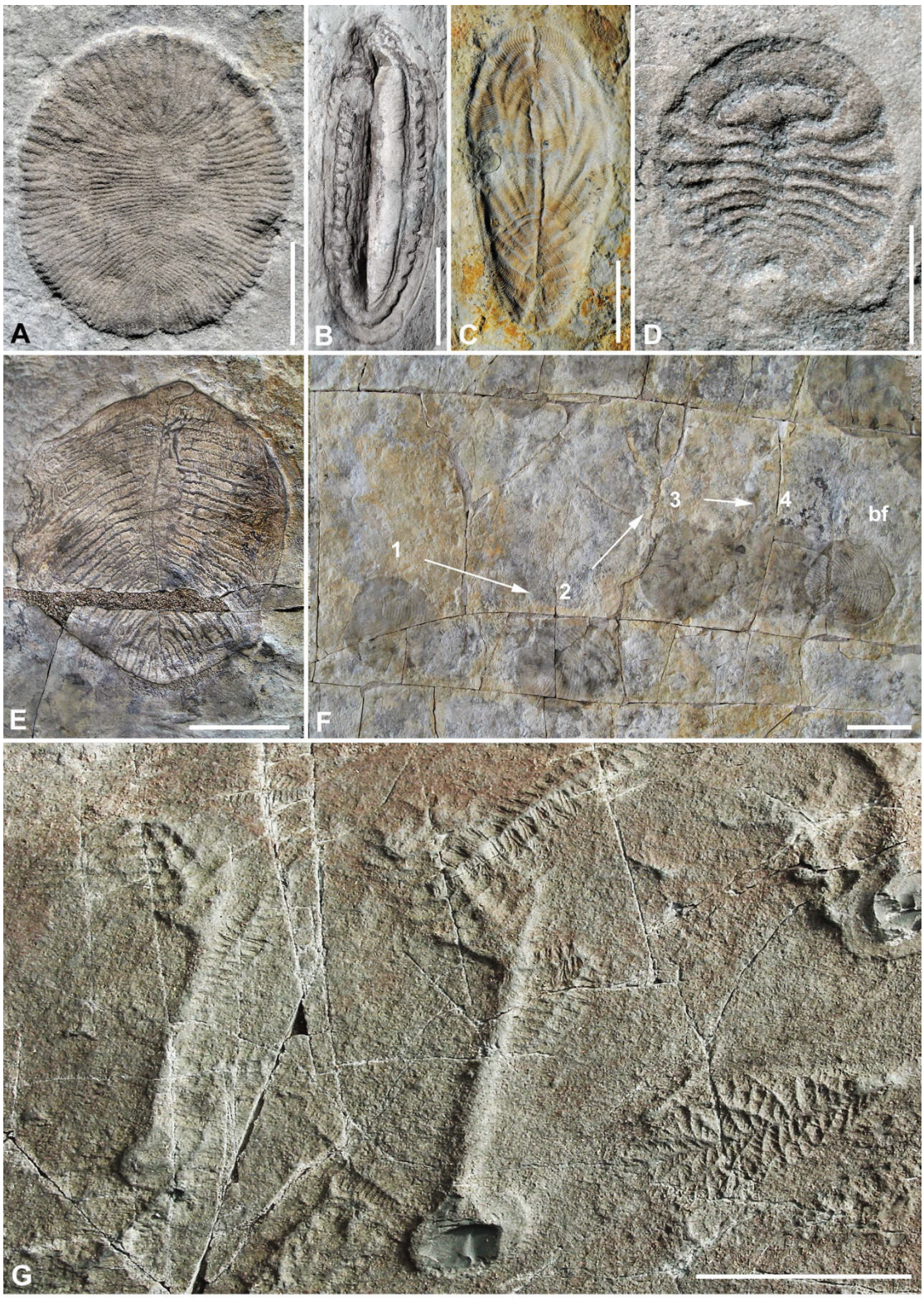

Fig. 3. Late Precambrian (Ediacaran) macro-organisms. A-F. White Sea biota from northern Russia. A. *Dickinsonia*; B. *Kimberella*; C. undet. dickinsoniid. D. *Archaeaspinus*. E. *Yorgia*. F. Body fossil (bf) of *Yorgia* and its associated trace fossils. G. Frond-like organisms (rangeomorphs) from Mistaken Point, Newfoundland, Canada. Scale bars: 10 cm in G, 5 cm in F, 1 cm in A-E. (A-F: J. Vannier; G: courtesy M. Laflamme).

Fig. 4. Artistic reconstructions of the Ediacaran fauna. From BBC at http://www.bbc.co.uk/nature

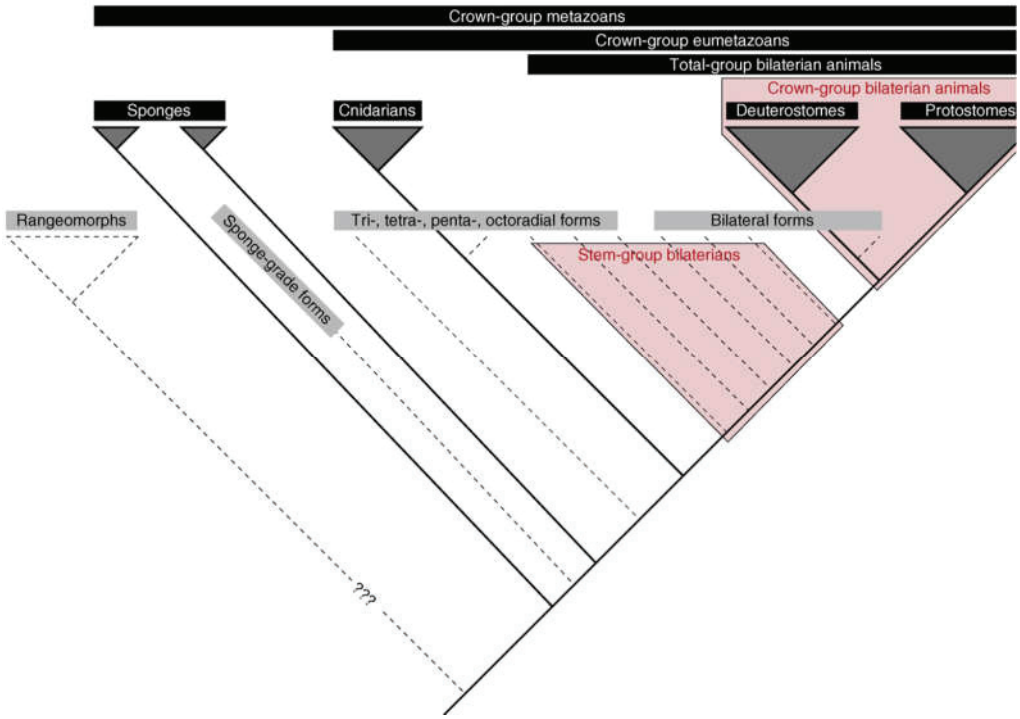

Fig. 5. Possible phylogenetic placement of bilateral Ediacara fossils (vendomorphs, parvancorinomorphs, *Yorgia*, *Kimberella* and *Dickinsonia*), tri-, tetra-, penta- and octoradial forms, and rangeomorphs in the metazoan tree. The diverse array of morphological constructions exemplified by the Ediacara biota suggests a greater phylogenetic diversity than typically assumed. Ediacara fossils are represented by dotted lines or triangles, extant animals by gray triangles. From Xiao and Laflamme, 2009.

Ediacaran micro-organisms such as the phosphatized embryos (Fig. 6) from the 570 million-year-old Doushantuo Formation (Guizhou Province, China) have generated controversial interpretations since their discovery. Although remarkably preserved in three dimensions at cell or possible intracellular level their phylogenetic affinities remain uncertain. Although detailed comparisons with the cleavage and development of modern embryos would suggest affinities with animals (Xiao, Zhang and Knoll 1998) some authors would rather place these enigmatic embryonic forms between Fungi and Metazoa, possibly among Holozoans (e.g. (Butterfield 2011)) which represent a simpler level of eucaryotic organization (Fig. 7).

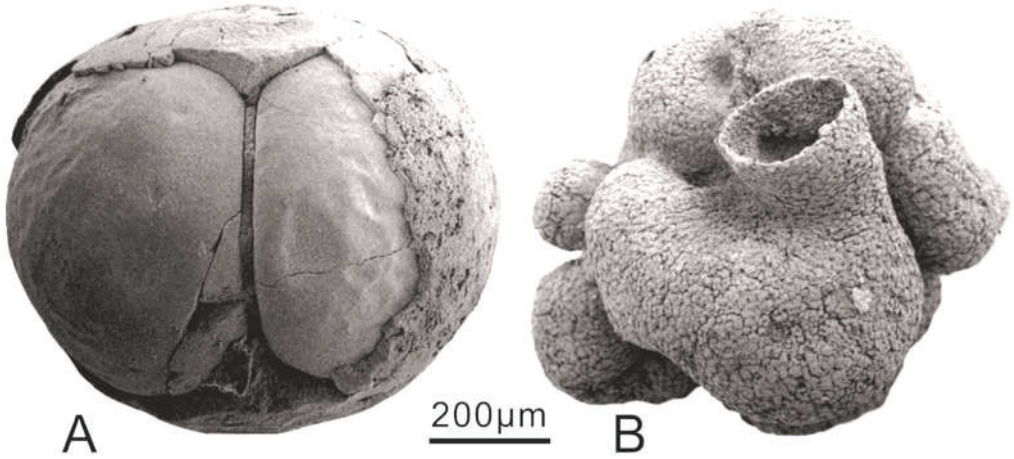

Fig. 6. Phosphatized micro fossils from the late Neoproterozoic Doushantuo Formation, Weng'an, Guizhou Province, south China. A. Assumed fossil animal embryo at two-cell stage. B. Earliest known sponge colony. Modified from Xiao et al., 1998; Yin et al., 2015.

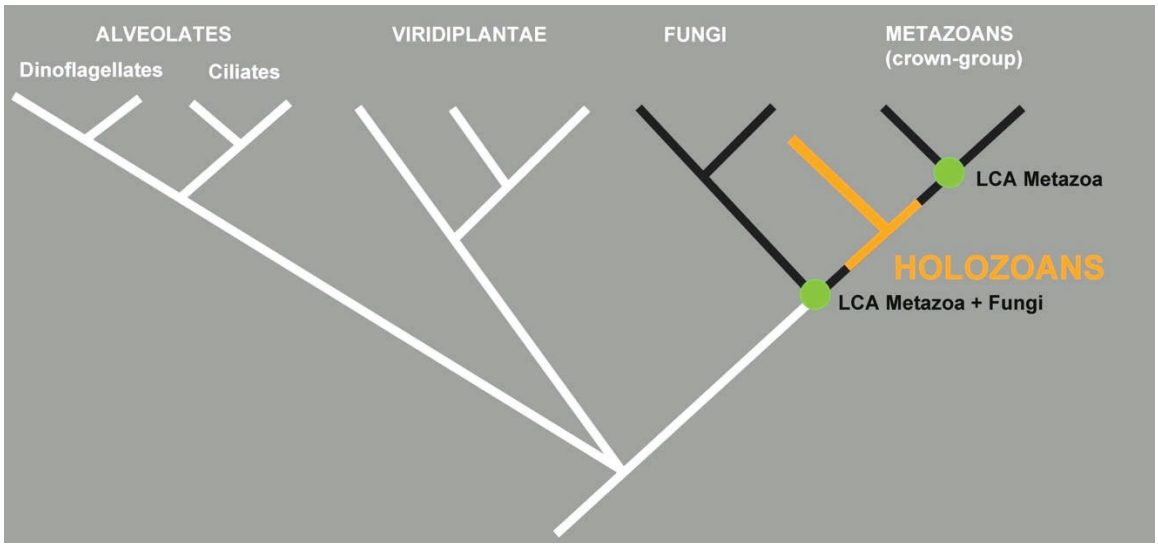

Fig. 7. Possible affinities of the Doushantuo embryos. Simplified cladogram in which they are placed between Fungi and Metazoa. Simplified from Butterfield, 2011.

1.4 First animals

Eucaryotes have three important components: plants, fungi and animals (or Metazoa). Animals form a relatively low proportion of the huge eucaryotic diversity (Fig. 2). They have diagnostic features that set them apart from other living things. Unlike plants and algae, animals are heterotrophic, feed on organic material and digest it via a more or less complex digestive systems in which enzymatic reactions take place. All animals are motile during at least part of their life cycle, many of them being able to move through their environment via nerves transmitting signals to muscles. Most animals develop through the blastula during their embryonic development and their cells differentiate into specialized tissues and organs (except in basal metazoans such as sponges and placozoans). Choanoflagellates are generally considered as the closest relatives of animals and the sister group of Metazoa (Carr et al. 2008), based on genome sequencing. They are free-living unicellular of colonial unicellular eucaryotes with a microscopic ovoid or spherical cell body of 3–10 µm in diameter and a single apical flagellum surrounded 30–40 microvilli. Sponges (Porifera) have long been regarded as the most basal animals with assumed intimate relationship with Choanoflagellata (Philippe et al. 2009). However, detailed genomic studies of *Mnemiopsis leidyi* suggest that ctenophores (comb jellyfish) are the earliest off-shot of the animal tree (Ryan et al. 2013). Additionally, the analysis of amino acid positionsalso confirm the view that sponges are the sister group of all other animals. (Dunn et al. 2014) (Fig. 2)

The earliest unambiguous evidence for animal life in the fossil record are sponges. Exceptionally three dimensionally preserved sponges occur in the ca. 600 Ma-old Doushantuo Formation from south China (Yin et al. 2015) (Fig. 6 B).

The early diversification of animal life occurs during the Cambrian and is known as the “Cambrian Explosion” (Conway Morris 2000). This event is by definition the relatively sudden appearance in the fossil record of a great variety of new animal body plans that have modern counterparts in present-animal groups (e.g. arthropods). Evidence come from 1) body fossils (Fig. 8), 2) trace fossils attesting to the existence of animal activity at or within the sediment as soon as the earliest Cambrian (e.g. the burrow systems called *Treptichnus pedum* which characterize the Precambrian-Cambrian boundary and were probably made by priapulid-like worms; see (Vannier et al. 2010) and 3) Small Shelly Fossils (SSFs) representing the exoskeletal remains of the first biomineralized animals (e.g. Kuanchuanpu biota; see (Qian 1977) and see Chapters 3, 5 of this thesis). One of the most spectacular feature of the “Cambrian Explosion” is the rise of bilaterians (animals with an antero-posterior and dorsa-ventral polarity, a head concentrating brain tissues) exemplified by arthropods and fish-like deuterostomes (Shu 2003). The emergence of animals is one of the major events in the history of life on Earth that gave rise to the present-day biological diversity, generated the prototypes of modern-style trophic webs and deeply impacted the dynamics of interchange between life and the Earth system. Over the last two decades,

intensive research on exceptional fossil sites (Lagerstätten), such as those of Chengjiang in China (*ca.* 521 Ma;(Hou et al. 2017, Shu et al. 2003a, Zhang et al. 2014)), Sirius Passet in Greenland (*ca.* 520 Ma; (Budd 1998, Morris and Peel 2008)), Emu Bay Shale in Australia (Briggs and Nedin 1997, Paterson et al. 2010), the Burgess Shale in Canada (*ca.* 508 Ma; e.g. (Morris 1989, Briggs, Collier and Erwin 1994, Vannier et al. 2018); see also https://burgess-shale.rom.on.ca/en/index.php) and more recently that of the Fezouata in Morocco (ca 480 Ma; (Martin 2016)) has provided a wealth of new anatomical, ecological and even behavioral (Caron and Vannier 2016) information on the early stages of animal life and has clarified its relation to present-day animal groups (e.g. Arthropoda, Crustacea, Chordata).

Fig. 8. Exceptionally preserved soft-bodied or lightly sclerotized marine animals from Cambrian Burgess Shale-type Lagerstätten. A. *Wiwaxia corrugata*, a soft bodied organism protected by numerous sclerites (Vannier 2012). B. Cricocosmia jinningensis, a cycloneuralia worm with a double row of sclerites. C. Ottoia prolifica, a priapulid worm showing its everted pharynx (left) and

the remains of undigested food (brachiopod shells) in the posterior part of its gut (up right) (Vannier 2012). D. Paucipodia haikouensis, a lobopodian with soft unjointed legs. E. *Hallucigenia sparsa*, a lobopodian interpreted (Smith and Ortega-Hernández 2014, Smith and Caron 2015) as a possible stem-group onychophoran with pointed sclerites on its back. F. Anomalocaridid (juvenile) showing prehensile frontal appendages. G. Waptia fieldensis, an arthropod with a flexible abdomen and well-preserved head and trunk appendages (Caron and Vannier 2016). H-J. Sidneyia inexpectans, an arthropod in general view (H) with details of its gut contents (I) (e.g. trilobite elements) and trunk appendage (J) (see gnathobase) (Zacaï, Vannier and Lerosey-Aubril 2016). A, C, E, G-J are from the middle Cambrian Burgess Shale (British Columbia, Canada) biota; B, D, F are from the early Cambrian Chengjiang biota (Yunnan, China). All photographs from J. Vannier except E (courtesy J. B. Caron). Scale bars: 1 cm in A, C, D, F-H; 5 mm in B, E, J; 1 mm in I.

Fig. 9. Artistic reconstructions of middle Cambrian Burgess Shale fauna, Canada. From BBC at http://www.bbc.co.uk/nature. For videos on Burgess Shale animals (e.g. predators, filterers, scavengers), see: https://burgess-shale.rom.on.ca/en.

The "Cambrian Explosion" has fueled intensive scientific debates, especially as whether it represents a real diversification or a preservational artefact (Conway Morris 1989, Conway Morris 2000, Smith and Harper 2013). Various hypotheses have been proposed by authors who invoke environmental, developmental, and ecological factors and triggers (Fig. 10) to explain the timing and magnitude of this unique event in the history of life and its apparently fast evolution pace (e.g. (Smith and Harper 2013, Zhang et al. 2014)). Potential biological causes include the following:
1) changes in primary productivity and the emergence of complex food webs; 2) the vacancy of ecological niches and redistribution of resources created by the extinction

of the Ediacaran organisms; 3) major innovations among bilaterians (e.g. brains, digestive systems, sensory organs) which boosted capacities of animals to explore their environment, exploit new and richer food sources (e.g. predation, the appearance of carnivores) and 4) arms race between predator and prey which introduced new selection pressure and increased evolutionary rates (Peterson 2005, Butterfield 2011). Non-biological factors may have been crucial triggers, too. Among them, 1) the rise of oxygen level (Canfield, Poulton and Narbonne 2007, Cook and Shergold 1984, Peters and Gaines 2012), 2) the increase of nutrients (e.g. calcium, phosphate) which may have boosted primary production and allowed animals to increase their body size; 3) the rise of sea-level expanding the ecological niches (Smith and Harper 2013) (Fig. 10).

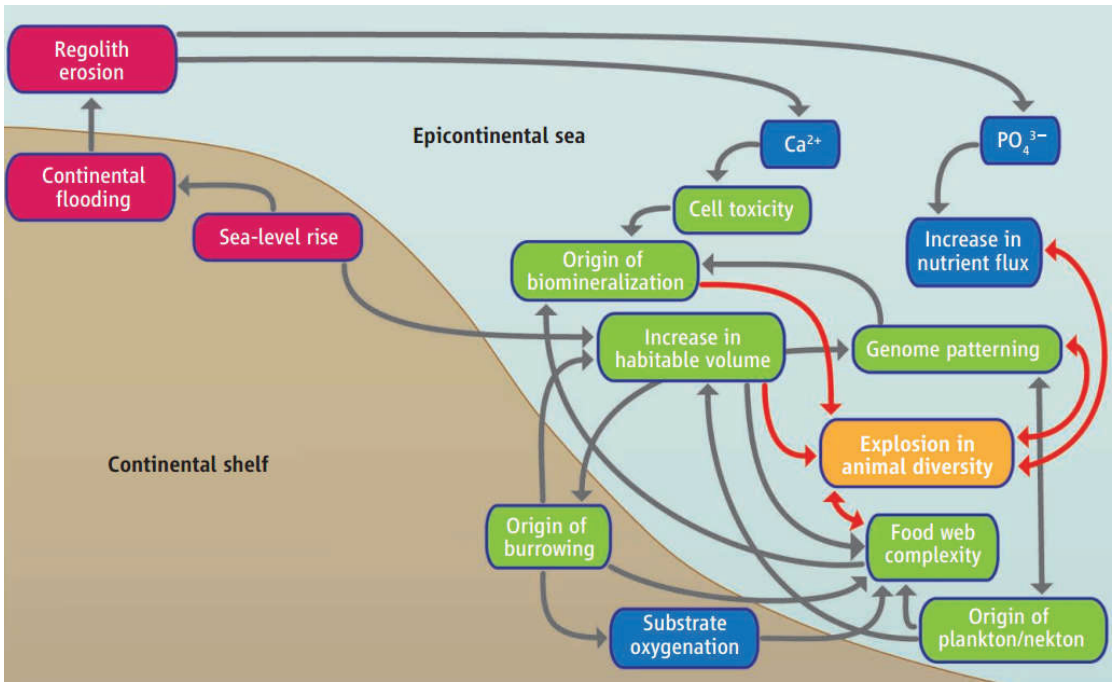

Fig. 10. Possible geological, geochemical and biological factors that led to the "Cambrian explosion" (red bar, geological; blue bar, geochemical; green bar, biological). From Smith and Harper, 2013.

The Kuanchuanpu Formation (Qian 1977) from the Shaanxi Province, south China (lowermost Cambrian; Fortunian Stage; *ca.* 535 Ma) provides the unique opportunity to study the diversity of animal life before the Cambrian radiation reached its peak (Cambrian Stage 3; *ca.* 521 Ma; e.g. Chengjiang biota) and to better understand the timing and amplitude of the animal diversification. It contains abundant and diverse assemblages of Small Shelly Fossils (SSFs) and, over the recent years, has become an important source of information to study the early diversification of a variety of bilaterians and non-bilaterians animal groups (Dong et al. 2013, Dong et al. 2016, Han et al. 2013, Han et al. 2016c, Liu et al. 2017, Wang et al. 2017, Zhang and Dong 2015) . For example, embryonic forms interpreted as possible cnidarians, ecdysozoan worms

and small deuterostomes (a large clade which include the present-day vertebrates) have been the focus of recent studies (Zhang et al. 2015, Liu et al. 2014c, Han et al. 2017). Previous work on this biota and results obtained in the framework of the present thesis are presented in Chapters 3 and 5, respectively.

Chapter 2: Evolution of cnidarians from Precambrian to Recent

Chapter 2: Evolution of cnidarians from Precambrian to Recent

2.1 Extant cnidarians

The phylum Cnidaria is diverse group of basal animals with at least 10000 species known to science which occupy a wide ecological spectrum in pelagic and epibenthic environments (Brusca and Brusca 2003) (Fig. 11). They comprise corals, see anemones, sea fans, sea pens, a huge variety of jellyfish, hydroids and some parasitic forms (Raikova 1988, Raikova 2008, Evans et al. 2008). Their morphological and ecological diversity contrasts with a relatively simple body plan compared with bilaterian groups. Corals, sea anemones and jellyfish are the most familiar cnidarians that people can observe easily in shallow waters. Whereas climatic changes severely threaten the existence of corals and may lead them to extinction, present day environmental disturbances largely due to human activity seem to favor the proliferation of jellyfish. Overfishing which wipes out their predators and competitors, global warming, depletion of oxygen in coastal waters, creates optimal conditions to the proliferation of jellyfish which can proliferate by taking advantage of their unique lifestyle and asexual reproduction mode. Their remarkable capacities to colonize marine environments may explain the evolutionary success of these animals which have a remote origin and survived all major biodiversity crisis throughout the Phanerozoic. Cnidarians appeared very early in the evolution of metazoans as predicted by phylogenies based on genomic data and molecular clock hypotheses (Erwin et al. 2011) (Fig. 12) and indicated by fossil evidence in the Cambrian and possibly the Precambrian. However, numerous questions remain unanswered, especially the chronology of their early diversification, and the morphology, lifestyle and environment of their earliest ancestors.

Fig. 11. A jellyfish drifting in the shallow waters of Bonne Bay, Canada. Photograph: David Doubilet / NG / Getty Images at https://www.theguardian.com/environment/2015/aug/21/are-jellyfish-going-to-take-over-oceans.

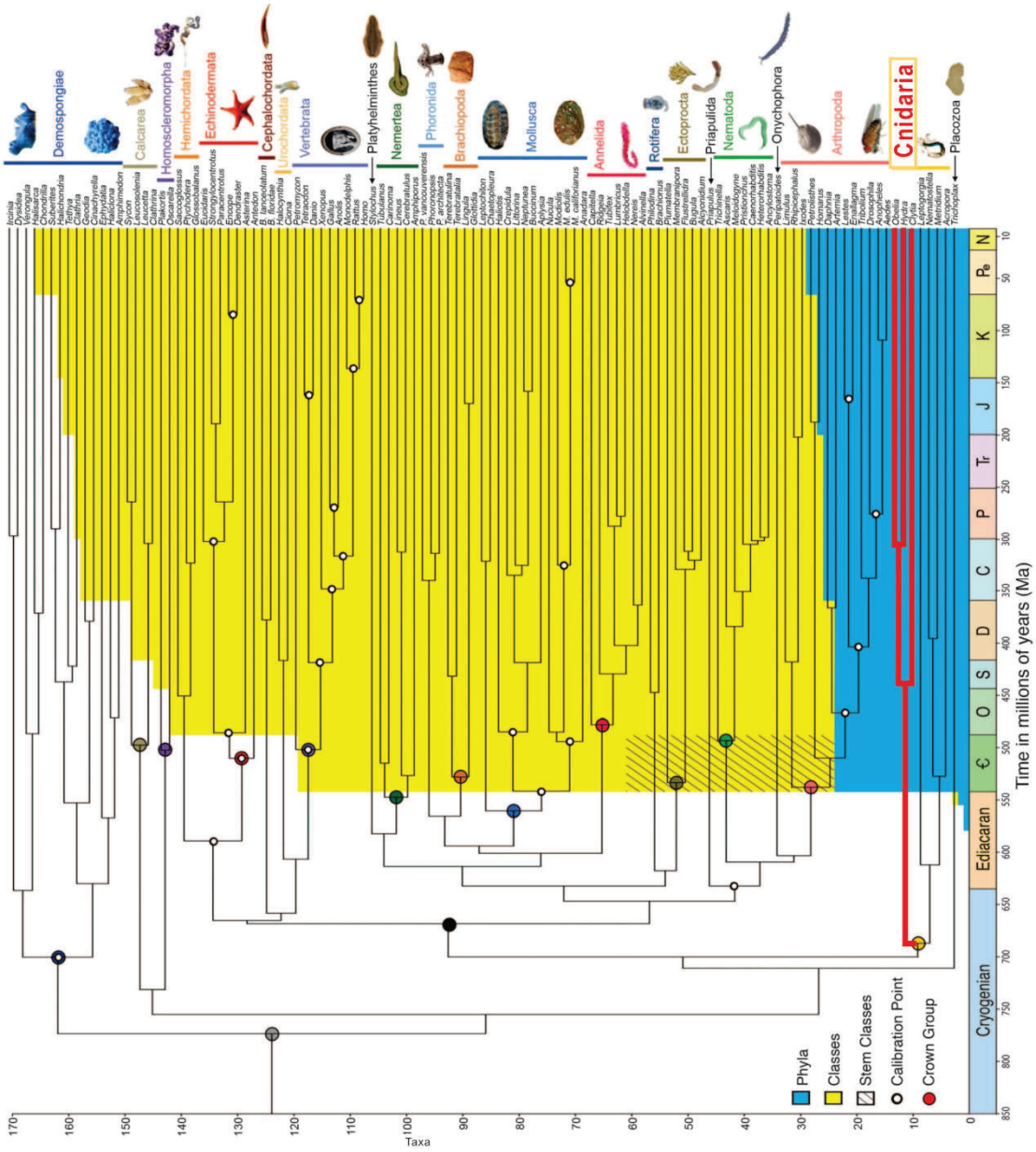

Fig. 12. Position of Cnidaria (highlighted in red line) in the metazoan tree based on genomic phylogenies and fossil occurrences. Modified from Erwin et al., 2011.

2.1.1 Definition, body plan and symmetry

Cnidarians owe their name to the cnidocytes, a unique and diagnostic cellular type involved in prey capture, defense, locomotion and attachment. In contrast with triploblatic bilaterian animals, cnidarians have only two embryonic germ layers, the ectoderm and the endoderm which give rise to the epidermis (e.g. umbrella of medusa) and the gastrodermis in adult forms (Fig. 13 A-B). The interspace between the endoderm and the ectoderm is filled with a jelly-like substance called the mesoglea. The mesoglea is derived from ectoderm but is by definition a non-cellular feature which produces no complex tissues and organs. It is generally thicker in polyps than in

medusae. Cnidarians differ markedly from bilaterians by the lack of anterior-posterior polarity and by a radial symmetry which has important implications on all vital aspects of their biology such as locomotion and feeding and sensing. The alternation of two distinct forms in the lifecycle of most cnidarians, the polypoid and medusoid forms, is another original character of the group which exemplifies their remarkable anatomical plasticity (Brusca and Brusca 2003, Harrison 1991, Hyman 1940, Mayer 1910).

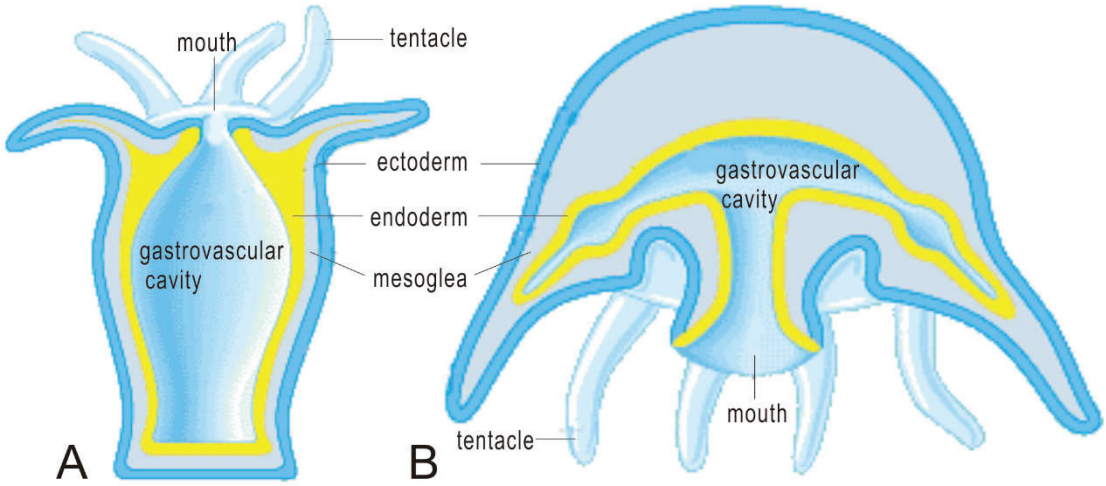

Fig. 13. Simplified diagram showing the main features of the cnidarian body plan. A. Polypoid form; B. Medusoid form. Endoderm layer in yellow. Ectoderm layer in dark blue. The interspace between the ectoderm and the endoderm is filled by the mesoglea (pale blue). Modified from Harrison, 1991.

The polypoid form

The polypoid stage occurs in the four classes of cnidarians although greatly reduced in the Scyphozoa and Cubozoa. The basic symmetry is radial with the main body axis running through the mouth (oral pole) to the base (aboral pole) of the polyp which is generally attached to the substratum (e.g. via a pedal disc in sea anemones). The mouth is either located in the middle of an oral disc (anthozoans) or at the distal end of an elevated manubrium (hydrozoans). The gastrovascular cavity (coelenteron) may be undivided, partially subdivided (scyphozoan polyps) or extensively compartmented by ridge-like mesenteries. Tentacles usually surround the mouth (Brusca and Brusca 2003, Harrison 1991). Polyps have the capacity to form colonies and some groups such as the siphonophoran hydrozoan exhibit a remarkable polymorphism among their polyps (Fig. 13).

The medusoid form

Free medusoid forms occur in all cnidarian classes except Anthozoa. In contrast with polyps, their body plan is relatively uniform, partly as a result of their pelagic lifestyle and their inability to form colonies. Typical medusae have a bell shape and closely resemble an open umbrella with its shaft representing the manubrium. The aboral or

outer convex surface of the bell is called the exumbrella and the concave and inner surface, the subumbrella. Medusae have a tubular shaft-like extension called the manubrium rooted in a central position (Fig. 14). Its unique and distal opening is the equivalent of the mouth. The gastrovascular cavity occupies a major part of the umbrella and extends radially to form a four-fold system of radial canals supported by septa. The distal parts of the radial canals are connected to a ring canal. Most extant jellyfish such as scyphozoans exhibit a tetraradial symmetry exemplified by the division of the gastrovascular cavity into four gastric subcavities separated by four primary septa and termed gastric pouches. Additional series of secondary septa (associated with canals) usually divide the cavity into smaller units. The terminology used to describe and orientate these tetraradial animals is as follows (see diagram Fig. 15) and applies to the fossils described in this thesis. The planes crossing the gastric subcavities and the oral arms are termed the peradii. At 45° from both sides of the perradii are the interradial planes or interradii. Halfway between the perradii and the interradii are the adradial planes (Fig. 15). Each septum usually branches off into numerous tiny canals near to the bell border. Tentacles generally in multiples of fours distribute evenly around the bell margin. The bell margin of some cnidarians (cubomedusae and scyphomedusae) also accommodates important sensory organs called rhopalia, each containing a concentration of epidermal neurons, a statocyst and in some cases an ocellus. Rhopalia lie in a perradial position and are also indicators of the tetraradial symmetry. Gonads generally occur as four distinct masses around the manubrium in an interradial position. In summary, medusoid cnidarians have primary radial, biradial body symmetry and their body axis is oral-aboral (Harrison 1991, Brusca and Brusca 2003).

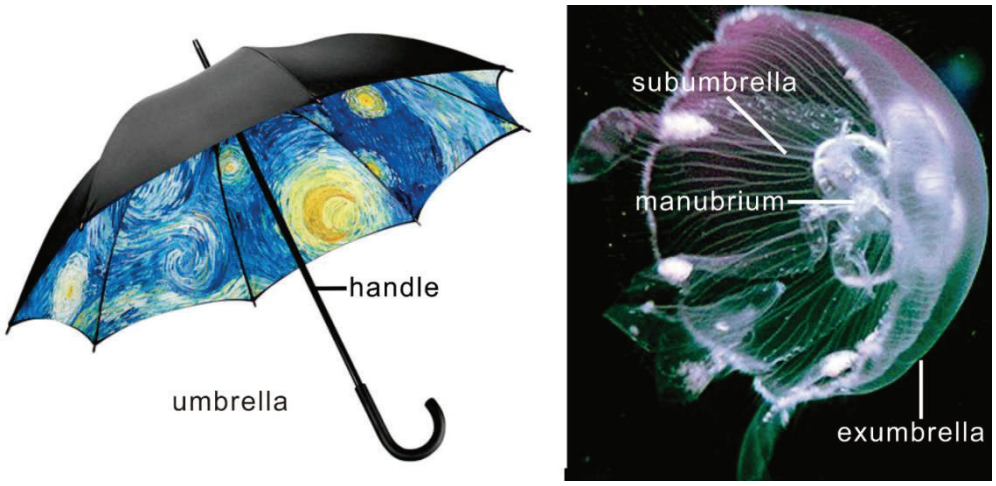

Fig. 14. An open umbrella resembling the overall shape of a scyphozoan medusa (*Aurelia*). The exumbrella and subumbrella are the outer and inner surface of the medusa bell, respectively. The manubrium occupies a central position.

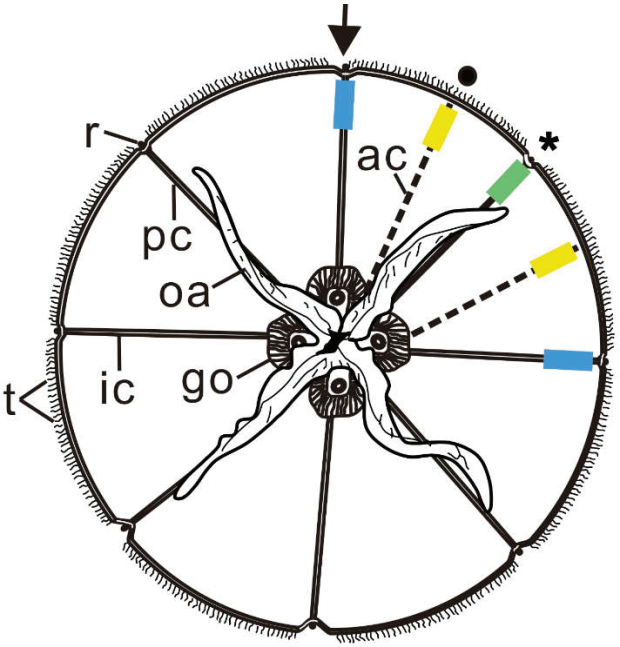

Fig. 15. Simplified oral view of a scyphomedusa showing its tetraradial symmetry. The interradial, adradial and perradial planes (interradii, adradii, perradii) crossing the medusa bell are marked with blue, yellow and green colours, respectively. The gonads and oral arms surrounding the mouth are in an interradial and perradial position, respectively. Abbreviations: ac, adradial canal; go, gonad; ic, interradial canal; oa, oral arm; pc, perradial canal; r, rhopalium; t, tentacle. •, adradii; →, interradii; *, perradii. Modified from Lesh Laurie and Suchy, 1991 in (Harrison 1991).

2.1.2 Reproductive cycles

Cnidarians typically exhibit alternation of asexual polypoid and sexual medusoid generations but there are considerable variations on this basic pattern. The purpose here is not to describe the huge variety of reproductive cycles that occur in cnidarians but to succinctly present some of them, especially the reproduction modes that may have possible equivalent in the fossil record or may be of interest in comparative studies between extinct and extant cnidarians. Cambrian species tentatively assigned to cnidarians have been described by several authors who reconstructed their possible life cycles (Han et al. 2013, Steiner et al. 2014). Basic knowledge on the early developmental stages of extant cnidarians is a pre-requisite for testing these interpretations. Sexual reproduction in cnidarians gives rise to a planula larva which corresponds to the dispersal phase of the life cycle. The planula is a flattened, free-swimming or creeping, non-feeding and ciliated larval form with an elliptical outline (Otto 1976), a flattened shape and a bilateral symmetry. Its size is about 1 mm long. It has an anterior-posterior polarity, the trailing posterior end of the larva becoming the

oral end of the adult (Fig. 16). The planula larva is common to all cnidarian groups. We briefly review here the main characteristics of the reproduction and development of hydrozoans, scyphozoans, anthozoans and cubozoans which have potential and putative ancestors in the Cambrian.

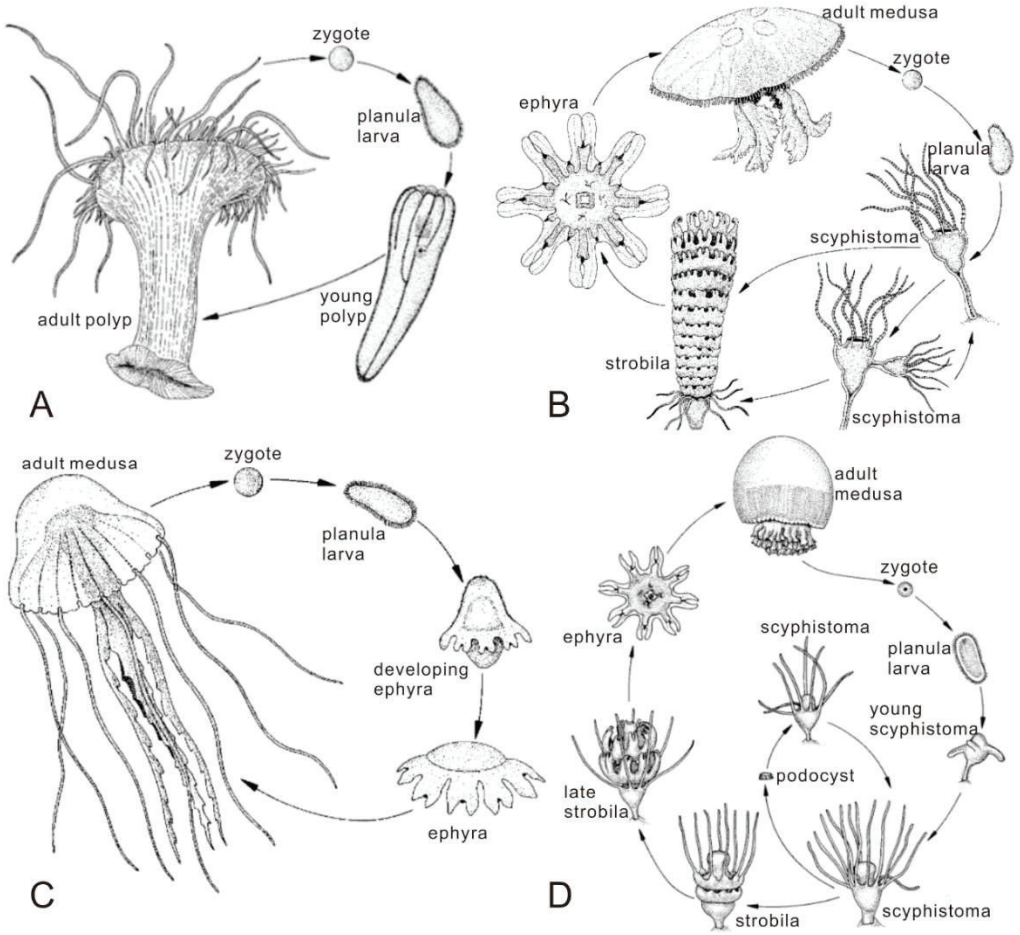

Fig. 16. Life cycles in typical representatives of extant cnidarians. A. Anthozoa (*Edwardsia*); B. Scyphozoa (*Aurelia*); C. Scyphozoa (*Pelagia*); D. Scyphozoa (*Stomolophus meleagris*). Modified from Brusca and Brusca, 2003.

Anthozoans- Extant representatives of this cnidarian group have no medusoid stage in their developmental cycle (Fig. 16 A). Assexual reproduction is common through longitudinal fission. In sea-anemones and corals, gonads are located on the gastrodermis of mesenteries and release gametes. Eggs are fertilized either in the coelenteron or outside the body. Most planula larvae of anthozoans are planktotrophic and therefore differ from the non-feeding larvae of other cnidarian groups. This feeding mode increases the probability of larvae to survive a longer time during the dispersal phase (Brusca and Brusca 2003).

Hydrozoans- Hydrozoan polyps reproduce assexually by budding but have also a sexual phase in their cycle. The polyps develop epidermal gamete-producing

structures called sporosacs. A different process occurs in most colonial hydroids. They produce medusa buds (gonophores) which may become free-swimming sexually mature medusae or may remain attached to the polyps as incipient reproducing medusae. Hydromedusae are gonochoristic, sperms and eggs being released into the water where fertilization occurs. The resulting hydrozoan planula larva swim for a few hours or days and and settles by attaching its anterior end to the substratum. The mouth opens at the opposite oral end and tentacular buds develop around the mouth as the larva metamorphoses into a solitary polyp (Brusca and Brusca 2003).

Scyphozoans- The asexual form of scyphozoans is a small polyp called the scyphostoma (Fig. 16 B-D). Repeated transverse fission of the scyphostoma produces medusae through a process called strobilation. This process gives rise to stacked immature medusae which are released in the surrounding medium as ephyrae. Ephyrae are extremely small medusae with incised bell margins and primary tentacles. The following developmental stage lead to sxually mature adult cyphozoans. Gonads appear on the floor of the gastric pouches and gametes are released through the mouth. Fertilization may be external or internal within the gastric pouch of the female. Blastulation and gastrulation give rise to a planula larva which marks the beginning of a new cycle. Numerous pelagic forms lack the scyphostoma stage and develop directly a medusa from the planula larval stage (Brusca and Brusca 2003).

Cubozoans- The reproduction cycle of this cnidarian group is relatively poorly documented in comparison with that of other groups. Each polyp metamorphoses directly into a medusa. No strobilation is known to occur in cubozoans. A sexual behaviour recalling copulation is used by cubozoans in which sperm is transfered directly by the male to the female, contrasting with the passive dispersal of gametes in the sexual reproduction of other groups (Harrison 1991).

Staurozoans- Staurozoa was originally grouped with Scyphozoa but now forms a distinct class based on its morphology and sessile lifestyle (Daly et al. 2007, Marques and Collins 2004). The lifecycle of staurozoans is similar to that of scyphozoans.

2.1.3 Systematic classification

Cnidarians are currently divided into six classes based (Daly et al. 2007, Collins 2002, Collins et al. 2006a, Raikova 2008, Raikova 1988) (Table 1). Typical representatives of Anthozoa, Hydrozoa, Cubozoa, Staurozoa and Scyphozoa are shown in Fig. 17.

Anthozoa- They lack a meduzoid stage and are characterized by a coelenteron divided by longitudinal mesenteries. Their polyp has a biradial and radial symmetry. The tentacles are generally 8 or occur in multiple of 6 and contains extensions of the

coelenteron. The well-developed pharynx bears one or more ciliated grooves. Polyps may reproduce both sexually and asexually (Collins 2002, Daly et al. 2007).

Cubozoa- The medusa bell is nearly square in cross-section. They are characterized by blade-like structures called pedalia which bear hollow interradial tentacles, one at each corner of the cube-like umbrella. The bell margin is folded inward to form a specific feature called the velarium into which gut diverticula extend. The sting of cubozoans are very toxic. Four sensory structures (rhopalia) are present in a perradial position and house remarkable complex eyes bearing a lens and ocelli. Each polyp produces a single medusa by complete metamorphosis with no strobilation stage (Hyman 1940, Mayer 1910, Coates et al. 2006).

Staurozoa- This Class was redefined by (Marques and Collins 2004). Staurozoans develop directly from benthic planula larvae and attach to substratum via a stalked adhesive disc. They have eight arms bearing tentacles. This configuration had led people to describe them as sessile medusae although scientists view them as polyps. They also form a relatively small group in terms of species and genera (Van Iten et al. 2006, Zapata et al. 2015).

Scyphozoans- This large group encompasses the jellyfish. The medusoid stage predominates. The coelenteron of scyphozoans is divided into 4 longitudinal mesenteries. Medusae lack a velum and typically have a thick mesogleam layer. Tentacles are filiform or capitate. Marginal notches with lappets alternate with tentacles around the margin and accomodate sense oragans. They mouth may or may not be on a manubrium. Scyphozoans heve usually no ring canal Polyps produce medusae by asexual budding (strobilation) (Hyman 1940, Mayer 1910).

Hydrozoans- The coelenteron of their representatives lacks a pharynx and mesenteries both in the polyp and medusa stage. Medusae lack rhopalia and usually possess a velum and two nerve rings.The mouth is typically borne on a manubrium. The exoskeleton is usually chitinous and occasionally calcified hydrocorals). Polyps are usually colonial with interconnected coelenterons and are typically polymorphic with individuals specialized in feeding, reproduction, defense or prey capture. Alternation of generations occurs in most hydrozoans with typically asexual benthic polyps alternating with sexual planctonic medusae (Mayer 1910, Schuchert 2009).

Phylum Cnidaria		
Class Anthozoa	**Subclass Hexacorallia**	Order Actiniaria
		Order Antipatharia
		Order Ceriantharia
		Order Corallimorpharia
		Order Scleractinia
		Order Zoanthidea
	Subclass Octocorallia	Order Alcyonacea
		Order Helioporacea
		Order Pennatulacea
Class Cubozoa		Order Carybdeida
		Order Chirodropida
Class Hydrozoa	**Subclass Hydroidolina**	Order Anthoathecata
		Order Leptothecata
		Order Siphonophorae
	Subclass Trachylina	Order Actinulida
		Order Limnomedusae
		Order Narcomedusae
		Order Trachymedusae
Class Scyphozoa	**Subclass Discomedusae**	Order Semaeostomeae
		Order Rhizostomeae
		Order Coronatae
Class Staurozoa		Order Stauromedusae
Class Polypodiozoa		Order Polypodiidae

Table 1. Classification of Cnidaria. Adapted from Daly et al., 2007; Collins et al., 2002; 2006; Raikova, 1988; 2008.

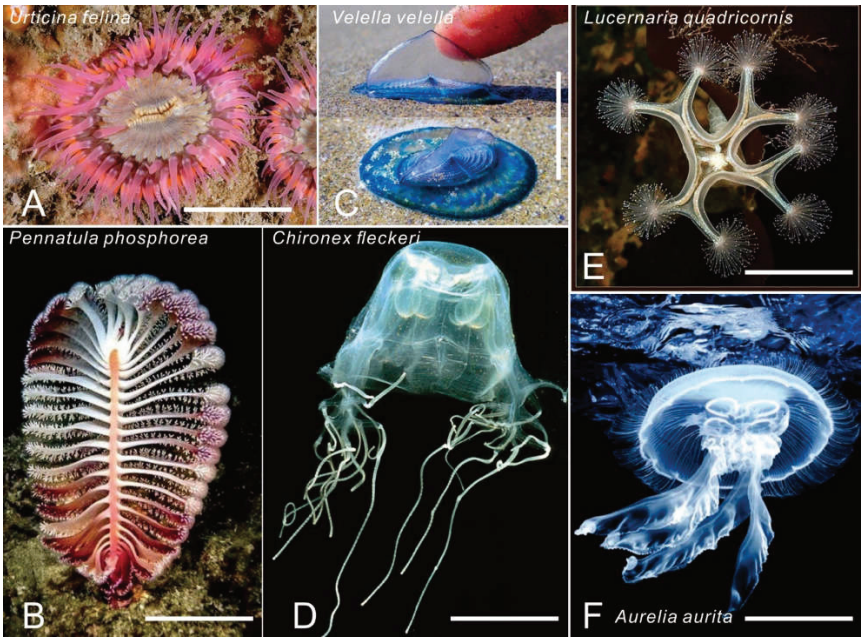

Fig. 17. Representatives of extant cnidarians. A. Anthozoa (Hexacorallia); B. Anthozoa (Octocorallia); C. Hydrozoa; D. Cubozoa; E. Staurozoa; F. Scyphozoa. Scale bars: 2 cm in A, C-E; 5 cm in B; 10 cm in F.

2.1.4 The ancestral cnidarian and phylogenies

It is widely accepted that cnidarians occupy a basal position in the Tree of Metazoa. Cnidarians have a long fossil record of nearly 600 million years if we include some late Precambrian cnidarian-like fossils. Phylogenies based on molecular data and molecular clock hypothesis but incorporating fossil data suggest that cnidarians have a very remote, possibly Cryogenian origin (720-635 Ma) (Erwin et al. 2011, Park et al. 2012). However, these predictions need to be tested by fossil evidence. The nature of the first ancestral cnidarian has puzzled both biologists and palaeontologists until now and several hypotheses have been proposed on the origin of cnidarians.

There are two opposite theories on the origin of cnidarians. The so-called 'medusa theory' is that of (Hyman 1940) who proposed that the ancestral cnidarian was a medusoid form. At the beginning of the 20th century, ctenophores were considered as ancestral to cnidarians in the tree of life (based on morphological and developmental considerations). Hyman suggested that trachyline medusae (cnidaria with only a medusoid stage) probably represented the ancestral cnidarian bodyplan because of numerous resemblances with ctenophores. An alternative so-called 'polyp theory' proposed by (Hadzi 1944, Hadži 1953) suggested that the most primitive cnidarian resembled extant anthozoans but was asymmtrical and the radial symmetry of cnidarians was secondaryly evovled (Hadži 1953, Hadzi 1944, Hand 1959).

Authors generally assume that ancestral cnidarians developed in a similar way as do extant representatives of the group i.e. via a planula larval stage. However this assumption is based on no fossil evidence and lack solid ground. As other soft-bodied

organisms, the planula larvae are prone to decay extremely rapidly after death. Their absence from the fossil record may result from taphonomy biais or may simply indicate that ancestral cnidarians had no planula stage in their developmental cycle. The fact that no phosphatized microfossil resembling the planula larva had been found among the SSF assemblages from the Kuanchuanpu Formation which otherwise contain numerous well-preserved embryos, might support the hypothesis that ancestral cnidarians had no planula stage.

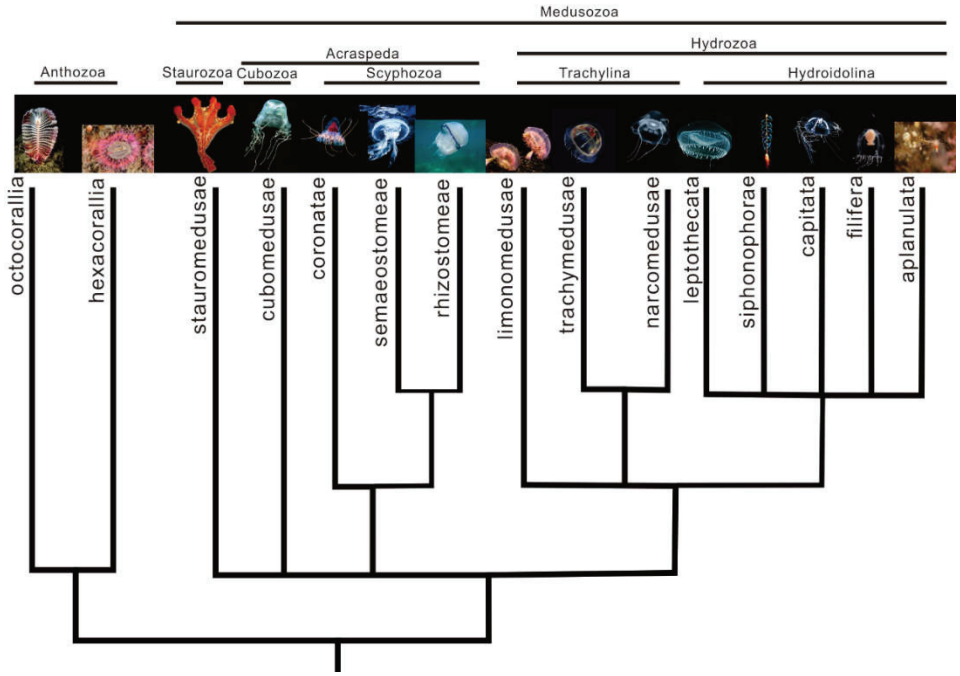

Fig. 18. Possible cnidarian relationships based on molecular and morphological data. Modified from Collins et al., 2002; 2006; Marques & Collins, 2004 and Daly et al., 2007.

According to recent phylogenies based on the molecular analysis, Anthozoa represents the most basal cnidarian lineage (Collins et al. 2006a, Marques and Collins 2004). Anthozoa appears as a monophyletic group (Zapata et al. 2015) with Hexacorallia and Octocorallia as distinct branches. Medusozoa are also monophyletic and comprise the Staurozoa, Cubozoa, Scyphozoa and Hydrozoa (Collins 2002, Collins et al. 2006a, Marques and Collins 2004) (Fig. 18).

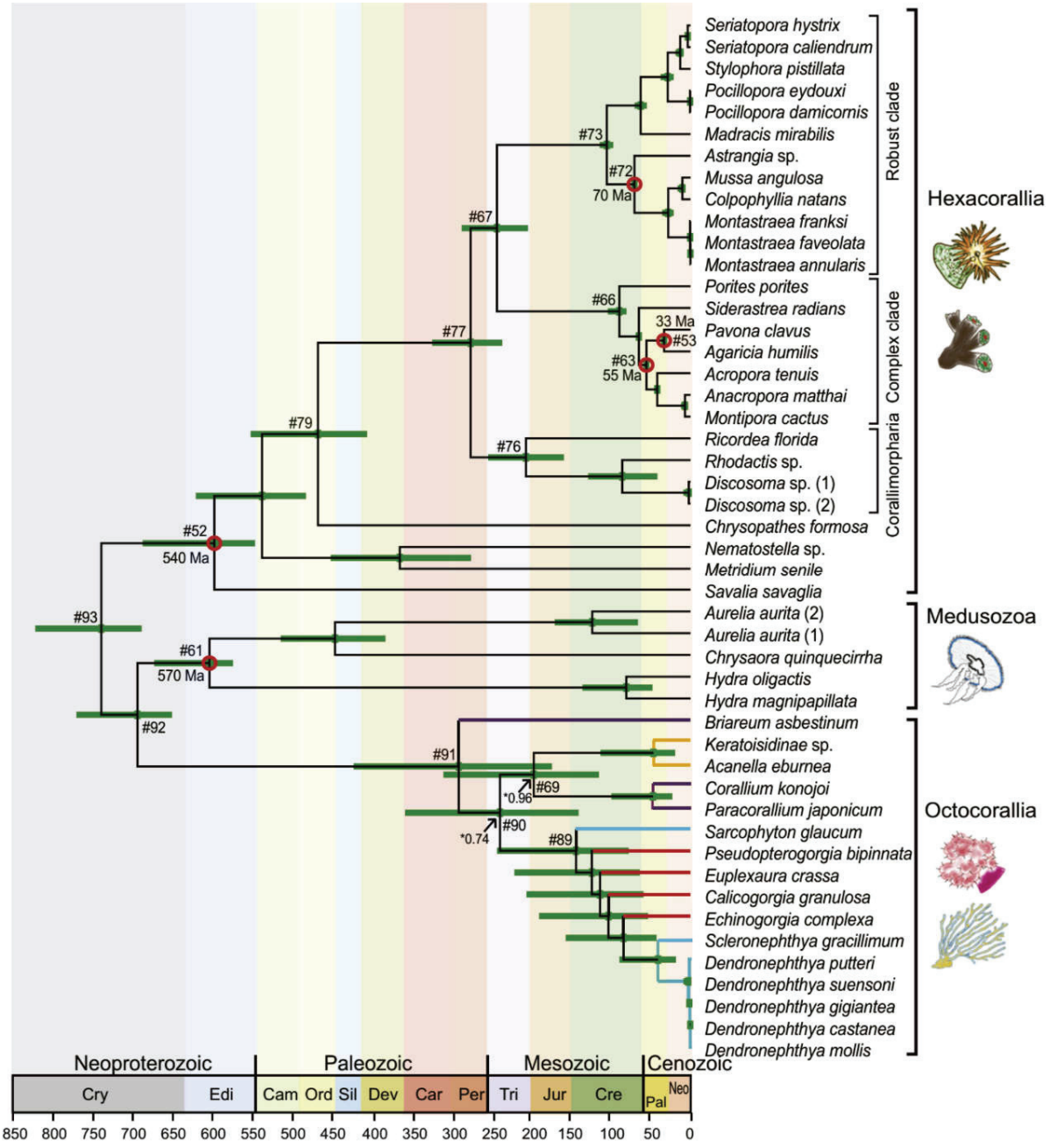

Fig. 19. Diagram on Bayesian estimates of divergence times for cnidarians. From Park et al., 2012.

Park et al. (2012) using data from mitochondrial protein-coding genes and from the fossil record, proposed a chnorology of divergence for cnidarian lineages. According to their scenario Cnidaria is a monophyletic group which may appear in the Precambrian (Cryogenian). Anthozoa appears as the sisiter group of Medusozoa. However, the anthozoan Octocorallia is seems to be closer to Medusozoa than to Hexacorallia (Fig. 19).

Other attempts have been made recently to clarify the cnidarian phylogeny by using fossil data, especially those obtained from the Cambrian Kuanchuanpu Formation. Jian Han and his collaborators assume that several group of extant cnidarians (Cubozoa, etc.) may have had ancestors in the lowermost Cambrian (Han et al. 2013, Han et al.

2016b) (Fig. 20). However these assumed early cnidarians are mostly embryonic forms with no exact counterparts in modern groups.

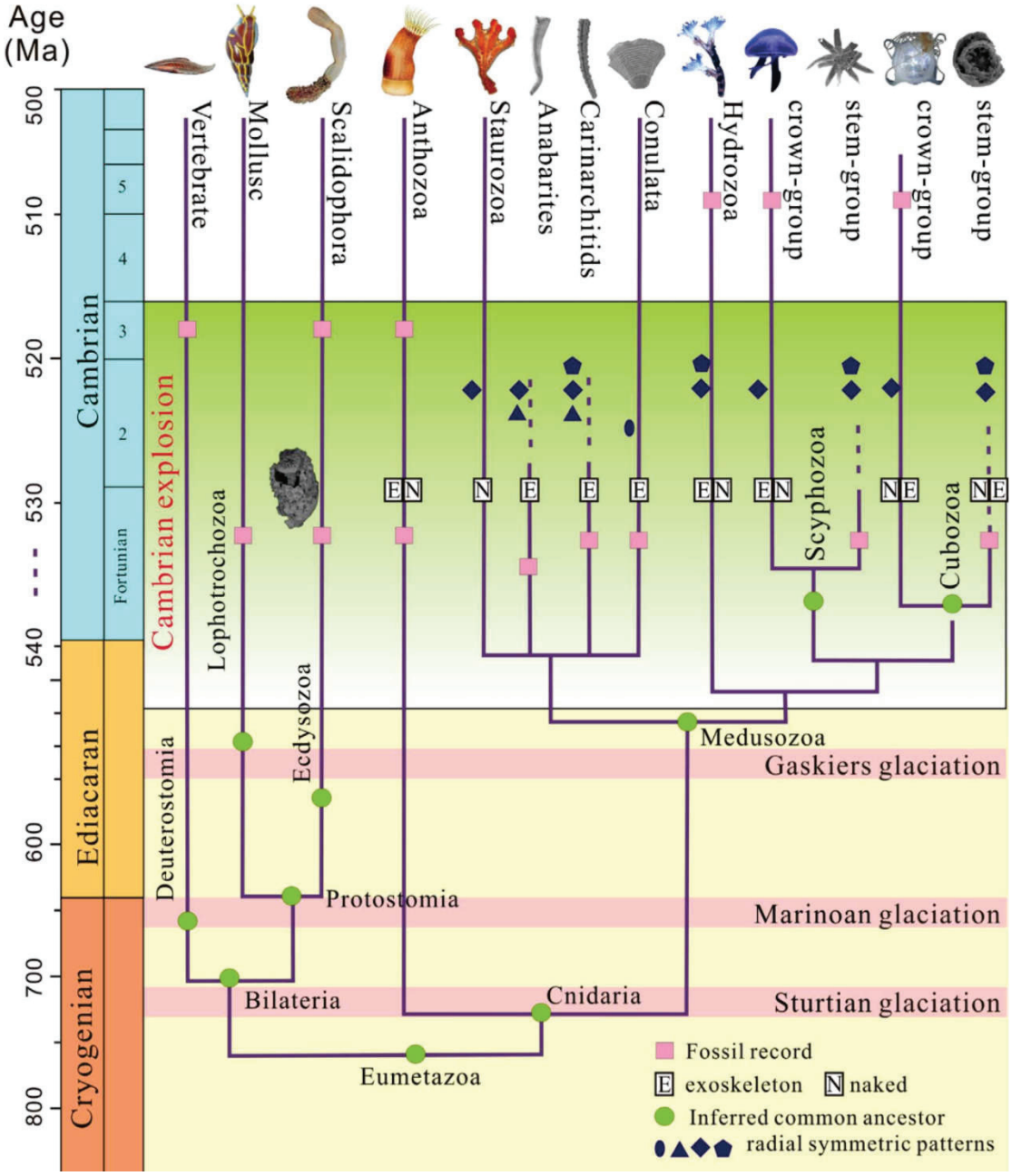

Fig. 20. Possible evolutionary relationships among extant and fossil cnidarians. Based on fossil data from the early Cambrian Kuanchuanpu Formation, Shannxi Province, south China. From Han et al., 2016a.

2.1.5 Ecology

Cnidaria is a huge phylum containing over 10,000 living species (Brusca and Brusca 2003). Except a few species, like *Hydra*, most cnidarians live in marine environments. Usually, the cnidarians have two life phases: the sessile polyp and the free-swimming

medusa. The adult medusae can drift or swim actively in the water freely via muscle contractions. The muscles of cnidarians are derived from their myoepithelial cells (endoderm). There are two muscle categories in cnidarians, the retractor muscles and the circular ones. The former are made of longitudinal fibers along the body axis whereas the circular muscles are concentrated on the bell margin. Contractions of the muscular system can help the bells up / downwards move and keep balance in the water column (Harrison 1991).

Most cnidarians are carnivores (involving the active predation) or suspension feeders (e.g. sea pen). A remarkable exception is *Polypodium hydriforme*, a unique cnidarian adapted to intracellular parasitism inside the oocytes of acipenseriform fish (Raikova 2008). Cnidarians prey on other sea animals such as small fish and crustaceans, even other medusae (Fig. 21), by using their extended tentacles which are lined with venomous cnidae. There is no diffrentiated circulation system in cnidarians. The endodermal (gastrodermal) cilia acid help digest food within the gastrovascular cavity. The undigested wastes are expelled through the mouth. The muscle contractions play a major role in conveying oxygen and nutrients to internal tissues and organs and expelling metabolic wastes (Harrison 1991).

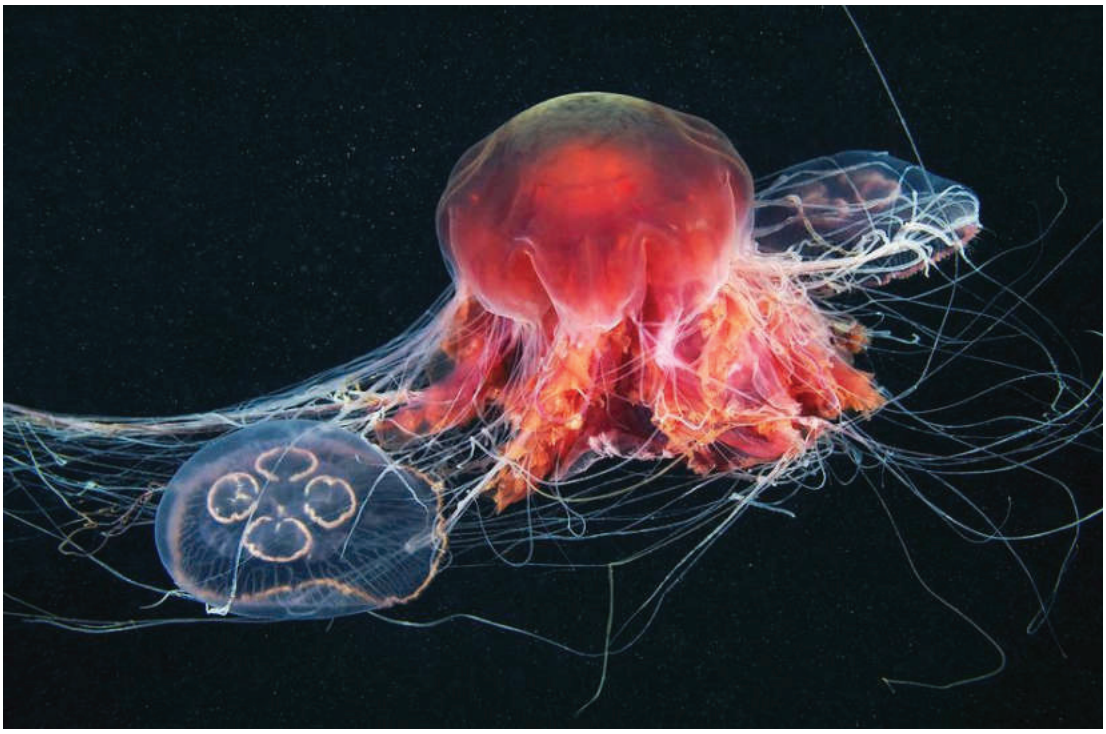

Fig. 21. The Lion's Mane jellyfish (*Cyanea capillata*) feeding on the Moon jellyfish (*Aurelia aurita*). Photograph by Alexander Semenov. https://fineartamerica.com/featured/jellyfish-feeding-alexander-semenov.html

They have no distinct brain. Their neurons are distributed throughout their body and form nerve networks. Most nerve cells in cnidarians are nonpolar and the impulses can travel in either direction along the cell and then up to the whole nerve net. In

general, polyps have no highly developed sensory organ. They cilia-shaped minute structures distributed on their tentacles and around the oral part are sensitive and receive external signals which are conveyed to other body regions. In contrast, other cnidarians such,as box jellyfish (cubozoans) usually have well-developed sense organs (rhopalia) which house a high concentration of epidermal neurons, a pair of chemosensory pits, a statocyst and ocelli (e.g. *Tripedalia cystophora* ; see (Coates et al. 2006)) with visual pigments and two kinds of lens eyes (Fig. 22).

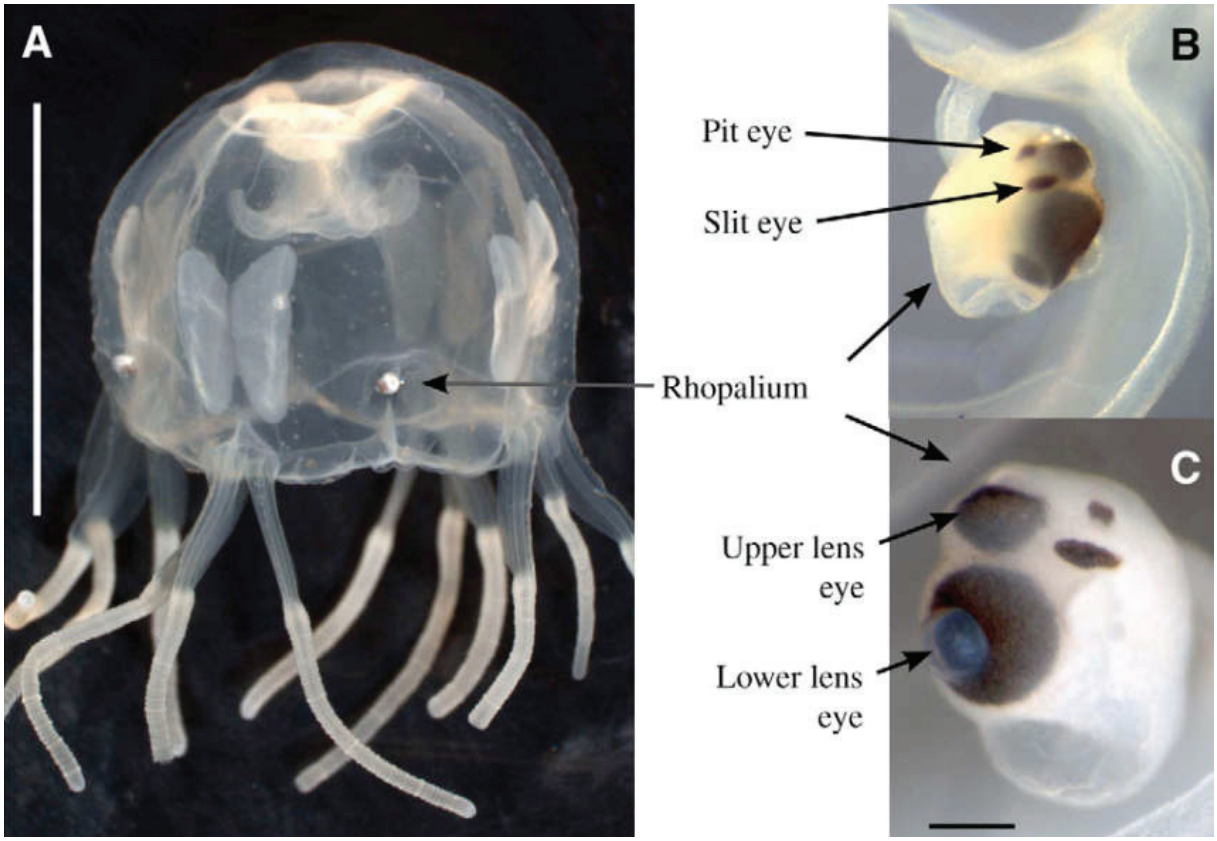

Fig. 22. Eyes in the cubozoan *Tripedalia cystophora*. From Coates et al., 2006.

Bioluminescence (the chemical generation of light) is common in cnidarians (Widder 2010) (Fig. 23).

Fig. 23. Bioluminescence of Moon jellyfish (*Aurelia aurita*).
https://www.petjellyfish.co.uk/shop/live-jellyfish/moon-jellyfish/

The polyps of anthozoans are strenghtened by a cuticular layer made of protein, such as chitin, which may be thin and flexible or thick and rigid. In corals, the cuticle secretes calcium carbonate (Harrison 1991). After death, the cuticle is degraded by microorganisms. Except its calcified part which resists to decay. Eventually, reefs formed by generations of organisms (Fig. 24) create a variety of habitats for other marine organisms which will find sufficient nourishment in this new ecosystem.

Fig. 24. Coral reef ecosystem. From www.tripplus.tw/blog/.

Cnidarians are diploblastic metazoans with a primary radial symmetry, which occupy a basal position in the animal tree. Most of them are dimorphic and assume two markedly different morphologies and ecologies during their life cycle, a polypoid stage and a medusoid stage. Phylogenies based on molecular data resolve Anthozoa as the most basal cnidarian lineage, and as the sister group of Anthozoa, the Medusozoa consisting of the Staurozoa, Scyphozoa, Cubozoa and Hydrozoa. Although their internal organizatio is relatively simple compared with that of bilaterian animals (e.g. lack of cephalization and circulatory system), numerous cnidarians have sophisticated sensory organs and feed on other animals via predation involving specialized stinging and adhesive structures.

2.2 Fossil cnidarians

Molecular data obtained via genomic comparisons between extant species using molecular clock phylogenetic methods have led to evolutionary scenarios that predict the chronology of divergence of major animal groups, including cnidarians (Erwin et al. 2011). These estimates often suggest that the origin and earliest diversification of cnidarians occurred during the Ediacaran (*ca*. 541-635 Ma) and possibly even earlier in the Cryogenian (*ca.* 635-720 Ma), many tens of millions of years before their first appearance in the fossil record (Park et al. 2012). This discrepancy deeply questions the validity of these molecular models and requires testing from fossil evidence within the geological time frame that preceded the "Cambrian Explosion". Obtaining new and accurate fossil evidence concerning this critical period is vital for improving our knowledge of the early steps of cnidarian evolution and an essential requirement for calibrating molecular models. We are reviewing here possible cnidarian occurrences in the Precambrian and Cambrian periods from previous work.

2.2.1 Precambrian

Some fossils from the late Precambrian (Ediacaran) of various regions have been tentatively assigned to cnidarians. However, their affinities remains uncertain and controversial (Glaessner and Wade 1966, Wade 1972, Ford 1958).

Typically, the frond-like organism (rangeomorph) *Charnia* from England and Australia (*ca.* 560 Ma), was first interpreted as the giant algae, and then assigned to pennatulacean hydrozoans (sea pens), on the basis of its bilateral series of lobate fronds attached to a central stalk and a disc-shaped holdfast (Ford 1958, Ford 1999, Glaessner and Wade 1966). However, detailed comparisons show that the morphology of the *Charnia* is hardly comparable with that of pennatulaceans. *Charnia* consists of a series of parallel, sigmoidal to rectangular primary branches which display an alternating pattern along the central axis. In spite of appearances, *Charnia* is not a bilateral organism *sensu stricto*. Extant pennatulaceans, usually less than 2 cm in length, grow from a single unornamented polyp anchored into soft sediment via a muscular peduncle. Then numerous secondary polyps branch off from this initial polyp (Williams 2011) (Fig. 25). Rangeomorphs have four branching styles: *Arborea*-type, *Charnia*-type, *Rangea*-type and *Swartpuntia*-type (Laflamme and Narbonne 2008) (Fig. 26 a (1-4)). All characterized by a modular and fractal growth which has no counterpart in extant pennatulaceans and cnidarians in general (Xiao and Laflamme 2009).

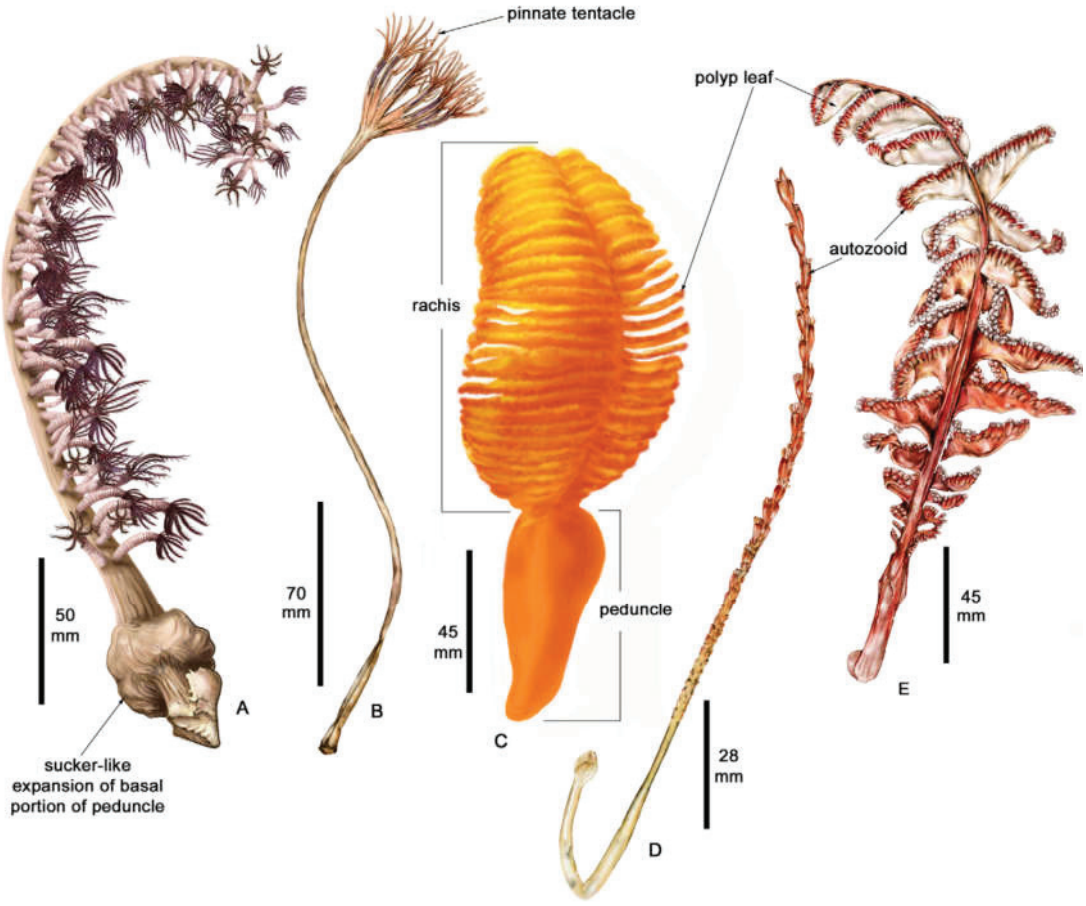

Fig. 25. Extant pennatulacean hydrozoa. From Williams, 2011.

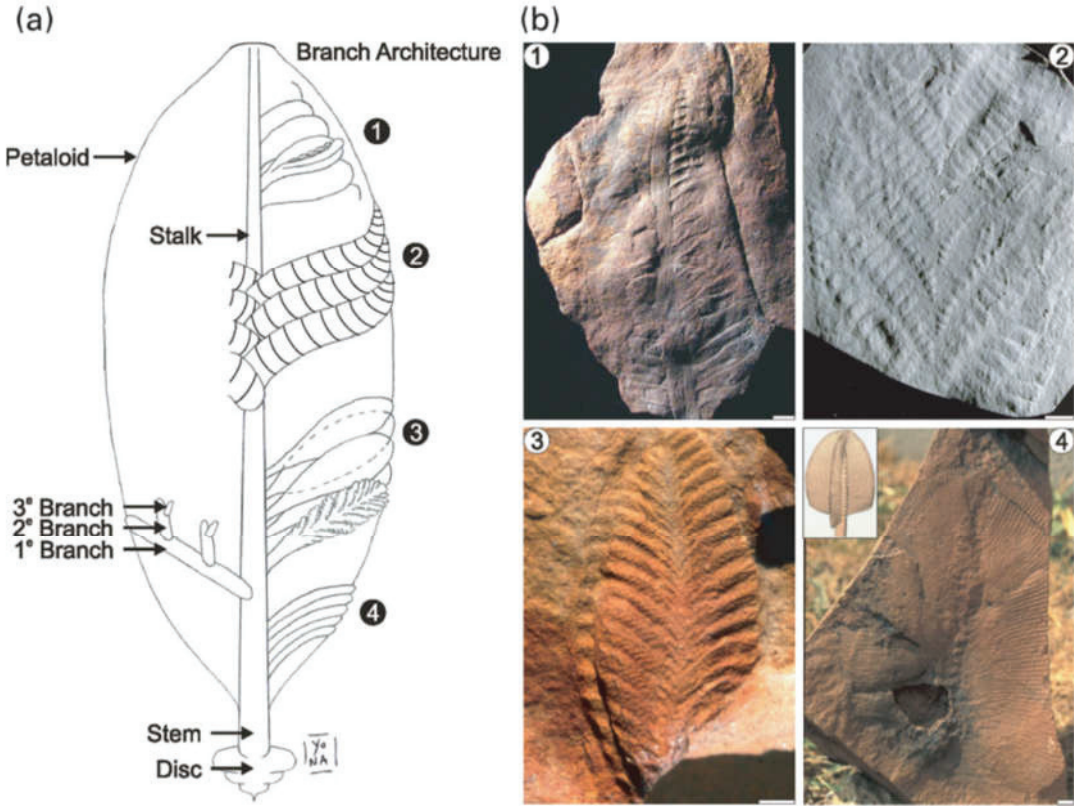

Fig. 26. Modular and fractal growth in Ediacaran rangeomorphs. a. simplified diagram showing the distribution of fronds along the central axix. b. Photographs showing the four branching types found in rangeomorphs. 1-4 represent *Arborea*-type, *Charnia*-type, *Rangea*-type and *Swartpuntia*-type, respectively. From Laflamme and Narbonne, 2008.

Conulariids are extinct cone-like organisms with early representatives in the late Precambrian and the Cambrian (Fig. 27). They have been tentatively assigned to various group of extant animals such as the Mollusca, Hemicordata and Cnidaria (Babcock and Feldmann 1986, Feldmann and Babcock 1986). However, discussions on the affinities of conulariids are severely limited because of the lack of information concerning their soft anatomy. More recent phylogenetical studies which combine morphological and molecular data (Van Iten 1991a, Van Iten 1991b, Van Iten 1992a, Van Iten 1992b, Van Iten et al. 2005a, Van Iten et al. 2005b, Van Iten et al. 2006, Van Iten et al. 2014) come to the conclusion that conulariids may belong to scyphozoan cnidarians, based on two supposed common features. The closely-spaced transverse ridges on the theca of conulariids recalls the segmented pattern of the stephanoscyphistoma of coronate polyps (Fig. 28). The perradial teeth-like projections on the inner surface of conulariids is reminiscent of comparable features in the coronate exoskeleton (Jarms 1991, Ivantsov 2017) (Fig. 27).

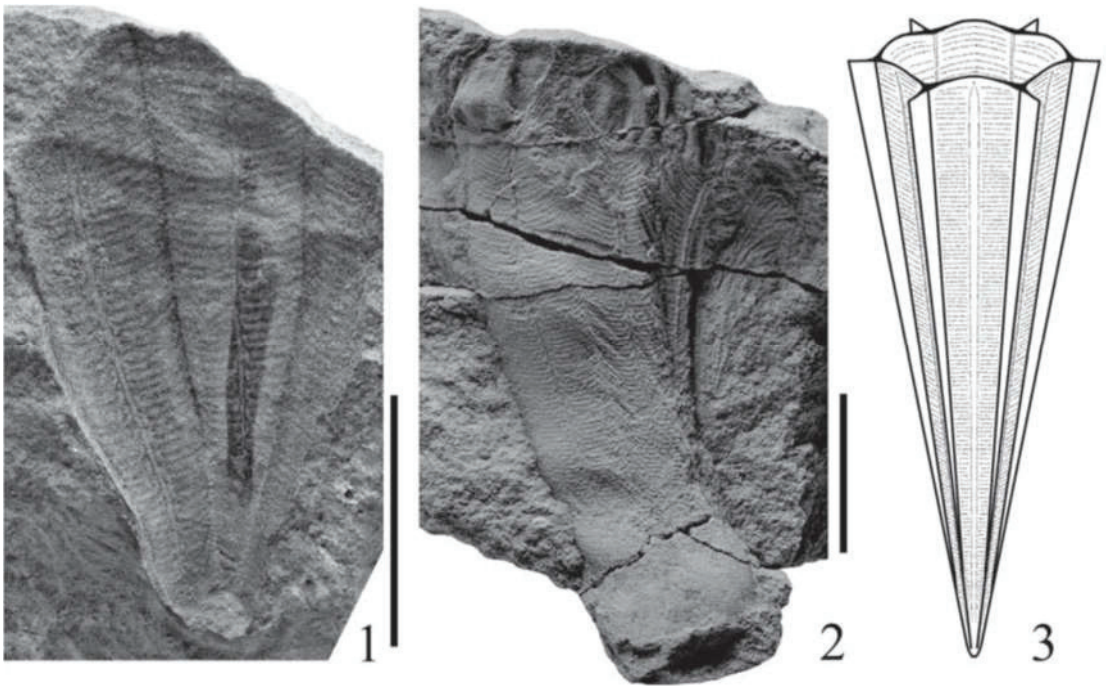

Fig. 27. Theca of *Vendoconularia triradiata* Ivantsov et Fedonkin, 2002 from the Ediacaran Ust'-Pinega Formation (*ca.* 560 Ma), the White Sea region, north of Russia. From Ivantsov, 2017.

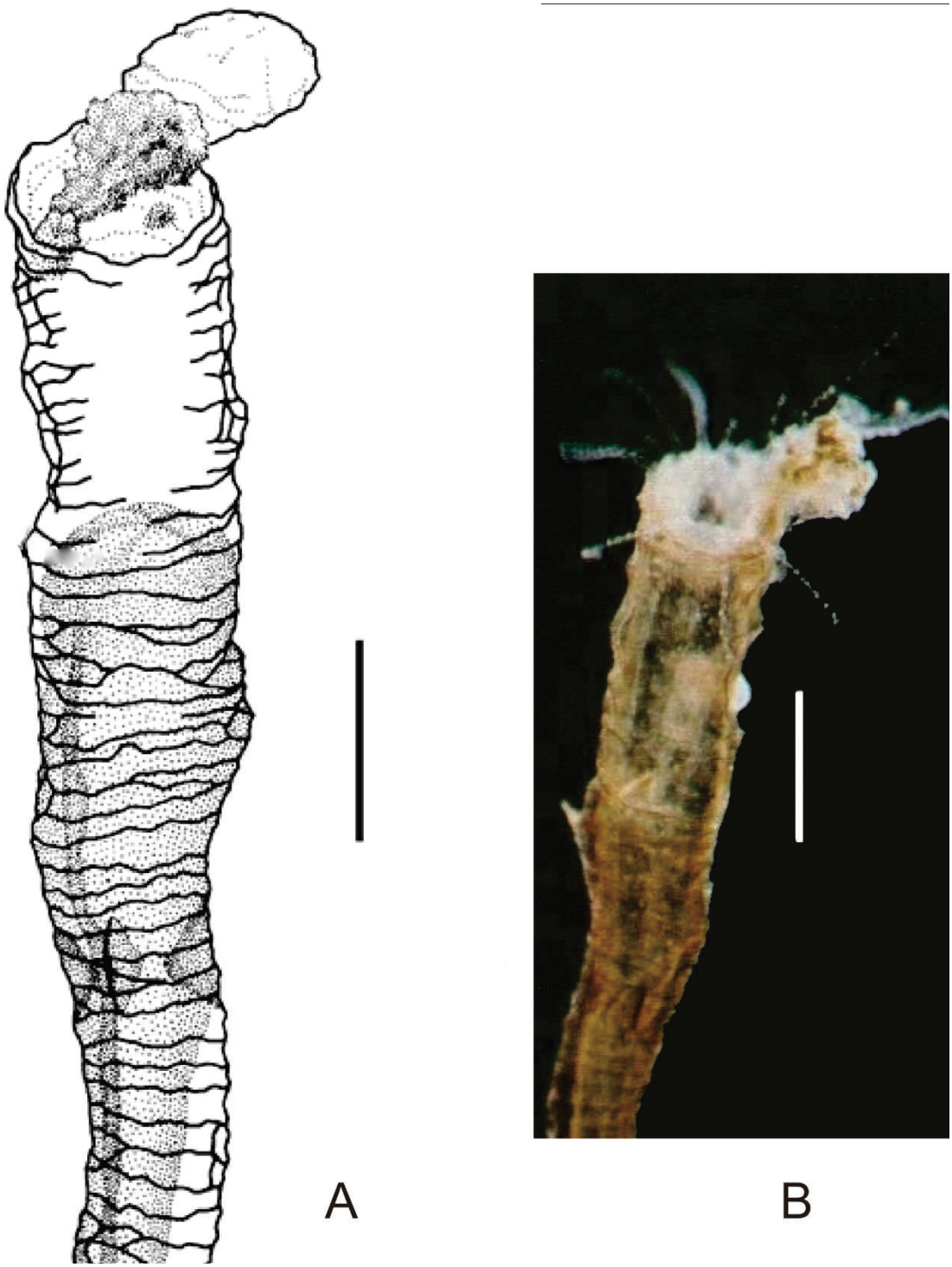

Fig. 28. A. Stephanoscyphistoma of *Nausithoe aurea* (coronate scyphozoan) from subtropical western South Atlantic waters (São Paulo State, Brazil; general drawing and proximal part. Scale: 0.3 mm (modified from (Silveira 2002)).

Corumbella is another supposed cnidarian from the Late Neoproterozoic of Brazil (Hahn et al. 1982, Babcock et al. 2005, Hagadorn and Waggoner 2000, Fairchild et al. 2012, Warren et al. 2012). It is characterized by narrow elongated tubes bearing transverse and evenly distributed ribs or ridges, a tetramerous symmetry and four

faces with a central midline. *Corumbella* show external resemblances with the periderm of coronate polyps such as *Nausithoe aurea* (Figs. 28-30).

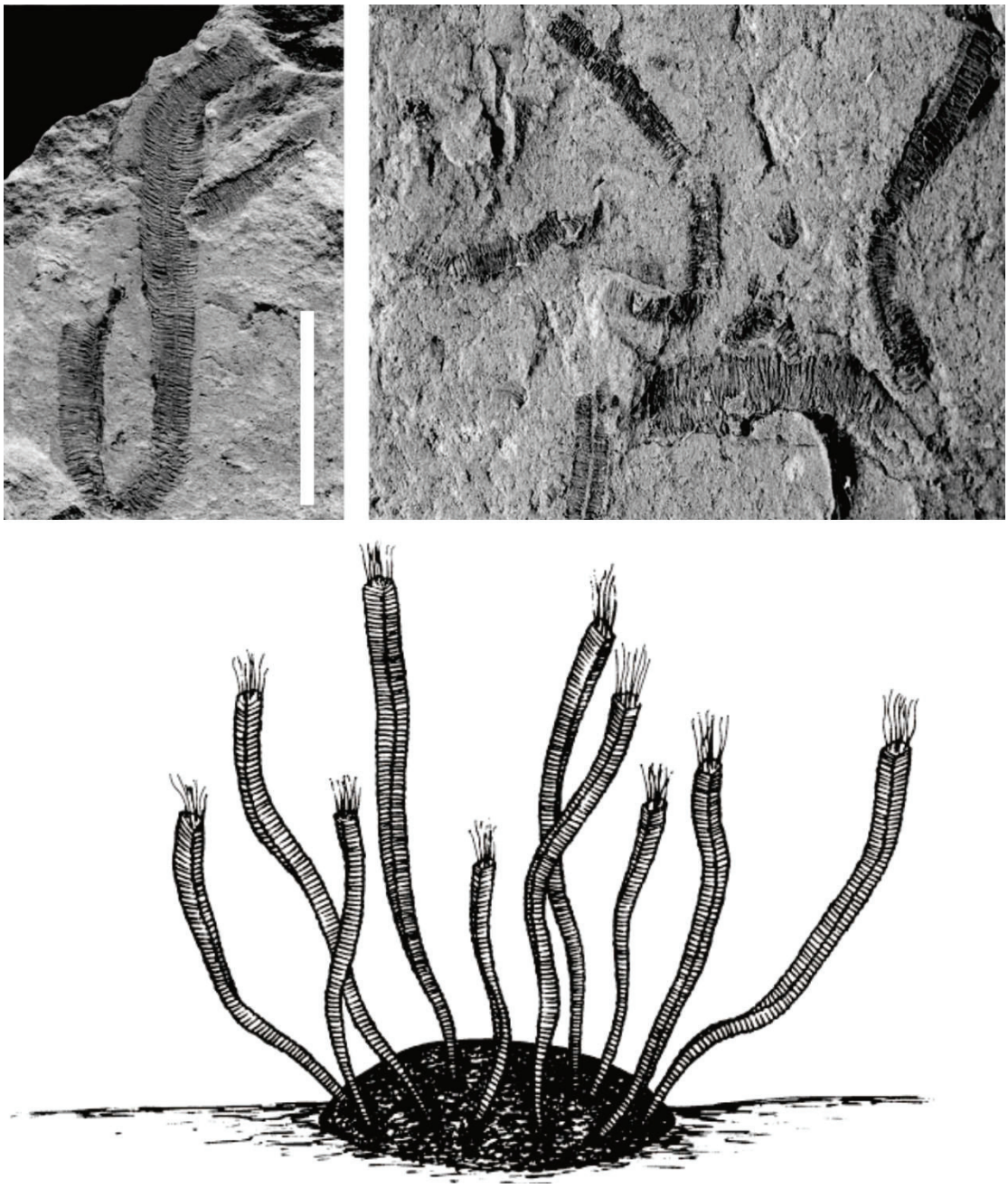

Fig. 29. *Corumbella werneri* Hahn et al., 1982, from the Itau´ quarry (Ediacaran; *ca.* 600 Ma), Lada´rio, Brazil; hotographs and reconstruction. Scale bar: 50 mm. From Babcock et al., 2005.

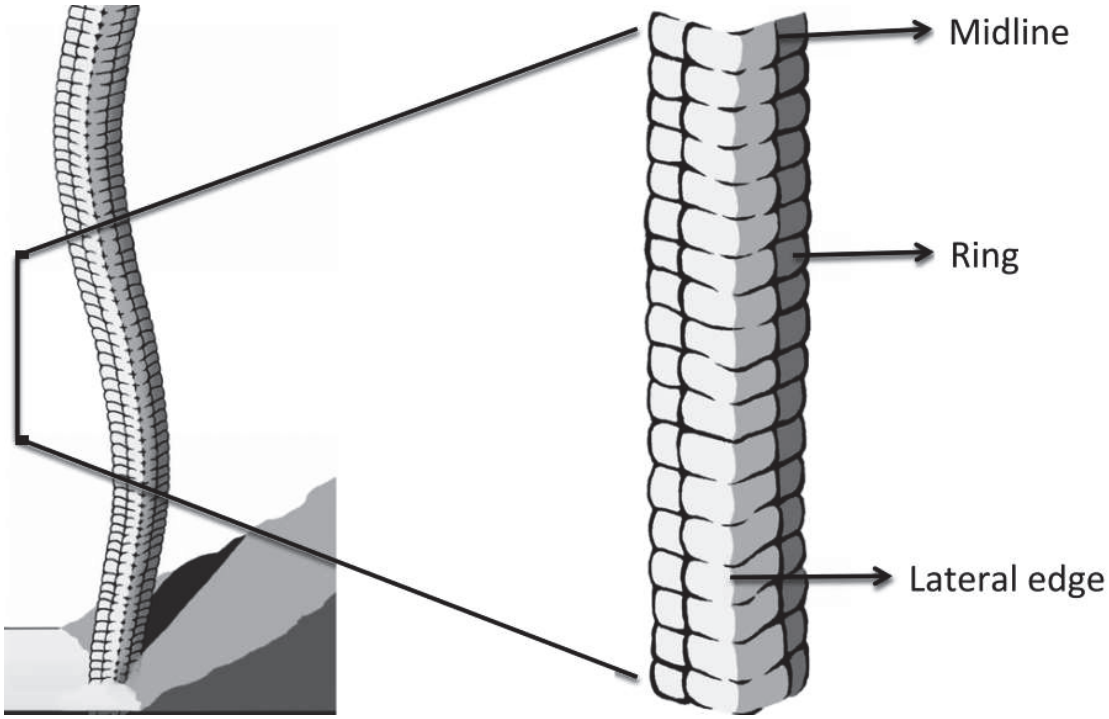

Fig. 30. Corumbella werneri, morphological details (from Van Iten et al., 2014).

Van Iten et al. (2014) noted external resemblances with coronate polyps and suggested possible affinities with scyphozoans (Fig. 31). However, the lack of information on the soft anatomy of *Corumbella* make these interpretations highly debatable.

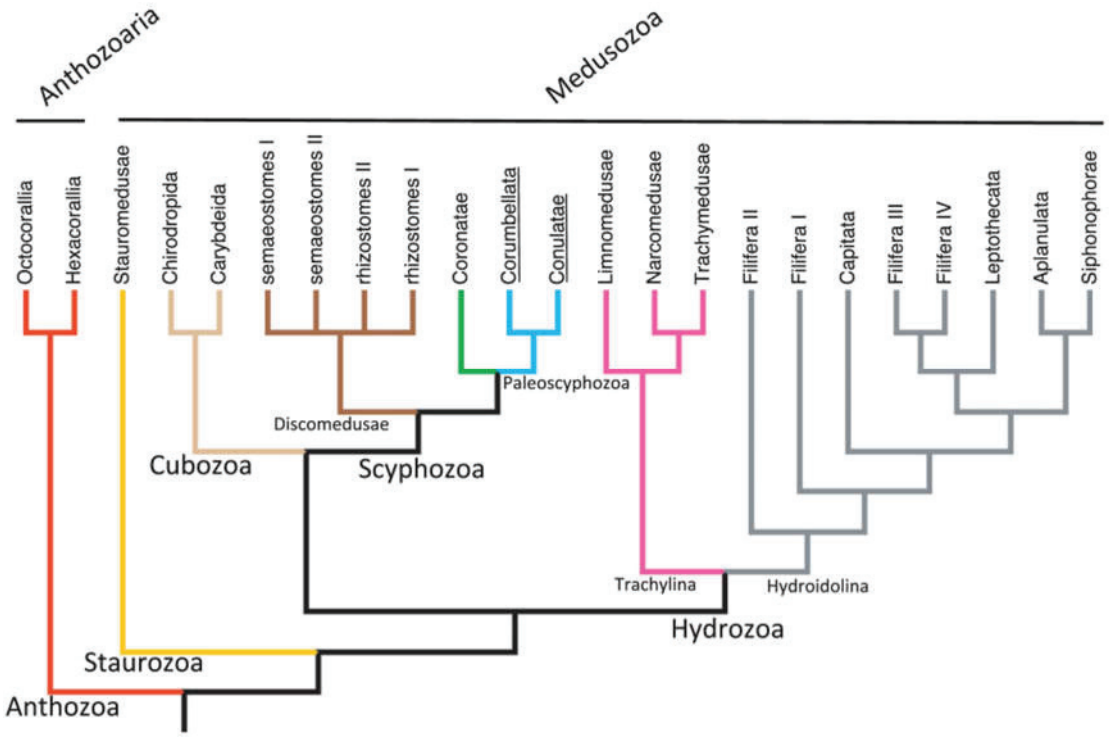

Fig. 31. Possible phylogenetic tree of Cnidaria. *Corumbella* and *Conulatae* (underlined; see (blue branches) show close relationships with Scyphozoa (from Van Iten et al., 2014).

Haootia quadriformis is another cnidarian-like fossil from the Ediacaran lower part of the Fermeuse Formation (*ca.* 560 Ma) of Newfoundland, eastern Canada which displays well-preserved body features imprinted in sediment, such as numerous closely spaced wrinkles interpreted as the remains of possible coronal muscles (Liu et al. 2014a, Liu et al. 2015) (Fig. 32). This led Liu et al. (2014a) to consider *Haootia* as a possible cnidarian close to staurozoans. However, extant medusozoans are known to possess longitudinal and circular muscles that are hardly comparable with the supposed muscular traces of the Ediacaran form (Miranda 2015). Moreover, the hypothetical presence of strong coronal muscles in *Haootia* appears to be poorly consistent a sessile lifestyle. No tentacle clusters typical of extant staurozoans occur in *Hootia*. This deeply questions the interpretations proposed by Liu et al. (2014a).

Fig. 32. *Haootia quadriformis* Liu et al., 2014 from the Ediacaran lower Fermeuse Formation (*ca.* 560 Ma), Bonavista Peninsula, Newfoundland, in Canada. Photograph of the holotype and reconstruction. Scale bar: 50 mm. Modified from Liu et al., 2014.

Cloudina is one of the oldest biomineralizing metazoans. This tubular fossil was first described by from specimens (Germs 1972) found in *ca.* 600 Ma-old limestones of the Nama Group in southwest Africa. Further accounts gave more detailed descriptions of *Cloudina* from the Dengying Formation (*ca.* 550 Ma) of the Shaanxi Province, south China (Hua et al. 2005, Cai et al. 2014) (Fig. 33 1), especially the microstructure of its tubular biomineralized exoskeleton (‘funnel in funnel’ structures; Fig. 33 2-4) and the asexual dichotomous growth mode of its exoskeleton with parent and daughter tubes communicating between each other. Some extant annelids such as serpulitiids secrete comparable tubes of calcium carbonate in which the animal withdraw. For example, *Salmacina amphidentat* reproduces asexually by growing its calcareous tube from a single bud (Pernet 2001, Vinn and Zaton 2012). There are two major differences between *Cloudina* and Serpulitiidae 1) the tube of serpulitiids bears a peristome (opening) anteriorly and a tiny opening in its basal part (Taylor and Vinn 2006) whereas

that of *Cloudina* has a closed rounded base (Hua et al. 2005); 2) tube dichotomy is unknown in serpulids (Vinn and Zaton 2012) (Fig. 33).

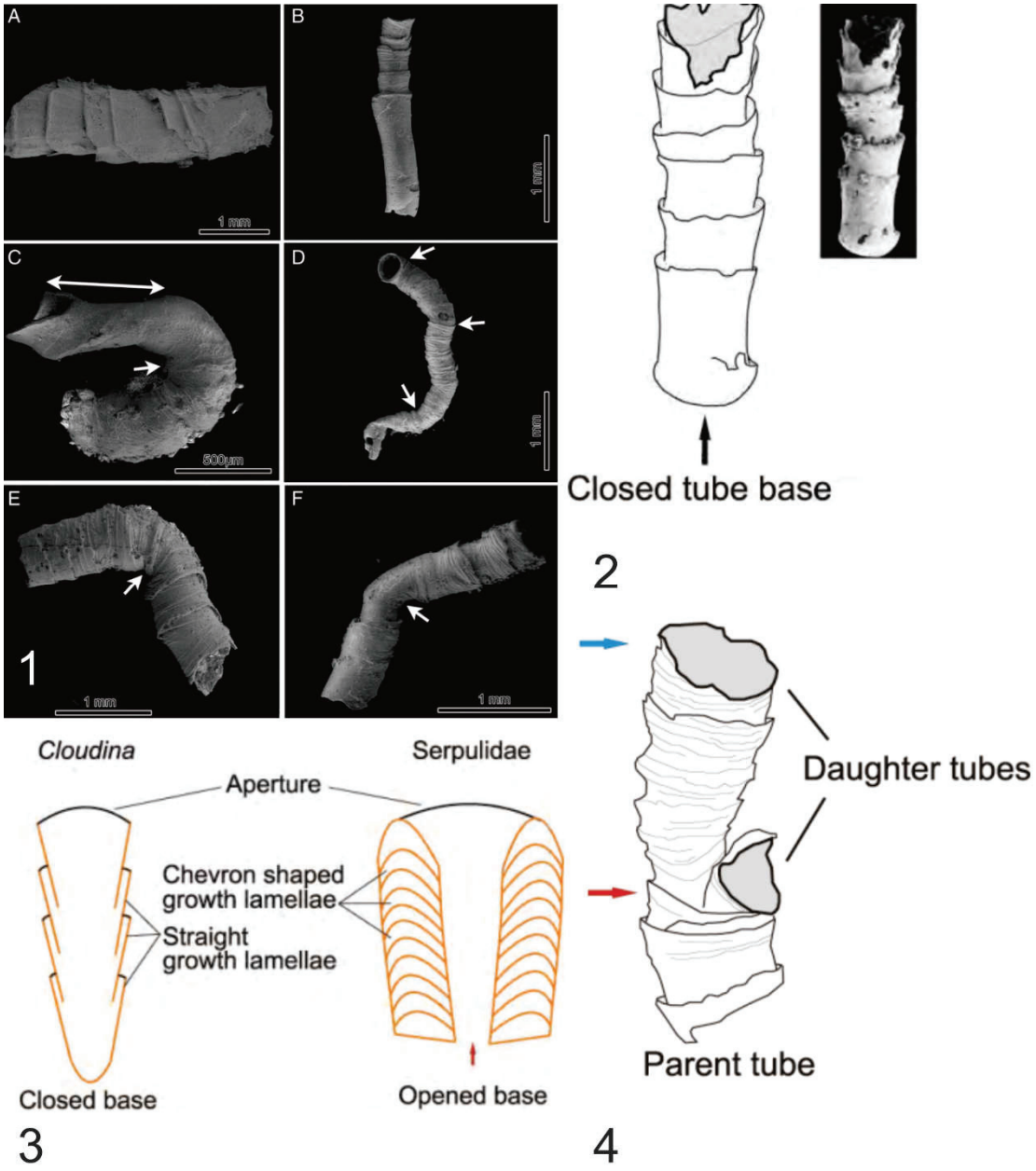

Fig. 33. *Cloudina.* 1. Specimens from the Gaojiashan Member, Dengying Formation (*ca.* 550 Ma), Lijiagou section, Shaanxi Province, south China. 2. Reconstruction of basal part. 3. Growth modes of *Cloudina* and extant Serpulitiidae. 4. Dichotomous branching in Cloudina. Modified from Cai et al., 2014; Vinn and Zaton, 2012.

Vinn and Zaton (2012) proposed an alternative hypothesis and regarded *Cloudina* as a possible cnidarian. As for the annelid option, the arguments set out in their study are weak, being based on superficial resemblances such as 1) the dichotomous branching mode; 2) the closed tube base; 3) the rapid growth ratio of both the parent and daughter tubes (Vinn and Zaton 2012).

In summary, several enigmatic groups of fossil organisms superficially resembling cnidarians have been found and described in the late Precambrian. These are mostly conical and tubular forms or frond-like organisms. Because of the lack of diagnostic features and detailed information on their soft anatomy, there are considerable uncertainties concerning their relationship with any extant cnidarian lineage. None of these forms closely resembles extant polyps and medusae.

2.2.2 Cambrian

2.2.2.1 Lowest Cambrian Kuanchuanpu biota

The microfossils from the Kuanchuanpu Formation (*ca.* 535 Ma) are phosphatized and preserved in three dimensions. They have been assigned to various groups of animals including cnidarians. The diversity and affinities of these possible cnidarians is the focus of the next chapters (Chapters 3 and 5).

2.2.2.2 Early Cambrian Chengjiang biota

The oldest occurrence of unambiguous cnidarians comes from the early Cambrian (*ca.* 521 Ma) Chengjiang biota which contains fossil jelly-fish resembling modern ones.

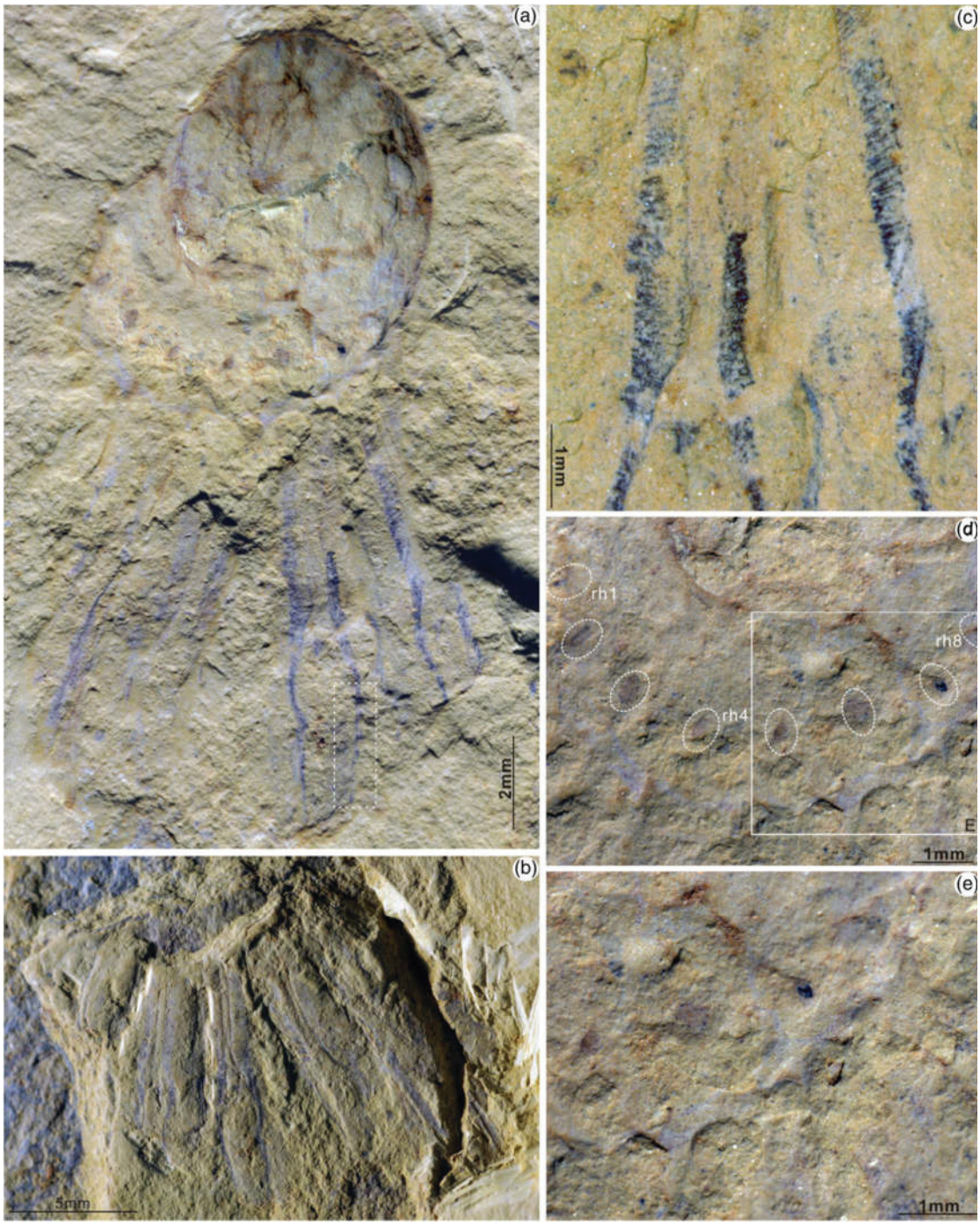

Fig. 34. *Yunnanoascus haikouensis* Hu et al. (2007), the oldest fossil jellyfish from the early Cambrian Chengjiang Lagerstätte, China. From Han et al., 2016c.

Yunnanoascus haikouensis closely resembles modern medusa. It has a tetramerous symmetry, sixteen rhopalia, sixteen pairs of long tentacles around the bell margin, a possible manubrium in the central part of the bell (Han et al. 2016a) (Fig. 34).
Yunnanoascus haikouensis Hu et al. (2007) was formerly interpreted as a crown group Ctenophora based on its 16 tentacles mistakenly interpreted as comb-rows (Hu et al. 2007).

Xianguangia sinica Chen and Erdtmann, 1991 in (Chen 1991) is found from the lower Cambrian Chengjiang biota, which is diagnosed by the sophisticated, feather-like tentacles surrounding the oral part, a column covered with the longitudinal external ridges, a circumferential constriction connected to the column and the holdfast (Hou et al. 2017). *X. sinica* recently is revised by Ou et al., (2017) consisting with the previous assumed affinity that it is a sister group of extant anthozoans based on the phylogenetic analysis and it is a suspension feeder (Ou et al. 2017) (Fig. 35).

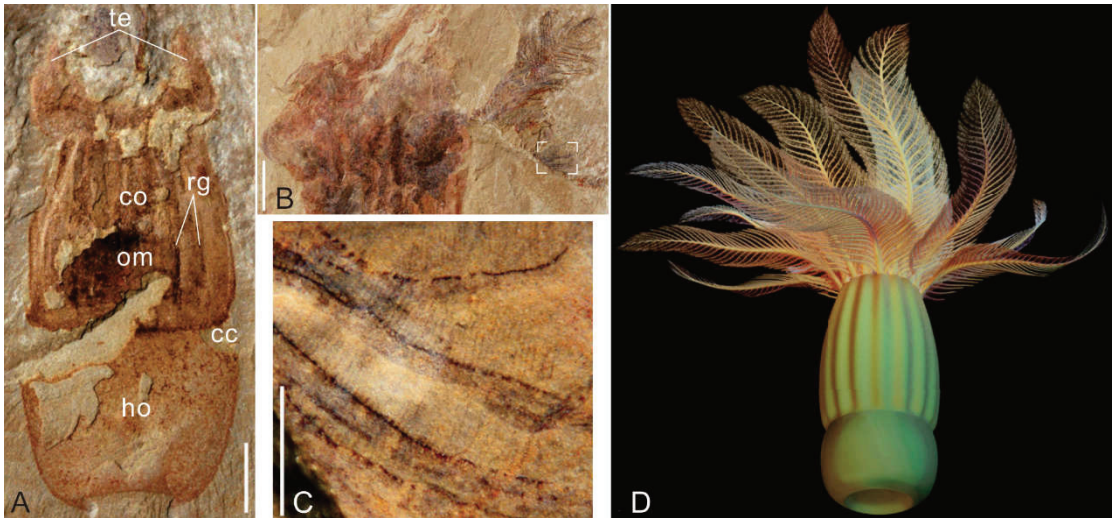

Fig. 35. *Xianguangia sinica* Chen and Erdtmann (1991), from the lower Cambrian (Series 2, Stage 3) Chengjiang biota. A. Specimen ELEL-SJ120379 showing column (co) with external ridges (rg) and internal dark remains (om, organic material), circumferential constriction (cc), holdfast (ho) and tentacles (te). B. Tentacle architecture of specimen ELEL-SJ080827B showing numerous pinnate tentacles. C. Zoomed area in B. D. Reconstruction of *X. sinica.* Scale bars: 2 mm in A; 10 mm in B; 1 mm in C. Modified from Ou et al., 2017.

Archisaccophyllia kunmingensis Hou et al., 2005 is another sessile fossil organisms which is suspected to close to the Anthozoa. It is diagnosed by a cylinder-shaped body covered the longitudinal ridges, the possible extending tentacle surrounding the oral disc, and a pedal disc (Hou et al. 2005, Hou et al. 2017) (Fig. 36). However, some authors reinterpreted it as a stem phoronid (horseshoe worm) with actinotroch-like larval characters (Zhang and Holmer 2014).

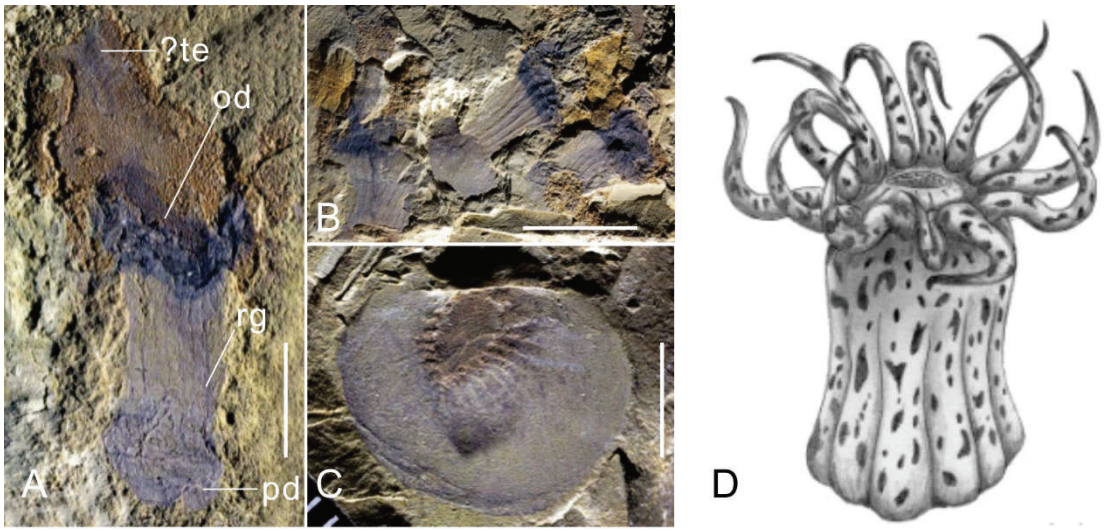

Fig. 36. *Archisaccophyllia kunmingensis* Hou et al., 2005, from the lower Cambrain Chengjiang biota. A. Specimen YKLP 13828 showing the possible tentacles (te) surrounding the oral disc (od), external longitudinal ridges (rg) and the pedal disc (pd). B. Specimen YKLP 10382-84 showing the colony of *A. kunmingensis*. C. Specimen YKLP 10165, longitudinal compressed direction showing a possible pharynx of *A. kunmingensis*. D. Reconstruction of *A. kunmingensis*. Scale bars: 0.5 cm. Modified from Hou et al., 2005; 2017.

2.2.2.3 Middle Cambrian

The jellyfish from the middle Cambrian Marjum Formation (*ca.* 505 Ma), Utah, USA are preserved in fine-grained dark grey mudstone. They provide very detailed and high-resolution information on the overall shape of medudae (bell, tentacles), coronal muscles and microstructures on the surface of tentacles, exumbrella and subumbrella. (Cartwright et al. 2007) (Fig. 37). The authors assigned these remarkably preserved jelly fish to extant lineage of crown group Medusozoa such as semaeostomeae and coronate scyphozoans, cubozoans and hydrozoans.

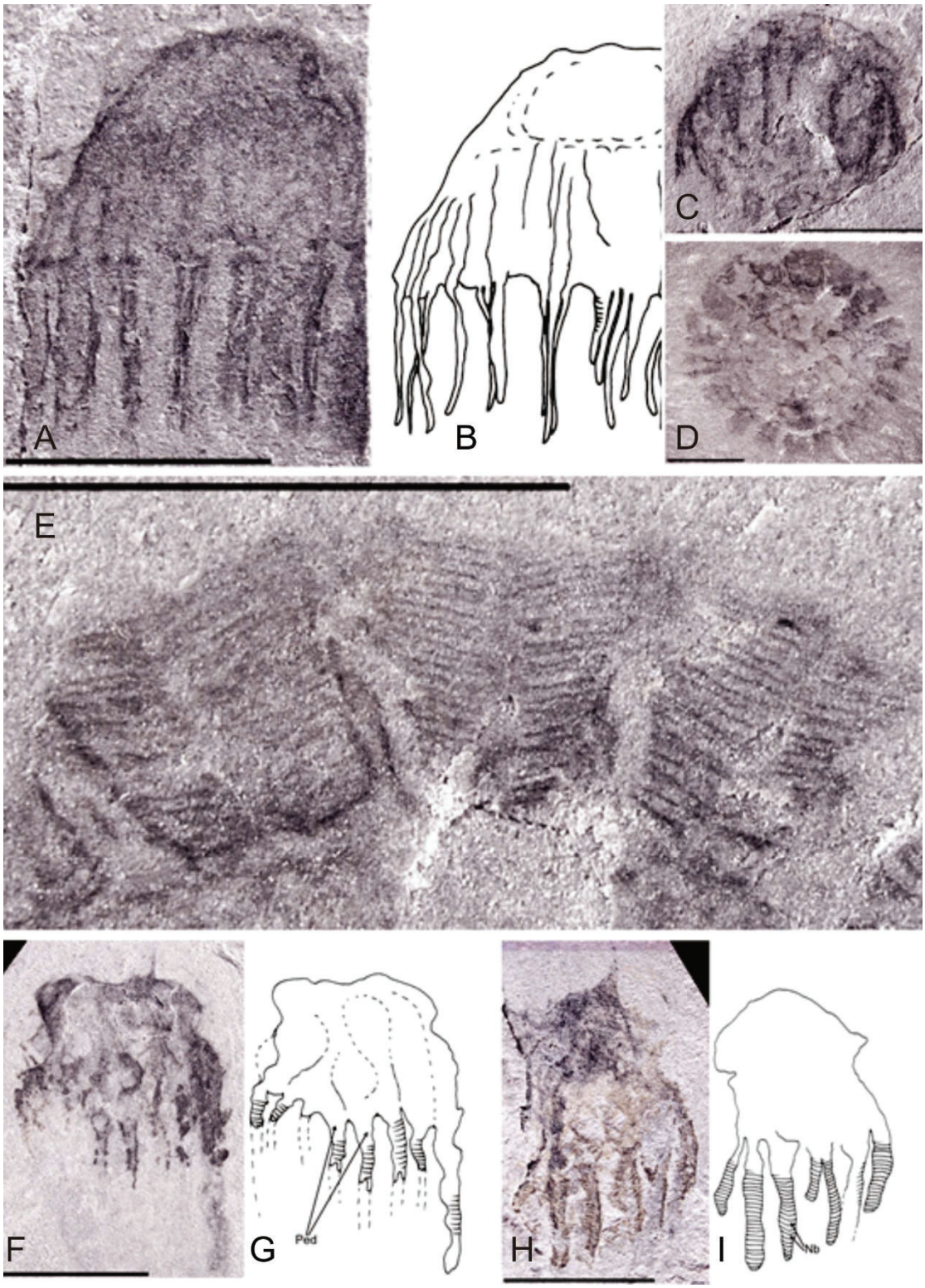

Fig. 37. Fossil jellyfish from the Marjum Formation in the middle Cambrian, Utah, USA. A-C. Fossil jellyfish possible referable to Narcomedusae, Hydrozoa. D. Fossil jellyfish possible referable to Semaeostomeae, Scyphozoa. E. Enlargement of the radially arranged coronal muscles. F-I. Fossil jellyfish possible referable to Cubozoa. Scale bars: 5 mm. Modified from Cartwright et al., 2007.

2.2.2.4 Post Cambrian medusae

Sporadic fossil cnidarian medusae occur in post-Cambrian deposits such as the late Ordovician Stony Mountain Formation (Williams Member) of Manitoba, Canada. These post-Cambrian fossils exhibit a wide range of soft-bodied structures such as the ex- and subumbrellae, manubria, tentacles, stomachs and radial canals (Young et al. 2007, Young and Hagadorn 2010) (Fig. 38), that were mineralized by calcium carbonate or pyrite, At least three extant classes of cnidarians the scyphozoans, cubozoans and hydrozoans, appear to be represented in the post-Cambrian fossil record. A large number of exceptionally preserved fossil medusozoans are known from the late Carboniferous Mazon Creek Lagerstätte of Illinois, USA (Young and Hagadorn 2010) (Fig. 38 E-H). Abundant well-preserved jellyfish impressions have been described from the late Jurassic Cerin Lagerstätte (lithographic limestones; Ain, SE France) indicating the presence of scyphozoans and cubozoans (Gaillard et al. 2006).

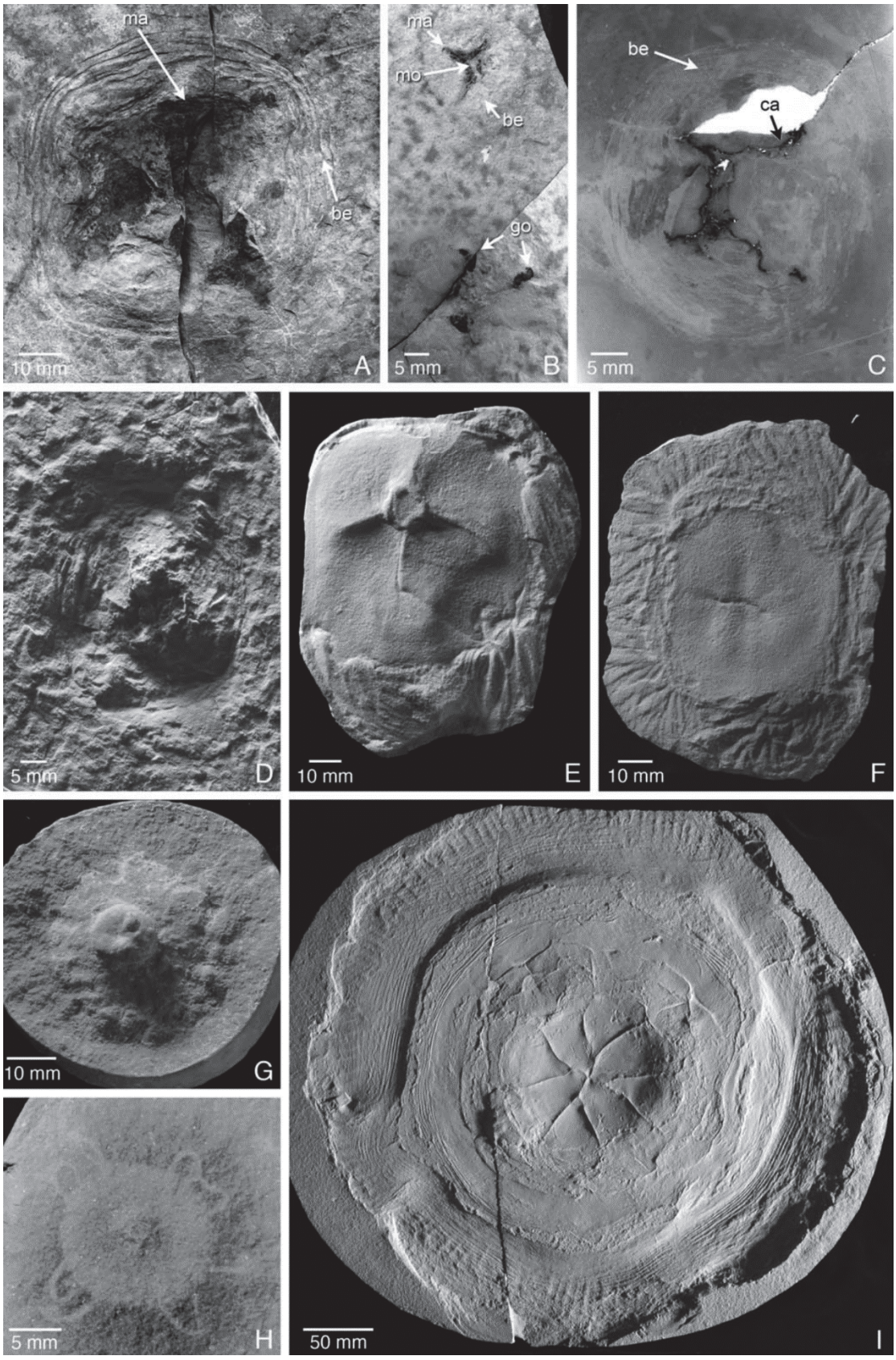

Fig. 38. Post-Cambrian medusozoans. A-C. Possible hydrozoans from the late Ordovician (Richmondian) Williams Member, Stony Mountain Formation, William Lake, Manitoba, Canada. D Possible scyphozoan from the same locality as A-C. E, F. *Anthracomedusa turnbulli*, a cubozoan

from the Carboniferous (Westphalian) Mazon Creek Lagerstätte (Francis Creek Shale Member, Carbondale Formation), Illinois, USA. G, H. *Reticulomedusa greenei*, a scyphozoan and *Octomedusa pieckorum* a problematic medusa, respectively, from the same locality as E and F. I. *Rhizostomites* sp. from the late Jurassic (Tithonian) Solnhofen Formation, Bavaria, Germany. From Young et al., 2007; Young and Hagadorn, 2010.

No strong fossil evidence supports the presence of cnidarians in the Precambrian. Most supposed Precambrian cnidarians do not show close resemblances with modern representatives of the group, expect that their tubular or conical shapes superficially resemble those of extant cnidarians. Because of the lack of information on their internal anatomy, most attempts to determine their affinities are inconclusive and doomed to fail. The only unambiguous Cambrian cnidarians are those from the Marjum biota and Chengjiang biota. They display a wide range of anatomical features typical of modern jellyfish, including tentacles and coronal muscles and gonads. The predictions based on molecular data that cnidarians have a very remote origin with possible early ancestors in the Ediacaran and Cryogenian has so far not been confirmed by fossil evidence. The cnidarian-like embryos from the 535 Ma-old Kuanchuanpu Formation give us the unique opportunity to go deeper into the early history and diversification of cnidarians before the metazoan radiation known as the “Cambrian Explosion” reaching its peak.

Chapter 3: The Kuanchuanpu Formation and biota

Chapter 3: The Kuanchuanpu Formation and biota

3.1 General background

3.1.1 Palaeogeographic setting

This chapter aims to provide the reader with some basic knowledge on the geological and palaeogeographical framework of the studied localities. The studied area belongs to the South China Block which was formed by the collision between the southern margin of the Yangtze Platform and the northern margin of the Cathaysia Platform during the early Neoproterozoic (*ca.* 900-880 Ma) (Li 1999, Powell et al. 1993, Wang et al. 2010b).
In the early Cambrian, the South China Block was located in north hemisphere, closed to the eastern margin of the Gondwana super-continent, under tropical latitudes (*ca.* 10° - 35°) (Li and Powell 2001, Elicki 2006) (Fig. 39). The studied area belongs to the northwestern margin of the Yangzte Platform (Qian 1977, Steiner et al. 2007, Steiner et al. 2014) (Fig. 40 A-B) and lies in the central part (Shaanxi Province) of the present-day Chinese territory.

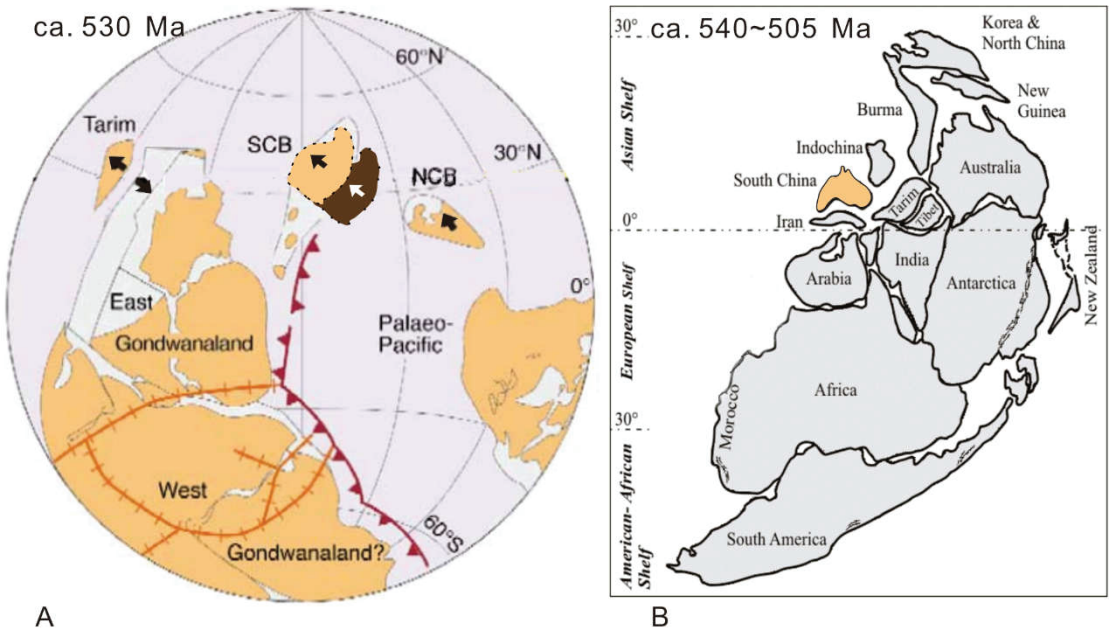

Fig. 39. Paleogeographic map of the super-continent Gondwana. A. Location and movement of the Chinese plates (*ca.* 530 Ma; SCB, South China block; NCB, North China block. The dark brown block represents the assumed position of the South China Block *ca.* 535 million years ago and the white arrow points to the direction of movement. The thick orange lines mark the sutures between blocks within the super-continent Gondwana. The line with small red triangles indicate Gondwana

boundaries. B. Paleogeographic map of Gondwana (early to middle Cambrian). The plate colored in orange is the south China block. Modified from Li and Powell, 2001 and Elichi, 2006.

3.1.2 Geology and localities

The fossils studied here come from the Kuanchuanpu Formation which was deposited during the lowermost Cambrian, more precisely the Fortunian Stage of the Terrenuvian Series, which is equivalent to the Meishucunian Stage in the Yunnan Province of China (Qian 1999, Peng 2003). Recent U-Pb zircon and previous U-Pb radiochronological dating indicate that the age of the Kuanchunpu Formation is approximately 535 Ma, which is consistent with the biostratigraphical data (Li et al. 2003, Peng, Babcock and Cooper 2012).

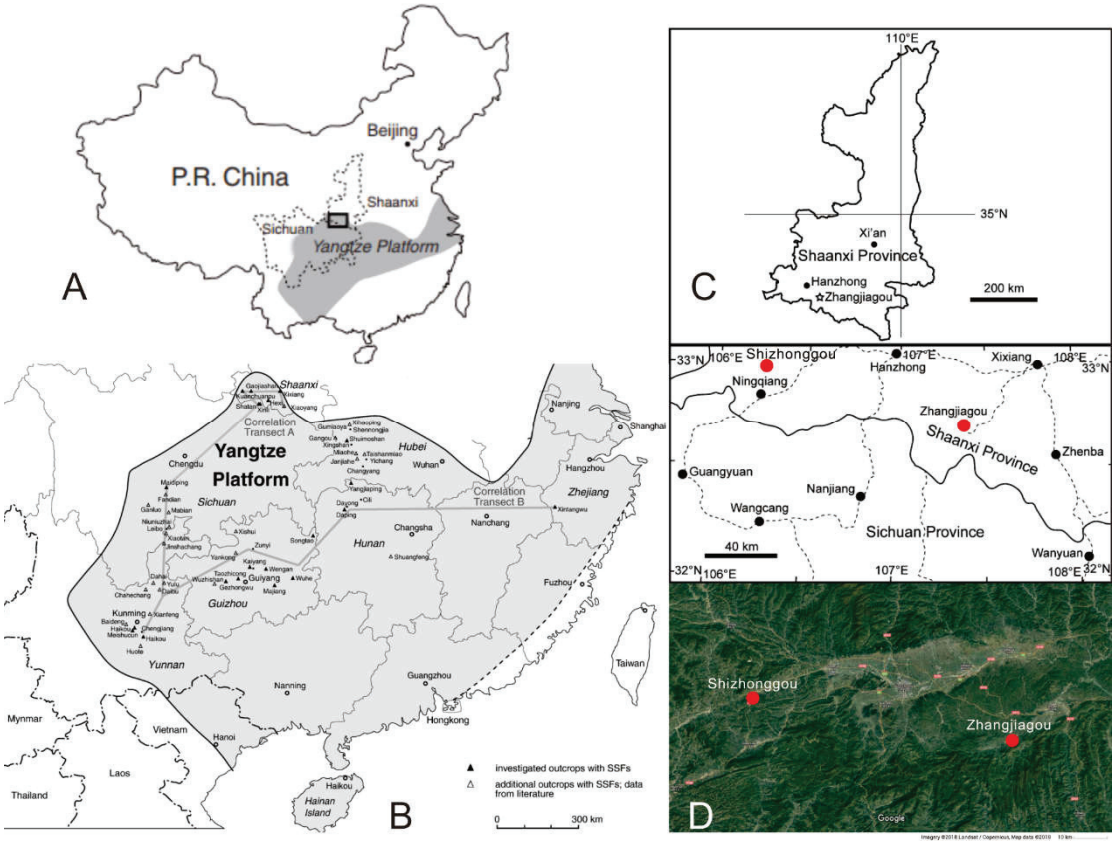

Fig. 40. Locality map. The dark grey area in A refers to the Yangtze Platform. B. Detailed map of the Yangtze platform. C-D, Close-ups showing the Shaanxi Province and the fossil localities (red dots) in the southern part of this province (D corresponds to the small rectangular area in A). The two localities are closed to the Shizhonggou village, Ningqiang County and the Zhangjiagou village, Xixiang County, respectively, both in the Shaanxi Province, China. Scale bars: 300 km in B; 40 km in C; 10 km in D. Copyright of D is from google map. Modified from (Steiner et al. 2007, Steiner et al. 2014, Liu et al. 2014c).

Our fossil material was collected from the Shizhonggou section and Zhangjiagou section (Figs. 40-41) where the Kuanchuanpu Formation outcrops, near the the Shizhonggou village (Ningqiang County) and the Zhangjiagou village (Xixiang County) both located in the southern part of the Shaanxi Province, China. The outcrop of the Shizhonggou section exposes a *ca.* 60 m succession of limestones and phosphatic limestones with interlayered cherts (Fig. 41 A). In this section, the Kuanchuanpu Formation overlies the thick dolostones of the Ediacaran Dengying Formation. The Shizhonggou section, from the bottom to the top, consists of basal light gray microsparitic limestones (8 m), a thick layer of chert (7 m), phosphatic limestones (12 m), the chert (10 m), phosphatic limestone (18 m) interlayered with thin-bedded chert (2 m), chert (8 m) and phosphatic limestone (12 m) (Fig. 41 A). This succession is overlaid by a siltstones which belong to the lower Cambrian Guojiaba Formation (Wang et al. 2010a). The Zhangjiagou section is about 22 m thick with the Kuanchuanpu Formation consisting successively of a basal unit of light gray microsparitic limestones (0.8 m), phosphatic limestones (3.2 m), thick-bedded dark microsparitic limestones (17.4 m), and thin-bedded dolomitic limestones (0.6 m) (Li 1984) (Fig. 41 B) overlaid by shales (lower Cambrian Guojiaba Formation). As in the Shizhonggou section, the Zhangjiagou section overlays a thick layer of Precambrian (Ediacaran) dolostones. In both sections SSFs are dominantly found in phosphatic limestones.

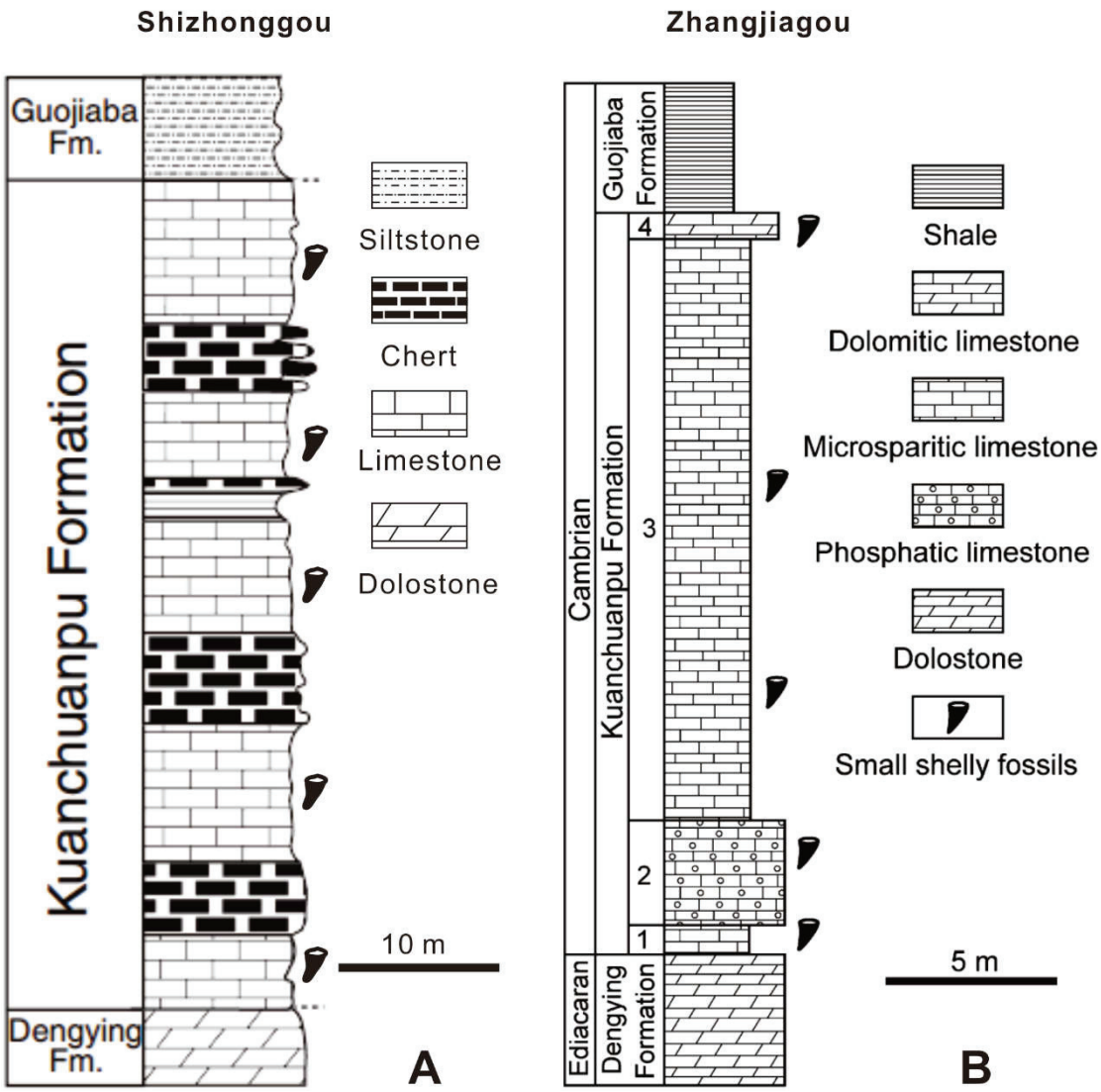

Fig. 41. Origin of the material: the Shizhonggou (A) and Zhangjiagou (B) sections. Scale bars: 10 m (A), 5 m (B). Modified from (Steiner et al. 2014, Liu et al. 2014c).

3.1.3 Biostratigraphy and correlations

The Kuanchuanpu Fromation is the equivalent to the Meishucun Formation (Meishucunian Stage) which represent the lowermost Cambrian in the Yunnan Province (Qian 1977). Three biostratigraphic zones based on SSFs are recognized from the bottom to the top of the Meisshucun referenced sections. These are *Anabarites – Protohertzina – Arthrochities* zone, the *Siphogonuchites – Paragloborilus* zone and *Lapworthella – Tannuolina – Sinosachites* zone. And the *Siphogonuchites – Paragloborilus* zone is considerd containing the most abundant fossils in Meishucun Formation (Narbonne et al. 1987, Peng 2003, Luo 1994).

The SSF assemblages from the Kuanchuanpu Formation resemble those from the Meishucun Formation. The phosphatized eggs or larvae or isolated skeletons, e.g. *Olivooides*, *Protohertzina*, *Anabarites, Hexaconularia*, *Siphogonuchites*, *Carinachites*,

etc., occur both in Meishucun Formations and Kuanzhuanpu Formation, that is why we can correlated these sections. And the *Sinosachites spp.* could not be clearly discovered in the Kuanchuanpu Foramtion (Qian 1977, Steiner et al. 2004).

3.1.4 Lithology and palaeoenvironmental setting

A comprehensive sedimentological study of the Kuanchuanpu Formation has, until now, never been carried out. Small Shell Fossils typically occur within phosphatic limestones, more precisely in concentrated layers embeded within a calcitic matrix (see thin section in Fig. 42). The sediment contains between 35% and 55% of sand grains (size range approx. 50-1000 µm). Skeletal elements are phosphatized, their original calcium carbonate being replaced by apatite. The shell in-fillings are also strongly enriched in phosphate (see thin section in Fig. 42). Low-angled (*ca.* 8°) hummocky cross-stratification (HCS) associated with the SSF-bearing layers suggests that the SSFs found in concentration layers might have been transported by currents and redeposited. HCS are known to form at a depth of water below fair-weather wave base and above storm-weather wave base. Wang et al. (2010) suggested that the HCS observed in the Kuanchuanpu Formation may correspond to a wave length and wave height of about 60-120 cm and 5-20 cm, respectively, indicating a relatively high energy shallow environment.

The most plausible taphonomic scenario is the following: both soft-bodied and biomineralized organisms accumulated at the sediment-water interface were phosphatized shortly after the death of organisms before microbial activity degraded and digested them, which would explain their three-dimensional excellent preservation. Phosphatisation probably continued after burial until the original calcium carbonate of shell was totally replaced by phosphate, and also led to the phosphatic in-filling of microscopic voids in shells and embryos (e.g. empty spaces between internal structures) (Xiao et al. 1998). Although some extremely fragile organisms such as embryos are well-preserved (due to rapid phosphatisation shortly after death), many fossils are incomplete (e.g. small fragments of worms) and numerous organisms are only represented by their sclerites dispersed within the sediment. This suggests that organisms were transported by currents and redeposited.

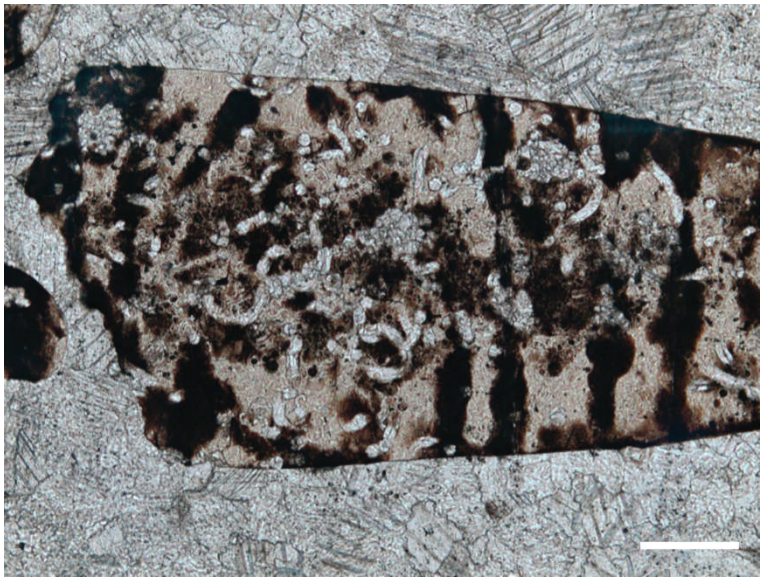

Fig. 42. Thin section of a unamed tubular fossil from the Kuanchuanpu Formation showing tubular SSFs preserved in calcium phosphate (black and brownish areas). Light photograph. Scale bars: 100 µm.

Abundant microstructures have been recently described (Yang et al. 2017) on the surface of numerous SSFs from the Kuanchuanpu formation. Some of them have a non-biological origin and are ambient inclusion trails (AITs), i.e. micro-tunnels formed by the diagenetic pyrite which releases gas such as CH_4 and CO_2 propelling small grain to move pass-through the shell surfaces (Xiao and Knoll 1999, Yang et al. 2017) (Figs. 42; 43 E-F). Others are tiny unbranched micro-borings preserved as internal moulds on the surface of SSFs (Fig. 43 B) and most likely made by euendolithic cyanobacteria (e.g. *Endoconchia lata*; see (Runnegar 1985, Bengtson, Conway Morris and Cooper 1990)). These microstructures give some clues concerning the chronology of taphonomic events. AITs often disturb and cross through the euendoliths (Fig. 43 C-D). It seems that the cyanobacteria drilled the shells prior to phosphate sedimentation whereas AITs were most probaly generated during or after phosphatic mineralization but before the calcareous cementation of sediment (Yang et al. 2017).

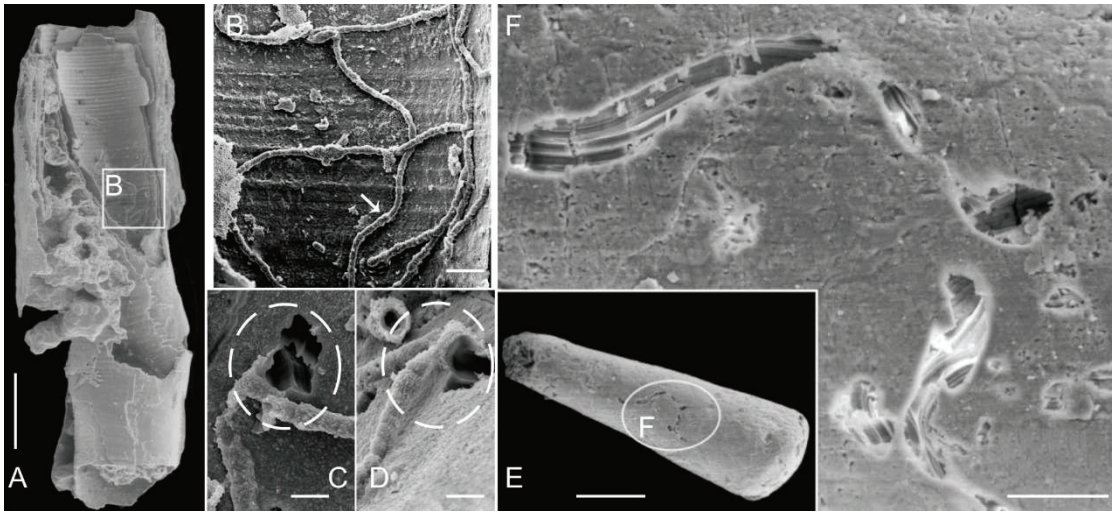

Fig. 43. Euendoliths and ambient inclusion trails (AITs) on the surface of the SSFs from the lower Cambrian Kuanchuanpu Formation, Zhangjiagou Scetion, south China. A. Inner surface of tubular shell of *Conotheca* with the phosphatic casts of *Endoconchia lata* (fossil cyanobacteria). B. Close-up of A in the rectangle area. The arrow pointing the phosphatic casts of euendoliths. C-D. Co-occurrence of *E. lata* and AITs, and the euendoliths interrupted by the AITs. E. Overview of AITs in *Conotheca*. F. Enlargement of E in ellipse area, showing the basic morphology of AITs as micro-tunnels and grooves. Scale bars: 300 μm in A, E; 30 μm in C-D; 10 μm in B, F. Modified from Yang et al., 2017.

The ambient inclusion trails (AITs, a new term) is considered as the micro-tunnels formed by the diagenetic pyrite which releases gas such as CH_4 and CO_2 propelling small grain to move pass-through the shell surfaces (Xiao and Knoll 1999, Yang et al. 2017) (Figs. 42; 43 E-F). The AITs can break or disturb the euendoliths (Fig. 43 C-D) indicating that the abiogenic microboring occurs later than the euendoliths in the early diagenesis.

The sedimentology and palaeoenvironmental conditions are awaiting to be studied in details.

The fossil material studied here comes from Small Shelly Fossil Assemblages extracted from the phosphatic limestones of the Kuanchuanpu Formation. The rocks have been dated from the lowest part of the Cambrian (*ca.* 535 Ma) by radio chronological methods and by correlations using SSFs biostratigraphical zones. The excellent preservation of our fossil material typically represented by embryos and larval stages is due to the rapid phosphatization of soft tissues and cuticle shortly after death. The relatively high proportion of incomplete specimens and isolated sclerites indicate that the Kuanchuanpu organisms may have been transported and redeposited by low energy currents. Uncertainty remains concerning the exact palaeoenvironmental setting of the Kuanchuanpu animal communities although authors suggest that they may have lived in shallow waters.

3.2 Previous work

The earliest descriptions of the Small Shelly Fossils (SSFs) from the lowermost Cambrian Kuanchuanpu Formation appeared in the 70's (Qian 1977). This pioneer work was mainly published in Chinese with English summary and is unfortunately hardly accessible to the majority of scholars. Collaboration with foreign laboratories which started in the 90's clearly boosted scientific research on Chinese SSFs from the Kuanchuanpu Formation and highlighted their scientific interest. In parallel with more accurate systematic descriptions, authors started to focus on two important scientific issues: the contribution of these microfossils to understanding the early evolution of metazoan groups at the base of the Cambrian (including ecdysozoans and deuterostomes) and the rise of biomineralized invertebrates.
A series of more recent studies (Bengtson and Yue 1997, Liu et al. 2014b, Zhang et al. 2015, Han et al. 2013, Steiner et al. 2014, Dong et al. 2013, Wang et al. 2017) has revealed the high diversity of the Kuanchuanpu biota which contains representatives of several key extant animal groups such as cnidarians, ecdysozoans, molluscs, and deuterostomes (Han et al. 2017), as well undetermined organisms which are awaiting to be studied. Micro-computed tomography (Micro-CT) (Micro-CT) and synchrotron radiation X-Ray tomographic microscopy (SRXTM) have revolutionized our way to explore the three-dimensional anatomy of these remarkable fossils and has become an essential tool for resolving their affinities.

3.2.1 Possible cnidarians

Numerous fossils from the Kuanchuanpu Formation are considered as possible members of the Cnidaria. Their assumed cnidarian affinities have been inferred from both external and more rarely internal morphological characters. A relatively complete review of the putative cnidarians from the Kuanchuanpu biota was made by Steiner et al. (2004) and is updated here (see table 2 below).

Cnidarians
***Olivooides / Punctatus* Qian, 1977**
Punctatus emeiensis He, 1980
Punctatus triangulicostalis Liu et al., 2006
Olivooides mirabilis Yue, 1984
Olivooides multisulcatus Qian, 1977
Olivooides / *Punctatus*-like forms
Sinaster Wang et al., 2017
Sinaster petalon Wang et al., 2017
Hanagyroia
Hanagyroia orientalis gen. et sp. nov. (unpublished)
Unnamed fossils
ELISN 31-5; ELISN 108343 (see Han et al., 2013)
GMPKU 3089 (see Dong et al., 2013)
Quadrapyrgites Li et al., 2007
Quadrapyrgites quadratacris Li, 1984 (revised in Li et al., 2007)
Quadrapyrgites ningqiangensis Li et al., 2007
Quadrapyrgites undulatuscostalis Liu et al., 2009
Eolympia Han et al., 2010
Eolympia pediculata Han et al., 2010
Qinscyphus Liu et al., 2017
Qinscyphus necopinus Liu et al., 2017
***Hexaconulariids* He, 1987**
Hexaconularia longelus He and Yang, 1986
Hexaconularia multicostata He and Yang, 1986
Hexaconularia formosa Qian, 1989
Hexaconularia xinliensis Qian, 1989
Hexaconularia breviculus He and Yang, 1986
Hexaconularia nanjiangesis He and Yang, 1986
Hexaconularia sichuanesis He and Yang, 1986
***Carinachites* Qian, 1977**
Carinachites spinatus Qian, 1977
Carinachites tetrasculus Luo et al., 1982
Pentaconularia ningqiangensis Liu et al., 2011
Emeiconularia trigemme Qian, 1997
Emeiconularia amplcanalis Liu, 2005

Table 2. Species and undetermined specimens from the Kuanchuanpu biota, tentatively assigned to Cnidaria.

Most genera and species tentatively assigned to Cnidaria (e.g. *Olivooides*, *Olivooides*-like, and unnamed microfossils) are represented by embryonic stages (size range between 450 µm and 600 µm). Other forms (e.g. *Hexaconulariids*, *Carinachites*), generally larger, belong to post-hatching stages and are also considered by many authors as possible cnidarians. The family Olivoodae erected by Steiner et al., 2014 which is identified their tower-shaped periderms after the hacthing stage and the round shape at the embryonic stages, involving *Olivooides*, *Quadrapyrgites*.

3.2.1.1 *Olivooides* / *Punctatus* and *Olivooides*-like forms

Olivooides was first described by Qian (1977) as the embryonic stage of an unknown animal. The lack of information from internal features and the absence of modern equivalent did not allow him to go further. *Punctatus* was erected by (Yin 1980) based on its conical shape and unique stellate external micro-ornament. Detailed comparative studies showed that both genera actually shared important morphological features such as the pentaradial symmetry and the stellate micro-ornament which occurs both on the periderm of *Punctatus* and the apertural lobes (around mouth) of *Olivooides*. This led authors to consider *Punctatus* as the post-hatching stage of *Olivooides* and to propose a reconstruction of the developmental stage of the animal (Bengtson and Yue 1997, Yue and Bengtson 1999). Although no formal decision has yet been taken regarding the status and the validity of these taxa, we consider here *Punctatus* as a younger synonym of *Olivooides*
Olivooides-like fossils resemble *Olivooides* in all major aspects of their morphology but lack the dense stellate ornament typical of the periderm of *Olivooides*.
Several unnamed *Olivooides*-like embryonic forms from the Kuanchuanpu biota are currently regarded (Han et al. 2013, Dong et al. 2013) as possible cubozoans or scyphozoans (e.g. ElISN 31-5, ElISN 108-343, ELISN 31-31, GMPKU 3089 ; see Han et al., 2013; Dong et al., 2013). Wang et al. (2017) erected *Sinaster* a new genus which is also assumed to belong to the stem group Cubozoa. Another embryonic form (submitted manuscript by Wang et al.; see Chapter 5) may have an intermediate position between cubozoans and scyphozoans.

1) External morphology

Olivooides has an ovoid shape, a stellate micro-ornament, a pentamerous body symmetry exemplified by five perradial oral apertural lappets and ten interradial apertural lappets (5 + 10 mode) surrounding the assumed mouth opening (Steiner et al. 2014) (Fig. 44). Their diameter ranges from 500 to 800 µm (Hua, Chen and Zhang 2004). *Punctatus* is characterized by a proximal cone-shaped apex followed distally by a series of annulated transverse ridges, interconnected by tiny longitudinal stripes (Bengtson and Yue 1997).

Olivooides often co-occurs with *Punctatus* in SSF-assemblages. It became rapidly evident to authors (e.g. (Bengtson and Yue 1997)) that *Olivooides* and *Punctatus* were probably two different developmental stages of a single type of organism. This interpretation is well supported by specimens having an intermediate morphology between *Olivooides* and *Punctatus*. Bengtson and Yue (1997), Steiner et al. (2014), Han et al. (2013) made tentative reconstructions of the life cycle *of Olivooides*/*Punctatus*, from an early stage (*Olivooides sensu stricto*; dividing embryo) to a more advanced possibly post-hatching stage (*Punctatus*).

Olivooides is represented by two distinct species namely *Olivooides multisulcatus* (Qian 1977) and *Olivooides mirabilis* (Yue, 1984). *O. multisulcatus* is characterized by a stellate ornament covering the periderm surface, five perradial apertural lappets and ten interradial apertural lappets surrounding the mouth opening. More advanced developmental stages of this species display an overall turret-like shape with a conical apex, transverse ridges and triangular structures overprinting the ridges at the post-hatching stage (Qian, 1977; Bengtson and Yue, 1997; Steiner et al., 2013) (Fig. 45). *O. mirabilis* lacks such triangular structures and instead has regular tiny longitudinal stripes between ridges (Yue 1986) (Fig. 46).

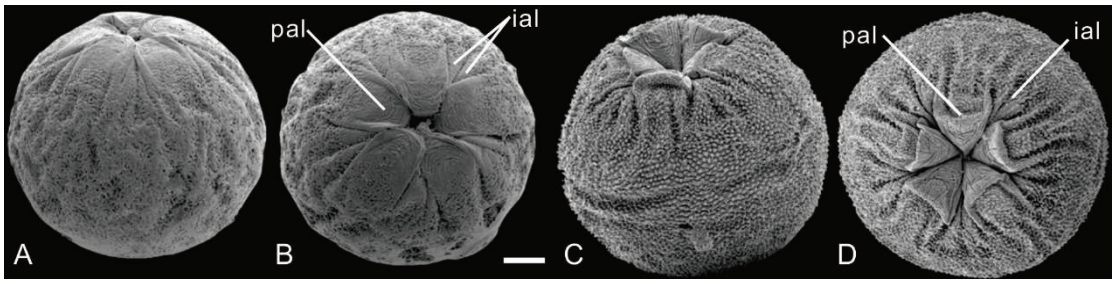

Fig. 44. *Olivooides multisulcatus* from the Kuanchuanpu Formation, Shizhonggou section, Shaanxi Province, China. Abbrevations: ial, interradial appertural lappet; pal, perradial appertural lappet. All scale bar: 100 µm. Modified from Steiner et al., 2014.

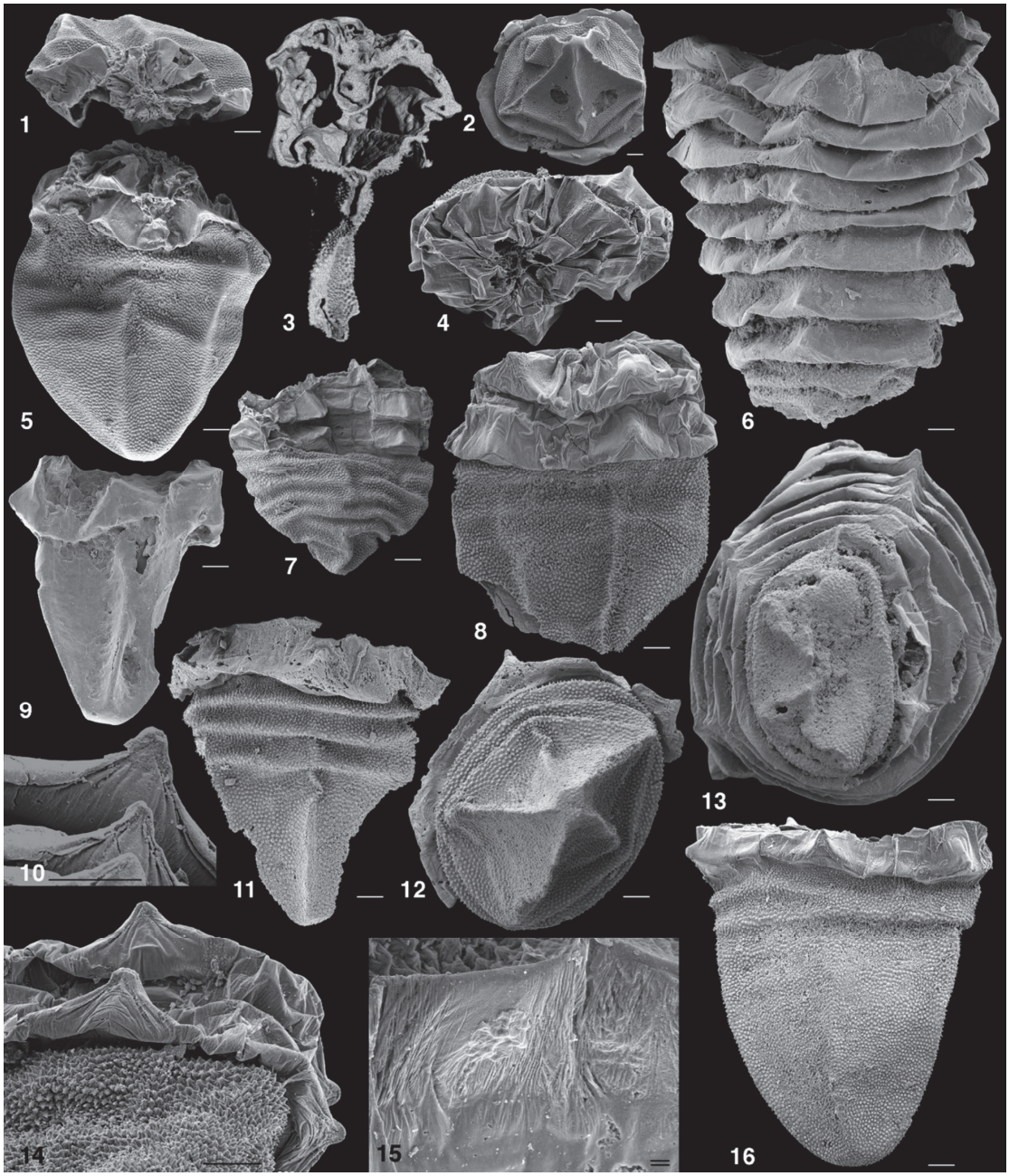

Fig. 45. *Olivooides multisulcatus* from the Kuanchuanpu Formation, Shizhonggou section, Shaanxi Province, China. Single and double scale bars correspond to 100 µm and 10 µm, respectively. From Steiner et al., 2014.

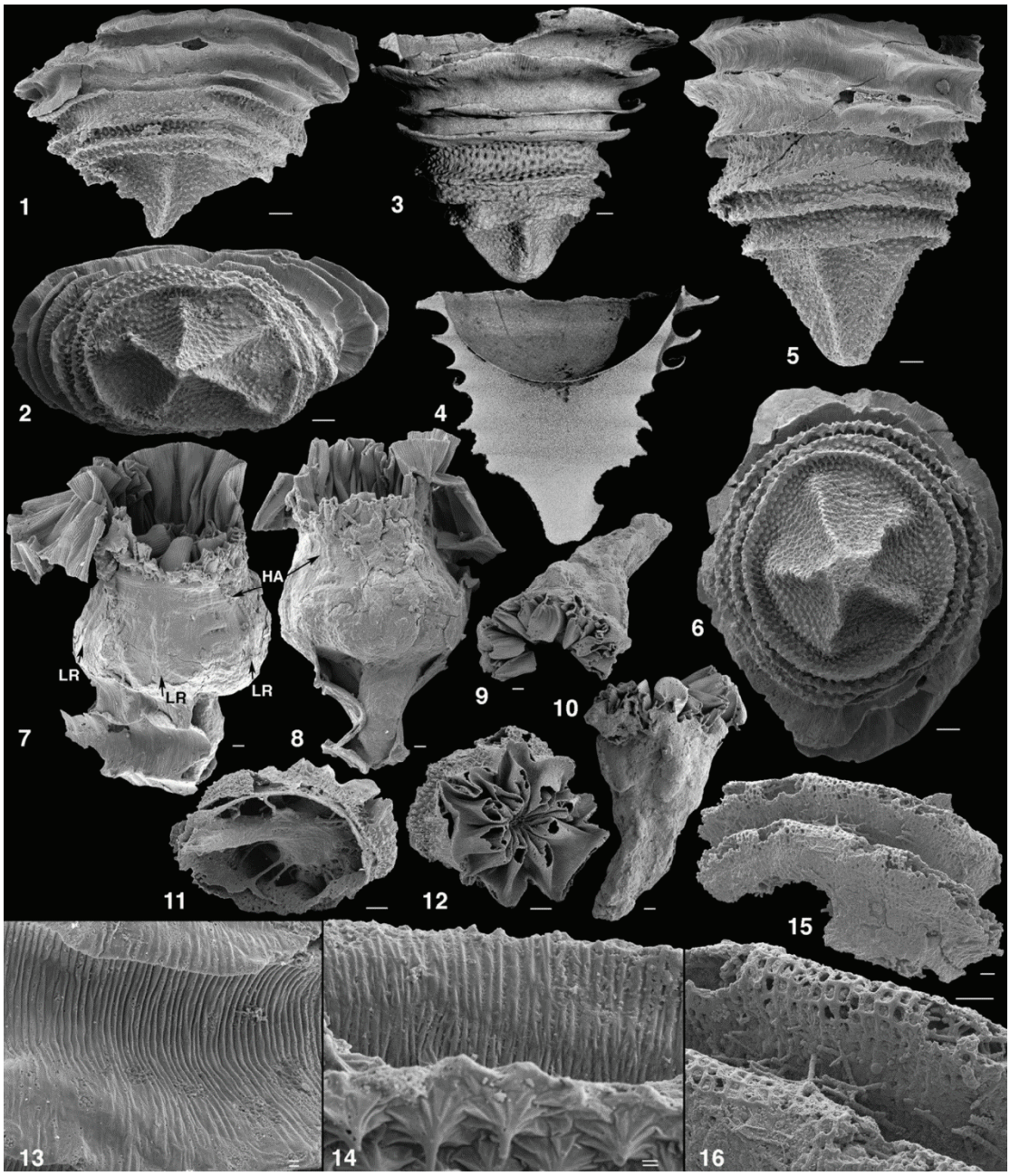

Fig. 46. *Olivooides mirabilis* from the early Cambrian Kuanchuanpu Formation, Shizhonggou section, Shaaxi Province, China. Single and double scale bars correspond to 100 μm and 10 μm, respectively. From Steiner et al., 2014.

2) Internal morphology

The external morphology of *Olivooide*s and allied forms has been repeatedly observed via Scanning Electron Microscopy (SEM). In contrast, the inner structures of *Olivooides* have remained virtually unknown until they were studied via new techniques such as micro-computed tomography (Micro-CT) and synchrotron radiation X-ray tomographic microscopy (SRXTM) (Han et al. 2013).

Microtomography allowed complex internal structures to be described such as the interradial septa, claustrum, gonad-lamella, suspensorium and velarium supported by the frenula. Direct comparisons with similar structures known in extant cnidarians (e.g. cubozoans; (Han et al. 2013, Conant 1898, Hyman 1940)) could be made as well. For example, microtomography revealed the complex partitioning of the gastrovascular cavity of some *Olivooides*-like fossils into at least 40 pockets (e.g. ELISN 31-5; see Han et al., 2013 and Figs. 47-48). The microtomographic exploration of these microfossils revealed unexpected details of their internal structures and added complexity to the problem of reconstructing and interpreting them.

Other research teams led by Dong (2013; 2016), Steiner (2014) and their respective collaborators also used synchrotron X-ray tomography to study the internal morphology of *Olivooides* and *Olivooides*-like fossils with the hope of resolving the affinities of these enigmatic organisms.

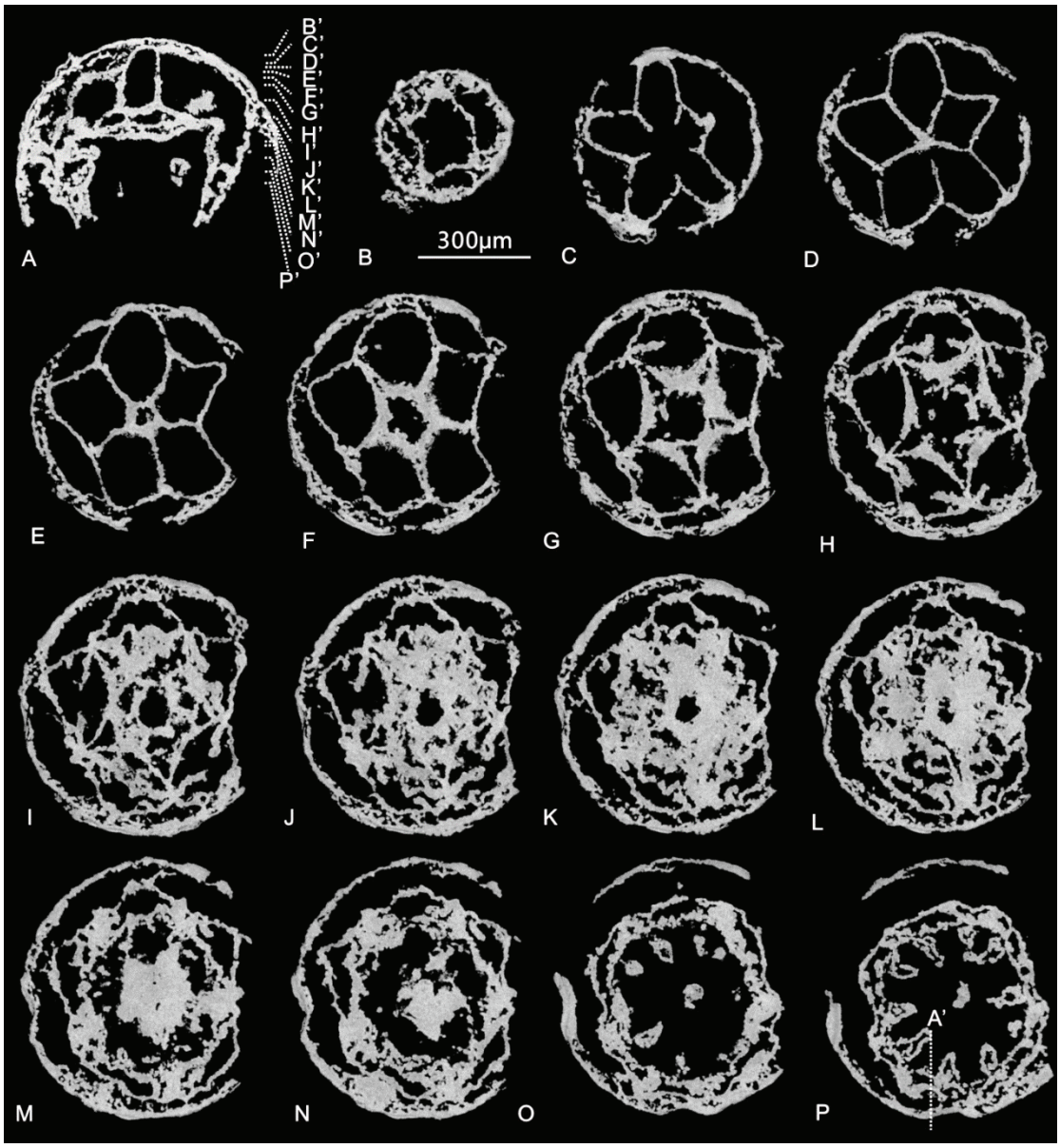

Fig. 47. X-Ray Microtomography applied to microfossils from the lower Cambrian Kuanchuanpu Formation, Shizhonggou section, Shaanxi Province, China. Virtual sections through embryonic forms (ELISN 31-5). A. Virtual vertical section of ELISN31-5 marked with a vertical dotted line by P9 in (P). B–P. Successive virtual horizontal sections of the same specimen from the oral-aboral axis; their horizontal levels are marked by B9–P9 in (A) with white dotted lines. Scale bar: 300 μm. From Han et al., 2013.

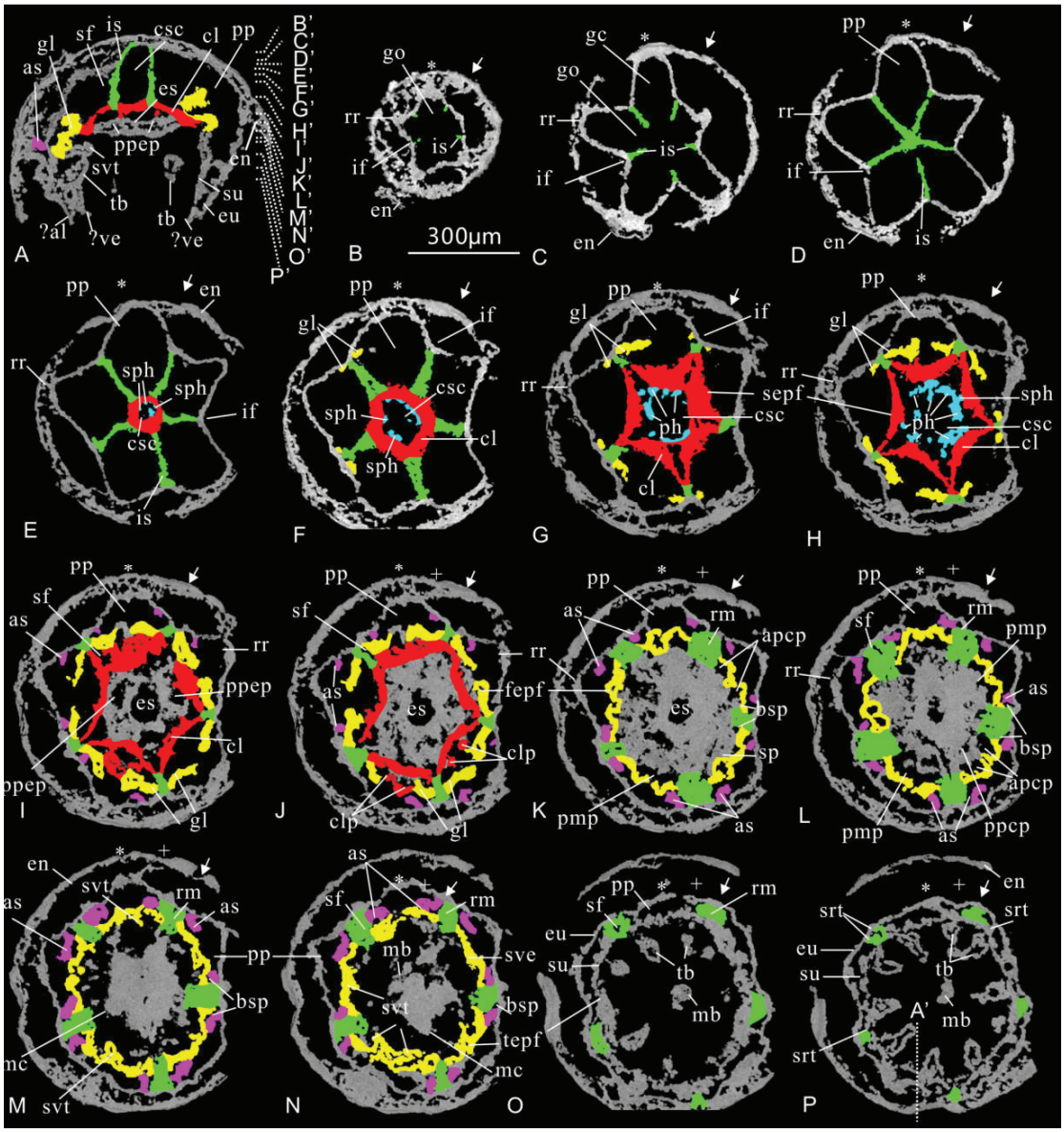

Fig. 48. X-Ray Microtomography applied to microfossils from the lower Cambrian Kuanchuanpu Formation, Shizhonggou section, Shaanxi Province, China; interpretation of the virtual sections shown in Fig. 47. Abbreviations: al, apertural lappet; apcp, adradial peri-claustral pocket; as, accessory septum; bsp, basal septal pocket; cl, claustrum; clp, claustral projections; cs, coronal stomach; csc, central stomach cavity; en, egg envelope; es, esophagus; eu, exumbrella; fepf, first endodermic pentagonal funnel; gc, gastric cavity; gl, gonad-lamella; go, gastric ostium; if, interradial furrow; is, interradial septa; mb, manubrium; mc, manubrial corner; pmp, perradial mesogonial pockets; pp, perradial pocket; ppep, perradial peri-esophageal pocket; rm, retractor muscle; rr, radial ridge; sepf, second endodermic pentagonal funnel; sf, septal funnel; sph, stalk of phacellus; srt, septal roots of tentacles; su, subumbrella; tb, tentacular bud; tepf, third endodermic pentagonal funnel; ve, velarium; *, perradius; +, adradius; →, interradius. Scale bar: 300 µm. From Han et al., 2013.

Although pentaradial symmetry seems to be dominant among *Olivooides* and *Olivooides*-like fossils, some tetraradial forms were found in the Kuanchuanpu biota (Han et al. 2016b). This important finding indicated 1) that at least two types of symmetry co-existed in *Olivooides* and allied forms and 2) that the tetramerous symmetry which is a diagnostic feature of most extant medusozoans also occurred among eraly Cambrian embryos interpreted as possible cnidarians. These tetraradial forms were tentatively placed within the crown group cubozoans, based on cladistic analysis (Han et al. 2016b) (Fig. 49).

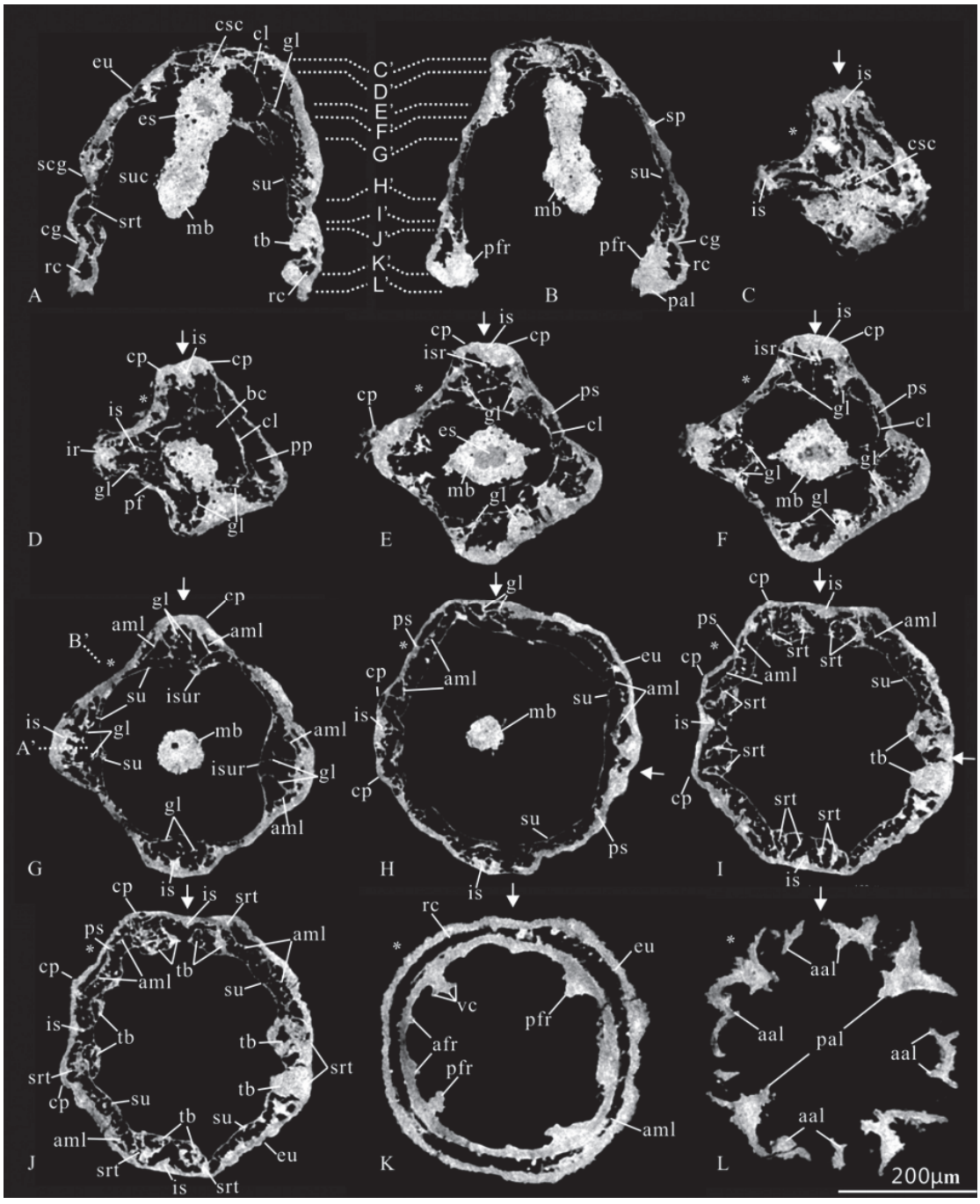

Fig. 49. Micro-CT sections of a tetramerous cubozoan (ELISN31-31) from the Lower Cambrian Kuanchuanpu Formation, South China. (A) Interradial and (B) perradial vertical sections marked with a horizontal dotted line by A' and B' in G. (C–L) Successive horizontal sections of the same specimen from the aboral pole downward, and their horizontal levels are marked by C'-L' in A–B with white dotted lines. Abbreviations: aal, adradial apertural lappets; afr, adradial frenulum; aml, adradial marginal lamellae; bc, bell cavity; cg, coronal groove; cl, claustrum; cp, corner pillar; en, egg envelope; es, esophagus; eu, exumbrella; gl, gonad-lamella; ir, interradial ridges; is interradial septa; isr, interradial septal ridge; isur, interradial subumbrellar ridges; mb, manubrium; pal, perradial apertural lappet; pf, perradial furrow; pfr, perradial frenulum; pp, perradial pocket; ps, perradial septum; rc, radial canal; srt, septal root of tentacles; su, subumbrella; suc, subumbrella cavity; sp, suspensorium; tb, tentacular bud; ve, velarium; vc, valarial canal; *, perradius; →, interradius; +, adradius. All sections share the same scale bar (=200 μm) as in L. From Han et al., 2016b.

3) Development and life cycle of *Olivooides* / *Punctatus*

Attempts to reconstruct the life cycle of *Olivooides / Punctatus* have been made (Bengtson and Yue 1997, Steiner et al. 2014) (Figs. 51-52), that show how organisms develop from fertilized egg to larva through a series of gradual stages (Hua et al. 2004, Yao, Han and Jiao 2011). However, the transition between the early dividing embryos to the blastula stage is still unclear. In *Olivooides*, five evenly distributed radial buds appear around the oral part during the interval which seems to correspond to the late blastula-gastrula stage. In the early stage of gastrulation, the surface of the periderm becomes granulate (Steiner et al. 2014), then the stellate micro-ornament appears on the periderm surface. This ornament is remarkably well preserved in some specimens (Fig. 50 a). A circular constriction can be seen between the oral and aboral poles (Hua et al. 2004) (Fig. 50 b). In the next steps, the whole periderm of *Olivooides* is entirely covered with stellate ornament except for the radial oral lobes. At the same time, a conical apical structure develop in the aboral region. The first circular furrow appears in the equatorial area of the larva (Fig. 44 C-D).

After the hatching stage, the globular embryos stretch along the oral-aboral axis. Four annulated circular ridges appear below the oral region and a cone-shaped apical structure develop at the opposite end. This conical structure has the same pentaradial symmetry as the rest of the body (Steiner et al. 2014) (Figs. 44-45). As the number of circular ridges gradually increases during ontogeny, the organism grows in length and transform into a cone with a corrugated appearance.

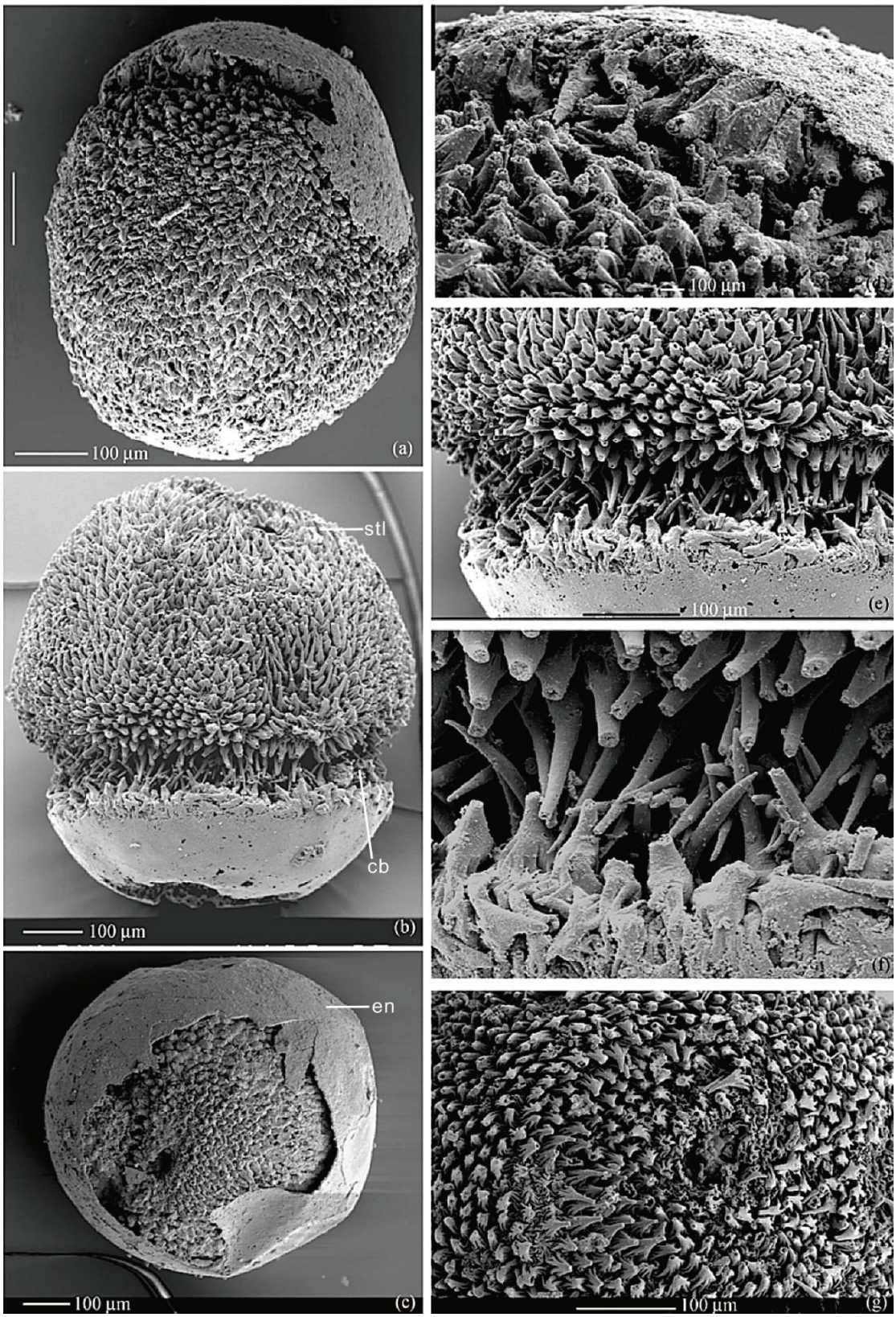

Fig. 50. Gastrula stage of *Olivooides* (unnamed species). Developmental sequence: (c), (a) and (b). d. Stellate ornament. e-f. Details on girdle (circular) belt in b. g. Possible blastopore. Abbreviations: cb, circular belt; en, envelope (periderm); stl, stellate ornament. Modified from Hua et al., 2004.

Olivooides embryos at the hatching stage display a clear radial symmetry, have a single body opening and apparently two tissue layers. Although these three characterics are found in modern cnidarians, *Olivooides* differs markedly from cnidarian embryos by the absence of a planula stage during its ontogeny. Whether *Olivooides* had originally a planula larval stage or not remains uncertain. The absence of planula might have a taphonomic origin since larvae are prone to decay extreme rapidly.

Although *Olivooides multisulcatus* and *Olivooides mirabilis* share numerous morphological characters and are closely related species, Steiner et al. (2014) noted slight differences in their development. For example, the triangular thickenings arising during the development of the transverse annulated ridges of *O. multisulcatus*, do not occur in *O. mirabilis* which instead develop thin connecting longitudinal strips between ridges.

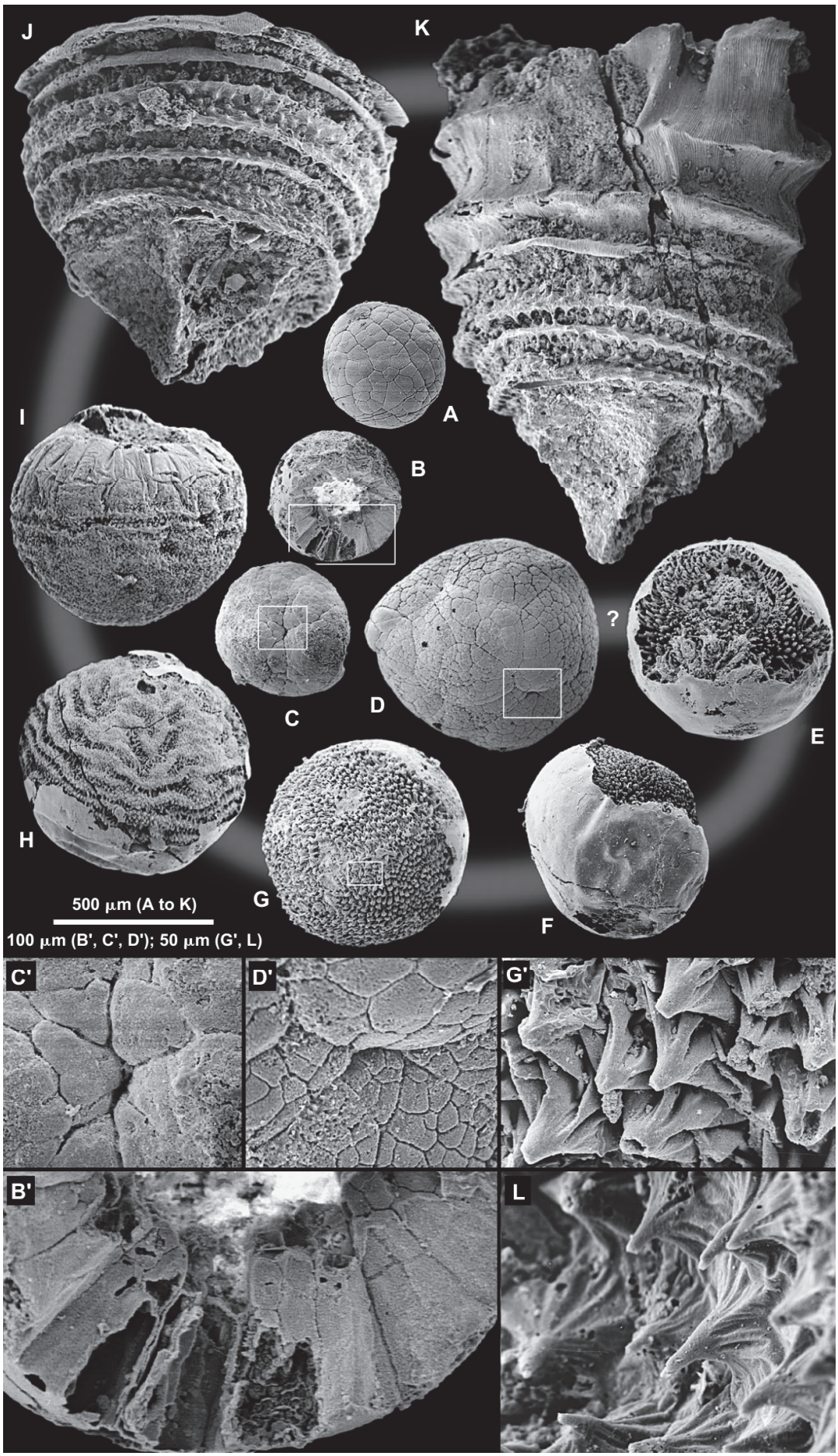
J
K
A
I
B
C
D
?
E
H
G
F
500 μm (A to K)
100 μm (B', C', D'); 50 μm (G', L)
C'
D'
G'
B'
L

Fig. 51. Successive stages in the development of *Olivooides mirabilis* from the lowest Cambrian Kuanchuanpu Formation, Shizhonggou section, Shaaxi Province, China (A-K). From Bengtson and Yue, 1997.

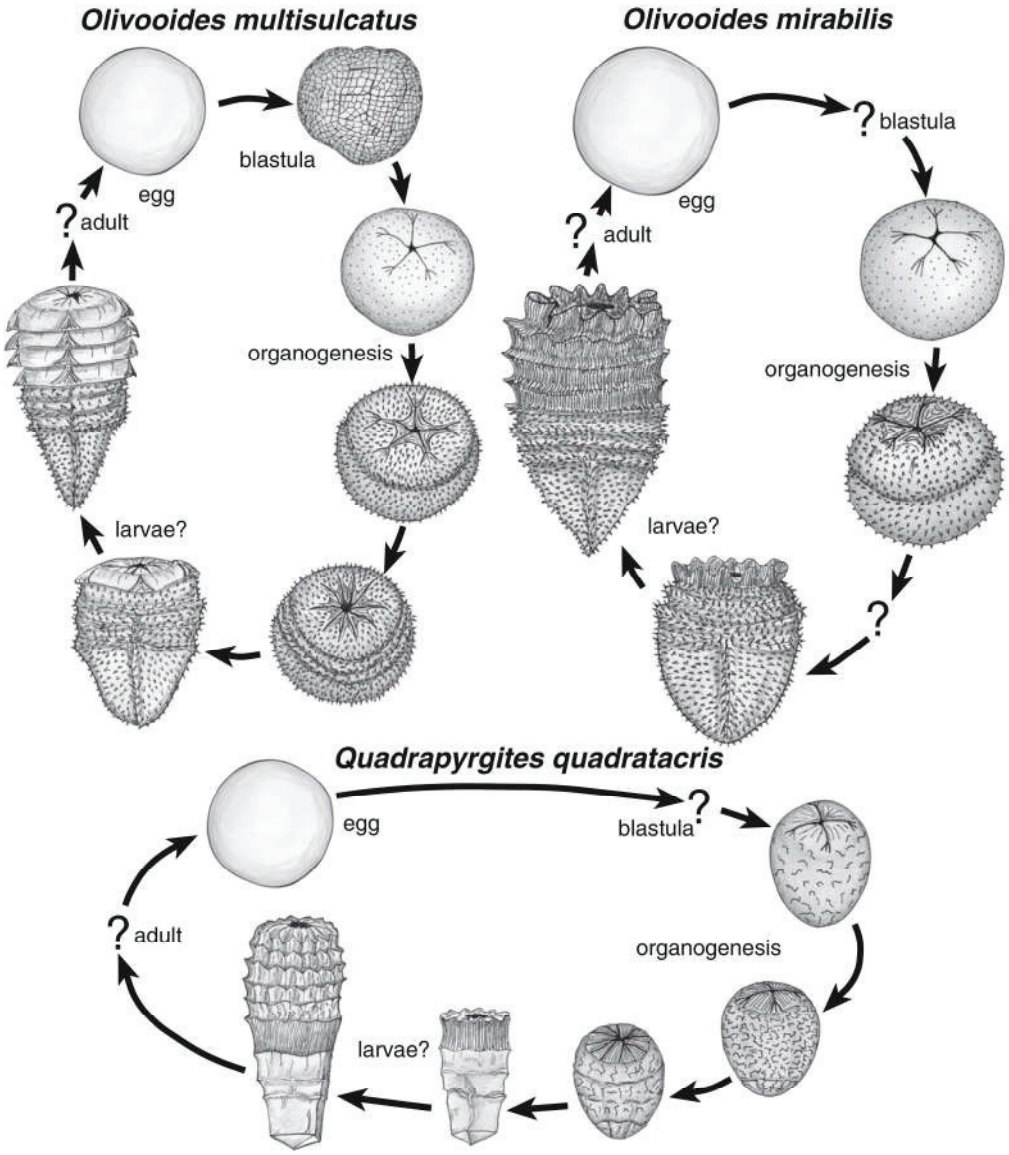

Fig. 52. Possible lifecycles of *Olivooides multisulcatus*, *O. mirabilis* and *Quadrapyrgites quadratacris*. From Steiner et al., 2014.

4) Affinities of *Olivooides* / *Punctatus* and allied forms

There are two opposing hypotheses regarding the affinities of *Olivooides* which has been considered either as a Scalidophora (Ecdysozoa) (Steiner et al. 2014) or a Cnidaria (Scyphozoa or Cubozoa) (Dong et al. 2013, Han et al. 2013, Liu et al. 2017, Steiner et al. 2014).

a) The scalidophoran hypothesis

Steiner et al. (2014) suggested that *Olivooides* / *Punctatus* may represent the larval stages of scalidophoran worms because of its pentamerous body symmetry and its tube-like feature (post hatching stage of *Olivooides*) recalling the protective outer case (lorica) secreted by loriciferans.

b) The cnidarian hypothesis

This option is more commonly accepted by researchers who provide the following arguments:

1) *Olivooides*/*Punctatus* fossils consist of two body layers (exumbrella and subumbrella) (Han et al. 2013, Wang et al. 2017) which are connected by interradial septa comparable with those of extant medusozoans (Hyman 1940);

2) These fossils have a single opening (mouth) with no through gut connecting the mouth to the anus, both in embryonic and and more advanced stages (Han et al. 2013, Liu et al. 2014b, Dong et al. 2016);

3) Paired features recalling tentacular buds occur in *Olivooides* fossils (Han et al. 2013, Wang et al. 2017).

Both hypotheses are discussed in more details in Chapters 5-6.

3.2.1.2 *Quadrapyrgites*

Quadrapyrgites was erected by Li et al. (2007) to accommodate three distinct species, namely *Quadrapyrgites ningqiangensis* Li et al., 2007, *Quadrapyrgites undulatuscostalis* Liu et al., 2009 and *Quadrapyrgites quadratacris* Li, 1984 (revised in (Li et al. 2007)) (Fig. 54). *Quadrapyrgites* replaces *Pyrgites* (Li 1984), a poorly defined and invalid genus.

Quadrapyrgites is characterized by a tetramerous body symmetry, a smooth apex (apical cone) with four regularly distributed radial ridges, annulated transverse ridges connecting to the cone-shaped apex, four perradial apertural and eight interradial apertrual lobes around the oral part (Figs. 53-54). The diameter of annulated ridges increases from aboral to oral end, and longitudinal tiny stripes run between them. Early developmental stages show zig-zag-shaped microstructures over the periderm surface (Fig. 53).

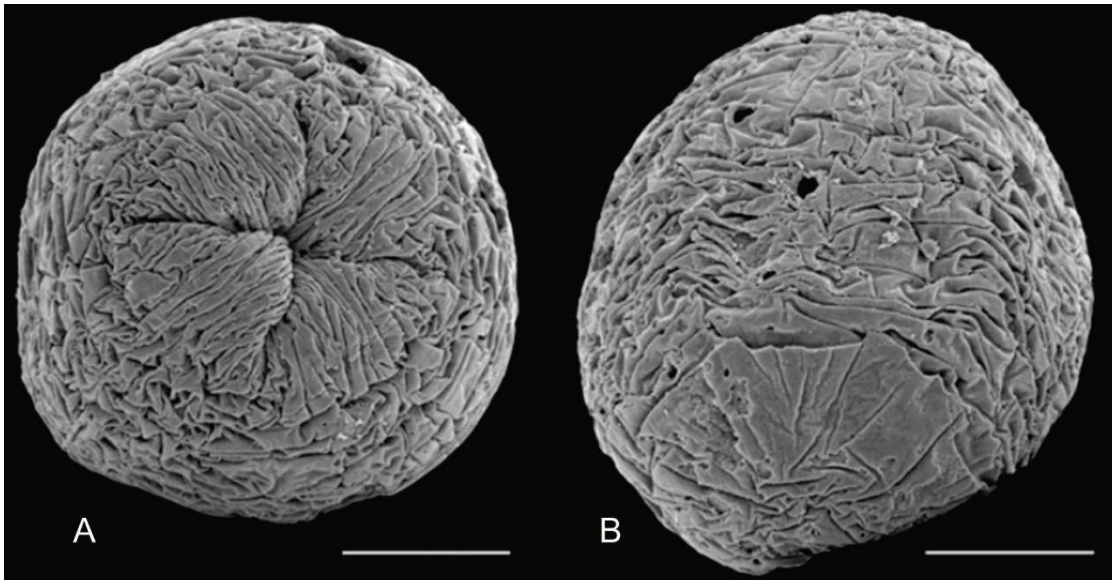

Fig. 53. Embryos of *Quadrapyrgites quadratacris* Li (1984) with tetramerous symmetry. A. View on tetramerous oral lobes. B. Lateral view of A. Scale equals 100 µm. From Steiner et al., 2014.

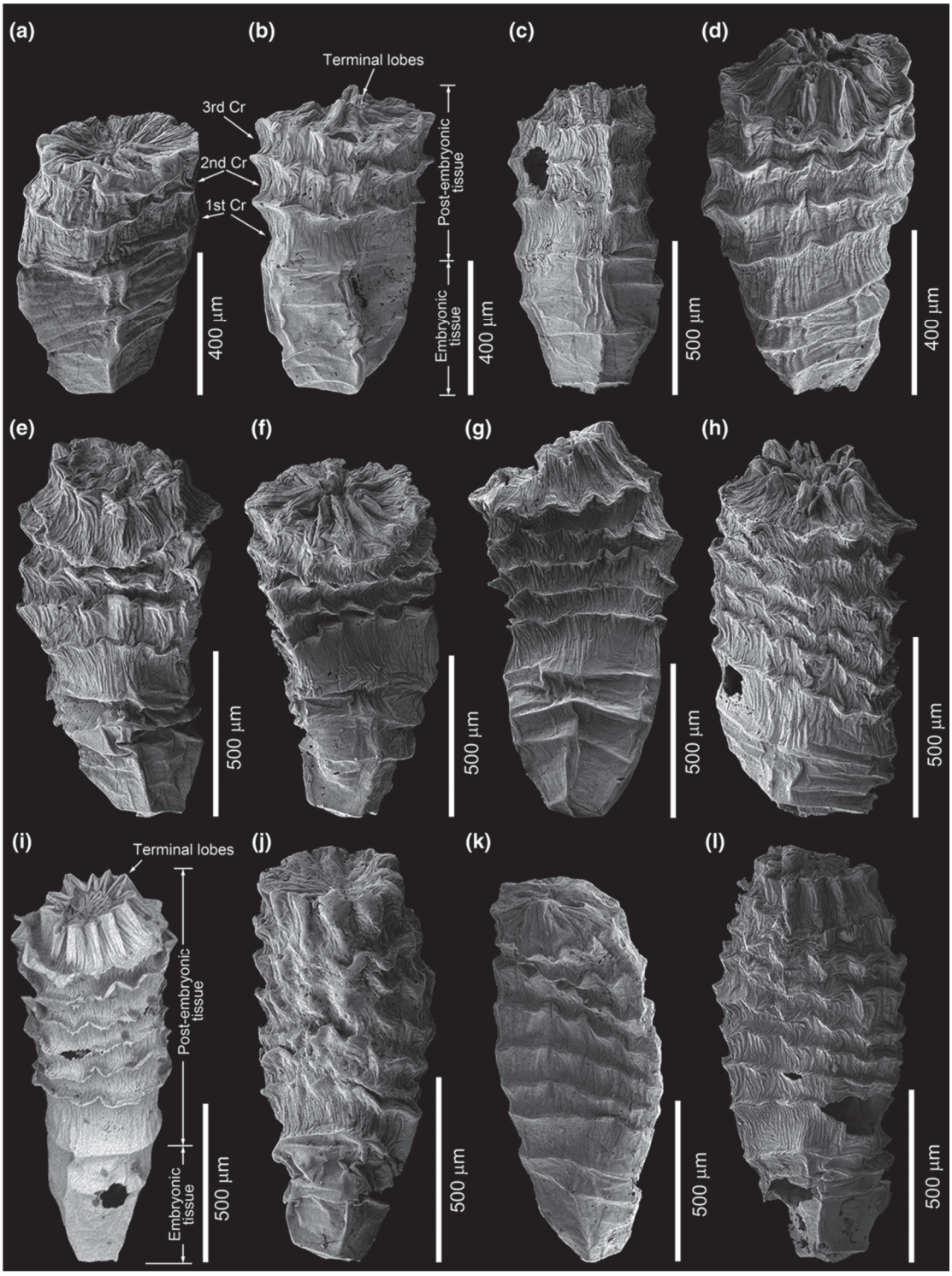

Fig. 54. Growth pattern of *Quadrapyrgites quadratacris* Li (1984) at post embryonic stage from the lower Cambrian, Kuanchuanpu Formation, Zhangjiagou section, Xixiang County, Shaanxi Province, China. From Liu et al., 2014b.

3.2.1.3 *Eolympia pediculata*

Eolympia pediculata is a minute (size *ca.* 450 µm) pedunculated form with a cylindrical upper part crowned by a ring of evenly spaced bud-like features. It was interpreted by Jian et al. (2010) as the tentaculated polyp of a solitary form with a pedicle at its aboral end (Fig. 55). *E. pediculata* is characterized by an upper cylindrical part and a lower stalk-shaped pedicle. These two parts are demarcated by a weak circumferential groove. Eighteen (multiple of 6) mesenteries occur within the inner cylindrical cavity (Fig. 55 B, D, F). The same number of tentacles are found around the margin of the upper cylindrical body. There is a named collar structure between the tentacles and the mesenteries. A single opening (mouth) can be seen at the distal end of pedicle (Han et al. 2010) (Fig. 55 D).

Han et al. (2010) considered *E. pediculata* as possibly belonging to the sister group of extant hexacorallians based on its 18 (multiple of 6) complete and incomplete mesenteries. The possible bilateral arrangement of its mesenteries also suggest resemblance with extant anthozoans.

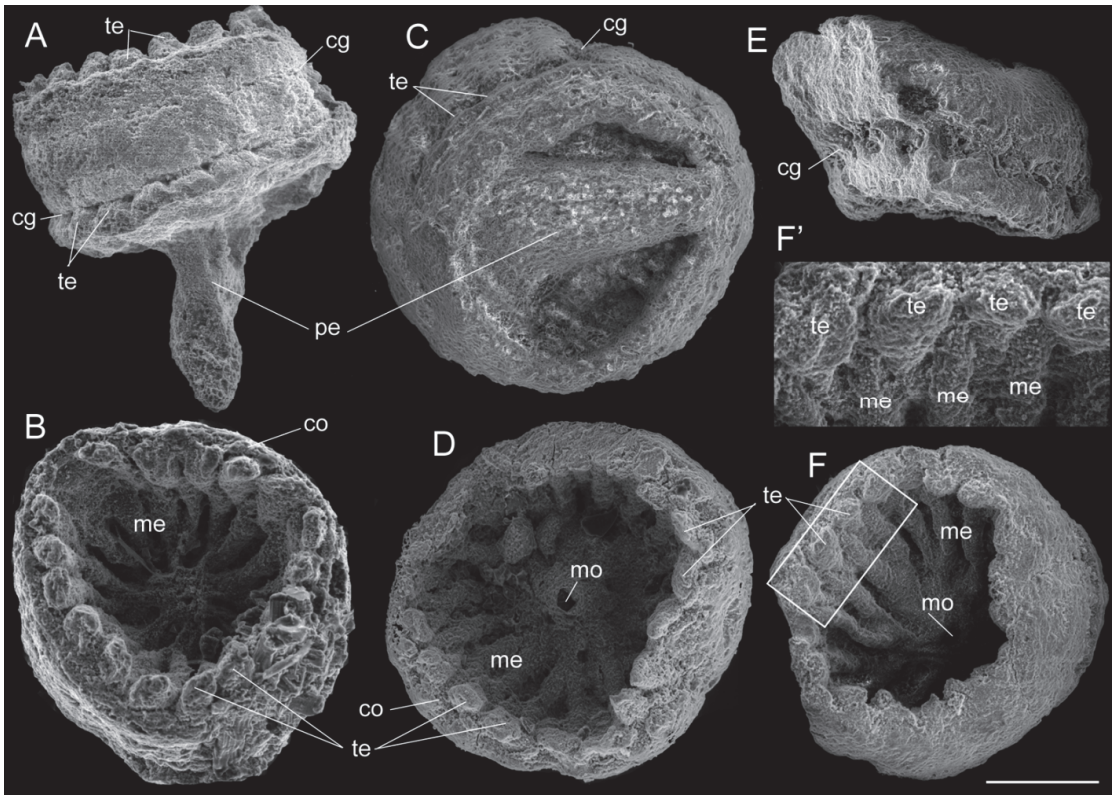

Fig. 55. ***Eolympia pediculata*** from lower Cambrian Kuanchuanpu Formation, Shizhonggou section, Shaanxi Province, China. Abbreviations: cg, circumferential groove; co, collar; me, mesentery; mo, mouth; pe, pedicle; te, tentacle. Scale bar: 0.2 mm. From Han et al., 2010.

3.2.1.4 *Qinscyphus necopinus*

Qinscyphus necopinus was reconstructed by Liu et al. (2017) (Fig. 56) as an elongated cone with an assumed oral region bearing five strong, pentaradial triangular features. These pointed features seem to converge towards the mouth opening. The external surface of the cone has numerous regularly spaced annuli. Repeated rows of five strong pyramidal features occur every four or seven annuli. *Qinscyphus* is placed by Liu et al. (2017) into the crown group of coronate scyphozoans based on its conical shape (Liu et al. 2017). However, this tentative assignment is supported by no evidence from internal features that X-Ray tomographic microscopy (XTM) would have the potential to reveal. *Q. necopinus* may be compared with the post embryonic stages of *Olivooides* and *Quadrapyrgites*. As *Olivooides Q. necopinus* is clearly pentamerous. However, it lacks the stellate ornament which characterizes *Olivooides*. The growth pattern of the thick triangular features found in *Q. necopinus* also differs from that of *Olivooides multisulcatus* Qian, 1977.

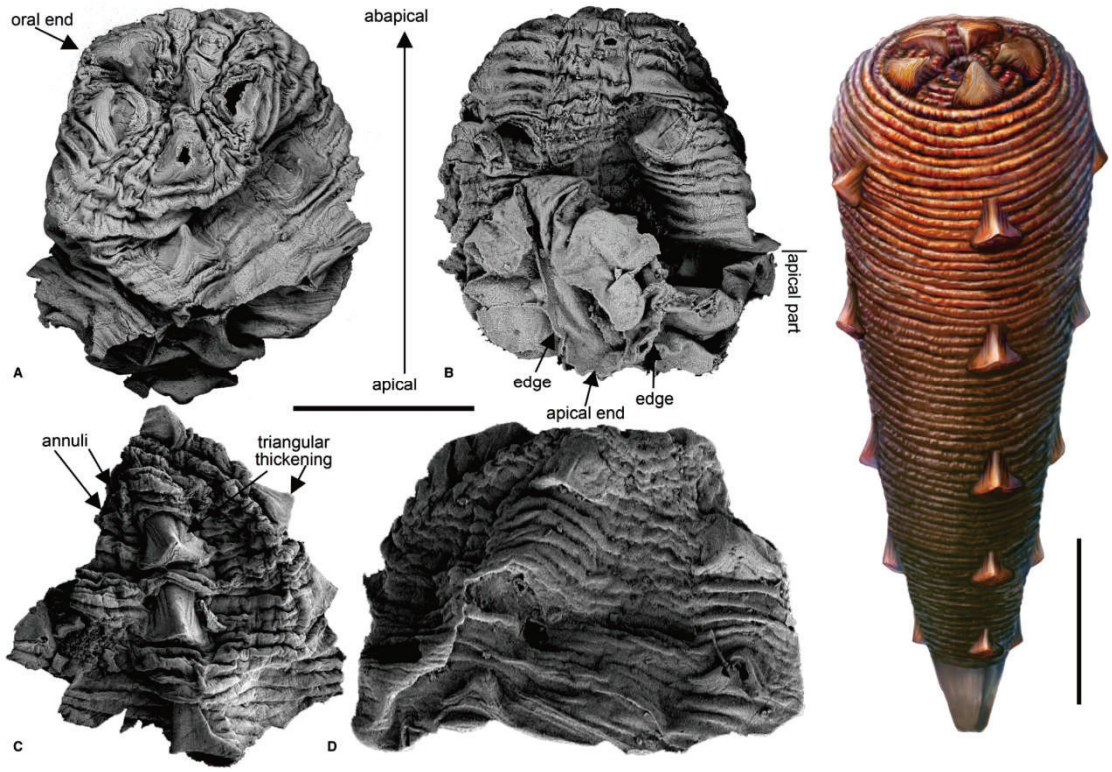

Fig. 56. *Qinscyphus necopinus* Liu et al. (2017) from the lower Cambrian, Kuanchuanpu Formation, Zhangjiagou section, Shaanxi Province, China. The SEM images on the left are the holotype (A-B) and paratype (C, UMCU 2015XQB087; D, UMCU 2015XQB089). The artistic reconstruction is shown on the right. Scale bars represent 500 µm. Modified from Liu et al., 2017.

3.2.1.5 Hexaconulariids

Conulariids is an extinct and poorly understood fossil group which appear in the fossil record from the Edicaran period and may have ancestor earlier (Jarms 1991, Van Iten et al. 2006, Ivantsov 2017). The group disappears during the Triassic period (Babcock and Feldmann 1986). Typical conulariids roughly resemble an ice-cream cone with a four-fold symmetry and a shell-like structure made up of rows of calcium phosphate rods. The soft anatomy of conulariids is poorly known. A holdfast seems to have maintain the pointed end of the cone attached to hard substrate (Babcock and Feldmann 1986). These characteristics and very superficial resemblances with modern sea anemones or coronate scyphozoans have led authors (Van Iten et al. 2006) to consider conulariids as possible cnidarians. The shell of conulariids is phosphatic (a variety of fluorapatite called francolite) and multilamellate with alternations of organic-rich and organic-poor layers (Ivantsov 2017).

Hexaconulariids are common elements in the Cambrian SSF-assemblages of China including those from the Kuanchuanpu Formation. The overal morphology of the phosphatized three-dimensionally preserved hexaconulariids is that of other conularids. Hexaconulariids have a conical shape with six faces (two pairs are relatively narrower than the remaining four; see Fig. 57), a round apical end and a wide opening. Four longitudinal grooves run between the narrow and broad faces. Faces are ornamented with closely-spaced ridges (He 1987, Van Iten, Maoyan and Li 2010) (Fig. 58).

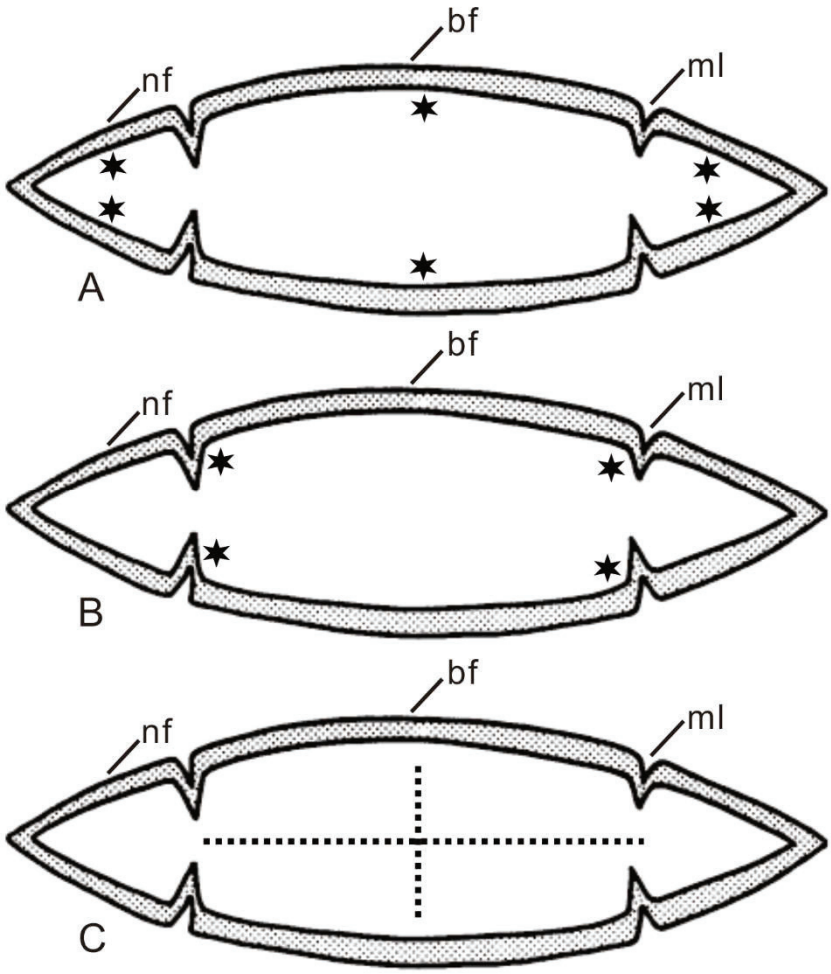

Fig. 57. Transverse section through an unnamed hexaconularids. A. Showing the possible hexaradial symmetry based on the six faces (marked by the solid hexagonal stars). B. Showing a tetraradial symmetry based on the four mid lines (marked by the solid hexagonal stars). C. Showing the possible bilateral symmetry (marked by the dotted lines). Abbreviations: nf, narrow face; bf, broad face; ml, mid line. Modified from Conway Morris and Chen, 1992.

Although hexaconularids display repeated features (e.g. six faces separated by four longitudinal mid line) (Conway Morris and Chen 1992, Van Iten et al. 2010, Ivantsov 2017) these organisms do not display a hexaradial (Fig. 58 A) or tetraradial symmetry (Fig. 57 B). Instead their shell has a bilateral symmetry (Fig. 57 C). The symmetric pattern of hexaconularids needs further studied.

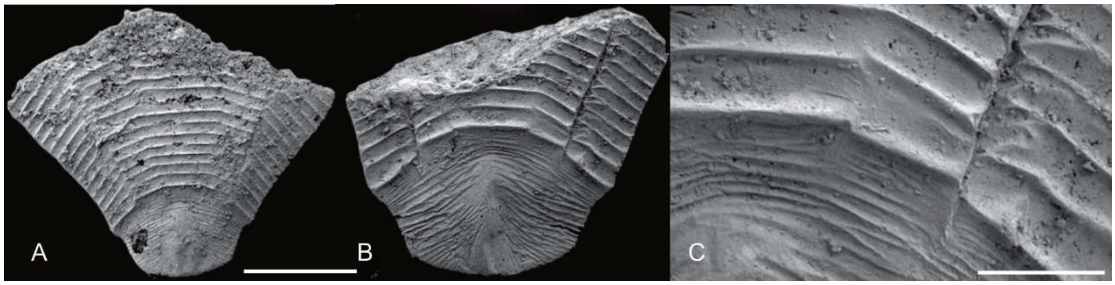

Fig. 58. ***Hexaconularia sichuanensis*** from the Kuanchuanpu Formation, Sichuan Province, China. A. Broad side view of the specimen NIGP 150159. B. Broad side view of the specimen NIGP 150162 (apertural end broken. C. Close-up of B, showing smooth transition between apical and abapical regions. Modified from Van Iten et al., 2010. Scale bars: 150 µm in A-B; 50 µm in C.

There is a considerable size difference between the hexaconulariids from the Kuanchuanpu Formation and the conulariids from other stratigraphic levels. Their size (cone length) is generally below 2mm (Van Iten 1991a, Van Iten et al. 2010). As for the vast majority of conulariids, the internal anatomy and soft parts of hexaconulariids is virtually unknown, which severly limits discussions concerning their phylogenetic affinities. However, Van Iten et al. (2005 a, b, 2006a; 2014) suggested possible affinities with scyphozoans based on the overall morphology of the shell resembling the segmented pattern of the stephanoscyphistoma of coronate polyps (Silveira 2002).

3.2.1.6 *Carinachitiids*

Carinachitids form a relatively large group of intriguing Small Shelly Fossils, which were first introduced by Qian (1977) based on material from the Kuanchuanpu Formation, Shizhonggou section, Shaanxi Province, China and comprise the following taxa: *Carinachites spinatus* (Qian 1977), *Carinachites tetrasculus* (Jiang 1980), *Pentaconularia ningqianggensis* (Liu et al. 2011), *Emeiconularia trigemme* (Qian 1999), and *Emeiconularia amplcanalis* (Liu et al. 2005). The exoskeleton of carinachitids is tubular with convex faces separated from each other by deep corner sulci. They generally have a tetraradial symmetry (Figs. 59-60) with the exception of rare triradial and pentaradial forms (Figs. 61-62). Typical carinachitids have four broad faces covered with crumpled ridges or spines, four corner sulci bearing dense tiny stripes (Liu et al. 2011, Conway Morris and Chen 1992, Qian 1977).

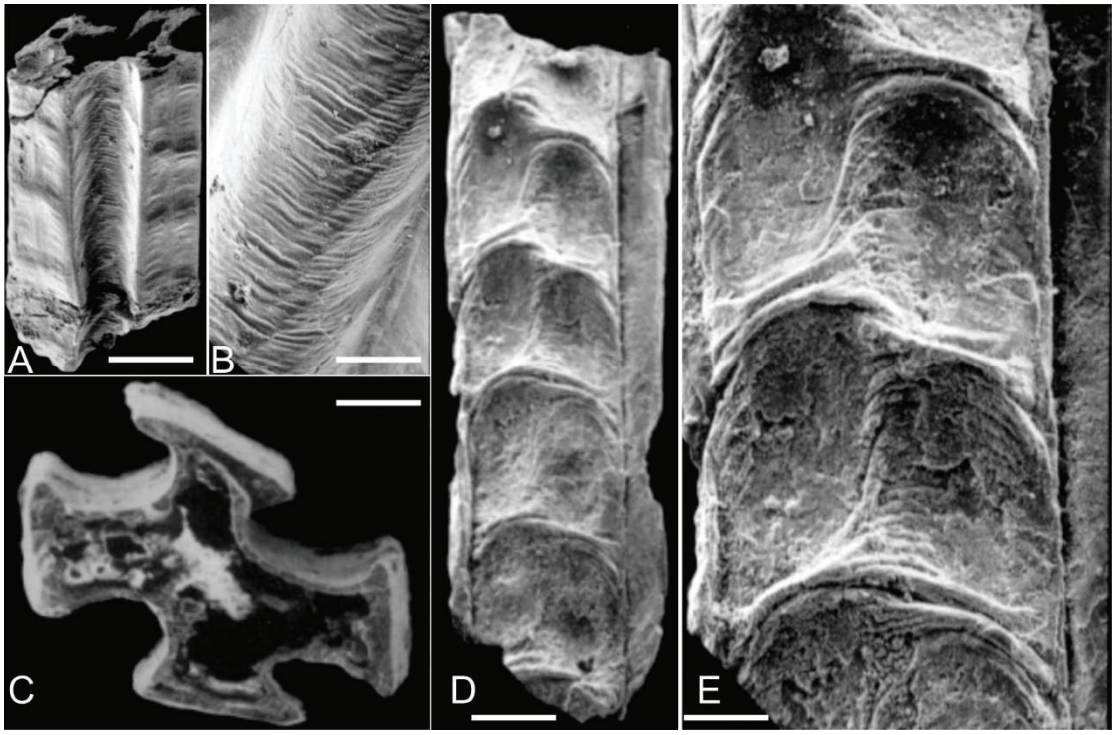

Fig. 59. ***Carinachites spinatus*** **Qian (1977)** from the Kuanchuanpu formation, Piaojiaya section, Shaanxi Province, China. A. Specimen 88-30215; longitudinal view on the overall morphology. B. Enlargement of A; showing the deep corner sulci growing densely tiny stripes. C. Specimen 88-30209, transverse section showing the tetraradial symmetry. D. Specimen 88-30216; showing the broad face covered with the crumpled ridges. E. Enlargement of D. Modified from Conway Morris and Chen, 1992. Scale bars: 150 µm in A, C-D; 20 µm in B; 50 µm in E.

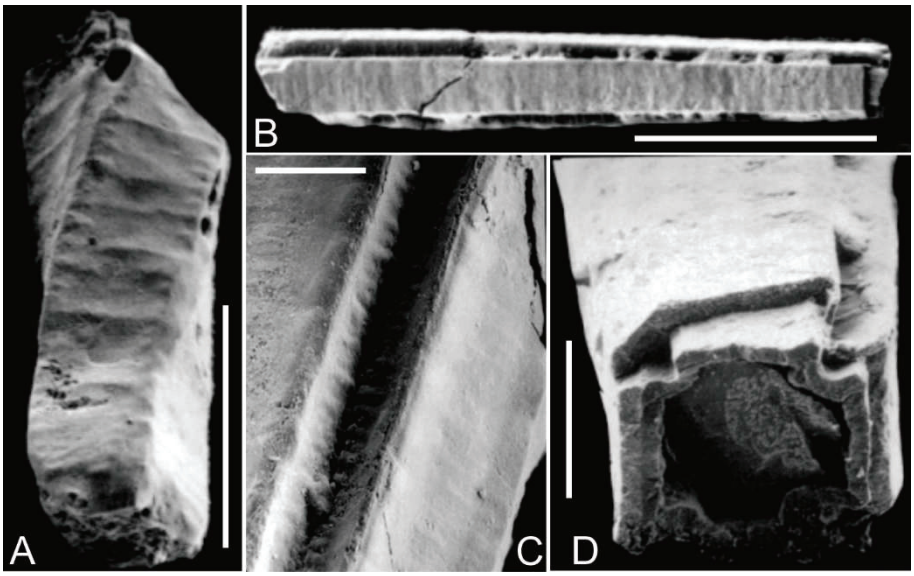

Fig. 60. ***Carinachites tetrasculus*** **Jiang, 1980** from the Kuanchuanpu Formation, Maidiping section, Sichuan Province, China. A. The specimen 88-30234; oblique view on the broad face covered with the gentle transverse ridge. B. The specimen 88-30245; flat view on overall morphology. C. Close-up of B; showing the narrow corner groove with the gentle transverse tiny stripes. D. The specimen

88-30245; showing the tetraradial symmetry. Modified from Conway Morris and Chen, 1992. Scale bars: 200 µm in A-B; 20 µm in C; 100 µm in D.

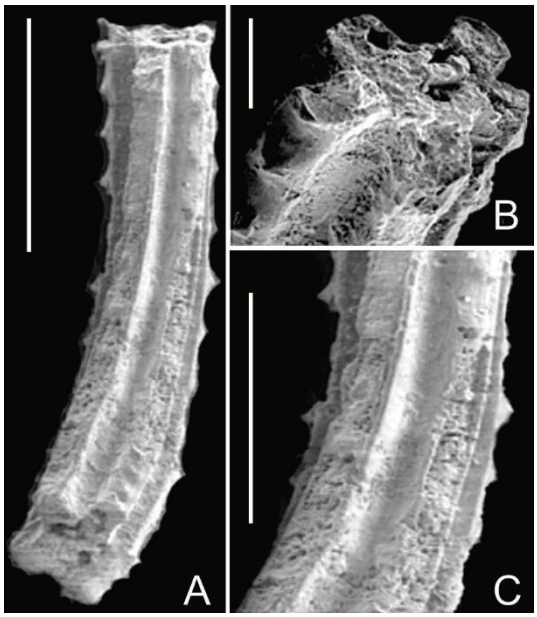

Fig. 61. ***Pentaconularia ningqianggensis*** **Liu et al., 2011** from the Kuanchuanpu Formation, Shizhonggou section, Shaanxi Province, China. A. Holotype of *P. ningqianggensis*, longitudinal view on the overall mophology (the broad face covered with the rough wrinkled ridges and the smooth corner groove). B. Cross section of A, showing the pentaradial symmetry. C. Close-up of A. Scale bars: 1 mm in A; 200 µm in B; 500 µm in C. Modified from Liu et al., 2011.

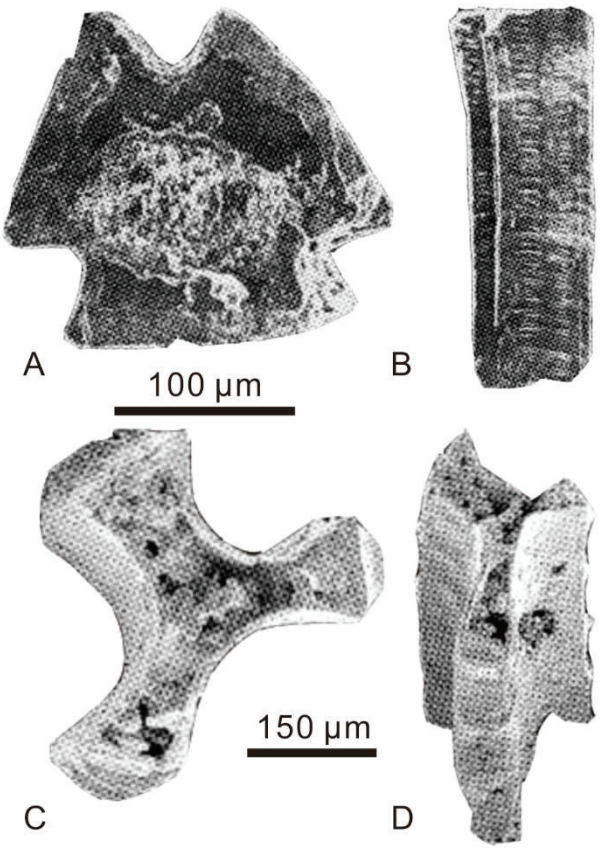

Fig. 62. A-B, *Emeiconularia trigemme* Qian, 1999 from the Kuanchuanpu Formation, Maidiping section, Sichuan Province, China. Showing the wide face covered with the gentle wrinkled ridges and the relative narrow sulci and the triradial symmetry. **C-D, *Emeiconularia amplcanalis* Liu et al., 2005** from the Kuanchuanpu Formation, Shizhonggou section, Shaanxi Province, China. Showing the narrow face covered with the rough wrinkled spines and the broad sulci. Scale bars: 100 µm in A-B; 150 µm in C-D. Modified from Liu et al., 2005.

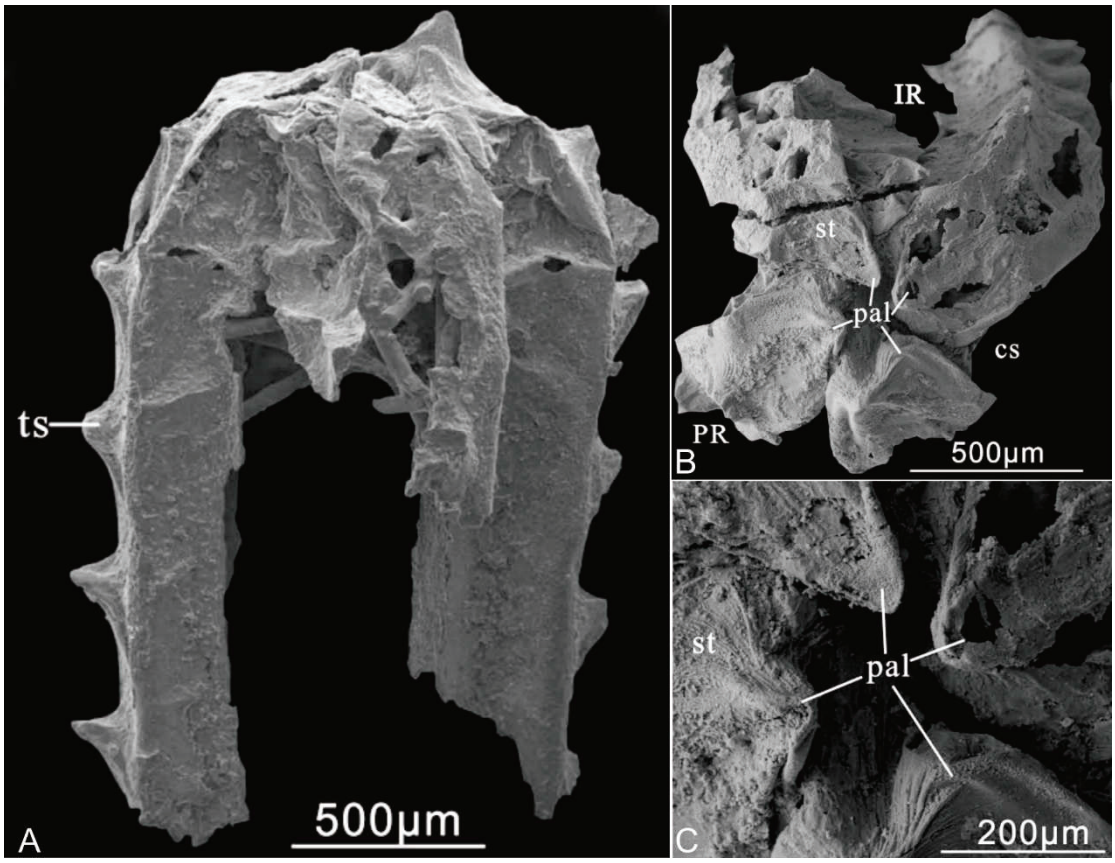

Fig. 63. *Carinachitids spinatus* with apertural lobes from the lower Cambrian Kuanchuanpu Formation in South China. A. Side view of the *C. spinatus*, showing the transverse thorn-like spines on the broad face. B. Vertical view of the *C. spinatus*, showing the four perradial apertural lobes evenly surrounding the oral part. Each lobe growing the regular tiny stripes. C. Zoomed area of oral part in B. IR, interradius; PR, perradius; cs, corner sulci; pal, perradial apertural lobes; st, striations; ts, thorn-like spines. Modified from Han et al., 2017.

Important key information is lacking concerning *Carinachitids*, especially the detailed 3D morphology of their aperture, their exoskeletal growth pattern and their internal organs. However, Han et al., (2017) described a single specimen of the tetramerous *Carinachites spinatus* Qian, 1977 which displays four oral apertural lobes surrounding the mouth opening (Han et al. 2018)(Fig. 63).

3.2.2 Other faunal components

The SSF-assemblages from the Kuanchuanpu Formation contain a great variety of other fossil organisms such as algal / bacterial colonies and the remains of several animal groups such as protostomes deuterostomes. They are represented by a huge variety of exoskeletal elements such as sclerites, shells, spines, cuticular remains and more rarely by whole minute organisms (e.g. ecdysozoan worms, early deuterostomes). Some of these microfossils may belong to molluscs, chaetognaths (e. g. *Protohertzina* spp.; see (Vannier et al. 2007)) whereas others such as *Anabarites* spp. (Bengtson et al. 1990, Qian 1977) remain more enigmatic. The problematic hyoliths are documented a wide geographical distribution and a relative long startigraphic ranges not only found from studied fauna but the later SSFs assemblages, e.g. south Australia, north China (Skovsted et al. 2016).

3.2.2.1 Ecdysozoans

Ecdysozoans are protostome animals including Arthropoda (insects, chelicerates, crustaceans, and myriapods), Onychophora, Tardigrada, Nematoda, and several smaller phyla such as Priapulida, Kinorhyncha (both in Scalidophora) and Loricifera (Aguinaldo et al. 1997, Dunn et al. 2008). All members of the group grow by moulting their exoskeleton (ecdysis). Ecdysozoans are already highly diverse and abundant in Cambrian marine communities (especially arthropods) as exemplified by exceptionally preserved biota (e.g. Chengjiang, Burgess Shale).

Eopriapulites sphinx Liu et al. (2014a) is one of the best example of exceptionally well-preserved ecdysozoan worms found in the Kuanchuanpu Formation, that closely resembles extant priapulid scalidophorans. *Eopriapulites sphinx has* an annulated trunk, an introverted proboscis with a terminal mouth, 18 pharyngeal teeth surrounding the mouth and an eversible introvert with 18 longitudinal rows of conical scalids (Liu et al. 2014c) (Fig. 64 A-B). These features occur in modern scalidophorans. The morphology of the posterior end of *Eopriapulites sphinx* is repoted later which surpposes a possible anus at the body end (Shao et al. 2016) (Fig. 64 C-D).

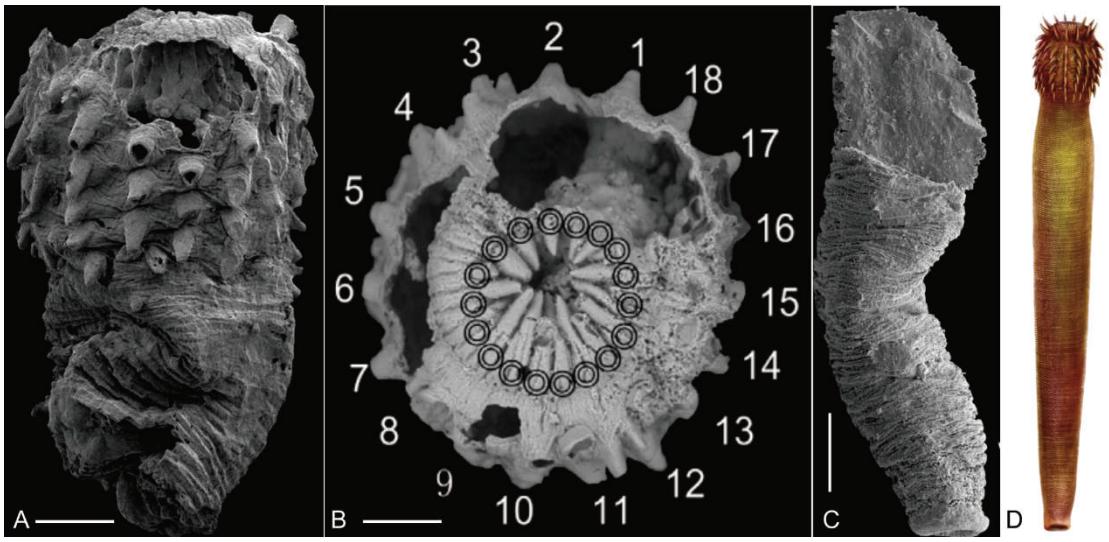

Fig. 64. *Eopriapulites sphinx* Liu et al., 2014c, a priapulids-like worm from the lower Cambrian Kuanchuanpu Formation, Zhangjiagou section, Shaanxi Province, China. A. Lateral view. B Oral view to show the 18 longitudinal rows of introvert scalids and 18 pharyngeal teeth in the basal circlet. C. The posterior end of *E. sphinx*. D. Artistic reconstructions. From Liu et al., 2014c and Shao et al., 2016.

Another scalidophoran animal, *Eokinorhynchus rarus* Zhang et al. (2015) closely similar with modern kinorhynchs also occcur in te Kunachuanpu biota (Zhang et al. 2015). As for *Eopriapulites sphinx*, the excellent preservation of the specimens allowed accurate 3D reconstructions to be made and close comparisons with extant representatives of Kinorhyncha. *Eokinorhynchus rarus* possessed an introvert with pentaradially arranged hollow scalids, a pharynx with octoradially arranged teeth, a neck with 5 circlets of scalids and caudal spines (Fig. 65).

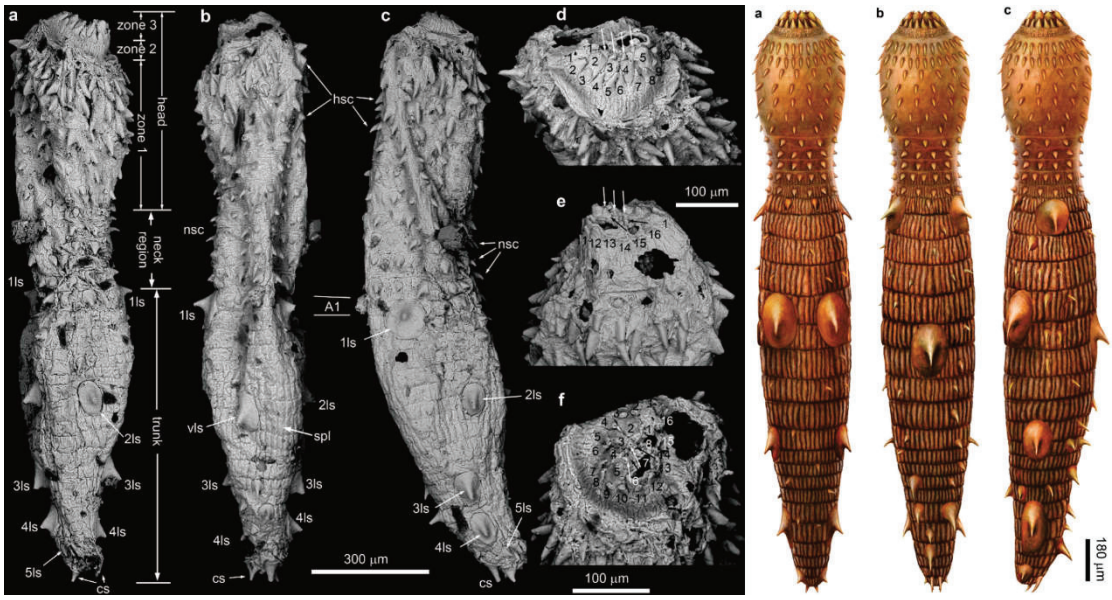

Fig. 65. *Eokinorhynchus rarus* Zhang et al., 2015 are supposed to close to kinorhynchs from from the lower Cambrian Kuanchuanpu Formation, Xinli section, Sichuan Province, China. SEM images show the holotype of *E. rarus*. Dorsal, ventral, and right lateral views of artistic reconstructions are shown on the left side. Abbreviations in SEM images: an, anus; cs, caudal spine; hsc, head scalid; ls, large sclerite; 1ls–5ls, 1st to 5th pair of large sclerites; nsc, neck scalid; spl, small plate; vls, ventral large sclerite. Modified from Zhang et al., 2015.

Many other cuticular remains which most probably belong to ecdysozoan animals occur in the SSF-assemblages from the Kuanchuanpu Formation (Zhang, Maas and Waloszek 2018) and are awaiting to be studied.

3.2.2.2 Deuterostomes

Deuterostomes are of particular significance because they include the group we belong to (chordates, vertebrates) as well as very diverse and abundant present-day animals such as echinoderms and hemichordates. The early Cambrian Chengjiang biota (*ca.* 521 Ma) has provided a wealth of information on the early evolution of chordates (Shu et al. 2003b, Shu et al. 1999) and has revealed the existence of several problematic deuterostome groups such as vetulicolians (Shu et al. 2010, Ou et al. 2012) and vetulocystids (Shu et al. 2004). The discovery of *Saccorhytus coronarius* (Han et al. 2017) in the Kuanchuanpu Formation (*ca.* 535 Ma) brings light on some of the most primitive deuterostomes ever found so far (Fig. 66). *Saccorhytus coronarius* is millimetric fossil with a bag-like body and single prominent opening interpreted as the mouth. The mouth is associated with folds, and followed by up to four conical openings on either side of the body as well as possible sensory structures. The lateral openings probably served to expel water and waste material. Although this animal has no modern counterparts, it shows similarities to both the vetulicolians and the vetulocystids from the Chengjiang biota. Han et al. (2017) suggested that *Saccorhytus* represented a key step in deuterostome evolution and that the development of lateral openings may have been co-opted as pharyngeal gills through the evolution of the group (Ou et al. 2012). *Saccorhytu*s was interpreted as a meiofaunal animal (Han et al. 2017).

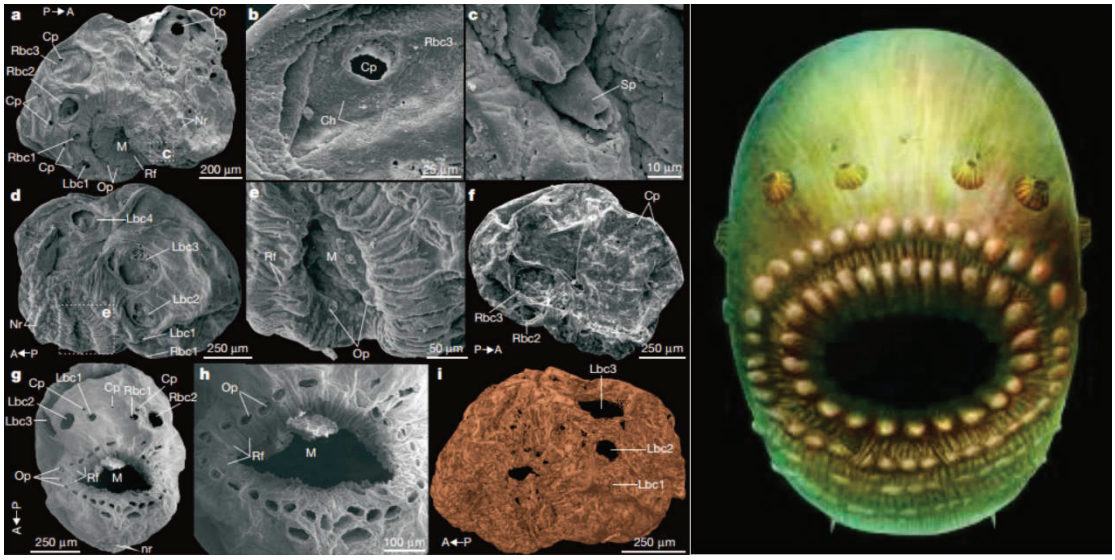

Fig. 66. ***Saccorhytus coronarius*** **Han et al., 2017**, possible ancient deuterostomes from the lower Cambrian Kuanchuanpu Formation, Zhangjiagou section, Shaanxi Province, South China. SEM images represent the holotype XX45-20 and the paratype XX45-56, XX48-64 on the left side. a – c. Holotype XX45-20. a. Right side. The mouth (M) arched dorsally along the anterior–posterior axis. b. Chevron pattern (Ch) on the inner surface of the integument. c. A spine (Sp) close to the mouth. d – f. XX45-56. d. Left side. e. Detail of the dorsally arched and folded mouth with radial folds (Rf) and oral protrusions (Op) in d. f. Circular pores (Cp) on the dorsal, right side. g – i. XX48-64 with limited compression. g. Ventral view, showing body cones (Bc) bilaterally arranged around the anterior, including the mouth. Two circular pores are adjacent to the first body cones (Bc1) and a small circular pore is on the mid-ventral line of the body. h. Oral protrusions lacking distal ends and appearing as a circle of pores. i. Left view reconstructed by microcomputerized tomography data. Lbc1 – Lbc4, left body cones; Nr, nodular rugae; Rbc1 – Rbc4, right body cones; Rf, radial folds; Sc, sub-layer of cuticle; arrowed AP, anterior–posterior axis. Artistic reconstruction of S. coronarius on the right side. Modified from Han et al., 2017.

The SSF assemblages from the lower Cambrian Kuanchuanpu Formation have yielded a remarkable variety of fossil organisms represented by whole or fragments of bodies, and isolated exoskletal elements. Previous authors have described scalidophoran worms possibly related to Kinorhyncha and Priapulida, deuterostomes and assumed cnidarians. The cnidarian affinities of numerous embryonic and larval forms seems to be well established and is supported by X-Ray microtomographic data. Although the ontogeny of these assumed cnidarians has no counterpart in modern representatives of the groups, authors suggest possible affinities with modern lineages such as scyphozoans, cubozoans, anthozoans. The position of numerous, more enigmatic, groups such as hexaconulariids and carinachitiids remains uncertain due to the lack of information concerning their internal structure and anatomy.

Chapter 4: Material and methods

Chapter 4: Material and methods

4.1 Sampling and extracting microfossils from rock

The fossil material studied here was collected from the lower Cambrian Kuanchuanpu Formation in the Shaanxi Province, South China (see geological and stratigraphical framework in Chapter 3). Rock samples were taken from the Shizhonggou section (Ningqiang County) and the Zhangjiagou section (Xixiang County) (see locality map in Fig. 40) to be processed in laboratory. Microfossils were extracted from phosphatic limestones via a standard acid digestion of phosphatic limestones using 7% acetic acid (Fig. 67). Dried residues with a grain-size >60 µm were sorted and picked under a binocular microscope.

All microfossil specimens from the Kuanchuanpu Formation are deposited at the Early Life Institute (ELI, collection numbers), Northwest University, Xi'an, Shaanxi Province, China. This fossil material and the corresponding microtomography data are available on request via Prof. Jian Han (Northwest University, Xi'an). The holotype of *Yunnanoascus haikouensis* (No. YDKS-35; see Hu et al. (2007) is deposited at the Nanjing Institute of Geology and Palaeontology, Chinese Academy of Sciences.

Fig. 67. A. One sampling point of the Kuanchuanpu Formation, Shizhonggou section, Shaanxi Province, China. B. Dissolving the phosphatic limestone at room. C. The residues after dissolution of the phosphatic limestone.

4.2 Observations and reconstructions

Specimens of interest were mounted on stubs and sputtered with gold to be observed under the Scanning Electron Microscope (SEM). Primary and backscattered electron microscopy (BSE) and energy-dispersive spectroscopy (EDS) analysis without coating were conducted with a HITACHI SU3500 SEM. Light photographs were taken using a Canon 5D Mark II camera.

Fig. 68. A-B. The computed X-ray Microtomography (XTM) at Tohoku University, Japan. C-D. The synchrotron X-ray Microtomography (SRXTM) at Spring-8 in Hyogo, Japan.

The best preserved microfossils or those with the potential to have internal structures preserved, were prepared for more detailed investigations via Computed X-ray Microtomography (XTM) at Tohoku University, Japan and Synchrotron X-ray Microtomography (SRXTM) at Spring-8 (third-generation large synchrotron radiation facility) in Hyogo, Japan (Fig. 68). SEM and XTM were used in order to obtain high-resolution images of the external and internal features, respectively. Thousands of images of virtual thin-sections through specimens were acquired at a resolution of 1004 * 1004 pixels (XTM) and 1920 * 1920 pixels (synchrotron XTM) (e.g. (Wang et al.

2017)). XTM data were processed using V.G. Studio 2.2 Max in order to enhance contrast between key internal anatomical features (artificial colours) and to generate detailed three-dimensional reconstructions of the microfossils (see examples in Chapter 5). Cladistic analysis was carried out using PAUP* v. 4.0 b10 (Swofford 2003) and TNT 1.1 (Goloboff, Farris and Nixon 2008). The analyzed characters are taken from (Marques and Collins 2004, Van Iten et al. 2006, Han et al. 2016a).

4.3 Interpretations

The terminology used here to described cnidarian or cnidarian-like fossils is that of previous works on Cambrian and extant cnidarians (Thiel 1966, Harrison 1991, Hyman 1940, Werner 1973, Gershwin and Alderslade 2006, Han et al. 2013, Han et al. 2016b). The definition of the meridian plane in these specimens follows Han et al. (2013, 2016b). We follow the current classification of Cnidaria which encompasses the Class Anthozoa and the Subphylum Medusozoa with the four following classes: Cubozoa (box jellyfish and sea wasps), Hydrozoa (hydroids and hydra-like animals), Scyphozoa (true jellyfish), Staurozoa (stalked jellyfish) (Daly et al. 2007).
The abbreviations used in the text and text-figures are as follows:
aal, adradial apertural lobe; al, apertural lappet; ac, adradial canal; af, adradial furrow; afl, adradial fold lappet; afr, adradial frenulum; aml, adradial marginal lamellae; an, annuli; an, anus; apcp, adradial peri-claustral pocket; as, accessory septum; bc, bell cavity; bf, broad face; bsp, basal septal pocket; cb, circular belt; cc, circumferential constriction; cg, coronal groove; cg, circumferential groove; cl, claustrum; clp, claustral projections; co, column; co, collar; cp, corner pillar; crm, circumferential muscle; cs, coronal stomach; cs, corner sulci; cs, caudal spine; csc, central stomach cavity; en + pe, egg envelope + periderm; es, esophagus; eu, exumbrella; fepf, first endodermic pentagonal funnel; g, gonad; gc, gastric cavity; gl, gonad-lamella; go, gonad; go, gastric ostium; hsc, head scalid; ho, holdfast; ial, interradial apertural lobe; ic, interradial canal; icp, interradial corner pillar; if, interradial furrow; ir, interradial ridges; is, interradial septum; isr, interradial septal ridge; isur, interradial subumbrellar ridges; ln, lappet node; ls, large sclerite; mb, manubrium; mc, manubrial corner; me, mesentery; mf, mouth field; ml, marginal lappet; ml, mid line; mo, mouth; mp, mesogonial pockets; NCB, North China block; nf, narrow face; Nr, nodular rugae; nsc, neck scalid; oa, oral arm; od, oral disc; om, organic material; pal, perradial apertural lobe; pc, perradial canal; pd, pedal disc; pe, pedicle; pf, perradial furrow; pfl, perradial fold lappet; pfr, perradial frenulum; ph, phacellus; pmp, perradial mesogonial pockets; ps, perradial septum; pp, perradial pocket; ppep, perradial peri-esophageal pocket; pt, pharyngeal teeth; r, rhopalium; rc, radial canal; Rf, radial folds; rg, ridge; rm, retractor muscle; rr, radial ridge; sc, scalid; Sc, sub-layer of cuticle; SCB, South China block; sepf, second endodermic pentagonal funnel; sf, septal funnel; sn, septal nodes; sp, suspensorium; sph, stalk of phacellus; spl, small plate; srt, septal root of tentacles; st, striations; stl, stellate ornaments; su, subumbrella; suc, subumbrella cavity; t (te), tentacle; tb,

tentacular bud; tepf, third endodermic pentagonal funnel; ts, thorn-like spines; vc, valarial canal; ve, velarium; vls, ventral large sclerite; •, adradii; *, perradii; →, interradii.

Chapter 5: Results

Chapter 5: Results

This chapter presents the main results achieved during the course of my PhD, on early Cambrian cnidarians. They have been published (or are in the process of being published) in scientific journals in the form of articles which are reproduced here. An introductory paragraph summarizing the findings and conclusions accompanies each article.

1. Jian Han, Shixue Hu, Paulyn Cartwright, Fangchen Zhao, Qiang Ou, Shin Kubota, **Xing Wang**, Xiaoguang Yang. 2016. The earliest pelagic jellyfish with rhopalia from Cambrian Chengjiang Lagerstätte. *Palaeogeography*, *Palaeoclimatology*, *Palaeoecology*, 449, 166–173.
2. Jian Han, Yaoping Cai, James D. Schiffbauer, Hong Hua, **Xing Wang**, Xiaoguang Yang, Kentaro Uesudi, Tsuyoshi Komiya, Jie Sun. 2017. A *Cloudina*-like fossil with evidence of asexual reproduction from the lowest Cambrian, South China. *Geological Magazine*, 154 (6), 1294–1305.
3. Jian Han, Guoxiang Li, **Xing Wang**, Xiaoguang Yang, Junfeng Guo, Osamu Sasaki, Tsuyoshi Komiya. 2018. *Olivooides*-like tube aperture in early Cambrian carinachitids (Medusozoa, Cnidaria). *Journal of Palaeontology*, 92 (1), 3–13.
4. **Xing Wang**, Jian Han, Jean Vannier, Qiang Ou, Xiaoguang Yang, Kentaro Uesugi, Osamu Sasaki, Tsuyoshi Komiya. 2017. Anatomy and affinities of a new 535-million-year-old medusozoan from the Kuanchuanpu Formation, South China. *Palaeontology*, 60 (6), 853–867.
5. **Xing Wang**, Jean Vannier, Xiaoguang Yang, Shin Kubota, Qiang Ou, Xiaoyong Yao, Kentaro Uesugi, Osamu Sasaki, Tsuyoshi Komiya, Jian Han (submitted). A Coronate-like medusa from the early Cambrian Kuanchuanpu Formation, south China.

5.1 Pelagic jellyfish from the early Cambrian Chengjiang biota (*ca.* 521 Ma)

Modern cnidarian medusozoans forma huge group which includes four classes: Staurozoa, Scyphozoa, Cubozoa and Hydrozoa (Daly et al. 2007). They generally possess a diphasic life cycle with successively a larva, a sessile asexual polyp and a pelagic sexual medusa stage. As we have seen in Chapters 1-2, molecular data predict a Precambrian origin of cnidarians, but the fossil record fails to provide compelling evidence of their presence before the Cambrian. Exceptionally preserved fossil medusozoans from the Middle Cambrian (Series 3, Stage 5) of Utah have long been the oldest fossil record for jelly fish. Indeed their tentacles, manubrium, subumbrella and exumbrella have direct counterparts in modern medusae, and have been assigned (Cartwright et al. 2007) to three extant cnidarian classes: the Hydrozoa, Cubozoa and Scyphozoa.

The Chengjiang Lagerstätte has opened new perspectives for studying the early evolution and diversification of numerous animal groups, including soft-bodied organisms such as cnidarians. This fauna owes its exceptional preservation to the fact that it was buried by periodic turbidity currents and to the early pyritization of its soft tissues shortly after death (Hou et al. 2017).

The purpose of this work was to test whether the early Cambrian Chengjiang biota contains cnidarians or not. We showed that *Yunnanoascus haikouensis* Hu et al. (2007), which had been interpreted as a member of the stem group Ctenophora based on assumed longitudinal 'comb-rows' comparable with those of extant (Harbison, Madin and Swanberg 1978, Brusca and Brusca 2003) and fossil ctenophorans from the Chengjiang biota (*Maotianoasus octonarius* and *Sinoascus papillatus*; (Chen 1997)) is actually a cnidarian. *Yunnanoascus haikouensis* lacks important ctenophore characters such as equally spaced meridional comb rows converging toward the apical sensory organs.

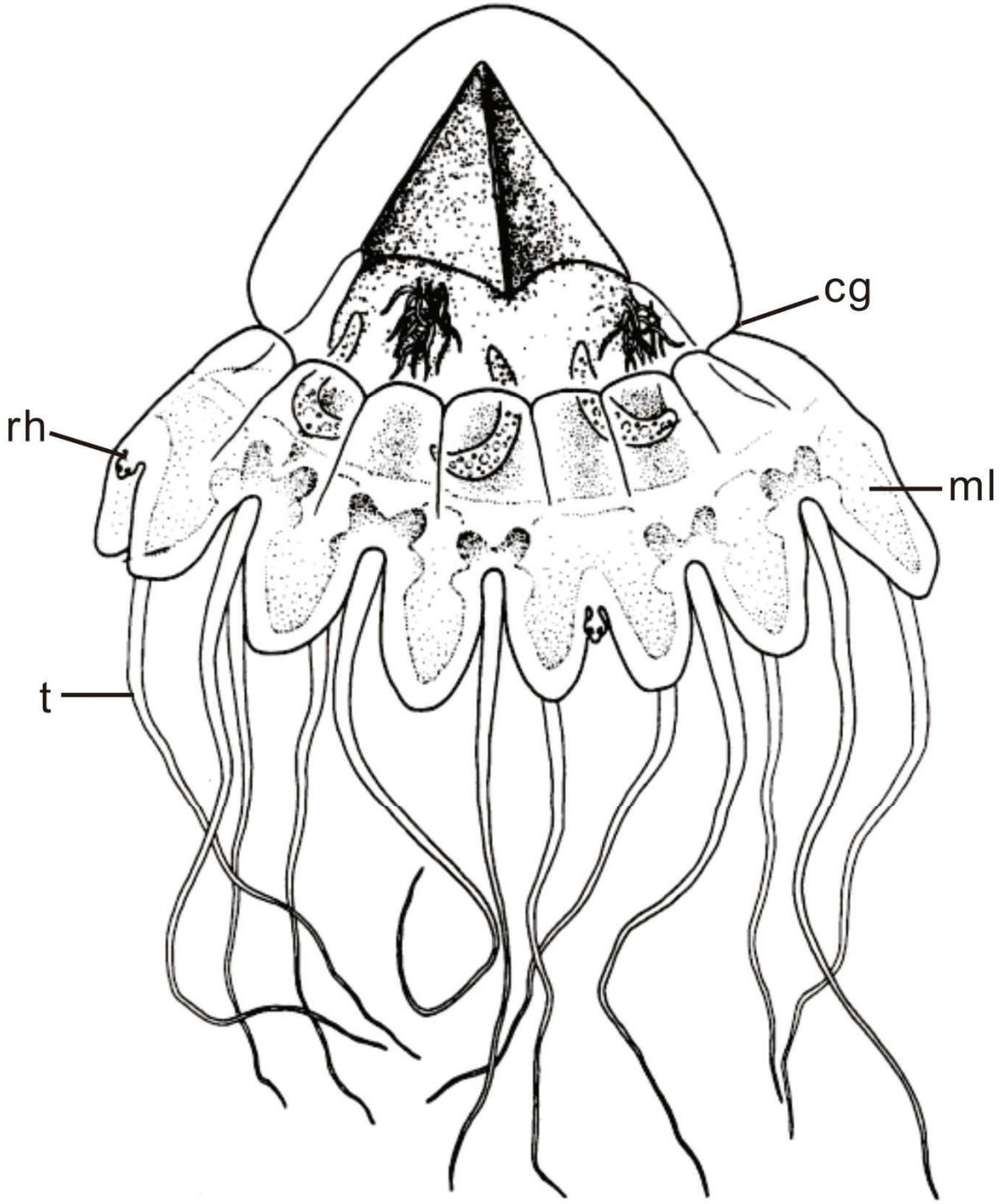

Fig. 69. Sketch of the extant coronate scyphozoan *Periphylla periphylla*. Abbreviations: cg, coronal groove; ml, margin lappet; rh, rhopalium; t, tentacle. Modified from Aria, 1997.

Detailed observations clearly revealed a set of evident medusozoan features: 1) tetraradial symmetry; 2) sixteen tentacles inserted along the bell margin; 3) 8 evenly spaced patches located between tentacles, interpreted as rhopalia; 4) coronal sinus; 5) marginal lappets; and 6) radial canals (Han et al. 2016a, Arai 1997) (Fig. 69).

An important conclusion of this study is that cnidarian medusozoans are represented in the 521-million-year-old Chengjiang biota and that *Yunnanoascus haikouensis* is the oldest indisputable fossil medusozoan. Another important implication of this study is that *Yunnanoascus haikouensis* was equipped with rhopalia which are known to play an important role in balancing the gravity of the medusa bell during swimming in the water column. These sophisticated organs indicate that early Cambrian jellyfish were adapted to living within the water column and do not seem to differ markedly from modern forms in terms of anatomy and lifestyles.

Palaeogeography, Palaeoclimatology, Palaeoecology 449 (2016) 166–173

Contents lists available at ScienceDirect

Palaeogeography, Palaeoclimatology, Palaeoecology

journal homepage: www.elsevier.com/locate/palaeo

The earliest pelagic jellyfish with rhopalia from Cambrian Chengjiang Lagerstätte

Jian Han [a,*], Shixue Hu [b], Paulyn Cartwright [c], Fangchen Zhao [d], Qiang Ou [e,f], Shin Kubota [g], Xing Wang [a], Xiaoguang Yang [a]

[a] State Key Laboratory of Continental Dynamics,Department of Geology, Northwest University, 229 Taibai Road, Xi'an 710069, P.R. China
[b] Chengdu Center, China Geological Survey, China
[c] Department of Ecology and Evolutionary Biology, University of Kansas, Lawrence, KS 66045, USA
[d] State Key Laboratory of Palaeobiology and Stratigraphy, Nanjing Institute of Geology and Palaeontology, Chinese Academy of Sciences, Nanjing 210008, China
[e] Early Life Evolution Laboratory, School of Earth Sciences and Resources, China
[f] University of Geosciences, Beijing 100083, China
[g] Seto Marine Biological Laboratory, Field Science Education and Research Center, Kyoto University, Shirahama, Nishimuro, Wakayama 649–2211, Japan

ARTICLE INFO

Article history:
Received 12 November 2015
Received in revised form 2 February 2016
Accepted 9 February 2016
Available online 20 February 2016

Keywords:
Pelagic
Medusozoa
Cambrian
Chengjiang
Medusa
Rhopalium

ABSTRACT

Modern cnidarian medusae generally show a triphasic life cycle with the succession of a larva, a sessile polyp and a pelagic medusa stage. The debate around the metagenesis of sessile polyps into pelagic medusae has lasted for more than 100 years. When pelagic forms originated is not clear. Hitherto, the earliest crown-group medusae have been found at Cambrian Stage 5 (traditional Middle Cambrian, 509 Ma) in Utah, while diverse stem-group medusozoans were found in the basal Cambrian Fortunian Stage. No reliable medusae have been found from Cambrian Series 2 Stage 3 (ca. 521 Ma), although the marine benthic community teemed with many phyla of bilaterians, sponges and ctenophores. Here, we reinterpret *Yunnanoascus haikouensis* Hu et al. (2007), originally described as a ctenophore, as a pelagic, predatory, crown-group medusozoan, based on the presence of rhopalia, possible radial canals and marginal tentacles. The medusae were a predatory member of the pelagic food web at the middle level of the ocean at Cambrian Stage 3.

1. Introduction

Cnidarian medusae are a conspicuous part of the modern marine realm. They typically exhibit a triphasic life cycle consisting of a planula larva, a sessile polyp stage and a pelagic, sexual medusa stage with sense organs, i.e. rhopalia. The rhopalia, which are in charginge of rhythmic body contraction and swimming (Ruppert et al., 2004), are a suite of club-shaped structures suited between a pair of marginal lappets, each containing a concentration of epidermal neurons, a pair of chemosensory pits, a statocyst, and often an ocelli. Given their different modes of development, it has been hypothesized that the medusoid form in different classes of Medusozoa might have been independently derived from a polyp-like form (Kraus et al., 2015; Salvini-Plawen, 1978). However, it is unclear when the pelagic forms arose. Molecular evidence suggests that cnidarian medusozoans originated deep within the Neoproterozoic (Park et al., 2012). The fossil record of medusae is rather sporadic. The soft-bodied fossil *Haootia quadriformis* Liu et al. (2014a) with possible muscular impressions reported from the lower Fermeuse Formation of the Bonavista Peninsula of Newfoundland (approx. 560 Ma) was compared to the sessile stauromedusans, although it lacks secondary tentacles, anchors, gonads and nematocyst clusters. Many exceptionally preserved stem-group medusozoans with a diverse set of internal anatomical structures arranged in tetra- or penta- radial symmetry were found in the basal Cambrian Fortunian Stage (ca. 535 Ma) in south China (Dong et al., 2013; Han et al., 2016; Han et al., 2013); however, most of them remain at the embryonic stage and some of their polypoid forms were contained inside a tubular peridermal theca (see Steiner et al., 2014). Even if some of them have developed strong coronal muscles (Han et al., 2016), all of them, including the putative ephyra (Dong et al., 2013), lack the rhopalia necessary for pelagic life, thus calling into question whether any of these fossils represent true pelagic medusae. Hitherto, representatives of most major lineages of nektonic medusozoans with umbrellar shape, gonads, coronal muscles and elongate retractile tentacles possibly with nematocyst batteries were present in Cambrian Stage 5 in Utah (Cartwright et al., 2007). In the Chengjiang fauna, pelagic forms including both diploblastic ctenophores (Ou et al., 2015) and various bilaterians have been well documented in Cambrian Stage 3 (Hu et al., 2007; Vannier et al., 2009; Zhao et al., 2010). Although some discoid Chengjiang fossils (i.e. *Rotadiscus grandis*, *Stellostomites eumorphus*, *Heliomedusa orienta*)

* Corresponding author at: Early Life Institute, Northwest University, 229 Taibai Road, Xi'an 710069, PR China.
E-mail address: elihanj@nwu.edu.cn (J. Han).

http://dx.doi.org/10.1016/j.palaeo.2016.02.025
0031-0182/

were previously reported as medusae (Sun and Hou, 1987), they were later reinterpreted as organisms closely related to either lophophorates (Dzik, 1991; Zhang et al., 2009; Zhu et al., 2002) or stem-group deuterostomes (Caron et al., 2010). Here, we reinterpret *Yunnanoascus haikouensis* Hu et al., 2007 as a tetraradial pelagic medusozoan, rather than a ctenophore, on the basis of medusozoan-like diagnostic features including 16 pairs of thick-based marginal tentacles, 16 rhopalia, 16 marginal lappets and a manubrium. The interpretation of this fossil as a crown-group medusozoan during this vital interval (520 Ma) suggests that crown-group pelagic medusa were present as far back as the early Cambrian.

2. Materials and methods

The holotype (No. YDKS-35), the unique specimen of *Y. haikouensis*, is deposited in the Nanjing Institute of Geology and Palaeontology, Chinese Academy of Sciences. Photographs were taken using a Canon 5D Mark II camera. Backscattered electron microscopy (BSE) and energy-dispersive spectroscopy (EDS) analysis without coating were conducted on a HITACHI SU3500 scanning electron microscope with an EDS system. A cladistic analysis containing 25 taxa and 105 characters (Appendix 1) was analyzed in both PAUP* 4.0 b10 (Swofford, 2003) and TNT 1.1 (Goloboff et al., 2008). The data matrix (Appendix 2) derives in large part from the data in Han et al. (2016); Marques and Collins (2004) and Van Iten et al. (2006). All 105 characters have equal weight, 8 of them are constant, 24 variable characters are parsimony-uninformative and the remaining 73 characters are parsimony-informative.

3. Result

Systematic palaeontology
Phylum Cnidaria Verrill, 1865.
Subphylum Medusozoa Peterson, 1979.
Class Scyphozoa Goette, 1887.
Order, Family uncertain.
Genus *Yunnanoascus.*
Type species: *Y. haikouensis* Hu et al. (2007).
Revised diagnosis: Body with tetra-radial symmetry. Hemispherical central disc surrounding a wider coronal sinus. Bell margin with a ring of sixteen pairs of long thick-based tentacles with possible nematocyst batteries. Sixteen rhopalia slightly away from scalloped bell margin. Sixteen short triangular marginal lappets intercalated with tentacles. Sixteen radial canals with possible branches. Short cone-shaped manubrium without conspicuous oral lips.
Occurrence: Lower Cambrian Heilinpu Formation, Kunming, Yunnan Province, China (equivalent to Cambrian Stage 3).
Description:

(a) **Body:** The obliquely-laterally compressed body, 20 mm long and 10 mm in maximal width, consisting of a hemispherical central disc and a wide peripheral coronal sinus trailing with a ring of sixteen long strips interpreted here as tentacles (t) (Figs. 1*a*, 2*a*).

(b) **Tentacles:** On the incomplete counterpart specimen, either two of the sixteen tentacles are clearly grouped into eight prominent pairs that are distributed in different micro-bedding planes and more or less deviating from the body axis (Figs. 1*b*, 2*b*). The tentacles measuring ca. 10 mm in maximal length and display a wider, straight basal part (0.5 mm in maximal diameter) followed by an elongate thinner distal part (Figs. 1*c*, 2*a*,*b*). The tentacle base, comprising half of the entire tentacle, has a sharp boundary with the surrounding host rocks. Neighboring tentacles in each pair are parallel to each other but are more or less overlapping. The distal part of the tentacles taper gradually, some of them are slightly twisted or undulatory, indicative of flexibility. As seen on the tentacles of Middle Cambrian medusae (Cartwright et al., 2007), the entire surface of the tentacles is dark and displays dense, fine transverse striations (Fig. 1*c*). The distal part of some tentacles (Figs. 1*a*, 2*a*) display bright zones intercalated with dense dark zones, highly reminiscent of contracted tentacles bearing nematocyst batteries. Notably, tentacles with dense dark striations were originally interpreted as characteristic comb rows of ctenophores; however, the host yellowish rocks between the tentacles (Fig. 1*a*) support the hypothesis that the tentacles extend from the bell rather than being part of the bell itself as found in ctenophores.

(c) **Coronal sinus, marginal lappets:** The bell peripheral to the central dome is preserved as a wider crescent-shaped zone delimited by a conspicuous arc-shaped groove (Fig. 1*a*). The outer margin of the crescent zone displays a consecutive series of small serrate structures that are quite close to the tentacles roots (Figs. 1*a*, 2*a*). The crescentic zone and the serrate structures probably represent the coronal sinus (cs) and the marginal lappets (ml) (Fig. 2*a*) along the scalloped bell margin, respectively.

(d) **Rhopalia:** Approximately 1 mm away from the bell margin, an arched row of eight evenly spaced patches, deep brown in color and located at the spaces between the pairs of tentacles (Fig. 1*a*, *d*,*e*). These slightly concaved patches, round to subrectangular in outline, are ca. 0.5 mm in length and 0.3 mm in width, with the long axis parallel with the body axis. Due to weathering of the rocks, only one of them has a black carbon film (0.2 mm wide) on the surface; and the carbon film on other two patches remain as a few dark spots; the others show a naked surface that is much more reddish in color than ambient bell tissue (Fig. 1*a*). SEM observations and energy dispersal analysis reveal that they are composed of pyrite and organic carbon (Fig. 3), identical to that of the statoliths of co-occurring ctenophores (Ou et al., 2015). Thus, based on their disposition, morphology and diagenesis, it is reasonable to interpret these patches as rhopalia (rh), which in living medusae are composed of statoliths and pigmented ocelli. In addition, the rhopalia of the fossil specimen are consistent in size with those of scyphozoans (Arai, 1997) and cubozoans (ca. 0.3 mm) (Sötje et al., 2011). As eight rhopalia are invariably aligned in an arched row parallel to the arched coronal groove and marginal lappets, they are not lined as an ellipse, we infer that the specimen was obliquely-laterally compressed and another half of the medusa was concealed at the host rocks. Therefore, the medusa most likely has a total of sixteen rhopalia and 32 tentacles (Fig. 5).

(e) **Manubrium:** The main components of the central bell are distributed on two micro-bedding planes well separated by host muddy rocks. On the lower bedding plane, five to six short radial lines extend from the bell floor and converge toward the bell center, thus forming a cone-shaped profile with its tapered end directed adorally (Fig. 1*a*). The cone, half the height of the central bell, is interpreted as a manubrium (mb) inside a spacious deep subumbrellar cavity (Fig. 2*a*). No conspicuous oral lips are visible at the distal end of the manubrium.

(f) **Radial canals.** In contrast to the lower bedding plane, the upper bedding plane on the right side of the central bell displays four incomplete but thick rectangular blocks (trb) delimited by five evenly-spaced deep radial lines parallel to the body axis. Due to probable taphonomic bias, the block near the body center is the widest one measuring ca. 5 mm wide. The radial lines, at an estimated number of sixteen in total, run orally and bifurcate toward the coronal groove (Fig. 2). Some of their adoral bifurcations are visible deep within the coronal sinus, and thus we interpret them as

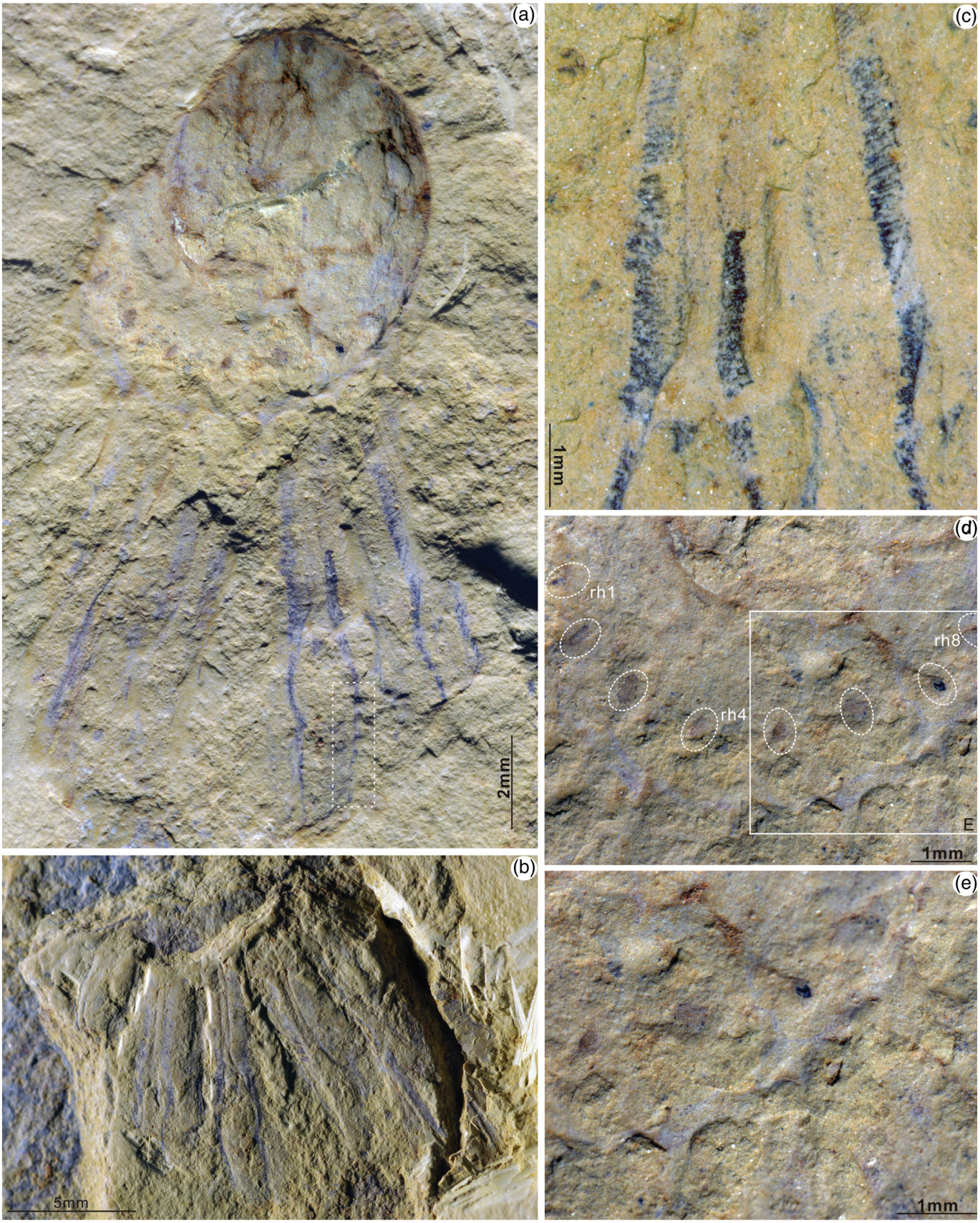

Fig. 1. *Y. haikouensis* Hu et al., 2007 from the early Cambrian Chengjiang Lagerstätte, China. (*a*) Part of the holotype; the 8th tentacle (rectangle area) likely bears nematocyst batteries. (*b*) Incomplete counterpart of the holotype. (*c*) Transverse stripes indicative of contracted tentacles with nematocyst batteries on the broad-based tentacles. (*d*) Close-up of the eight rhopalia (circled with white ellipses) and the scalloped bell margin. (*e*) Close-up of the bell margin showing the marginal lappets and four rhopalia (rh5–rh8) covered by carbon film.

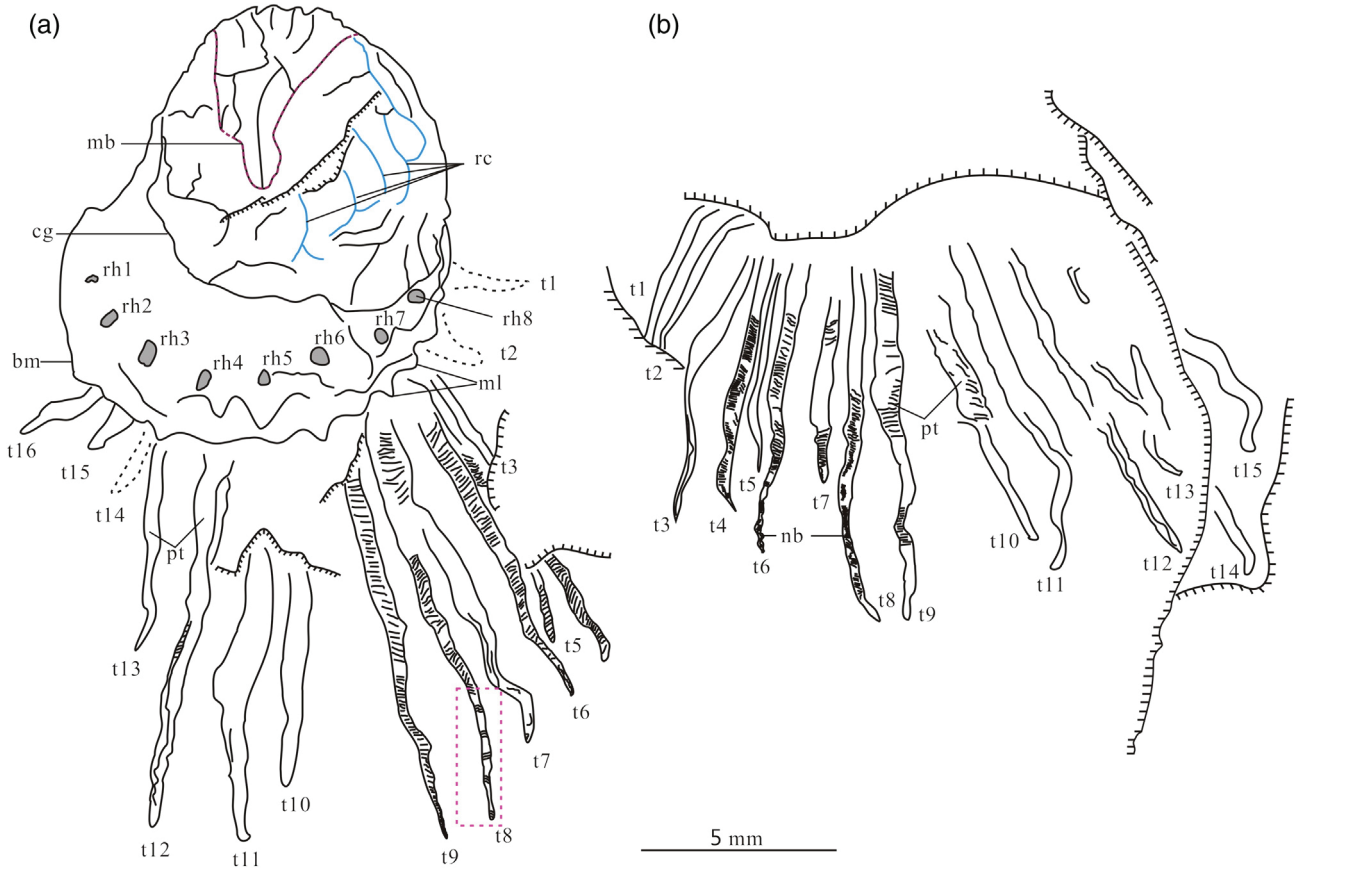

Fig. 2. Camera lucida drawings of the holotype specimen of *Y. haikouensis*. (*a*) Part of the holotype. (*b*) Counterpart. Abbreviations: bc, bifurcated canals; bm, bell margin; cg, coronal groove; cs, coronal sinus; m, mouth; mb, manubrium (red); ml, marginal lappets; nb, nematocyst battery; pt., proximal part of tentacle; rc, radial canals (blue); rh1–rh8, sc, subumbrellar cavity; serial number of rhopalia; t1–t16, serial number of tentacles; trb, thickened rectangle block. Scale bar = 5 mm.

radial canals (rc). The sub-rectangle blocks which alternate with the paralleling radial canals are apparently positive relief, possibly representing a ring of thickened mesoglea (Fig. 2*a*). No ring canal can be confirmed at the bell margin.

4. Taxonomic affinity

Y. haikouensis was originally interpreted as a ctenophoran as the longitudinal dark strips resemble comb rows of extant modern ctenophores (Hu et al., 2007). Now several lines of evidence can reject this hypothesis. First, the comb rows modern ctenophores are equally spaced meridional rows converging toward the apical sensory organs. Each row is composed of a transverse band of long, fused cilia on the body surface (Ruppert et al., 2004). In contrast, dark stripes on *Yunnanoascus*, which are separated by the host rocks, are connected to the body margin rather than distributed on the body surface; this is also supported by the twisted appearance of the distal part of dark strips, and thus, appreciate the current interpretation of strips as tentacles rather than comb rows. Second, Cambrian ctenophorans have diagnostic features of modern ctenophores such as an octamerous symmetry, prominent comb rows and an aboral sense organ with a statocyst; they are additionally characterized by a prominent aboral cone, conspicuous oral skirts and a sclerotized framework but are devoid of lateral tentacles (Conway Morris and Collins, 1996; Ou et al., 2015). *Yunnanoascus*, in contrast, has a hemispherical aboral bell floor, a series of rhopalia and multiple long tentacles extending from the bell margin, thus quite different from Cambrian ctenophores. Its absence of a stalk or pedal disc excludes affinity with either stauromedusans or anthozoans. *Yunnanoascus* seems unlikely to be a member of Hydrozoa as hydrozoans lack complex sense organs and their statocysts are located at the base of the tentacles. In addition, the characteristic velum of hydromedusae is not seen in the current specimen.

Yunnanoascus is less likely a cubomedusan. The wide-based tentacles arranged in pairs are highly reminiscent of the pedalia of extant cubomedusae (Conant, 1898). However, details of the gross morphology of *Yunnanoascus* differentiate it from extant cubomedusae. First, the cubozoan-type pedalia are smooth on the surface, and only the distal part of the tentacles bear rings of nematocyst-cells. In contrast, all tentacle surfaces of *Yunnanoascus* exhibits dense rings of transverse stripes similar to those of semaeostomeae scyphozoans (Russell, 1970). Second, marginal tentacles with a wide base are also seen in hydrozoans (i.e. *Sarsia princeps* Haeckel 1879)(Mayer, 1910) and scyphozoans (i.e. *Cyanea capillata* in (Russell, 1970)). Third, the paired tentacles in *Yunnanoascus* appear to be independent and they did not share the same tentacle base as extant chirodropida cubomedusae. Moreover, extant cubomedusans have only four groups of pedalia and four rhopalia, inconsistent with the sixteen rhopalia seen on *Yunnanoascus*. Finally, *Yunnanoascus* lacks other diagnostic features of cubomedusans such as box-like shape, four frenulae and a velarium.

Yunnanoascus appear to have a coronal groove and a coronal sinus resembling those of scyphozoan coronates; however, its coronal sinus shows no sign of coronate-type pedalia with solid tentacles sprouting from the exumbrellar wall. *Yunnanoascus* has some features of the Semaeostomeae scyphozoans, including marginal

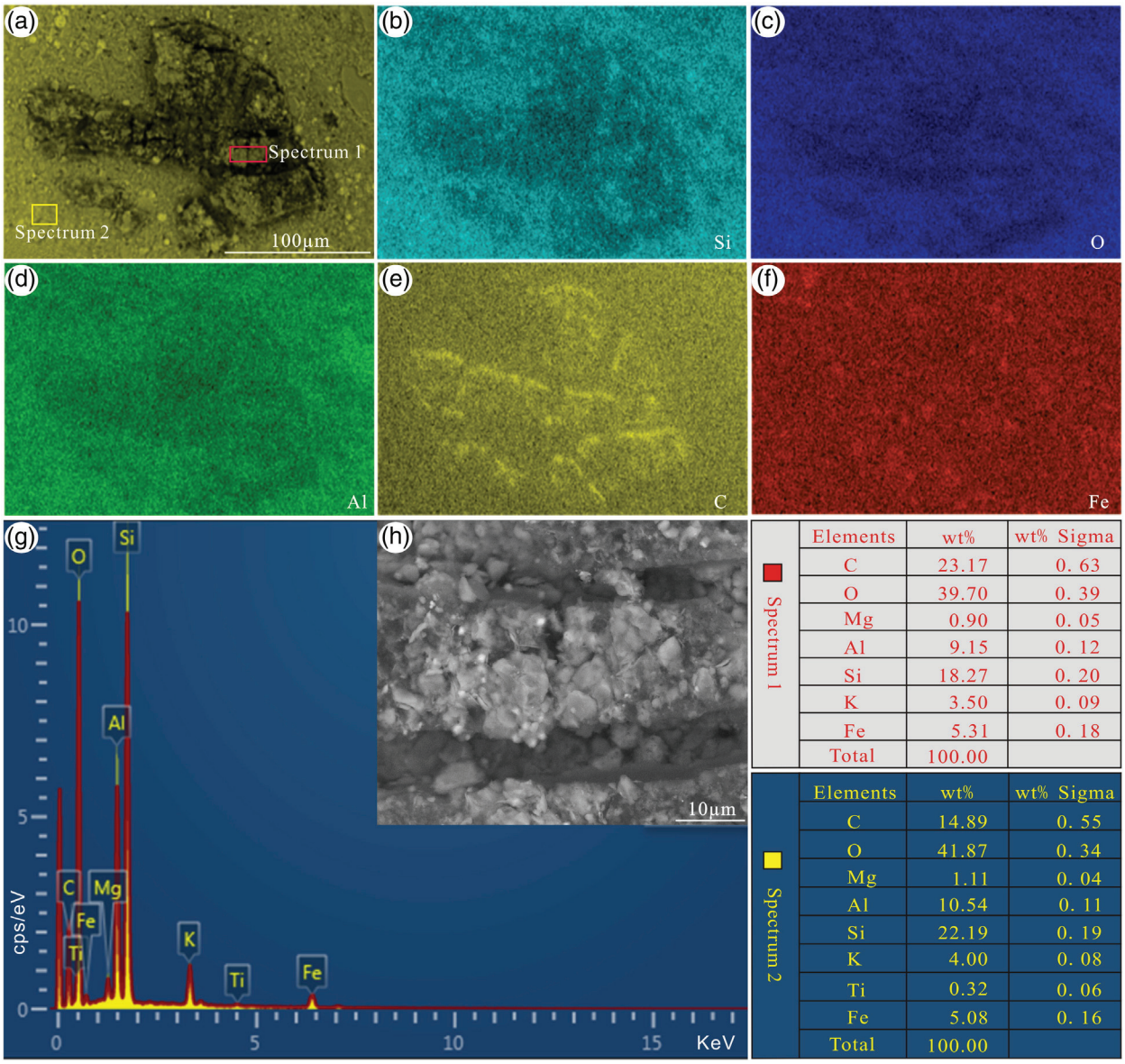

Fig. 3. Energy-dispersive spectroscopic analysis made at the seventh rhopalium on the holotype specimen of *Y. haikouensis* Hu et al., 2007. (*a*)–(*f*) Element maps of the seventh rhopalium. (*g*), Combined spectrum of rhopalium (spectrum 1, red rectangle in (*a*)) and background tissue (spectrum 2, yellow rectangle in (*a*)) of the bell. Note the high concentration of carbon on the rhopalium (spectrum 1). (*h*), Backscattered electron (BSE) image of the red rectangular area of the carbon in (*a*). (*a*)–(*h*) share the same scale bar in (*a*).

tentacles alternating with rhopalia, apertural lappets and bifurcated radial canals. Notably, 16 rhopalia and 16–48 tentacles are seen in *Diplulmaris* and *Phacellophora* (Semaeostomeae), particularly, the tentacles of the latter are arranged in 16 clusters (Mayer, 1910), quite resembling 16 pairs of tentacles in *Yunnanoascus*.

5. Phylogenetic analysis

We carried out a preliminary cladistic analysis based on 25 taxa and 105 characters in PAUP* 4.0 b10 and TNT 1.1. Unweighted branch-and-bound search of the data matrix in PAUP analysis yielded 189 shortest trees (tree length (TL) = 189, consistency index (CI) = 0.6243, rescaled consistency index (RC) = 0.4688). The successive weighting analysis (Marques and Collins, 2004; Van Iten et al., 2006) resulted in three trees (TL = 92.90023, CI = 0.864, RC = 0.794) that differ in the position of conulariids (Appendix 3). In the TNT analysis, we acquired a consensus tree based on three best trees (Appendix 4) generated by New-Technology search. These three trees differ in the position of Kuanchuanpu fossils between ELISN83-66 and ELISn31-31, and Utah fossils presumed to be Narcomedusae (Fig. 4*b*, Appendix 1). Apparently, the missing data of the fossils (up to 24 parsimony-uninformative characters) are the inherent sources of the partial inconsistency of both consensus trees acquired by PAUP* 4.0 b10 and TNT 1.1 (Fig. 4); it can also account for the inconsistency with the most accepted hypothesis that cubozoans and scyphozoans are more accepted as sister groups (Marques and Collins, 2004; Van Iten et al., 2006). However, all of these best trees, including the consensus trees, display *Yunnanoascus* as the sister taxon to the other fossil and extant Scyphozoa lineages (Fig. 4; Appendixes 3 and 4), compatible with morphological analysis mentioned above.

6. Life habit and the temporal constraint on the rise of medusoid stage

The rhopalia in extant medusae have been well documented as marginal centers generating rhythmic electrical impulses in the motor nerve net (Arai, 1997). When all of the rhopalia are removed from the medusae, the swimming rhythm and contractions of the coronal muscles

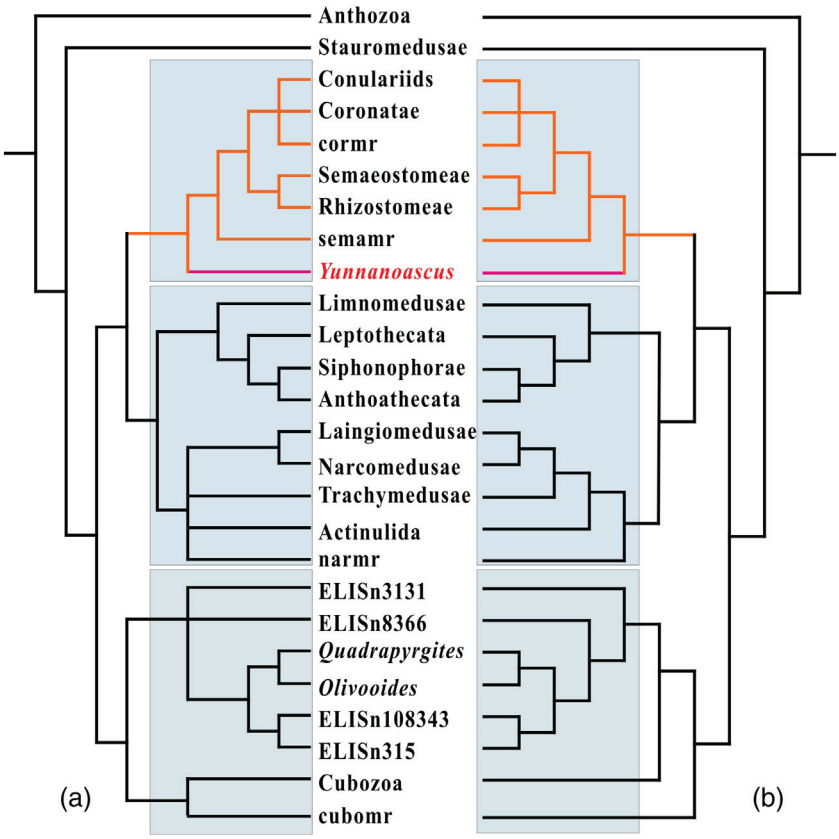

Fig. 4. Strict consensus trees for Medusozoa obtained respectively using TNT and PAUP based on morphologial phylogenetic analysis of medusozoans. (*a*) TNT analysis. (*b*) PAUP 4.0 beta 10. ELISn31-31, ELISn83-66, ELISn108-343, ELISn31-5 are undetermined taxa in Han et al. (2013, 2016); together with co-ocurring *Olivooides* and *Quadrapyrgites*, they come from the basal Cambrian Kuanchuanpu Formation in South China. Cormr, seamr, narmr, cubmr represent, respectively, unnamed fossils of the Coronata, Semaestomeae, Narcomedusae and Cubomedusa from the Middle Cambrian Marjum Formation, Utah (Cartwright et al., 2007).

will cease; and eventually the medusae usually will sink to the bottom (Spangenberg, 1968). The finding of 16 large rhopalia on *Yunnanoascus* strongly indicates a nektonic life style; and this hypothesis is further strengthened by its round aboral end devoid of stalk, and a spacious subumbrellar cavity adaptive for producing a jet of water (Fig.5). The predatory habit is indicated by up to 32 elongate tentacles each with a broad base, and particularly a twistable distal part with possible nematocyst batteries, which, in extant medusae, contain a large amount of toxic cnidae. The swimming pattern of extant medusae varies in species (Arai, 1997), basically they quickly move upwards and sink slowly (Gerritsen, 1980; Strand and Hamner, 1988). They have not been observed using sensory organs to make directed movement toward their prey; mostly during sinking they use tentacles to capture the preys by encounter (Arai, 1997). Likewise, a 'density' of 32 elongate tentacles of *Yunnanoascus* are adaptive for a high encounter probability.

The evidence supporting centimeter-scale, planktonic medusae at the Cambrian Stage 3 and 5 (Cartwright et al., 2007) is of great significance for our understanding of the evolution of the three-phase life

Fig. 5. Reconstruction of *Y. haikouensis* Hu et al., 2007. Artwork by Mr. Dinghua Yang at Nanjing Institute of Geology and Palaeontology.

cycle of medusozoans, particularly, the temporal origin of the pelagic medusoid phase. Hitherto, no reliable evidence of pelagic medusae was known from basal Cambrian or Precambrian deposits (Young and Hagadorn, 2010). The earliest reliable stem group medusozoans (Dong et al., 2013; Han et al., 2013), including ephyra-like organisms (Dong et al., 2013; Han et al., 2010) were known from the early Cambrian (Fortune Stage), but these are minute forms less than 5 mm; particularly, they lack the features for swimming such as sense organs (Han et al., 2016; Han et al., 2013). In addition, many of Cambrian medusozoans possess an external cone-shaped organic periderm (i.e. *Olivooides* and *Quadrapyrgites*) (Liu et al., 2014b; Steiner et al., 2014) or biomineralized tubes (i.e. conulariids, anabaritiids, *Sphenothallus*) (Kouchinsky et al., 2009; Van Iten et al., 2014); thus they are suspected to be benthic or sessile forms probably related to polyps (Van Iten et al., 2006). It appears that the medusozoan communities at the Cambrian Fortune Stage were dominated in both ecology and diversity by micrometer-scale benthic or sessile forms that inhabited shallow water. From the Cambrian III onward, the fossil record of sessile medusozoans, in either ecology or diversity were rather scarce (Van Iten et al., 2014), even in the worldwide fossil *Lagerstätten*. It turns out that the interval between Cambrian stages 1 and 3 most likely represents a period of competition between the polypoid and medusoid phases, and finally the dominant phase of medusozoan communities most probably had undergone a transition from benthic polyps to pelagic medusae. This transition might be ascribable to the great advantages of the medusa phase in positive feeding, broader dispersal, settlement selection, escaping from harsh environments and exploiting different ecological spaces of ancient oceans.

The early Cambrian record of medusae also has implications for understanding the ecological and evolutionary history of the marine pelagic realm. The evolution of rhopalia for both gravity and light in Cambrian medusae enable them to discriminate 'up' from 'down', and to excurse vertically (Gerritsen, 1980). Thus, it is most likely a precondition for the rise of diurnal/nocturnal vertical migrations (DVM) of entire population as seen in modern epipelagic and mesopelagic medusae (see Arai, 1997; Yasuda, 1973; Youngbluth and Båmstedt, 2001; Graham et al., 2001). Contrasting with other pelagic bilaterians, i.e. arthropods of *Ercaia*, *Misszhouia*, *Naraoia*, *Pectocaris*, *Pisnnocaris* and deuterostomes of *Yunnanozoa*, *Haikouella*, *Haikouichthys*, which were preserved by rapid burying as a large population (Han et al., 2006), direct evidence of medusa populations in Chengjiang have not yet been reported. Modern medusae are eaten by a variety of predators, i.e. other pelagic coelenterates, arthropods, fishes and turtles (Arai, 1997). As all known Cambrian vertebrates are filter-feeders (Shu et al., 1999, 2003), and only one species of medusae is reported herein, thus the medusae population in Chengjiang, if present, might have been consumed by some large predatory arthropods and anomolocarids. The evidence of nektonic medusae, together with pelagic populations mentioned above, further strengthens the hypothesis that a complex, modern-style pelagic ecosystem may have been developed by the time of early Cambrian Stage 3 (Hu et al., 2007; Vannier et al., 2009). The rise of such a highly complex pelagic ecosystem might have been accompanied, in part, by the origins of various well-developed sense organs among pelagic cnidarians and ctenophores (Ou et al., 2015), as well as pelagic bilaterians (Zhao et al., 2010).

7. Preservation of the medusae

In contrast with abundant medusae in modern ocean, the fossil record of medusae is sporadic. Apart from lacking hard tissue, the reason of their artefactual rareness is ascribable to three aspects unfavorable for fossilization: (1) Compared with sessile forms, pelagic medusa have nearly same density as seawater, and thus are difficult to bury. Generally, they would have decayed within the water column before being buried. (2) Medusae are extremely fragile organisms which probably decay extremely rapidly after death. (3) Specifically, pelagic medusae have thick mesoglea with low contents of organic materials. Most known medusae are fossilized as moulds (Young and Hagadorn, 2010), whereas the reason for the exceptional soft-tissue preservation of the medusae in Chengjiang and Utah (Cartwright et al., 2007) remains problematic. Energy-dispersive spectroscopic analysis of *Y. haikouensis* (Fig. 3) reveals that the soft tissue was mainly mineralized as organic carbon and pyrite, similar to the case of other Chengjiang organisms (Gabbott et al., 2004; Gaines et al., 2008; Zhu et al., 2005). If correct, a rapid burial caused by periodic storms would be capable of capturing both benthic and pelagic forms (Han et al., 2006; Hu, 2005; Hu et al., 2007; Zhao et al., 2009); a rapid burial of medusae by fine clay minerals would have inhibited microbial decay (Butler et al., 2015; Forchielli et al. 2014). In addition, infilling the subumbrellar cavity of the medusae by clay minerals will lead to the dehydration of the medusa mesoglea, thus the concentration of organic materials will be greatly improved.

Supplementary data to this article can be found online at http://dx.doi.org/10.1016/j.palaeo.2016.02.025.

Competing interests

The authors declare that they have no competing interests.

Author Contributions

J. H. conceived and designed the work; S.X. H. and F.C. Z. acquired the data; All authors analyzed and interpreted the data; J. H., P. C., S.X., H and Q, O. wrote the paper.

Acknowledgments

We thank Dinghua Yang for his colorful reconstruction of the specimen, and J. Sun. and M.R. Cheng (State Key Laboratory for Continental Dynamics, Northwest University, Xi'an, China) for their assistance in both field and lab work. This study was supported by the Natural Science Foundation of China (NSFC grants: 41272019, 41472012), the, 41102012, 41572017 National Basic Research Program of China (2013CB835002, 2013CB835006, 2013CB837100), the Programs of Introducing Talents of Discipline to Universities (No: W20136100061). We are grateful to Prof. Jean Vannier (France) and an anonymous reviewer for invaluable suggestions and linguistic improvement.

References

Arai, M.N., 1997. A Functional Biology of Scyphozoa. Chapman & Hall, London.
Butler, A.D., Cunningham, J.A., Budd, G.E., Donoghue, P.C., 2015. Experimental taphonomy of *Artemia* reveals the role of endogenous microbes in mediating decay and fossilization. Proc. R. Soc. Lond. B Biol. Sci. 282, 20150476.
Caron, J.-B., Conway Morris, S., Shu, D.G., 2010. Tentaculate fossils from the Cambrian of Canada (British Columbia) and China (Yunnan) interpreted as primitive deuterostomes. PLoS One 5, e9586.
Cartwright, P., Halgedahl, S.L., Hendricks, J.R., Jarrard, R.D., Marques, A.C., Collins, A.G., Lieberman, B.S., 2007. Exceptionally preserved jellyfishes from the Middle Cambrian. PLoS One 2, e1121.
Conant, F.S., 1898. The Cubomedusæ: A Memorial Volume. The Johns Hopkins Press, Baltimore.
Conway Morris, S., Collins, D., 1996. Middle Cambrian Ctenophores from the Stephen Formation, British Columbia, Canada. Philosophical Transactions, Biological Sciences, pp. 279–308.
Dong, X.-P., Cunningham, J.A., Bengtson, S., Thomas, C.-W., Liu, J., Stampanoni, M., Donoghue, P.C., 2013. Embryos, polyps and medusae of the Early Cambrian scyphozoan *Olivooides*. Proceedings of the Royal Society B: Biological Sciences 280.
Dzik, J., 1991. Is Fossil Evidence Consistent with Traditional Views of the Early Metazoan Phylogeny. In: Simonneta, A.M., Conway Morris, S. (Eds.), The Early Evolution of Metazoa and the Significance of Problematic Taxa. Cambridge University Press, Cambridge, pp. 47–58.
Forchielli, A., Steiner, M., Hu, S., Lüter, C., Keupp, H., 2014. Taphonomy of the earliest Cambrian linguliform brachiopods. Acta Palaeontol. Pol. 59, 185–207.
Gabbott, S.E., Xian-Guang, H., Norry, M.J., Siveter, D.J., 2004. Preservation of Early Cambrian animals of the Chengjiang biota. Geology 32, 901–904.
Gaines, R.R., Briggs, D.E., Yuanlong, Z., 2008. Cambrian Burgess Shale–type deposits share a common mode of fossilization. Geology 36, 755–758.

Gerritsen, J., 1980. Adaptive Responses to Encounter Problems. In: Kerfoot, W.C. (Ed.), Evolution and Ecology of Zooplankton Communities. University Press of New England, Hannover, N. H., pp. 52–62.
Goloboff, P.A., Farris, J.S., Nixon, K.C., 2008. TNT, a free program for phylogenetic analysis. Cladistics 24, 774–786.
Graham, W.M., Pagès, F., Hamner, W.M., 2001. A physical context for gelatinous zooplankton aggregations: a review. Hydrobiologia 451, 199–212.
Han, J., Shu, D., Zhang, Z., Liu, J., Zhang, X., Yao, Y., 2006. Preliminary notes on soft-bodied fossil concentrations from the Early Cambrian Chengjiang deposits. Chin. Sci. Bull. 51, 2482–2492.
Han, J., Kubota, S., Uchida, H., Stanley Jr., G.D., Yao, X.Y., Shu, D.G., Li, Y., Yasui, K., 2010. Tiny sea anemone from the Lower Cambrian of China. PLoS One 5, e13276.
Han, J., Kubota, S., Li, G.X., Yao, X.Y., Yang, X.G., Shu, D., Li, Y., Kinoshita, S., Sasaki, O., Komiya, T., Yan, G., 2013. Early Cambrian pentamerous cubozoan embryos from South China. PLoS One 8, e70741.
Han, J., Kubota, S., Li, G.X., Ou, Q., Wang, X., Yao, X.Y., Shu, D., Li, Y., Uesugi, K., Hoshino, M., 2016. Divergent evolution of medusozoan symmetric patterns: evidence from the microanatomy of Cambrian tetramerous cubozoans from South China. Gondwana Res 31, 150–163.
Hu, S., 2005. Taphonomy and palaeoecology of the Early Cambrian Chengjiang biota from Eastern Yunnan, China. Berliner Palaobiologische Abhandlungen 7, pp. 182–185.
Hu, S.X., Steiner, M., Zhu, M.Y., Erdtmann, B.D., Luo, H.L., Chen, L.Z., Weber, B., 2007. Diverse pelagic predators from the Chengjiang Lagerstätte and the establishment of modern-style pelagic ecosystems in the early Cambrian. Palaeogeogr. Palaeoclimatol. Palaeoecol. 254, 307–316.
Kouchinsky, A., Bengtson, S., Feng, W., Kutygin, R., Val'kov, A., 2009. The Lower Cambrian fossil anabaritids: affinities, occurrences and systematics. J. Syst. Palaeontol. 7, 241–298.
Kraus, J.E., Fredman, D., Wang, W., Khalturin, K., Technau, U., 2015. Adoption of conserved developmental genes in development and origin of the medusa body plan. Evol. Dev. 6, 23.
Liu, A.G., Matthews, J.J., Menon, L.R., McIlroy, D., Brasier, M.D., 2014a. *Haootia quadriformis* n. gen., n. sp., interpreted as a muscular cnidarian impression from the Late Ediacaran period (approx. 560 Ma). Proc. R. Soc. B Biol. Sci. 281, 20141202.
Liu, Y.H., Li, Y., Shao, T.Q., Zhang, H.Q., Wang, Q., Qiao, J., 2014b. *Quadrapyrgites* from the lower Cambrian of South China: growth pattern, post-embryonic development, and affinity. Chin. Sci. Bull. 59, 4086–4095.
Marques, A.C., Collins, A.G., 2004. Cladistic analysis of Medusozoa and cnidarian evolution. Invertebr. Biol. 23–42.
Mayer, A.G., 1910. Medusae of the World: the Scyphomedusae. Carnegie Institution of Washington, Washington.
Ou, Q., Xiao, S.H., Han, J., Sun, G., Zhang, F., Zhang, Z.F., Shu, D.G., 2015. A vanished history of skeletonization in Cambrian comb jellies. Sci. Adv. 1, e1500092.
Park, E., Hwang, D.-S., Lee, J.-S., Song, J.-I., Seo, T.-K., Won, Y.-J., 2012. Estimation of divergence times in cnidarian evolution based on mitochondrial protein-coding genes and the fossil record. Mol. Phylogenet. Evol. 62, 329–345.
Ruppert, E.E., Fox, R.S., Barnes, R.D., 2004. Invertebrate Zoology: A Functional Evolutionary Approach. Cole Publishing, Belmont, CA, Brooks.
Russell, F.S., 1970. The Medusae of the British Isles: 2. Pelagic Scyphozoa with a Supplement to the First Volume on Hydromedusae.
Salvini-Plawen, L.V., 1978. On the origin and evolution of the Lower Metazoa. J. Zool. Syst. Evol. Res. 16, 40–87.
Shu, D.G., Luo, H.L., Conway Morris, S., Zhang, X.L., Hu, S.X., Chen, L., Han, J., Zhu, M., Li, Y., Chen, L.Z., 1999. Lower Cambrian vertebrates from South China. Nature 402, 42–46.
Shu, D.G., Conway Morris, S., Han, J., Zhang, Z.F., Yasui, K., Janvier, P., Chen, L., Zhang, X.L., Liu, J.N., Li, Y., Liu, H.Q., 2003. Head and backbone of the Early Cambrian vertebrate *Haikouichthys*. Nature 421, 526–529.
Sötje, I., Neues, F., Epple, M., Ludwig, W., Rack, A., Gordon, M., Boese, R., Tiemann, H., 2011. Comparison of the statolith structures of *Chironex fleckeri* (Cnidaria, Cubozoa) and *Periphylla periphylla* (Cnidaria, Scyphozoa): a phylogenetic approach. Mar. Biol. 158, 1149–1161.
Spangenberg, D.B., 1968. Statolith differentiation in *Aurelia aurita*. J. Exp. Zool. 169 (4), 487–499.
Steiner, M., Qian, Y., Li, G., Hagadorn, J.W., Zhu, M., 2014. The developmental cycles of early Cambrian Olivooidae fam. nov. (?Cycloneuralia) from the Yangtze Platform (China). Palaeogeogr. Palaeoclimatol. Palaeoecol. 398, 97–124.
Strand, S.W., Hamner, W.M., 1988. Predatory behavior of *Phacellophora camtschatica* and size-selective predation upon *Aurelia aurita* (Scyphozoa: Cnidaria) in Saanich Inlet, British Columbia. Mar. Biol. 99, 409–414.
Sun, W.-G., Hou, X.-G., 1987. Early Cambrian medusae from Chengjiang, Yunnan, China. Acta Palaeontol. Sin. 26, 257–271.
Swofford, D.L., 2003. PAUP*. Phylogenetic Analysis Using Parsimony (and Other Methods). Version 4. Sinauer Associates, Sunderland, Massachusetts.
Van Iten, H., de Moraes Leme, J., Simões, M.G., Marques, A.C., Collins, A.G., 2006. Reassessment of the phylogenetic position of conulariids (? Ediacaran–Triassic) within the subphylum Medusozoa (phylum Cnidaria). J. Syst. Palaeontol. 4, 109–118.
Van Iten, H., Marques, A.C., Leme, J.d.M., Pacheco, M.L., Simões, M.G., 2014. Origin and early diversification of the phylum Cnidaria Verrill: major developments in the analysis of the taxon's Proterozoic–Cambrian history. Palaeontology 57, 1–14.
Vannier, J., García-Bellido, D., Hu, S.-X., Chen, A.-L., 2009. Arthropod visual predators in the early pelagic ecosystem: evidence from the Burgess Shale and Chengjiang biotas. Proc. R. Soc. Lond. B Biol. Sci. 276, 2567–2574.
Yasuda, T., 1973. Ecological studies on the jelly-fish, *Aurelia aurita* (Linné). Urazoko Bay, Fukui prefecture-VIII. diel vertical migration of the medusa in early fall, 1969. publ. seto mar. Biol. Lab 20, pp. 491–500.
Young, G.A., Hagadorn, J.W., 2010. The fossil record of cnidarian medusae. Palaeoworld 19, 212–221.
Youngbluth, M.J., Båmstedt, U., 2001. Distribution, abundance, behavior and metabolism of *Periphylla periphylla*, a mesopelagic coronate medusa in a Norwegian fjord. Jellyfish Blooms: Ecological and Societal Importance. Springer, pp. 321–333.
Zhang, Z.F., Li, G.X., Emig, C.C., Han, J., Holmer, L.E., Shu, D.G., 2009. Architecture and function of the lophophore in the problematic brachiopod *Heliomedusa orienta* (Early Cambrian, South China). Geobios-Lyon 42, 649–661.
Zhao, F., Caron, J.-B., Hu, S., Zhu, M., 2009. Quantitative analysis of taphofacies and paleocommunities in the Early Cambrian Chengjiang Lagerstätte. PALAIOS 24, 826–839.
Zhao, F.C., Zhu, M.Y., Hu, S.X., 2010. Community structure and composition of the Cambrian Chengjiang biota. Sci. China Earth Sci. 53, 1784–1799.
Zhu, M.Y., Zhao, Y.L., Chen, J.Y., 2002. Revision of the Cambrian discoidal animals *Stellostomites eumorphus* and *Pararotadiscus guizhouensis* from South China. Geobios-Lyon 35, 165–185.
Zhu, M., Babcock, L.E., Steiner, M., 2005. Fossilization modes in the Chengjiang Lagerstätte (Cambrian of China): testing the roles of organic preservation and diagenetic alteration in exceptional preservation. Palaeogeogr. Palaeoclimatol. Palaeoecol. 220, 31–46.

5.2 *Cloudina*-like fossils from the Kuanchuanpu Formation

One of the most important event in the evolutionary evolution of animals is the biomineralization of their exoskeleton in the form of tubes, shells or sclerites. The first animals with a biomineralized exoskeleton appear in the late Precambrian (e.g. Ediacaran; *ca.* 550 Ma, (Germs 1972, Hua et al. 2005)), as exemplified by *Cloudina* which is the earliest and most abundant biomineralized organism in rocks with attested occurrences in most regions of the world. SSF-assemblages which contain a huge variety of originally mineralized exoskeletons show that this event intensified during the early and middle Cambrian and spread to a wide range of animal groups. Although the physiological and biogeochemical processes associated with animal biomineralization are not completely understood, this event is often considered as an important episode of the "Cambrian explosion" and a possible response to the intensification of predation.

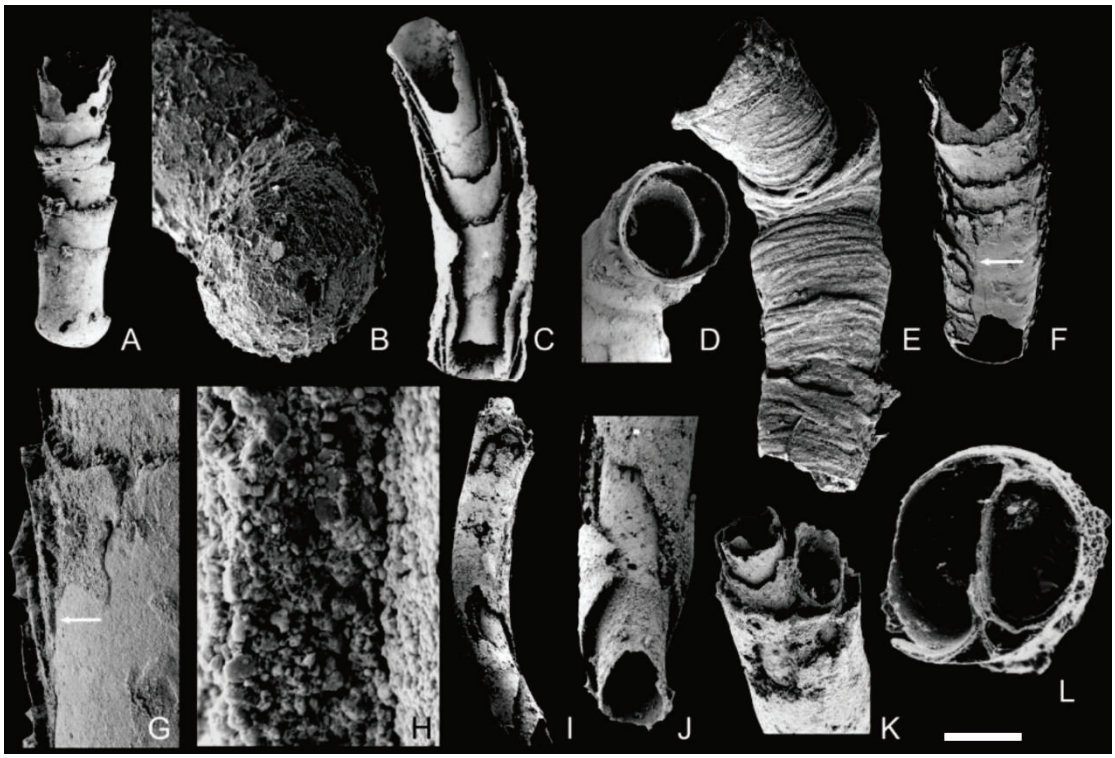

Fig. 70. *Cloudina hartmannae* Germs (1972) from the Dengying Formation, Gaojiashan Member at Lijiagou section, Shaanxi Province, China. A-B. Hemispherical or bulbous basal end. C. Deeply nested funnels. D-E. Eccentrically nested funnels with external annulations or corrugations (E). F. Tube with funnel walls peeled off. No transverse cross-walls are present within tube. G. Magnified view (arrow in F) showing stacked funnels. H, magnified view (arrow in G) showing granular crystals in funnel walls. Exterior to left. I. Dichotomous branching (at upper end) within parent funnel. J-K. Magnified views of lower (J) and upper (K) ends of specimen illustrated in I. L. Transverse cross section of two daughter funnels within parent funnel. Scale bars: 400 µm in A, F, I; 100 µm in B, G;

1000 µm in C; 200 µm in D-E, J-L; 4 µm in H. From Hua et al., 2005.

Cloudina is a tube-like organisms with a diameter varying from 0.3 to more than 5 mm and length of 8 to ca 150 mm. The tube consists of a series of stacked vase-like elements, each cone stacking eccentrically in the one below. It is curved and sinuous and branches off occasionally. It has an open base although considerably thickened. The tube wall is relatively thin (8-50 µm), possibly flexible, and usually covered with annular ridges of different sizes (Germs 1972, Hua et al. 2005, Wood 2011) (Fig. 70). *Cloudina* resembles other co-occurring biomineralized fossils, such as *Conotubus hemiannulatus* Zhang and Lin in Lin et al. (1986) from the Dengying Formation (*ca.* 550 Ma). *Conotubus* is characterized by a segmented tube with a periodical growth pattern. The apex of the tube is smooth and may represent an embryonic cone. The rest of the tube bears transverse annuli (Cai et al. 2011) (Fig. 71) but, contrasting with that of *Cloudina,* is not branched.

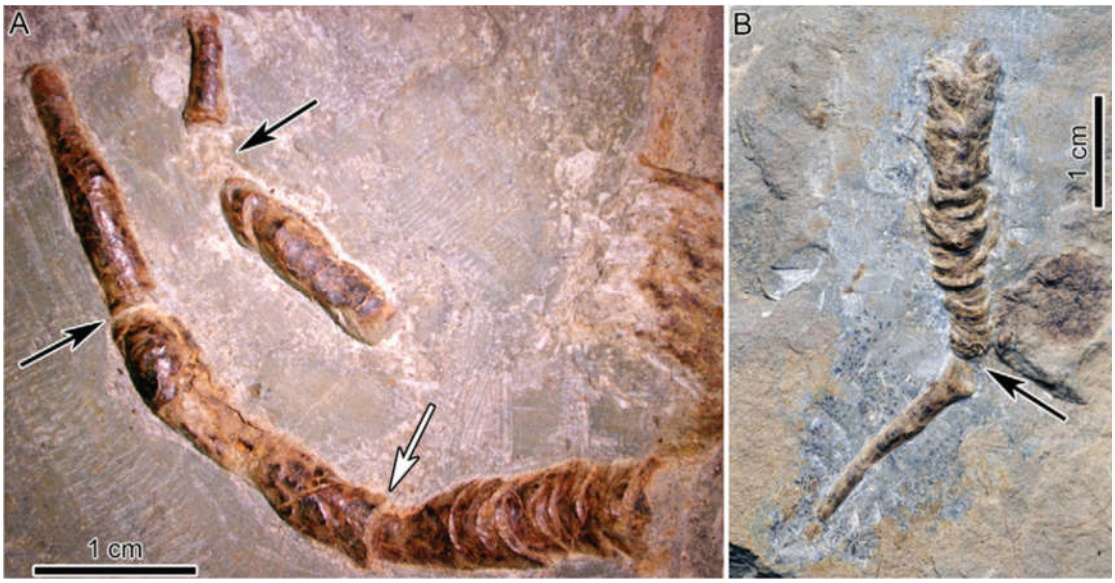

Fig. 71. Pyritized *Conotubus hemiannulatus* Zhang and Lin in Lin et al., 1986 from the Dengying Formation, Gaojiashan Member, Shaanxi Province, China. Black arrow shows the first disarticulation. White arrow shows the second disarticulation. From Cai et al., 2011.

Two hypotheses have been proposed concerning the zoological affinities of *Cloudina*. One of them suggests that it was an early tubicolous annelid secreting a tube comparable with that of modern serpulids such as *Salmacina dysteri*. Indeed, the tubes secreted by serpulids superficially resemble those of *Cloudina*, such as the tube-shaped form, the smooth cavities, more important the similar asexual reproduction through dichotomous branching (Germs 1972, Hua et al. 2005). However, Vinn and Zaton (2012) suggested that *Cloudina* might have cnidarian affinities based on more detailed morphological characteristics, not only the same tubicolous shells, the smooth inner cavities, the asexual reproduction, but the round-shaped closed tube

base, the similar size of both the parent tube and the daughter tubes. In addition, the morphology of dichotomous branching of tubes found in *Cloudina* has no counterpart of extant serpulids (Vinn and Zaton 2012) (Table 3).

Characters	*Cloudina*	Calcareous polychaetes (Serpulidae, Sabellidae, Cirratulidae)	Cnidaria
Tubicolous shell	x	x	x
Smooth lumen	x	x	x
Peristomes	x	x	x
Asexual reproduction	x	x	x
Granular microstructure	x	-	x
Closed tube base	x	-	x
Semicircular tube cross section	x	-	x
Rapid increase of the tube diameter	x	-	x
Diameter of daughter tubes about equal	x	-	x
Attachment surfaces lacking	x	-	x

Table. 3. Table summarizing resemblances between *Cloudina*, cnidarians and polychaetes. From Vinn and Zaton, 2012.

In this paper, we describe *Feiyanella manica* gen. et sp. nov., a conical tube with a 'funnel-in-funnel' structure, from lowermost Cambrian Kuanchuanpu Formation by using high-resolution tomographic methods. This new form shows close morphological resemblances with *Cloudina*, *Conotubus,* and also *Sinotubulites* from the Dengying Formation by the presence of corrugated features in the most external layer of the tubes (Chen et al. 1981). However it differs from them in having a unique "tube-in-tube" structure and longitudinal features.

We show that *Cloudina, Conotubus, Sinotubulites* and *Feiyanella* probably constitute a monophyletic group with representatives in the lowermost Cambrian and ancestors in the Ediacaran, which indicating the relics of Ediacaran that traversed the Ediacaran–Cambrian boundary.

We also highlight some important features in *Feiyanella* that would suggest cnidarian affinities. These are: 1) the asexual reproduction by longitudinal and transverse splitting of the soft body as in some extant cnidarians (anthozoans); 2) the corrugated ornament of the outermost layer of the tube which is reminiscent of the periderm of medusozoan polyps.

Geol. Mag.: page 1 of 12 © Cambridge University Press 2017
doi:10.1017/S0016756816001187

A *Cloudina*-like fossil with evidence of asexual reproduction from the lowest Cambrian, South China

JIAN HAN*, YAOPING CAI*†, JAMES D. SCHIFFBAUER‡, HONG HUA*, XING WANG*, XIAOGUANG YANG*, KENTARO UESUGI§, TSUYOSHI KOMIYA¶ & JIE SUN*

*Early Life Institute and Department of Geology and State Key Laboratory of Continental Dynamics, Northwest University, No. 229 Taibai Road, Xi'an 710069, China
‡Department of Geological Sciences, University of Missouri, 101 Geology Building, Columbia, MO, 65211, USA
§Japan Synchrotron Radiation Research Institute (JASRI), 1-1-1 Kouto, Sayo-cho, Sayo-gun, Hyogo, Japan
¶Department of Earth Science and Astronomy, Graduate School of Arts and Sciences, University of Tokyo, Tokyo 153–8902, Japan

(*Received* 30 August 2016; *accepted* 30 November 2016)

Abstract – The earliest fossil record of animal biomineralization occurs in the latest Ediacaran Period (*c*. 550 Ma). *Cloudina* and *Sinotubulites* are two important tubular taxa among these earliest skeletal fossils. The evolutionary fate of *Cloudina*-type fossils across the Ediacaran–Cambrian transition, however, remains poorly understood. Here we report a multi-layered tubular microfossil *Feiyanella manica* gen. et sp. nov. from a phosphorite interval of the lowest Cambrian Kuanchuanpu Formation, southern Shaanxi Province, South China. This newly discovered fossil is a conical tube with a 'funnel-in-funnel' construction, showing profound morphological similarities to *Cloudina* and *Conotubus*. On the other hand, the outer few layers, and particularly the outermost layer, of *Feiyanella* tubes are regularly to irregularly corrugated, a feature strikingly similar to the variably folded/wrinkled tube walls of *Sinotubulites*. The *Feiyanella* tubes additionally exhibit two orders of dichotomous branching, similar to branching structures reported occasionally in *Cloudina* and possibly indicative of asexual reproduction. Owing to broad similarities in tube morphology, tube wall construction and features presumably indicative of asexual reproduction, *Cloudina*, *Conotubus*, *Sinotubulites* and the here described *Feiyanella* may thus constitute a monophyletic group traversing the Ediacaran–Cambrian boundary. The tube construction and palaeoecological strategy of *Feiyanella* putatively indicate evolutionary continuity in morphology and palaeoecology of benthic metazoan communities across the Ediacaran–Cambrian transition.

Keywords: *Cloudina*, *Sinotubulites*, asexual reproduction, early Cambrian, Kuanchuanpu Formation.

1. Introduction

Although molecular clock studies estimate the origin and earliest diversification of animals within the Cryogenian Period, evidence from the fossil record reveals that crown members of nearly all animal phyla appear in a relatively rapid diversification event in early Cambrian time (the 'Cambrian explosion'). This evolutionary radiation follows after a global mass extinction of the Ediacaran fauna (Erwin *et al*. 2011), a benthic community dominated by sessile, substrate-sticking organisms (Seilacher, 1999; Fedonkin *et al*. 2007; Yuan *et al*. 2011). In addition, geological and geochemical data suggest that the Ediacaran–Cambrian transition was not only a transition in biological diversity and ecosystem structure, but was also associated with drastic environmental change. These changes in environment and biology were likely highly intertwined; for instance, the rise of oxygen (e.g. Fike *et al*. 2006; Canfield *et al*. 2008; Komiya *et al*. 2008; Canfield & Farquhar, 2009; Li *et al*. 2010) has been suggested to have had profound effects on the evolution and diversification of metazoans (Sperling *et al*. 2013). Further, the innovation of novel ecological strategies, such as ecosystem engineering and predation, in Ediacaran communities nearing the Cambrian boundary may have served to set the stage for the impending Cambrian radiation (e.g. Schiffbauer *et al*. 2016). Thus, the Ediacaran–Cambrian boundary represents a revolutionary transition, wherein the combined effects of environmental, biological and ecological change impart a large influence on phylogenetic patterns for the next *c*. 540 million years of evolutionary history.

With several reports of the survival of a few taxa from the Ediacaran fauna into the early and middle Cambrian period (e.g. Jensen, Gehling & Droser, 1998; Hagadorn & Waggoner, 2000; Shu *et al*. 2006; Van Iten *et al*. 2006), palaeontologists have sought to better understand the nature of biotic replacement at the Ediacaran–Cambrian transition (Laflamme *et al*. 2013; Darroch *et al*. 2015), and moreover, to explore the possible extinction hold-overs and their place within this evolutionary story. One such group of possible hold-overs comprises the terminal Ediacaran

†Author for correspondence: yaopingcai@nwu.edu.cn

tubular biomineralizing assemblage (part of the 'wormworld fauna', Schiffbauer *et al*. 2016), exemplified by such organisms as *Cloudina*, *Sinotubulites* and *Namacalathus* (e.g. Germs, 1972; Signor, Mount & Onken, 1987; Grant, 1990; Grotzinger, Watters & Knoll, 2000; Hofmann & Mointjoy, 2001; Cortijo *et al*. 2010; Zhuravlev *et al*. 2012; Cortijo *et al*. 2015). Although the presence of these and broadly comparable genera in Cambrian rocks is rare (e.g. Yochelson & Stump, 1977; McIlroy, Green & Brasier, 2001; Rogov *et al*. 2015), they may be evolutionarily tied to tubular forms present in small shelly fossil assemblages of the lowest Cambrian, such as the anabaritids.

The lower Cambrian Kuanchuanpu fauna (Fortunian Stage, *c*. 535 Ma) in South China has become increasingly significant in understanding the evolutionary history of animals in the Ediacaran–Cambrian transition. Apart from small shelly fossils, including various molluscs and protoconodonts (Bengtson *et al*. 1990; Qian, 1999), the Kuanchuanpu Formation has yielded several extraordinary discoveries including putative arthropod embryos (Steiner *et al*. 2004*b*), scalidophorans (Liu *et al*. 2014*b*; Zhang *et al*. 2015) and markedly diverse types of cnidarians (Han *et al*. 2010, 2013; Dong *et al*. 2013; Han *et al*. 2016*a*) with biomineralized exoskeletons. Particularly, the scalidophorans, molluscs and protoconodonts have established phylogenetic connections with the emerging complex Cambrian marine ecosystem, for example, the diversity of arthropods as represented by the Chengjiang fauna (Vannier *et al*. 2007, 2009). Perhaps more importantly, the abundant millimetre-scale tubular fossils in the Kuanchuanpu fauna at least superficially resemble the terminal Ediacaran tubular ecosystem (Fedonkin *et al*. 2007; Yang *et al.* 2016).

Here we describe a three-dimensionally preserved tubular microfossil–*Feiyanella manica* gen. et sp. nov.–from the lower Cambrian Kuanchuanpu Formation, Shaanxi Province, South China. It exhibits similar funnel-in-funnel tube construction to the late Ediacaran tubular fossil *Cloudina* (Hua *et al*. 2005), and also shows broadly comparable dichotomous branching features posited to indicate asexual reproduction. Further, it shows a similar wrinkled/folded tube wall exterior comparable to that of *Sinotubulites* (Chen *et al*. 2008; Cai *et al*. 2015). This newly described organism may therefore provide an important palaeobiological and palaeoecological link between tubular fossils in the latest Ediacaran Period and earliest Cambrian Period.

2. Stratigraphic setting, fossil material and methods

The specimens described here were recovered from Bed 31 of the lower Cambrian Kuanchuanpu Formation (Fortunian Stage, Terreneuvian Series) at the Shizhonggou section of Ningqiang County, and Bed 2 at the Zhangjiagou section, Xixiang, Shaanxi Province, South China. The Ningqiang and Xixiang areas were palaeogeographically located on the northwestern margin of the Yangtze Platform during Ediacaran and Cambrian times. The fossil-bearing beds belong to the classic *Anabarites trisulcatus – Protohertzina anabarica* small shelly fossil biozone, indicating a stratigraphic equivalent of the Nemakit–Daldynian interval in Siberia (Steiner *et al*. 2004*a*).

Insoluble phosphatized fossils were liberated from the phosphatic limestone using 10% acetic acid digestion. A *Hyolithellus* sp. specimen (ELIXX35-465) and a well-preserved specimen of *Feiyanella manica* gen. et sp. nov. (ELISN141-14) were imaged by scanning electron microscopy (SEM) (Fig. 1), and ELISN141-14 was three-dimensionally analysed using Synchrotron radiation X-ray tomographic microscopy (SRXTM) at SPring-8 in Hyogo, Japan (Figs 2–4). The 3D reconstructions of X-ray data were processed using VG Studio 2.2 Max, allowing us to document interior anatomic details of the tube structure. All specimens are reposited at the Early Life Institute (ELI), Northwest University, Xi'an, China.

3. Systematic palaeontology

Incertae sedis

Genus *Feiyanella* new genus

Type species. Feiyanella manica new species, by monotypy

Diagnosis. Minute, multi-layered sub-cylindrical fossil tube consisting of a number of nested funnel-shaped layers. Outermost layer strongly wrinkled/folded, inner layers ornamented with weaker transverse annulations. Tube exhibits two orders of dichotomous branching, forming three generations of tubes. Parent tube layers are fully nested in the preserved length, whereas daughter and granddaughter tube layers are partially stacked/overlapped.

Feiyanella manica gen. et sp. nov.
Figures 1–5

Etymology. Feiyan (Feiyan Zhao), an ancient Chinese beauty famous for her slender build, similar to the slight gross appearance of the tube; manica, Latin, referring to the wrinkled outermost layer of the tube that resembles a folded shirt sleeve.

Holotype. ELISN141-14.

Type locality and horizon. The Shizhonggou section in Ningqiang County, Shaanxi Province, South China. Lower Cambrian Kuanchuanpu Formation (Fortunian Stage).

4. Description

The holotype specimen of *Feiyanella manica* gen. et sp. nov. (ELISN141-14) is three-dimensionally preserved through authigenic phosphatization. The fossil is incomplete (Fig. 1a), with both apical and apertural

https://doi.org/10.1017/S0016756816001187

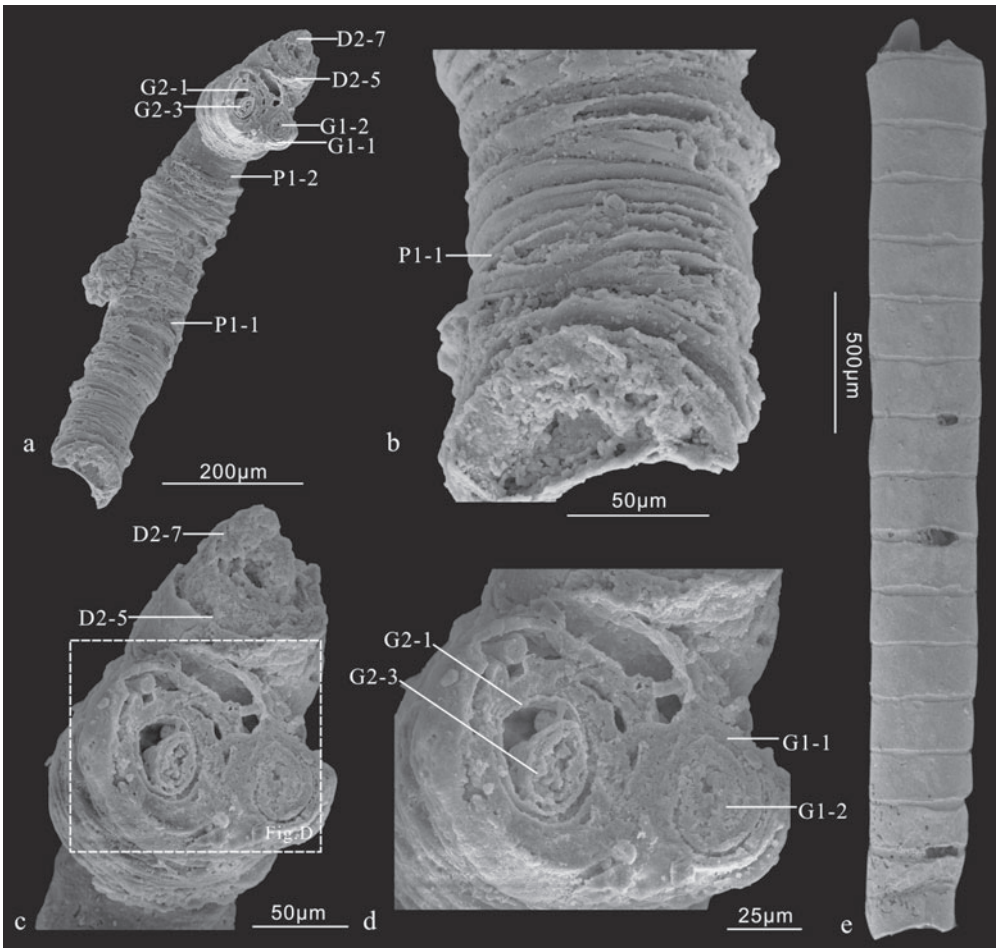

Figure 1. Secondary electron photomicrographs of *Feiyanella manica* gen. et sp. nov. (a–d) and *Hyolithellus* sp. (e). Fossils were recovered from the basal Cambrian Kuanchuanpu Formation at the Shizhonggou (a–d; Ningqiang County) and the Zhangjiagou (e; Xixiang County) sections. (a) Holotype specimen (ELISN141-14). Exterior view of the tube. (b) and (c) are enlarged views of the apical and apertural part, respectively. (d) is close up of (c). The tube is generally conical in shape, with the apical end (lower left) slightly tapering and the apertural end flaring (upper right) (a). The outermost layer of the tube is ornamented with transverse corrugations (b). Two daughter tubes (D1 and D2) and two granddaughter tubes (G1 and G2) can be seen in apertural fracture (c–d). (e) *Hyolithellus* sp. (ELIXX35-465). Abbreviations: P – parent tube; D – daughter tube; G – granddaughter tube. One parent tube (P1), two daughter tubes (D1 and D2) and three granddaughter tubes (G1, G2, and G3) are identified. Numberings suffixed P1, D1, D2, G1, G2 and G3 represent layers of walls in the parent, daughter and granddaughter tubes, respectively.

ends not intact (Fig. 1b–d). The preserved portion of the tube is roughly conical and gently curved (Fig. 1a). The apertural end flares with three slightly divergent, concentric sub-units (Fig. 1a, c, d). The tube is multi-layered and nested, composed of a number of stacked layers with varying overlap (Figs 1–5). The outermost layer of the tube is corrugated with closely spaced transverse ridges, showing stronger folds or wrinkles (Figs 1a, b, 2a–d, 3a–c). Only weaker transverse annulations can be seen in inner layers (Fig. 4b–l). SRXTM analysis reveals that three units of tube layers with unambiguously different lengths and diameters can be identified in the holotype specimen. Although these three sets of tubes are of quite different sizes, they all show the funnel-in-funnel tube construction. They are here interpreted as representing three generations – namely the parent, the daughter and the granddaughter tubes, respectively – which are described separately below.

4.a. Parent tube

The parent tube is sub-cylindrical in gross morphology, with the apertural end slightly flaring. It consists, from exterior to interior, of four nested funnel-shaped layers (the outermost four layers of the tube of *Feiyanella*, marked with P1-1, P1-2, P1-3, P1-4 in all figures). The preserved length of the parent tube is *c*. 1379 μm (= the length of the longest third layer; P1-3). The four layers of funnels, ranging from 193 to 304 μm in diameter, are fully stacked and overlapped, reminiscent of the 'tube-in-tube' construction of late Ediacaran tubular fossil *Sinotubulites* (Cai *et al*. 2015). The first layer (P1-1) is strongly wrinkled and/or folded, forming stronger, closely spaced, irregular, transverse corrugations on the exterior surface of the tube (Fig. 1a, b), strongly distinct from those on the inner layers. Transverse corrugations often bear a few secondary transverse irregular folds (Fig. 1b), which

https://doi.org/10.1017/S0016756816001187

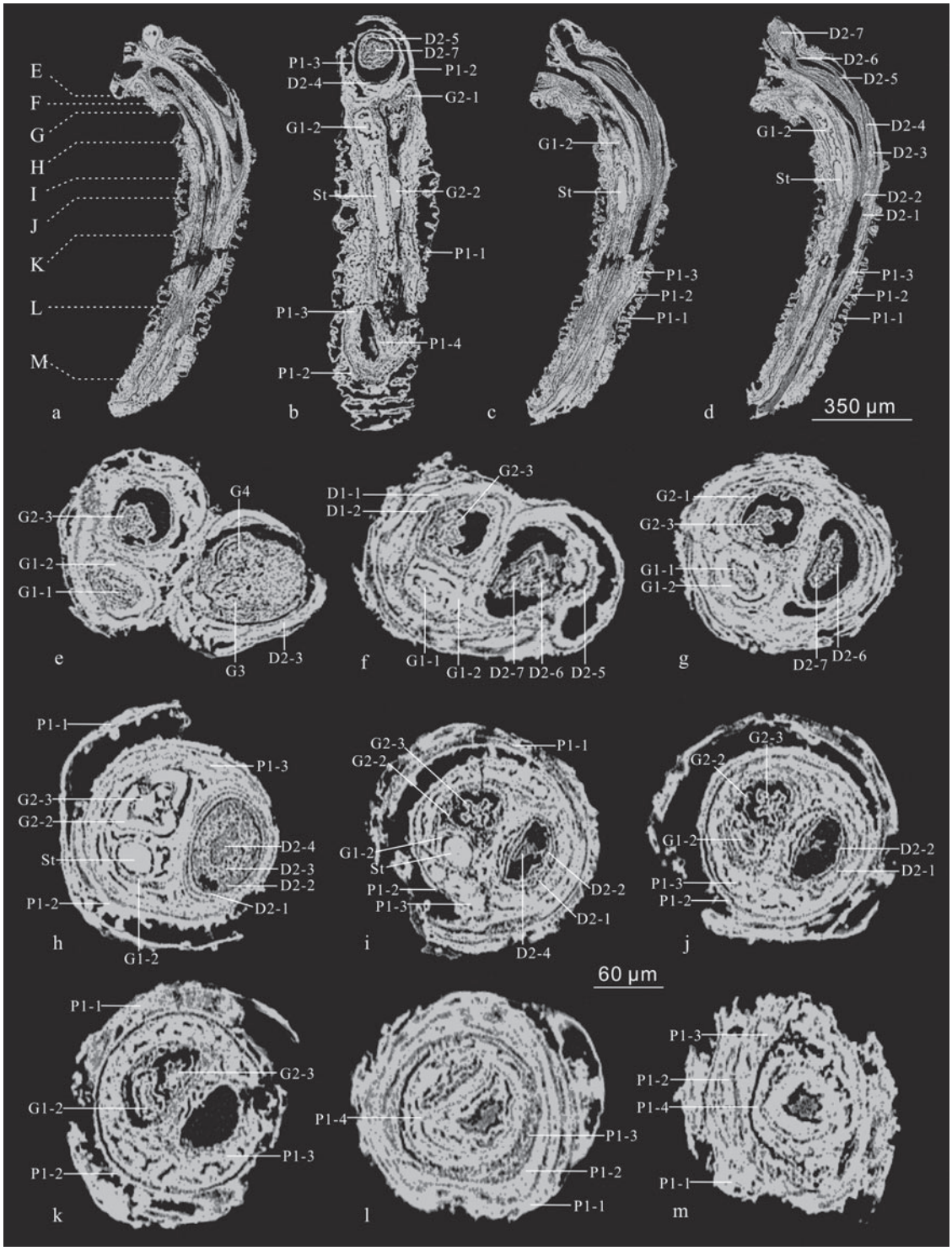

Figure 2. SRXTM virtual sections of the holotype specimen (ELISN141-14) of *Feiyanella manica* gen. et sp. nov. (a–d) Vertical bisections of the entire specimen; (e–m) transverse sections. Positions of the sections are indicated in (a). Abbreviations: St – soft tissue. For all other abbreviations, see Figure 1. Scale bars: 350 μm for (a–d) and 60 μm for (e–m).

form complex exterior corrugations and make this layer appear to be much thicker than any other layers (Figs 2a–d, 3b, c). The notably stronger corrugation on the outermost layer of *Feiyanella* is a diagnostic feature characterizing this taxon. The second, third and fourth parent layers (P1-2–P1-4) share a similar morphology with the first layer. However, layers P1-2–P1-4 are ornamented with weaker transverse annulations (Fig. 4b–d), quite different from those in layer P1-1. The second parent layer is *c*. 120 and *c*. 259 μm in minimum and maximum diameters, respectively. The third parent layer (P1-3) is the longest one (1379 μm) in the preserved specimen (Fig. 4c). The fourth parent layer is obviously shorter (631 μm) and smaller (77 and 108 μm in minimum and maximum diameters) than the other three parent funnels (Fig. 4d).

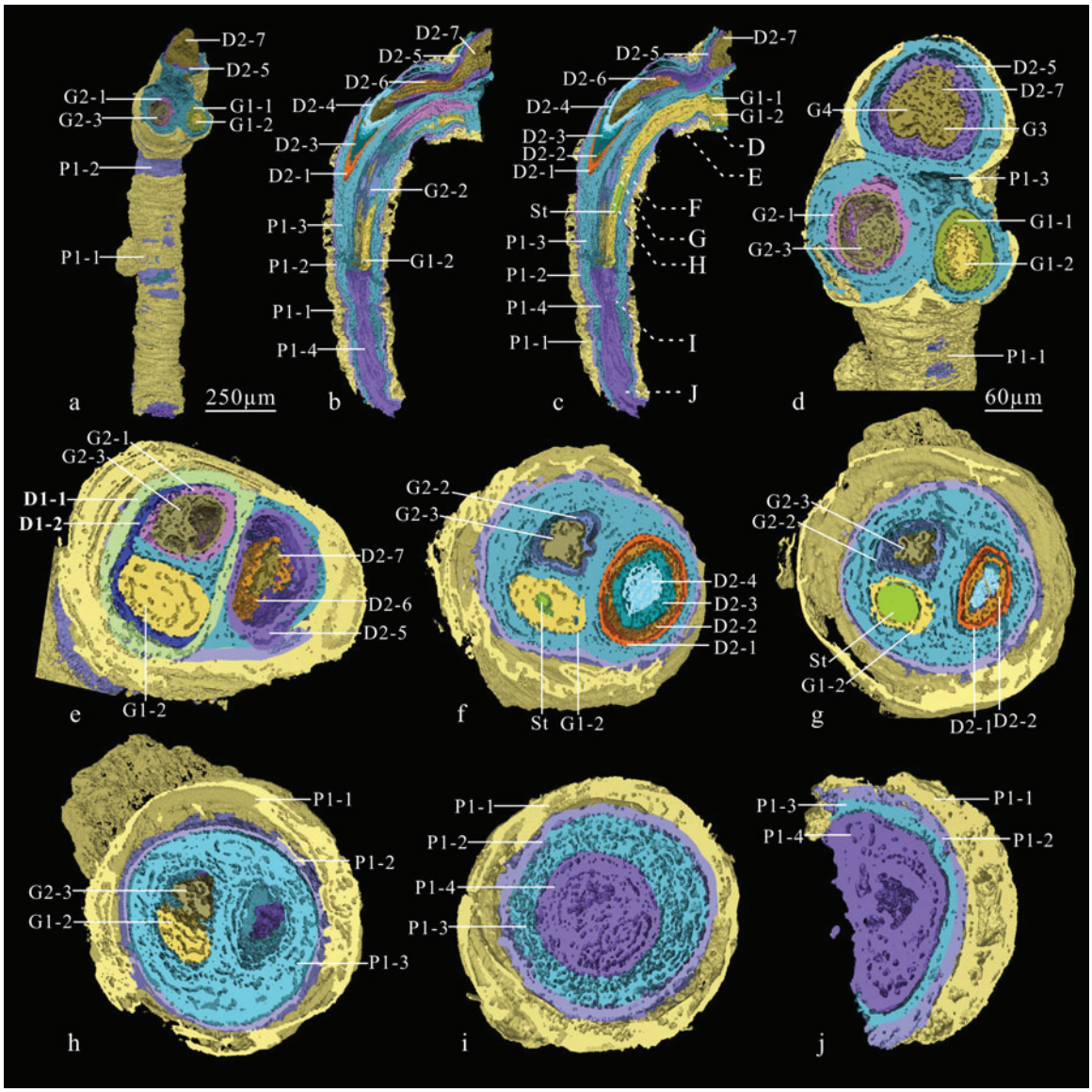

Figure 3. SRXTM reconstructions of the holotype specimen (ELISN141-14) of *Feiyanella manica* gen. et sp. nov. (a) External view of entire specimen; (b–c) vertical bisection of the specimen; (d–j) transverse sections. Positions of the sections are indicated in (c). Abbreviations: see Figure 1. Scale bars: 250 μm for (a–c) and 60 μm bar (d–j).

4.b. Daughter tube

Two daughter tubes (denoted as D1 and D2 in all figures) are discernible at the apertural end of the tube of *Feiyanella* (Figs 1c, 2, 3, 4), which extend from the apertural opening of the fourth parent funnel (Fig. 4d). The two daughter tubes stand side-by-side, and the outermost funnel of each daughter tube appears nearly cemented together (Fig. 2e). The daughter tubes consist of a number of nested, funnel-shaped layers, sharing similarities in tube wall morphology and nesting patterns with the parent tube. The two daughter tubes are not equal in size. The larger one (D1) consists of two tube wall layers (Fig. 2f) and is irregular in cross-section (Fig. 2e–g). The two layers (D1-1 and D1-2) are only situated in the apertural part of *Feiyanella*. Its width increases greatly towards the apertural end (Fig. 4a–d). The smaller daughter tube (D2) is composed of seven tube wall layers (D2-1–D2-7 in Figs 2d–j, 3b–c, 4d–f). In contrast, ornamentations on the daughter funnels are noticeably diminished, with closely spaced transverse annulations but without complicated corrugations (e.g. funnel D2-1), as compared to the parent funnels.

4.c. Granddaughter tube

Four granddaughter tubes are identified in *Feiyanella*: two (G1 and G2) originated from the larger daughter tube (D1) and the other two (G3 and G4) from the smaller daughter tube (D2). The granddaughter tubes G1 and G2 are situated at the upper half of the preserved parent tube (Fig. 3b, c), whereas G3 and G4 are at the apertural end (Figs 2e, 3d). Morphological details of G3 and G4 are very limited, as they can only be identified in cross-sections near the apertural end of the tube (Figs 2e, 3d). Granddaughter tubes G1

https://doi.org/10.1017/S0016756816001187

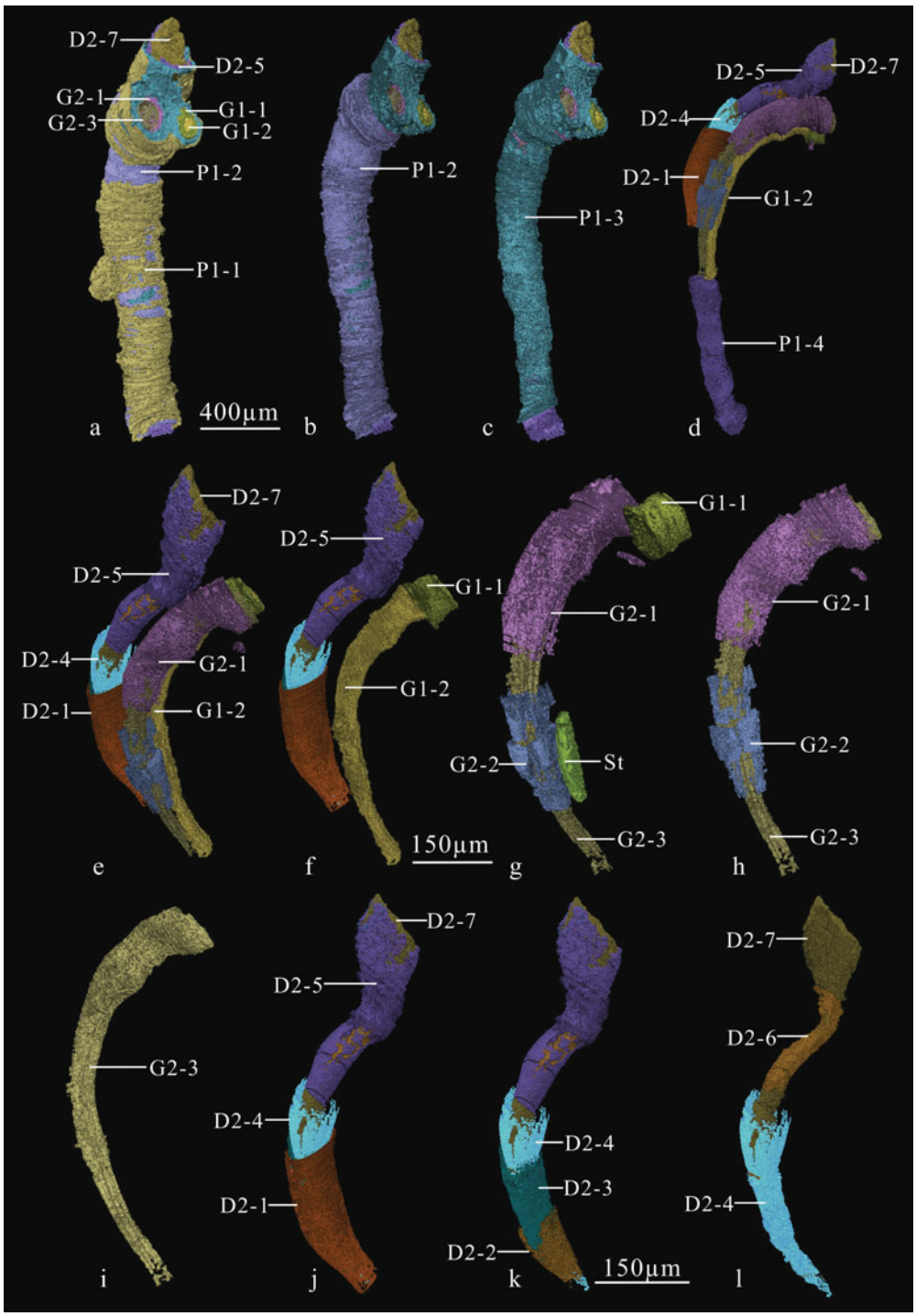

Figure 4. SRXTM reconstruction of the holotype specimen (ELISN141-14) of *Feiyanella manica* gen. et sp. nov. Different tube layers are in different colours. The outer layers are stepwise removed (from a–l) to expose the inner layers. Abbreviations: see Figure 1. Scale bars: 400 μm for (a–d) and 150 μm for (e–l).

and G2 are deeply nested into the daughter tube D1 (located at the middle to apertural portion of the parent tube; Fig. 2e–k). G1 and G2 are more or less equal in size (*c*. 39 μm). Notably, the splitting plane along the tube between the two granddaughter tubes G1 and G2 is orientated perpendicular to the splitting plane of the daughter tubes (Figs 2e, 5). G1 contains two layers of funnels (G1-1 and G1-2) and G2 has three layers (G2-1–G2-3) (Fig. 4d–i). The innermost layer of the granddaughter tube G2 (G2-3) displays four lobes separated by four longitudinal furrows in cross-section (Figs 2i, j, 3g). This tetraradial symmetry only occurs at the apical end, and traverses approximately one-fourth of the granddaughter tube G2 (Fig. 4g–i). A spindle-shaped structure was preserved in the innermost funnel of the granddaughter tube G1 (denoted as St in Figs 2b, h, i, 3g, 4g). It is situated in the central portion of the granddaughter tube G1 and is oval (Fig. 2h, i)

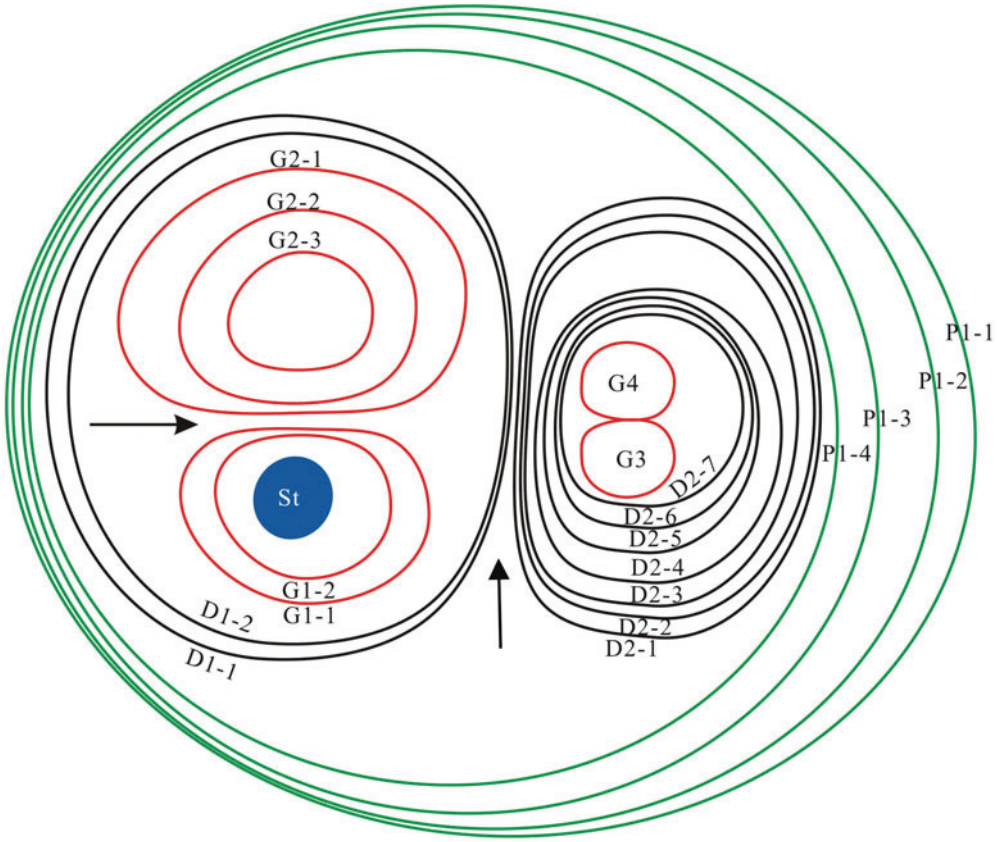

Figure 5. (Colour online) Schematic drawing of the cross-section of *Feiyanella manica* gen. et sp. nov. illustrating growth patterns between parent, daughter and granddaughter tubes. Note the orthogonal splitting planes between daughter (rightward arrow) and granddaughter (upward arrow) tubes. Abbreviations: see Figure 1.

in cross-section. The spindle exhibits a bright phase under SRXTM observation, *c*. 39 μm in diameter and 188 μm in length, occupying nearly one-third of the full length of granddaughter tube G1 (Fig. 4g).

5. Discussion

The incomplete preservation of the *Feiyanella* tube leaves uncertainties as to its full morphology and nesting patterns of the parent layers. Two overlapping patterns can be identified from the preserved portion, however: the outer parent tube layers (P1-1–P1-4) fully overlap (Fig. 4a–d), whereas all of the other inner tube layers only partially overlap (Fig. 4d–l). Two contrasting degrees of ornamentation are observed in *Feiyanella*: the outer parent tube layers (P1-1–P1-4) are visibly folded/wrinkled and form stronger transverse and/or slightly oblique corrugations (Fig. 4a–d), whereas all of the other inner tube layers are ornamented with weaker transverse annulations (Fig. 4d–l). The outermost layer of the tube in particular shows strongly folded/wrinkled corrugations (Figs 1a, b, 3a, 4a), making this layer appear much thicker (Figs 2a–d, 3b–c). With regard to nesting, although the four funnel-shaped parent layers (P1-1–P1-4) are completely nested in the preserved portion of the *Feiyanella* tube, it is uncertain whether their full morphology is funnel-shaped and whether they are fully or partially stacked.

As an Örsten-type Lagerstätte, the Kuanchuanpu Formation biota is characterized by the selective preservation of refractory cuticular tissues of meiofauna (see review in Schiffbauer *et al*. 2014) and only fragments of larger organisms (i.e. putative grasping spines of *Protohertzina anabarica*; see Steiner *et al*. 2004*a*). However, *Feiyanella* was not likely a fragment of a more complex organism: for example, an appendage of an annelid or ecdysozoan (panarthropod cycloneuralian). Several lines of evidence are summarized here: (1) Both annelids and ecdysozoans have a cuticularized integument overlying the epidermis, particularly a tri-layered cuticle (epi-, exo- and endocuticles) in cycloneuralians (Bereiter-Hahn, Matoltsy & Richards, 1984; Peterson & Eernisse, 2001). The appendages of these animals, if fossilized, would not be preserved as loosely multi-layered, funnel-in-funnel structures. (2) The cuticle of a complex organism usually bears complex ornaments, such as sensory organs, chaetae, glands, scalids and net-like structures. These ornaments are absent in *Feiyanella*. (3) The branched, segmented appendages in arthropods differ from the unsegmented funnel of *Feiyanella*. (4) The parapodium of annelids, although varying among species, tapers apparently towards one end, in visible

contrast with the sub-cylindrical shape of *Feiyanella*. (5) Some species of cycloneuralians (Liu *et al.* 2014*b*; Zhang *et al.* 2015) have been discovered from the Kuanchuanpu Formation. These fossils, together with a large number of specimens in our collection, collectively exhibit specific cuticle ornaments that are markedly different from *Feiyanella*. In addition, the integument of the cycloneuralian fossils is preserved as a single layer. In short, the characteristic multi-layered, funnel-in-funnel structure of *Feiyanella* is more appropriately interpreted as a dwelling tube of an organism, comparable to those known from the upper Ediacaran (e.g. Hua, Pratt & Zhang, 2003; Cai *et al.* 2011, 2014, 2015), rather than a body fragment of a larger complex organism.

Feiyanella is distinct from other early Cambrian tubular fossils, i.e. Hyolithelminths, *Byronia* and *Sphenothallus*. Hyolithelminths, a problematic group of mineralized tubular fossils characterized by more or less regular annulations or growth lines (Bengtson, *et al.* 1990; Li, 2004), exhibit a multi-laminated tube wall, and in some species, a cone-in-cone structure (see Kouchinsky *et al*. 2015, fig. 67). However, the micro-laminations of the tube wall are closely cemented together and each lamella (in some species) is composed of fine fibres (i.e. Bengtson *et al.* 1990; Vinn, 2006; Skovsted & Peel, 2011). *Hyolithellus* from the Kuanchuanpu Formation – a common element in the Kuanchuanpu Formation in the Xixiang and Ningqiang areas Steiner *et al.* (2004*a*) – is another tubular fossil sharing a similar morphology with *Feiyanella*. But the tubes of *Hyolithellus* are much larger in size (> 2 mm in length) than *Feiyanella* and the exterior smooth surface bears a number of wide-spaced circular grooves (Fig. 1e). In addition, ellipse-shaped pores occasionally occur in the grooves, which may be produced by soft tissue inside the tubes. *Hyolithellus* may have been a more complex organism (e.g. an annelid; Skovsted & Peel, 2011). The smooth tube, transverse grooves and ellipse-shaped pores indicate contrasting morphological and palaeobiological relationships with *Feiyanella*.

Byronia, a sessile tube-dwelling organism characterized by a lenticular cross-section and a deep split along the broader end (Bengtson *et al.* 1990), differs from *Feiyanella* in its wide-spaced transverse ridges and longitudinal ribs (see fig. 6 in Skovsted & Peel, 2011) that resemble the peridermal tube of olivooids (e.g. *Olivooides* and *Quadrapyrgites*; Liu *et al.* 2014*a*; Steiner *et al.* 2014) from the Kuanchuanpu Formation. Both *Byronia* and olivooids have been proposed to have close affinities with thecate medusozoans in the phylum Cnidaria (see Bengtson *et al.* 1990; Zhu *et al.* 2000; Dong *et al.* 2013; Han *et al.* 2016*b*).

Sphenothallus, a cone-shaped tube characterized by a more or less elliptical cross-section and a basal holdfast and proposed as a thecate medusozoan (Van Iten, Cox & Mapes, 1992; Zhu *et al.* 2000; Li, 2004), differs from *Feiyanella* in its finely laminated and cemented tube wall consisting of alternating apatite and organic laminae.

Instead, *Feiyanella* shares similarities in tube morphology and construction with some late Ediacaran tubular fossils, including *Cloudina* (Hua *et al*. 2005; Cortijo *et al*. 2010, 2015), *Conotubus* (Cai *et al*. 2011) and *Sinotubulites* (Chen *et al*. 2008; Cai *et al*. 2015). Each of these taxa shows a nested tube construction, cylindrical or oval-shaped cross-section and the absence of transverse internal structures such as septae or tabulae.

The perceived nesting pattern and the wrinkled tube-wall features of the parent layers (particularly P1-1) of *Feiyanella* are visibly similar to those of *Sinotubulites* (Cai *et al*. 2015). This may indicate that the parent layers of *Feiyanella* fully overlap, which would thus be comparable to the nesting patterns of *Sinotubulites*. On the other hand, the funnel-shaped tube layers of *Feiyanella* are strikingly similar to those of *Cloudina* (Hua, Pratt & Zhang, 2003; Hua *et al*. 2005; Cortijo *et al*. 2010) and *Conotubus* (Cai *et al*. 2011). Furthermore, the dichotomous branching of *Feiyanella*, which is most likely indicative of an asexual reproduction strategy, is also comparable to that of *Cloudina* (Hua *et al*. 2005; Cortijo *et al*. 2010, 2015).

While similar, *Feiyanella* also shows distinct differences from *Cloudina*, *Conotubus* and *Sinotubulites*. First, as compared to *Sinotubulites*, *Feiyanella* differs in tube layer morphology and overlapping patterns: *Feiyanella* is composed exclusively of funnel-shaped layers with partial overlap between adjacent layers (except for those of the parent funnels), whereas *Sinotubulites* is composed exclusively of cylinder-shaped layers with full overlap between two adjacent layers. The funnels of *Feiyanella* differ from the funnels of *Cloudina* and *Conotubus* in that the former lacks thickened rims on the apical and apertural ends of the funnels (Hua *et al*. 2005; Cortijo *et al*. 2010; Cai *et al*. 2011). In addition, *Feiyanella* differs from *Cloudina* in the manner of asexual reproduction. *Cloudina* is characterized by two manners of asexual reproduction strategies: dichotomous branching of daughter tubes in the same parent tube (see fig. 1L of Hua *et al*. 2005 and fig. 8 of Cortijo *et al*. 2010, 2015) and budding of a daughter tube between two adjacent funnels (see fig. 1P of Hua *et al*. 2005). *Feiyanella*, however, displays a pattern of multiple-ordered dichotomous branching of the younger generation of tubes within the older generation tubes.

Most broadly, *Feiyanella* shares similarities in the tube morphology, nesting patterns and presence of asexual reproduction strategies with *Cloudina*, and in the corrugation and nesting patterns of outer layers with *Sinotubulites*. Considering its similarities with *Cloudina* (Cai *et al*. 2014) and *Conotubus* (Cai *et al*. 2011), *Feiyanella* is thus interpreted as a sessile organism with periodic growth by secretion of new funnels within the older funnels (Grant, 1990), with the animal presumed to have lived within the innermost, most recently secreted funnel (Cortijo *et al*. 2010). The tube

https://doi.org/10.1017/S0016756816001187

of *Feiyanella* is hollow, indicating the soft tissue of the organism likely was able to move up and down within the tube, rather than being fixed within an isolated chamber. Although the full morphology of the tube is unknown, the apical end may have been closed, comparable to the basally closed apical end of *Cloudina* (Cortijo *et al*. 2015).

6. Zoological affinities and evolutionary implications

Together, *Cloudina*, *Conotubus*, *Sinotubulites* and *Feiyanella* may constitute a monophyletic group, as they are morphologically quite different from other Ediacaran and Cambrian tubular fossils (see summary in Cai *et al*. 2011; Cai, Hua & Zhang, 2013). The zoological placement of these *Cloudina*-type organisms, however, has been controversial. For example, *Cloudina* has been compared with both serpulid annelids (e.g. Glaessner, 1976; Hua *et al*. 2005) and cnidarians (e.g. Vinn & Zaton, 2012; Van Iten *et al*. 2014); the lack of preserved soft tissues in these fossils hinders convincing establishment of a palaeobiological interpretation.

While not reported in any other similar fossils, the spindle-shaped structure reported here in the innermost funnel of the granddaughter tube G1 may help provide a clue for phylogenetic placement of *Feiyanella* and, by extension, potentially other *Cloudina*-type organisms. This structure is three-dimensionally replicated by phosphate minerals, and its spindle-shaped morphology and massive size compared to the tube volume does not support an interpretation of an incompletely preserved funnel or other mineralized structure. Instead, we suggest that the spindle-shaped mass may be the phosphatized remains of the long-awaited tube dweller. Although it is difficult to depict the full morphology of the soft tissue inside the hollow tube, this spindle-shaped structure may represent the degraded organic remains of the organism that lived within these tubes. This interpretation is consistent with the morphological and palaeoecological reconstruction in *Conotubus* and *Cloudina* (Cai *et al*. 2011, 2014); they all possess hollow tubes which allowed for the tube dwellers to move up and down freely. This interpretation is also in accordance with the periodic growth of the tubes; the funnels were not simultaneously secreted by the soft issue, but instead were episodically secreted in the innermost layers.

A cnidarian planula interpretation for *Feiyanella* is largely compatible, and can be supported by several lines of evidence: (1) The asexual reproduction by longitudinal and transverse fissions of the soft body is more popular in extant cnidarians than in bilaterians. In addition, transverse fission has been reported from the sea-anemone-like cnidarians in the lower Cambrian Kuanchuanpu Formation in South China (Han *et al*. 2010). (2) The corrugated outermost layer of the tube broadly resembles the periderm of medusozoan polyps (Werner, 1973; Jarms, 1991). (3) The four-lobed morphology seen in granddaughter tube G2 of *Feiyanella* shows symmetry comparable to another coeval fossil, *Carinachites spinatus* Qian, 1977 (Qian, 1977; Conway Morris & Chen, 1992) – a Cambrian medusozoan with a phosphatized skeleton showing triradial, tetraradial and pentaradial symmetries (Conway Morris & Chen, 1992; Qian *et al*. 1997; Liu *et al*. 2011). (4) A colonial life habit proposed for *Feiyanella* is common in cnidarian hydropolyps (Hyman, 1940) (5) The funnel-in-funnel tube architecture of *Feiyanella* has also been observed in a few hydrotheca (e.g. *Sertularelia quadrata*; plates 15 and 16 of Nutting, 1900). (6) The proposed closed apical end of *Feiyanella* is compatible with a cnidarian body plan, but inconvenient for defecating of a bilateral worm with a through gut.

The ontogeny of *Feiyanella* indicates a possible transition from cylindrical radial symmetry to tetraradial symmetry. A similar transition from cylindrical radial symmetry to triradial symmetry was observed from a coeval fossil, *Anabarites*, which is also an early Cambrian tubular small shelly fossil suspected to be a cnidarian (Kouchinsky *et al*. 2009).

It is well known that Cambrian communities are quite different from those of the Ediacaran Period. Cambrian communities, exemplified by the Chengjiang and Burgess Shale biotas, are characterized by a complex food web with diverse types of feeding behaviours (Vannier *et al*. 2007; Hou, Siveter & Aldridge, 2008) and complex reproduction strategies (Duan *et al*. 2014; Caron & Vannier, 2015) similar to modern ocean ecosystems. Ediacaran communities, however, were instead comprised of slow creeping mat feeders and sessile benthic suspension feeders and/or osmotrophic feeders (e.g. Fedonkin *et al*. 2007; Laflamme, Xiao & Kowalewski, 2009; Rahman *et al*. 2015; Wood & Curtis, 2015). Although the early Cambrian small shelly fossil community – exemplified by the Kuanchuanpu Formation organisms – contains mat feeders (molluscs) (Qian & Bengtson, 1989) and microscopic predators (cycloneurians) (Liu *et al*. 2014*b*; Zhang *et al*. 2015), this ecosystem was characterized by a high richness and diversity of sessile organisms (i.e. predominantly cnidarians). Although a zoological placement remains unresolved, *Feiyanella* represents a Cambrian relict containing significant similarities in tube morphology, tube construction and reproduction strategy to some terminal Ediacaran tubular fossils (e.g. *Cloudina*, *Conotubus* and *Sinotubulites*). The early Cambrian small shelly fossil community revealed in the Kuanchuanpu Formation exhibits palaeobiological and palaeoecological features seemingly intermixed between both late Ediacaran and early Cambrian faunas. As such, it may support the notion that the late Ediacaran tubular biotas and their descendants represent important elements in a broader evolutionary prelude of the Cambrian explosion (Shu *et al*. 2014; Schiffbauer *et al*. 2016), rather than disappearing from the fossil record in an end-Ediacaran extinction (Smith *et al*. 2016).

https://doi.org/10.1017/S0016756816001187

7. Conclusions

The early Cambrian tubular fossil *Feiyanella manica* gen. et sp. nov. shares morphological similarities with the late Ediacaran tubular fossils *Cloudina*, *Conotubus* and *Sinotubulites*. Together, these tubular organisms may constitute a monophyletic group in the late Ediacaran through early Cambrian periods. The 'funnel-in-funnel' tube construction and the two-ordered dichotomous branching of *Feiyanella manica* gen. et sp. nov. are all comparable to those reported in *Cloudina*. The strongly corrugated outermost funnel and the gradational variations in the degrees of folding and/or wrinkling from exterior to interior tube layers of *Feiyanella manica* gen. et sp. nov. resembles those of *Sinotubulites*. *Feiyanella* thus embraces evolutionary continuity of typical late Ediacaran 'funnel-in-funnel' tube construction (exemplified by *Cloudina* and *Conotubus*), asexual reproduction by dichotomous branching of the tube (exemplified by *Cloudina*) and a gradational decrease in degrees of wrinkles and/or ornamentation from exterior to interior layers (exemplified by *Sinotubulites*). These continuities provide pivotal palaeobiological and palaeoecological insights into our understanding of the evolutionary history of the Ediacaran–Cambrian transition.

Acknowledgements. We thank H. Gong, J. Luo, N. Liu and M. Cheng (State Key Laboratory for Continental Dynamics, Northwest University (NWU), Xi'an, China) for their assistance in both field and lab works. We are grateful to Prof. Li Guoxiang (Nanjing Institute of Geology and Palaeontology, Chinese Academy of Sciences) for invaluable advice. Current work was supported by the Natural Science Foundation of China (Nos. 41621003, 41272019 and 41572012), the '973 project' of the Ministry of Science and Technology of China (2013CB835002), and the State Key Laboratory of Palaeobiology and Stratigraphy (Nanjing Institute of Geology and Palaeontology, CAS) (No. 163107).

References

Bengtson, S., Conway Morris, S., Cooper, B., Jell, P. & Runnegar, B. 1990. Early Cambrian fossils from South Australia. *Memoirs of the Association of Australasian Palaeontologists* **9**, 1–364.

Bereiter-Hahn, J., Matoltsy, A. G. & Richards, K. S. 1984. *Biology of the Integument: Invertebrates*. Berlin: Springer-Verlag.

Cai, Y., Hua, H., Schiffbauer, J. D., Sun, B. & Yuan, X. 2014. Tube growth patterns and microbial mat-related lifestyles in the Ediacaran fossil *Cloudina*, Gaojiashan Lagerstätte, South China. *Gondwana Research* **25**, 1008–18.

Cai, Y., Hua, H., Xiao, S., Schiffbauer, J. D. & Li, P. 2010. Biostratinomy of the late Ediacaran pyritized Gaojiashan Lagerstätte from southern Shaanxi, South China: importance of event deposits. *Palaios* **25**, 487–506.

Cai, Y., Hua, H. & Zhang, X. 2013. Tube construction and life mode of the late Ediacaran tubular fossil *Gaojiashania cyclus* from the Gaojiashan Lagerstätte. *Precambrian Research* **224**, 255–67.

Cai, Y., Schiffbauer, J. D., Hua, H. & Xiao, S. 2011. Morphology and paleoecology of the late Ediacaran tubular fossil *Conotubus hemiannulatus* from the Gaojiashan Lagerstätte of southern Shaanxi Province, South China. *Precambrian Research* **191**, 46–57.

Cai, Y., Xiao, S., Hua, H. & Yuan, X. 2015. New material of the biomineralizing tubular fossil *Sinotubulites* from the late Ediacaran Dengying Formation, South China. *Precambrian Research* **261**, 12–24.

Canfield, D. E. & Farquhar, J. 2009. Animal evolution, bioturbation, and the sulfate concentration of the oceans. *Proceedings of the National Academy of Sciences* **106**, 8123–7.

Canfield, D. E., Poulton, S. W., Knoll, A. H., Narbonne, G. M., Ross, G., Goldberg, T. & Strauss, H. 2008. Ferruginous conditions dominated later Neoproterozoic deep-water chemistry. *Science* **321**(5891), 949–52.

Caron, J.-B. & Vannier, J. 2015. *Waptia* and the diversification of brood care in early arthropods. *Current Biology* **26**, 1–6.

Chen, Z., Bengtson, S., Zhou, C. M., Hua, H. & Yue, Z. 2008. Tube structure and original composition of *Sinotubulites*: shelly fossils from the late Neoproterozoic in southern Shaanxi, China. *Lethaia* **41**, 37–45.

Conway Morris, S. & Chen, M. E. 1992. Carinachitids, hexaconulariids, and *Punctatus*: problematic metazoans from the Early Cambrian of South China. *Journal of Paleontology* **66**, 384–406.

Cortijo, I., Mus, M. M., Jensen, S. & Palacios, T. 2010. A new species of *Cloudina* from the terminal Ediacaran of Spain. *Precambrian Research* **176**, 1–10.

Cortijo, I., Mus, M. M., Jensen, S. & Palacios, T. 2015. Late Ediacaran skeletal body fossil assemblage from the Navalpino anticline, central Spain. *Precambrian Research* **267**, 186–95.

Darroch, S. A., Sperling, E. A., Boag, T. H., Racicot, R. A., Mason, S. J., Morgan, A. S., Tweedt, S., Myrow, P., Johnston, D. T. & Erwin, D. H. 2015. Biotic replacement and mass extinction of the Ediacara biota. In *Proceedings of the Royal Society B: Biological Sciences* **282**, 20151003. doi: 10.1098/rspb.2015.1003.

Dong, X.-P., Cunningham, J. A., Bengtson, S., Thomas, C.-W., Liu, J., Stampanoni, M. & Donoghue, P. C. 2013. Embryos, polyps and medusae of the Early Cambrian scyphozoan *Olivooides*. *Proceedings of the Royal Society B: Biological Sciences* **280**, 130071. doi: 10.1098/rspb.2013.0071.

Duan, Y., Han, J., Fu, D., Zhang, X., Yang, X., Komiya, T. & Shu, D. 2014. Reproductive strategy of the bradoriid arthropod *Kunmingella douvillei* from the Lower Cambrian Chengjiang Lagerstätte, South China. *Gondwana Research* **25**, 983–90.

Erwin, D. H., Laflamme, M., Tweedt, S. M., Sperling, E. A., Pisani, D. & Peterson, K. J. 2011. The Cambrian conundrum: early divergence and later ecological success in the early history of animals. *Science* **334**(6059), 1091–7.

Fedonkin, M. A., Gehling, J. G., Grey, K., Narbonne, G. M. & Vickers-Rich, P. 2007. *The Rise of Animals: Evolution and Diversification of the Kingdom Animalia*. Baltimore: John Hopkins University Press.

Fike, D. A., Grotzinger, J. P., Pratt, L. M. & Summons, R. E. 2006. Oxidation of the Ediacaran ocean. *Nature* **444**, 744–7.

Germs, J. G. B. 1972. New shelly fossils from the Nama Group, South West Africa. *American Journal of Science* **272**, 752–61.

Glaessner, M. 1976. Early Phanerozoic annelid worms and their geological and biological significance. *Journal of the Geological Society, London* **132**, 259–75.

Grant, S. 1990. Shell structure and distribution of *Cloudina*, a potential index fossil for the terminal Proterozoic. *American Journal of Science* **290**, 261–94.

Grotzinger, J. P., Watters, W. A. & Knoll, A. H. 2000. Calcified metazoans in thrombolite–stromatolite reefs of the terminal Proterozoic Nama Group, Namibia. *Paleobiology* **26**, 334–59.

Hagadorn, J. W. & Waggoner, B. M. 2000. Ediacaran fossils from the southwestern Great Basin, United States. *Journal of Paleontology* **74**, 349–59.

Han, J., Kubota, S., Li, G., Ou, Q., Wang, X., Yao, X., Shu, D., Li, Y., Uesugi, K., Hoshino, M., Sasaki, O., Kano, H., Sato, T. & Komiya, T. 2016a. Divergent evolution of medusozoan symmetric patterns: evidence from the microanatomy of Cambrian tetramerous cubozoans from South China. *Gondwana Research* **31**, 150–63.

Han, J., Kubota, S., Li, G., Yao, X., Yang, X., Shu, D., Li, Y., Kinoshita, S., Sasaki, O., Komiya, T. & Yan, G. 2013. Early Cambrian pentamerous cubozoan embryos from South China. *PLoS One* **8**(8), e70741. doi: 10.1371/journal.pone.0070741.

Han, J., Kubota, S., Uchida, H., Stanley Jr, G. D., Yao, X. Y., Shu, D. G., Li, Y. & Yasui, K. 2010. Tiny sea anemone from the Lower Cambrian of China. *PLoS One* **5**(10), e13276. doi: 10.1371/journal.pone.0013276.

Han, J., Li, G. X., Kubota, S., Ou, Q., Toshino, S., Wang, X., Yang, X. G., Uesugi, K., Hoshino, M., Sasaki, O., Kano, H. & Komiya, T. 2016b. Internal microanatomy and zoological affinity of the early Cambrian *Olivooides*. *Acta Geologica Sinica (English Edition)* **90**(1), 38–65.

Hofmann, H. J. & Mointjoy, E. W. 2001. *Namacalathus–Cloudina* assemblage in Neoproterozoic Miette Group (Byng Formation), British Columbia: Canada's oldest shelly fossils. *Geology* **29**, 1091–4.

Hou, X. G., Siveter, D. J. & Aldridge, R. J. 2008. Collective behavior in an early Cambrian arthropod. *Science* **322**(5899), 224.

Hua, H., Chen, Z., Yuan, X. L., Zhang, L. Y. & Xiao, S. H. 2005. Skeletogenesis and asexual reproduction in the earliest biomineralizing animal *Cloudina*. *Geology* **33**, 277–80.

Hua, H., Pratt, B. R. & Zhang, L.-Y. 2003. Borings in *Cloudina* shells: complex predator-prey dynamics in the terminal Neoproterozoic. *Palaios* **18**, 454–9.

Hyman, L. H. 1940. *The Invertebrates*. New York: McGraw Hill.

Jarms, G. 1991. Taxonomic characters from the polyp tubes of coronate medusae (Scyphozoa, Coronatae). *Hydrobiologia* **216**, 463–70.

Jensen, S., Gehling, J. G. & Droser, M. L. 1998. Ediacara-type fossils in Cambrian sediments. *Nature* **393**, 567–9.

Komiya, T., Hirata, T., Kitajima, K., Yamamoto, S., Shibuya, T., Sawaki, Y., Ishikawa, T., Shu, D., Li, Y. & Han, J. 2008. Evolution of the composition of seawater through geologic time, and its influence on the evolution of life. *Gondwana Research* **14**, 159–74.

Kouchinsky, A., Bengtson, S., Clausen, S. & Vendrasco, M. J. 2015. An early Cambrian fauna of skeletal fossils from the Emyaksin Formation, northern Siberia. *Acta Palaeontologica Polonica* **60**, 421–512.

Kouchinsky, A., Bengtson, S., Feng, W., Kutygin, R. & Val'kov, A. 2009. The Lower Cambrian fossil anabaritids: affinities, occurrences and systematics. *Journal of Systematic Palaeontology* **7**, 241–98.

Laflamme, M., Darroch, S. A., Tweedt, S. M., Peterson, K. J. & Erwin, D. H. 2013. The end of the Ediacara biota: extinction, biotic replacement, or Cheshire Cat? *Gondwana Research* **23**, 558–73.

Laflamme, M., Xiao, S. & Kowalewski, M. 2009. Osmotrophy in modular Ediacara organisms. *Proceedings of the National Academy of Sciences* **106**, 14438–43.

Li, G. 2004. Early Cambrian Hyolithelminths – *Torellella bisulcata* sp. nov. from Zhenba, Southern Shaanxi. *Acta Palaeontologica Sinica* **43**, 571–8.

Li, C., Love, G. D., Lyons, T. W., Fike, D. A., Sessions, A. L. & Chu, X. 2010. A stratified redox model for the Ediacaran ocean. *Science* **328**(5974), 80–3.

Liu, Y., Li, Y., Shao, T., Zhang, H., Wang, Q. & Qiao, J. 2014a. *Quadrapyrgites* from the lower Cambrian of South China: Growth pattern, post-embryonic development, and affinity. *Chinese Science Bulletin* **59**(31), 4086–95.

Liu, Y., Li, Y., Shao, T., Zheng, X., Zheng, J., Wang, G., Wang, H. & Qwang, K. 2011. A new genus and species of protoconulariids from the early Cambrian in the south Shaanxi, China. *Acta Micropalaeontologica Sinica* **28**, 245–49.

Liu, Y. H., Xiao, S. H., Shao, T. Q., Broce, J. & Zhang, H. Q. 2014b. The oldest known priapulid-like scalidophoran animal and its implications for the early evolution of cycloneuralians and ecdysozoans. *Evolution & Development* **16**, 155–65.

McIlroy, D., Green, O. R. & Brasier, M. D. 2001. Palaeobiology and evolution of the earliest agglutinated Foraminifera: *Platysolenites*, *Spirosolenites* and related forms. *Lethaia* **34**, 13–29.

Nutting, C. C. 1900. *American Hydroids (II)*. Washington: US Government Printing Office.

Peterson, K. J. & Eernisse, D. J. 2001. Animal phylogeny and the ancestry of bilaterians: inferences from morphology and 18S rDNA gene sequences. *Evolution and Development* **3**, 170–205.

Qian, Y. 1977. Hyolitha and some problematica from the Lower Cambrian Meishucun Stage in central and SW China. *Acta Palaeontologica Sinica* **16**, 255–75.

Qian, Y. 1999. *Taxonomy and Biostratigraphy of Small Shelly Fossils in China*. Beijing: Science Press (in Chinese with English summary).

Qian, Y. & Bengtson, S. 1989. Palaeontology and biostratigraphy of the Early Cambrian Meishucunian Stage in Yunnan Province, South China. *Fossils and Strata* **24**, 1–156.

Qian, Y., Van Iten, H., Cox, R. S., Zhu, M. & Zhou, E. 1997. A brief account of *Emeiconularia trigemme*, a new genus and species of protoconulariid. *Acta Micropalaeontologica Sinica* **14**, 475–88.

Rahman, I. A., Darroch, S. A. F., Racicot, R. A. & Laflamme, M. 2015. Suspension feeding in the enigmatic Ediacaran organism Tribrachidium demonstrates complexity of Neoproterozoic ecosystems. *Science Advances* **1**, e1500800. doi: 10.1126/sciadv.1500800.

Rogov, V. I., Karlova, G. A., Marusin, V. V., Kochnev, B. B., Nagovitsin, K. E. & Grazhdankin, D. V. 2015. Duration of the first biozone in the Siberian hypostratotype of the Vendian. *Russian Geology and Geophysics* **56**, 573–83.

Schiffbauer, J. D., Huntley, J. W., O'Neil, G. R., Darroch, S. A. F., Laflamme, M. & Cai, Y. 2016. The latest Ediacaran Wormworld fauna: setting the

ecological stage for the Cambrian Explosion. *GSA Today* **26**, 4–11.

Schiffbauer, J. D., Wallace, A. F., Broce, J. & Xiao, S. 2014. Exceptional fossil conservation through phosphatization. *The Paleontological Society Papers* **20**, 59–82.

Seilacher, A. 1999. Biomat-related lifestyles in the Precambrian. *Palaios* **14**, 86–93.

Shu, D., Isozaki, Y., Zhang, X., Han, J. & Maruyama, S. 2014. Birth and early evolution of metazoans. *Gondwana Research* **25**, 884–95.

Shu, D. G., Morris, S. C., Han, J., Li, Y., Zhang, X. L., Hua, H., Zhang, Z. F., Liu, J. N., Guo, J. F., Yao, Y. & Yasui, K. 2006. Lower Cambrian vendobionts from China and early diploblast evolution. *Science* **312**(5774), 731–4.

Signor, P. W., Mount, J. F. & Onken, B. R. 1987. A pre–trilobite shelly fauna from the White–Inyo region of eastern California and western Nevada. *Journal of Paleontology* **61**, 425–38.

Skovsted, C. B. & Peel, J. S. 2011. *Hyolithellus* in life position from the Lower Cambrian of North Greenland. *Journal of Paleontology* **85**, 37–47.

Smith, E. F., Nelson, L. L., Strange, M. A., Eyster, A. E., Rowland, S. M., Schrag, D. P. & Macdonald, F. A. 2016. The end of the Ediacaran: two new exceptionally preserved body fossil assemblages from Mount Dunfee, Nevada, USA. *Geology* **44**, 911–4.

Sperling, E. A., Frieder, C. A., Raman, A. V., Girguis, P. R., Levin, L. A. & Knoll, A. H. 2013. Oxygen, ecology, and the Cambrian radiation of animals. *Proceedings of the National Academy of Sciences* **110**, 13446–51.

Steiner, M., Li, G. X., Qian, Y. & Zhu, M. Y. 2004a. Lower Cambrian Small Shelly Fossils of northern Sichuan and southern Shaanxi (China), and their biostratigraphic importance. *Geobios* **37**, 259–75.

Steiner, M., Qian, Y., Li, G., Hagadorn, J. W. & Zhu, M. 2014. The developmental cycles of early Cambrian Olivooidae fam. nov. (?Cycloneuralia) from the Yangtze Platform (China). *Palaeogeography, Palaeoclimatology, Palaeoecology* **398**, 97–124.

Steiner, M., Zhu, M. Y., Li, G. X., Qian, Y. & Erdtmann, B. D. 2004b. New early Cambrian bilaterian embryos and larvae from China. *Geology* **32**, 833–6.

Van Iten, H., Cox, R. S. & Mapes, R. H. 1992. New data on the morphology of *Sphenothallus* Hall: implications for its affinities. *Lethaia* **25**, 135–44.

Van Iten, H., De Moraes Leme, J., Sim Es, M. G., Marques, A. C. & Collins, A. G. 2006. Reassessment of the phylogenetic position of conulariids (? Ediacaran–Triassic) within the subphylum Medusozoa (phylum Cnidaria). *Journal of Systematic Palaeontology* **4**, 109–18.

Van Iten, H., Marques, A. C., Leme, J. D. M., Pacheco, M. L. & Sim Es, M. G. 2014. Origin and early diversification of the phylum Cnidaria Verrill: major developments in the analysis of the taxon's Proterozoic–Cambrian history. *Palaeontology* **57**(4), 1–14.

Vannier, J., Garc A-Bellido, D., Hu, S.-X. & Chen, A.-L. 2009. Arthropod visual predators in the early pelagic ecosystem: evidence from the Burgess Shale and Chengjiang biotas. *Proceedings of the Royal Society of London B: Biological Sciences* **276**(1667), 2567–74.

Vannier, J., Steiner, M., Renvoise, E., Hu, S. X. & Casanova, J. P. 2007. Early Cambrian origin of modern food webs: evidence from predator arrow worms. *Proceedings of the Royal Society B: Biological Sciences* **274**(1610), 627–33.

Vinn, O. 2006. Possible cnidarian affinities of *Torellella* (Hyolithelminthes, Upper Cambrian, Estonia). *Paläontologische Zeitschrift* **80**, 384–9.

Vinn, O. & Zaton, M. 2012. Inconsistencies in proposed annelid affinities of early biomineralized organism *Cloudina* (Ediacaran): structural and ontogenetic evidences. *Carnets de Geologie [Notebooks on Geology]* **CG2012**(A03), 39–46.

Werner, B. 1973. New investigations on systematics and evolution of the class Scyphozoa and the phylum Cnidaria. *Publications of the Seto Marine Biological Laboratory* **20**, 35–61.

Wood, R. & Curtis, A. 2015. Extensive metazoan reefs from the Ediacaran Nama Group, Namibia: the rise of benthic suspension feeding. *Geobiology* **13**, 112–22.

Yang, B., Steiner, M., Zhu, M., Li, G., Liu, J. & Liu, P. 2016. Transitional Ediacaran–Cambrian small skeletal fossil assemblages from South China and Kazakhstan: Implications for chronostratigraphy and metazoan evolution. *Precambrian Research* **285**, 202–15.

Yochelson, E. L. & Stump, E. 1977. Discovery of early Cambrian fossils at Taylor Nunatak, 936 Antarctica. *Journal of Paleontology* **51**, 872–5.

Yuan, X., Chen, Z., Xiao, S., Zhou, C. & Hua, H. 2011. An early Ediacaran assemblage of macroscopic and morphologically differentiated eukaryotes. *Nature* **470**(7334), 390–3.

Zhang, H., Xiao, S., Liu, Y., Yuan, X., Wan, B., Muscente, A., Shao, T., Gong, H. & Cao, G. 2015. Armored kinorhynch-like scalidophoran animals from the early Cambrian. *Scientific Reports* **5**, 16521. doi: 10.1038/srep16521.

Zhu, M., Van Iten, H., Cox, R. S., Zhao, Y. & Erdtmann, B. D. 2000. Occurrence of *Byronia* Matthew and *Sphenothallus* Hall in the Lower Cambrian of China. *Palaeontologische Zeitschrift* **74**, 227–38.

Zhuravlev, A. Y., Li, N, E., Vintaned, J. A. G., Debrenne, F. & Fedorov, A. B. 2012. New finds of skeletal fossils in the terminal Neoproterozoic of the Siberian Platform and Spain. *Acta Palaeontologica Polonica* **57**, 205–24.

5.3 Carinachitids with apertural lobes

As noted in Chapter 3, carinachitids are important elements of early Cambrian SSF-assemblages from the Kuanchuanpu Formation. The purpose of this study was to explore the morphology these microfossils in three dimensions by using high-resolution tomographic methods and test hypotheses concerning their assumed cnidarian affinities (Qian 1977, Conway Morris and Chen 1992).

Carinachitids display a remarkable variety of symmetry patterns with triradial, tetraradial and pentaradial forms. Their tubular skeletons consist of convex faces separated by longitudinal furrows (corner sulci; see (Qian 1977, Qian et al. 1997, Liu et al. 2011)).

In this paper, we described new carinachitid specimens resembling *Carinachites spinatus* Qian (1977). X-Ray micro tomography allows the authors to reconstruct its general architecture and revealed important details of its soft anatomy and apertural region. These specimens have four perradial plicate apertural lobes in connection with possible remains of soft tissue and converging radially towards the mouth. This configuration suggests that these four folded lobes could partially close the tube aperture bearing the mouth, thus recalling the oral lappets of *Olivooides*-like organisms from the same biota (Steiner et al. 2014).

Similarities between transverse rough spines on the faces and the oral lobes indicate that the transverse ribs of *Carinachites* were periodically displaced from the perradial portion of the aperture during formation of new ribs. In addition, the tube walls of the new specimen of *C. spinatus* may have undergone secondary thickening during growth. These findings strengthen previous hypotheses (Conway Morris and Chen 1992) that coeval *Carinachites*, *Olivooides*, *hexaconulariids*, and Paleozoic conulariids are closely related taxa within the subphylum Medusozoa. Finally, *Carinachites* may represent an evolutionary intermediate step between *Olivooides* and *hexaconulariids*.

Journal of Paleontology, page 1 of 11

0022-3360/15/0088-0906
doi: 10.1017/jpa.2017.10

JOURNAL OF PALEONTOLOGY
A PUBLICATION OF THE Paleontological SOCIETY

Olivooides-like tube aperture in early Cambrian carinachitids (Medusozoa, Cnidaria)

Jian Han,[1] Guoxiang Li,[2] Xing Wang,[1] Xiaoguang Yang,[1] Junfeng Guo,[3] Osamu Sasaki,[4] and Tsuyoshi Komiya[5]

[1]Department of Geology and State Key Laboratory of Continental Dynamics, Northwest University, 229 Taibai Road, Xi'an 710069, P.R. China ⟨elihanj@nwu.edu.cn⟩, ⟨799179701@qq.com⟩, ⟨lqzy0301@gmail.com⟩
[2]State Key Laboratory of Palaeobiology and Stratigraphy, Nanjing Institute of Geology and Palaeontology, Chinese Academy of Sciences, Nanjing 210008, China ⟨gxli@nigpas.ac.cn⟩
[3]School of Earth Science and Land Resources, Key Laboratory of Western China's Mineral Resources and Geological Engineering, Ministry of Education, Chang'an University, Xi'an 710054, China ⟨junfengg@chd.edu.cn⟩
[4]Tohoku University Museum, Tohoku University, 6-3 Aoba, Aramaki, Aoba-ku, Sendai, Japan ⟨Sasaki@museum.tohoku.ac.jp⟩
[5]Department of Earth Science and Astronomy, Graduate School of Arts and Sciences, The University of Tokyo, Tokyo 153-8902, Japan ⟨komiya@ea.c.u-tokyo.ac.jp⟩

Abstract.—The early Cambrian Carinachitidae, a family in the subclass Conulata, are intriguing and important small shelly fossils. Their gently tapering, tube-shaped skeletons consist of convex faces separated from each other by broad, deep corner sulci, and they exhibit triradial, pentaradial, or predominantly tetraradial symmetry. However, the morphology of the aperture and the modes of growth of carinachitid skeletons as well as the anatomy of their soft parts are unknown. Examination of a single new, exceptionally well-preserved specimen of tetramerous *Carinachites spinatus* Qian, 1977, collected from the lower Cambrian Kuanchuanpu Formation in South China, reveals: (1) that its aperture is connected to a small mass of relic soft tissue and (2) that the apertural end of each of the four faces is developed into a subtriangular lappet or oral lobe that is smoothly folded toward the long axis of the tube, partially closing the tube aperture. Similarities between thorn-like spines on the faces and the oral lobes indicate that the transverse ribs were periodically displaced from the perradial portion of the aperture during formation of new ribs. In addition, the tube walls may have undergone secondary thickening during growth. The growth pattern of the tube and the spatial relationships between the tube aperture and soft parts are analogous to those of co-occurring olivooids. These findings further strengthen the previously proposed hypothesis that coeval carinachitids, olivooids, hexangulaconulariids, and Paleozoic conulariids are closely related taxa within the subphylum Medusozoa. Finally, carinachitids most likely represent an evolutionary intermediate between olivooids and hexangulaconulariids.

Introduction

The abrupt appearance of diverse small shelly fossils (SSFs) during the earliest Cambrian signals the initial stages of the Cambrian explosion (G. Li et al., 2007; Maloof et al., 2010). It therefore seems axiomatic that SSFs are of great importance for understanding the early rise of metazoan phyla and the origins of animal skeletogeny. Paleoecological reconstruction of SSF communities is a challenging task as the majority of SSFs are fragmentary or consist of isolated sclerites. A critical exception to this rule is the set of phosphatic SSFs in Orsten-type Lagerstätten, for example the Kuanchuanpu Biota in South China (ca. 535 Ma), which together have the potential to provide unique insights into the nature and significance of these fossils thanks to their high potential for exceptional preservation of both hard parts and soft tissues.

Carinachitids are an important component of early Cambrian SSFs in South China (Conway Morris and Chen, 1992). Their gently conical skeletal tubes exhibit several (three to five) transversely ribbed faces separated from each other by wide and deep corner sulci that usually bear fine transverse wrinkles (tw) (Fig. 1). To date, three genera and six species of carinachitids—*Emeiconularia trigemme* Qian in Qian et al., 1997; *E. amplicanalis* Liu et al., 2005 (Fig. 1.1); *Pentaconularia ningqiangensis* Liu et al., 2011 (Fig. 2); *Carinachites spinatus* Qian, 1977 (Figs. 3–5); *C. tetrasulcatus* Jiang in Luo et al., 1982; and *C. curvatornatus* Chen, 1982—have been reported from the Kuanchuanpu Formation and equivalent horizons in South China (Qian, 1977; He, 1987; Conway Morris and Chen, 1992; Qian et al., 1997; Liu et al., 2005, 2011). These fossils collectively exhibit tri-, tetra-, or pentaradial symmetry in transverse sections (Liu et al., 2011), and these symmetries may have arisen independently in different lineages (Han et al., 2016a, b). In addition, the tube wall appears to have been flexible and composed of organic material and/or calcium phosphate (Conway Morris and Chen, 1992; Qian et al., 1999).

Carinachitids, together with co-occurring hexangulaconulariids (Yue and Bengtson, 1999; Van Iten et al., 2010) and olivooids

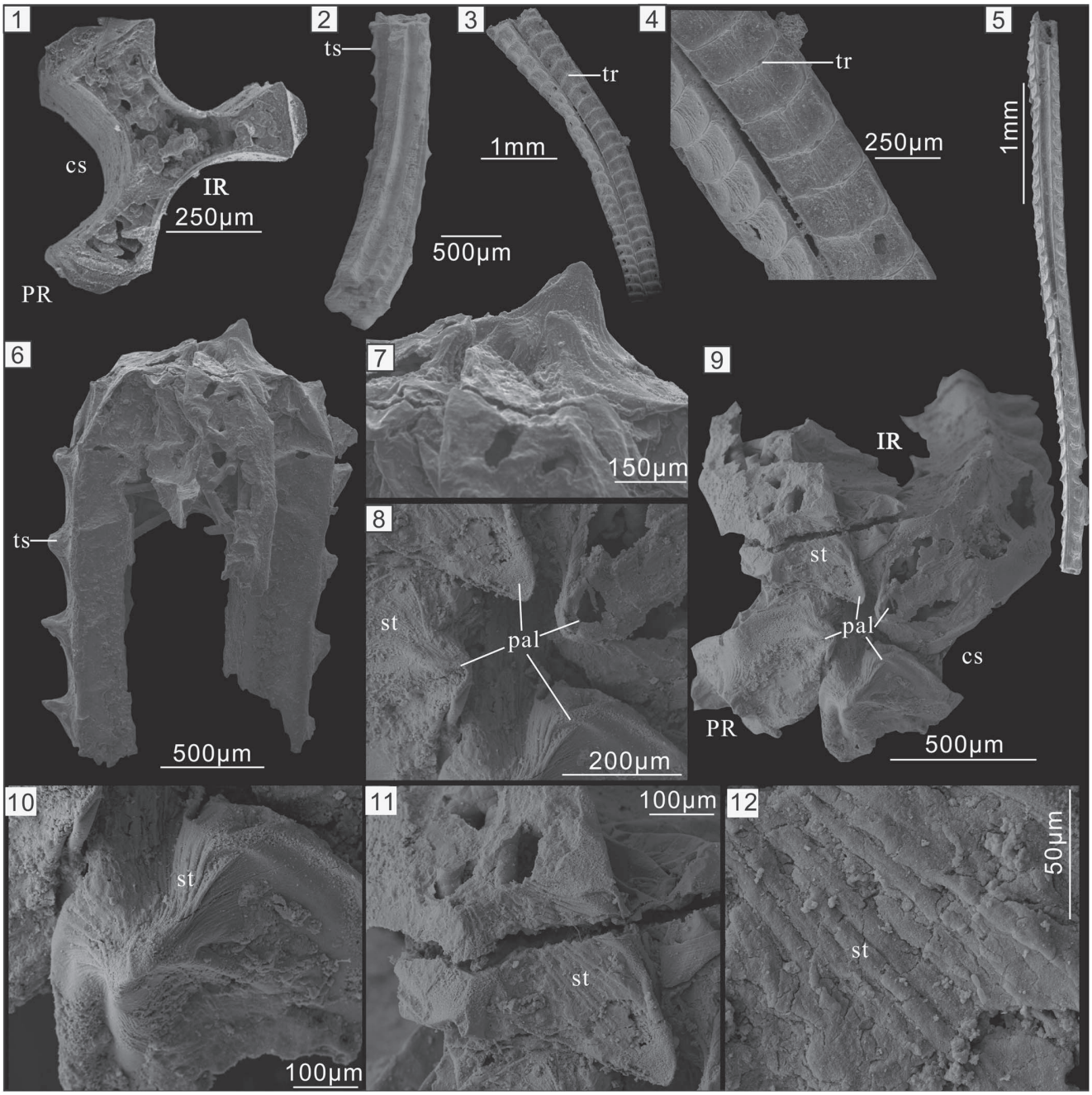

Figure 1. Carinachitids from the lower Cambrian Kuanchuanpu Formation in South China. (**1**) Triradiate *Emeiconularia amplicanalis* Liu et al., 2005. (**2**) Pentamerous *Pentaconularia ningqiangensis* Liu et al., 2011. (**1, 2**) Courtesy of Y.H. Liu. (**3–6**) Tetraradiate *Carinachites spinatus* Qian, 1977. (**3, 4**) ELISN93-157, showing the displacement between neighboring arcuate ribs, which are connected in the middle by striations. Both the faces and ribs widen slightly toward the apertural end of the skeleton. (**5**) ELISN93-45. (**6–12**) ELISN148-52. (**6, 7**) Lateral view of the tube. (**8, 9**) Close-up of the tube aperture shows one of the plicate apertural lobes being elevated above the others. (**10**) The elevated, plicate apertural lobes with converging striated folds. (**11**) Single plicate apertural lobe with converging striated folds and the corner sulci with parallel striations. (**12**) Close-up of (**11**) showing secondary cracks on the striated surface. IR = interradius; PR = perradius; cs = corner sulci; pal = plicate apertural lobes; st = striations; tr = transverse ribs; ts = thorn-like spines.

(see Steiner et al., 2014), have been assigned to the order Conulariida of the subclass Conulata (He, 1987; Qian et al., 1999). Because carinachitids and hexangulaconulariids are very small (<5 mm long) and lack the facial midline and carina typical of many Ordovician and younger conulariids, they have been classified as protoconulariids (Qian et al., 1999). The zoological affinities of Conulata have been controversial (Babcock et al., 1986; Brood, 1995), but the group is now generally assigned to the subphylum Medusozoa of the phylum Cnidaria (Bengtson and Yue, 1997; Van Iten et al., 2006, 2010, 2014). Phylogenetic relationships among protoconulariids remain poorly understood as all previously collected specimens of carinachitids lack both the apical and apertural regions, and thus their complete morphology and growth patterns are unknown. Here we describe a tetramerous

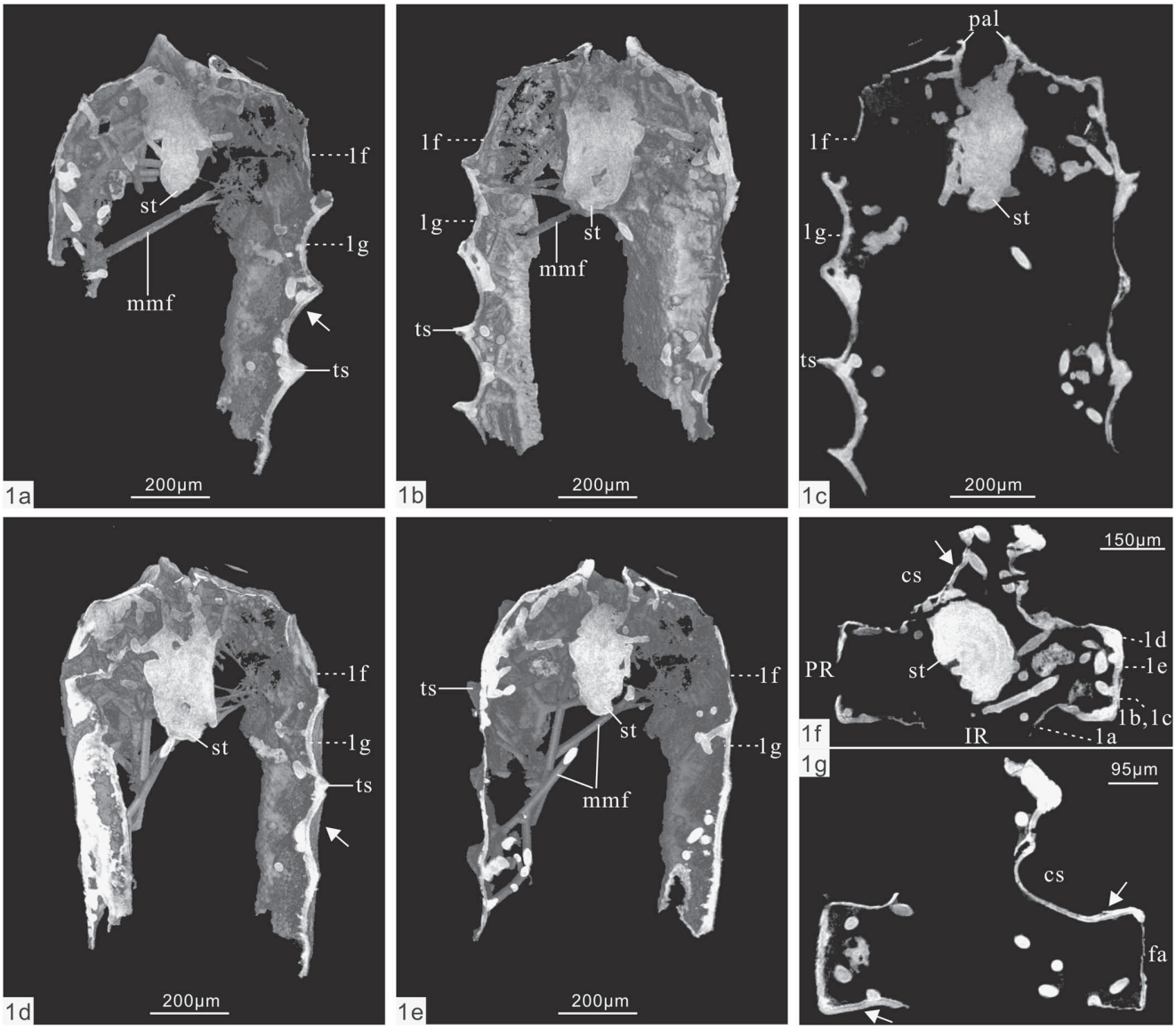

Figure 2. Micro-CT reconstruction of specimen ELISN148-52. (**1a–1e**) lateral view; (**1f, 1g**) oral view of the virtual cross sections. The sagittal positions of (**1a–1e**) are indicated respectively by '1a,' '1b,' '1c,' '1d,' '1e,' and '1f' in (**1f, 1g**). The horizontal levels of (**1f, 1g**) are respectively indicated by '1f' and '1g' in (**1a–1f**). White arrows indicate double-layered tube wall. cs = corner sulcus; fa = face; mmf = microbial-mediated filaments; pal = plicate apertural lobes; st = soft tissue; ts = thorn-like spines; PR = perradius; IR = interradius.

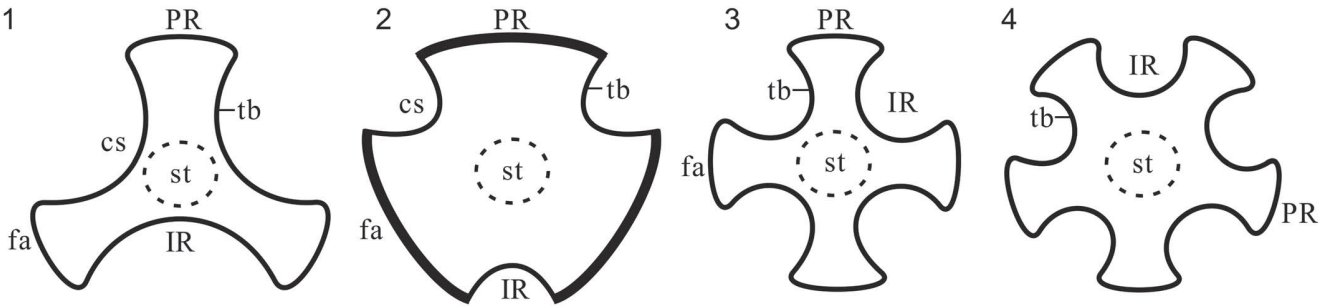

Figure 3. Cross sections and proposed orientation of the main radial symmetry planes in Cambrian carinachitids. (**1, 2**) Inferred triradial symmetry in *Emeiconularia*; (**1**) *E. amplicanalis*; (**2**) *Emeiconularia trigemme* with thickened faces sensu Qian et al., 1999; (**3**) tetraradial symmetry in *Carinachites*; (**4**) pentaradial symmetry in *Pentaconularia* (Modified from Liu et al., 2011). cs = corner sulcus; fa = face; st = soft tissue; tb = tube; PR = perradius; IR = interradius.

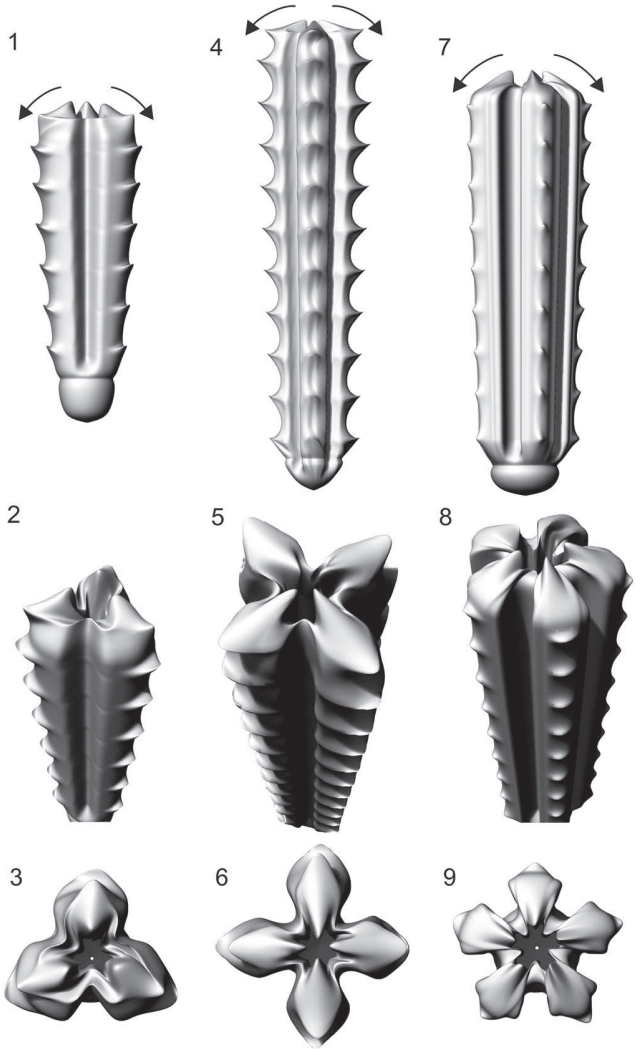

Figure 4. 3D reconstructions of Cambrian carinachitids with a hypothetical apical tip. (**1–3**) Lateral, oblique, and oral views, respectively, of *Emeiconularia*; (**4–6**) lateral, oblique, and oral views, respectively, of *Carinachites spinatus*; (**7–9**) lateral, oblique, and oral views, respectively, of *Pentaconularia*.

specimen of *Carinachites spinatus* that preserves the tube aperture. This specimen provides critical new insights into the morphology, systematic classification, and paleoautecology of carinachitids.

Materials and methods

Specimens of *Carinachites spinatus* were obtained from samples of phosphatic limestone collected from the Kuanchuanpu Formation in southern Shaanxi Province, South China, and digested in 10% acetic acid. Specimens ELISN148-52, ELISN93-45, ELISN93-157, ELISN19-20, ELISN23-240, and ELISN12-154 come from the Shizhonggou section in Ningqiang County, while specimen XX30-127 is from the Yangjiagou section in Xixiang County (for localities, see Steiner et al., 2007, fig.1). All specimens were coated with gold and then imaged using an FEI Quanta 400 FEG scanning electron microscope (SEM). Micro-CT data for specimen

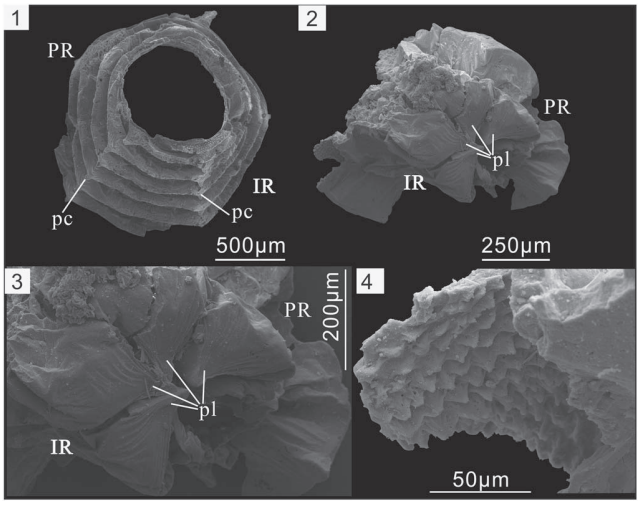

Figure 5. Peridermal tube of *Olivooides multisulcatus* from the Cambrian Kuanchuanpu Formation in South China. (**1**) Specimen ELISN19-20, aboral view showing five longitudinal rows of plicate corners (pc); (**2–4**) XX30-127. Oral view of the specimen. (**2**) Tube aperture with five plicate lobes (pl); (**3**) close-up of (**2**). (**4**) Diagnostic stellate ornament of the aboral ends. PR = perradii; IR = interradii.

ELISN148-52 were acquired at the Tohoku University (Fig. 2) and were processed using VG Studio 2.2 Max for 3D reconstructions. The terminology used herein mostly follows that of Conway Morris and Chen (1992), Van Iten (1992a), and Han et al., 2016a.

Repository and institutional abbreviation.—The figured specimens in this study are housed in the Early Life Institute (ELI), Northwest University, Xi'an, China.

Results

Tube morphology of Carinachites spinatus.—Carinachitids are abundantly represented by tetramerous *C. spinatus* Qian 1977 in the Kuanchuanpu Formation in the Shizhonggou section in Shaanxi Province. The tube of this species exhibits four prominent, equidimensional convex faces separated from each other by deep corner sulci (Figs. 1.3–1.6, 2.6). Each face usually bears a longitudinal series of arcuate transverse ribs that range in shape from simple welts to more complex folds (Conway Morris and Chen, 1992). The distance between adjacent ribs increases slightly toward the wide or oral end of the tube (Fig. 1.3). Near the facial midline, the region between any two adjacent ribs exhibits several, mutually parallel or irregular, longitudinal striated folds that in most cases are separated from each other by an inconspicuous shallow groove (Fig. 1.4).

The transverse ribs in some specimens are arcuate near the distal end and as wide as the faces (Fig. 1.3, 1.4), while in other specimens the ribs consist of a prominent, sharp, thorn-like spine (ts) such as those exhibited by specimens ELISN93-45 (Fig. 1.5) and ELISN148-52 (Fig. 1.6). The ribs on any two neighboring faces usually are located at the same levels above the apex, but some ribs exhibit longitudinal offset (Fig. 1.3, 1.4) (Conway Morris and Chen, 1992). In addition, the ribs of some specimens are offset along the facial midline (Conway Morris and Chen, 1992, fig. 6.1).

The apertural region, preserved only in the relatively large specimen ELISN148-52, is superficially dome-shaped (Fig. 1.6–1.9). The maximum diameter of the tube is approximately 1.3 mm, but near its apertural end the tube tapers rapidly, with the faces curving smoothly toward the longitudinal axis of the tube and becoming more or less perpendicular to it. Close to the longitudinal axis, the faces and intervening corner sulci are inclined toward the aboral end of the tube (Fig. 1.6, 1.7, 1.9). Present on each face, at the summit of the aperture, is a triangular tongue-shaped structure, and the distal ends of the faces almost meet near the longitudinal axis of the tube, leaving just a narrow central opening. One of the tongue-shaped structures projects much farther than the others beyond the aperture (Fig. 1.6). The tongue-shaped structures are not flat features but rather fold-like structures having two main, arched sides separated by two flanks. For this reason, we term the tongue-shaped structures 'plicate apertural lobes' (pal). The vertical abapertural side of the apertural lobes extends far into the apertural opening and exhibits a medial subtriangular groove bordered by two elevated flanks (Fig. 1.8, 1.9). The abapertural side is either flat or outwardly convex with a central ridge, and there are many longitudinal striations on the two sides. These striations converge on the tip of the lobes, and there are some oblique, irregular cracks on the striated surface (Fig. 1.11, 1.12). Situated peripheral to the apertural lobes are four longitudinal rows of nearly evenly spaced, nose-shaped, thorn-like spines aligned along the lateral sides of the faces. In addition, the distance between the apertural lobes and the marginal thorn-like spines is approximately equal to the distance between adjacent thorn-like spines. The adapertural side of the lobes, which is more or less perpendicular to the lateral faces, is concave aborally. The abapertural side, like the bridge of a nose, is inclined at approximately 30º to the lateral faces. The four corner sulci, which are substantially lower than the apertural lobes, follow the inward foldings of the adjacent faces and extend far into the tube cavity (Fig. 1.9). The external surface of the sulci is highly and irregularly folded and exhibits fine parallel striations. The summit of the four corner sulci is evidently lower than that of the faces (Fig. 1.9). Clearly, then, the tube aperture, including the inwardly folded portion, is a smooth continuation of the faces and corner sulci.

Tube wall and internal anatomy.—Micro-CT observations confirm the presence of a narrow apertural opening and the continuation of the tube walls into the inwardly and downwardly folded apertural lobes (Fig. 2.1a–e). The tube wall of carinachitids generally exhibits a prismatic inner layer of uniform thickness and a granular outer layer that is much thinner in the corner sulci than in the faces (e.g., Conway Morris and Chen, 1992, fig. 8.19; Qian et al., 1997, plate 2, 1c, 3c; Liu et al., 2005, plate 2, 1e, j; Liu et al., 2011, fig. 2f-g). The prismatic layer originally was thought to consist of overgrowths of diagenetic apatite, while the granular layer was thought to have been originally organic but later replaced by diagenetic apatite (Qian et al., 1999). Although we are mindful of possible preservational artefacts, Micro-CT imaging revealed that the thickness of the tube wall in specimen ELISN148-52 appears to vary, and that the apertural walls are much thinner than the lateral tube walls (Fig. 2.1a, 2.1c, 2.1e). High magnification imaging revealed a single-layered wall in the apertural region (Fig. 2.1c) and bilayered lateral tube walls (white arrows in Fig. 2.1a, 2.1g). In addition, the facial walls are thicker than those of the corner sulci (Fig. 2.1a, 2.1g). Finally, both the thorn-like spines and the apertural lobes are hollow (Fig. 2.1b).

Present within the tube is a short, subcylindrical mass measuring ~200 μm in diameter and 400 μm in length. The upper part of this feature is in direct contact with the inward folds of the faces and corner sulci (Fig. 2.1b–e), and it is connected to the lateral tube wall by numerous fine, straight filaments (mmf) (Fig. 2.1a–g). No additional details of the subcylindrical mass can be discerned.

Discussion

Relic soft-tissue of Carinachites spinatus.—Similar fine filaments commonly occur within associated fossils, including poorly preserved *Carinachites* (Conway Morris and Chen, 1992, fig. 7.9–7.11), other tubular microfossils (e.g., Steiner et al., 2014, figs. 7.21, 11.9, 11.12, 11.15), and egg envelopes with partly decayed embryos (e.g., Steiner et al., 2014, fig. 4.6–4.9). Because these internal filaments are generally interpreted as microbial in origin and derived from partly decomposed soft tissue (Yue and Bengtson, 1999), we interpret the subcylindrical mass surrounded by these fine filaments in specimens of *C. spinatus* as remains of soft tissue that underwent partial decay.

Relic soft tissue similar to that near the tube aperture of *Carinachites spinatus* also is present in *Hexaconularia* (Steiner et al., 2014, fig. 7.18), *Olivooides* (e.g., P. Li et al., 2007, fig. 4d; Steiner et al., 2014, figs. 10.3, 11.6, 11.12, 11.15), and *Quadrapygites* (e.g., Steiner et al., 2014, figs. 14.19, 15.13, 15.15). In addition, an intact, trumpet-shaped mass of relic soft tissue consisting of an upper calyx and a slender basal stalk extending to the aboral end has been documented in *Olivooides* (see Steiner et al., 2014, fig. 12.7–12.10). The presence of relic soft tissues in *Olivooides* embryos has been demonstrated convincingly by the discovery of exceptionally well-preserved, primary internal anatomy (Han et al., 2016b). All of these relic soft-tissue structures are smaller in diameter than the surrounding tube wall. Whether the soft tissues of *Carinachites spinatus* reached the aboral end of the tube cannot be determined at present.

Growth of the tubes of Carinachites spinatus.—The thorn-like spines on the transverse ribs of this taxon resemble the plicate apertural lobes in many respects including shape, size, surface ornament, spacing, and tip directions. Thus, it seems clear that the spines and lobes are substantially the same kind of structure and are simply located in different positions on the faces. The tube aperture was a kind of extracellular matrix that was most likely secreted by epithelial tissue at the oral end, as only in this area was the tube in direct contact with the soft body. If this hypothesis is correct, then one can make the following additional inferences: (1) the thorn-like spines most probably were derived from the plicate lobes and not vice versa. Delimited by the corner sulci, the transverse extension of the two flanks of the plicate lobes may have undergone ontogenetic transformation into the lateral face ribs. The abapertural groove of the plicate lobes was transformed into the middle groove or the central ridges between adjacent ribs. The converging striations on the

plicate lobes are equivalent to the striated folds on the lateral thorn-like spines. (2) The distance between neighboring ribs on the same face is approximately equal to or less than the radius of the tube aperture and the depth of the inward portion of the plicate lobes. The displacement of the ribs reflects the displacement of the segmented faces and the corner sulcus and thus the migration of the entire tube aperture. (3) Following the previous inward portion of tube aperture, new inward portion skeleton was secreted by the epithelium of soft tissue at the oral region. The new skeleton may have been primarily attached with the epithelium, and afterward the new apertural parts may have detached with the epithelium of the oral region and been pushed onward and outward with centrifugal expansion, finally being displaced to the lateral side of the tube and becoming the lateral components of the lateral walls. (4) Periodic renewal of the tube aperture necessarily led to orally addition of iterated ribs and 'segmentation' of the faces. Together, these processes reflect the growth of the tube by apertural extension (Fig. 4.4–4.6).

The multiple thorn-like spines on specimens ELISN93-45 (Fig. 1.5) and ELISN148-52 (Fig. 1.6) indicate that the morphology of the ribs on the faces of a single individual is essentially uniform and constant, without gradual transformation from welts to arcuate ribs or other, more complex folds. Probably, this replacement began at the basal end of the tube and continued to the upper part without metamorphosis. If this hypothesis is correct, then the specimens of *C. spinatus* described in Conway Morris and Chen (1992) are likely a mixture of several species. Specimens with sharp, thorn-like spines or arcuate ribs as well as welts should be reinterpreted as different species rather than different developmental stages, unless these variants can be shown to co-occur in the same individual of *C. spinatus*.

In addition to sequential adoral addition of ribs on the faces, growth of the *Carinachites* tube also involved increase in the diameter of the tube and the width of the corner sulci. Along the longitudinal axis, the corner sulcus expands gradually toward the aperture (Fig. 1.5). In the most complete specimen (ELISN93-45), which however lacks the apex and apertural margin, at least 35 ribs are present on each face (Fig. 1.5). If the tube could grow up to 1.3 mm in width, as indicated by specimen ELISN148-52 (Fig. 1.6), then we infer that a single face may have contained at least 130 ribs over a total length of approximately 25 mm. With regard to the apertural extension model mentioned in the preceding, neighboring ribs at the same level indicate that the plicate apertural lobes were replaced synchronously by new ones (Fig. 4.4–4.6). In contrast, longitudinal offset of ribs along the corner sulci may reflect diachronous replacement of previously formed plicate lobes, indicating that the tube opening was always more or less partly closed. The corner sulci are generally thinner and more flexible than the faces (Qian et al., 1997), and in most fragmentary specimens, the sulci exhibit secondary breakage. Probably in life the flexible corner sulci served as buffer zones that prevented tearing of the tube during diachronous replacement of the ribs on neighboring faces. The reason for longitudinal offset of the ribs along the facial midline (Conway Morris and Chen, 1992, fig. 6.1) remains unclear, though probably each apertural lobe was formed asynchronously by two adjacent subunits of soft tissue. It is important to note that longitudinal offset or asynchronous displacement of the ribs also can be seen on hexangulaconulariids, but it has never been observed in olivooids.

Tube morphology and growth of other carinachitids.—Since the ribs most likely constitute displaced plicate lobes, the four uniform plicate lobes in tetraradiate *Carinachites spinatus* correspond to the four rows of lateral facial ribs. Similarly, triradiate *Emeiconularia* and pentamerous *Pentaconularia ningqiangensis* Liu et al., 2011 most likely possessed three (Fig. 4.1, 4.2) and five centripetal plicate lobes (Fig. 4.7–4.9), respectively. Similarly, specimens with arcuate ribs reflect the presence of a set of centripetal arcuate lobes in the apertural region. Nevertheless, the apertural region of *Carinachites tetrasulcatus* (Chen, 1982) is difficult to reconstruct as its ribs are low and inconspicuous (Conway Morris and Chen, 1992, fig. 8.22). Probably the aperture of this species resembled a four-sided pyramid with deep, concave corner sulci similar to those of *Hexaconularia sichuanensis* He and Yang, 1986 (e.g., Steiner et al., 2014, fig. 7.13–7.16, 7.19–7.21). We hypothesize that this species exhibited periodical growth similar to that of *Carinachites spinatus*. However, such eversion probably was possible only in organic or lightly sclerotized exoskeletons and not in those with thick and rigid hard parts such as tubes of *Emeiconularia trigemme* (Qian et al., 1997). Thus, secondary, subsequent thickening of the lateral walls, suggested by the double-layered wall structure (Fig. 2), is proposed here to resolve conflicts between the flexibility of the primary apertural wall and the rigidity of the thick secondary tube wall. The thin primary apertural wall in *Carinachites spinatus*, represented by the outer layer with fine transverse wrinkles, may have been rich in organic material. The outer layer may have undergone subsequent thickening on its inner surface by a mixture of inorganic materials (represented by the smooth granular layer), thus resulting in a double-layered structure similar to that of conulariids (Brood, 1995; Ford et al., 2016). This model could account for: (1) the flexibility of the external tube surface (as indicated by the striations and welts shown in Conway Morris and Chen, 1992) and the relative rigidity of the entire tube wall, (2) the high abundance of fragmentary specimens of carinachitids and the extremely rare preservation of their aperture, and (3) probable variation in mechanical properties between the different layers as reflected in the secondary cracks on the tube surface (Fig. 1.11, 1.12). However, because the relic soft tissue is much smaller in diameter than the host tube, the sides of the soft body may not have been in direct contact with the lateral tube wall. How the organic or inorganic material was deposited on the inner surface of the outer layer remains unknown.

Feeding habits of carinachitids.—Despite the absence of in situ preservation of carinachitid tubes, it was originally assumed that carinachitids were solitary sessile forms having their aboral end attached to hard or firm substrates (He, 1987) as in extant medusozoan polyps. A pelagic habit for carinachitids is unlikely as their skeletonized tube appears to have been too dense to float in seawater. However, because the soft body was almost entirely enclosed within the tube, filter-feeding on microorganisms seems highly likely. Besides the function of supporting the growing soft tissues, periodic tube growth and thickening of

carinachitids reflects competition for ecological tiering among a varied benthos. In contrast to the reduced vestigial peridermal theca of cubopolyps and most scyphistomae, the thickening of the tube wall in carinachitids, and coeval tubular fossils (anabaritiids, hyolithelminths), indicate an adaptive strategy focusing on defense against predators such as cycloneuralians (e.g., Liu et al., 2014a; Zhang et al., 2015). Interestingly, suspension feeding by the hypostome rather than normal elongate tentacles with nematocysts has also been observed in extant polyps of *Eudendrium* (Hydrozoa) (Puce et al., 2002), in which the mucous-lined gastroderm plays a major role in capturing food particles such as zooplankton. Such behavior correlates with high concentrations of food particles and intense water movement, a scenario that seems compatible with the marine shelf environment favored by Cambrian small shelly fossils (Yin et al., 1999; Steiner et al., 2004, 2007).

The asynchronous displacement of the ribs in *Carinachites spinatus* indicates that the flexible tube aperture may have opened to a greater extent in this taxon than in olivooids. Relative to the radius of the tube, both the width and height of the ribs on *Emeiconularia amplicanalis* are smaller than in *E. trigemme*. This fact indicates that the oral lobes of *E. amplicanalis* could only partially cover the tube aperture, thus allowing continual contact of the soft body with the ambient environment. Presumably, retractile tentacles in *E. amplicanalis*, if present, could protrude beyond the tube opening, thus enabling limited predatorial behavior.

Comparisons

Carinachitids versus coronate polyps.—Carinachitid tubes resemble the chitinous periderm of coronate scyphozoans (i.e., *Stephanoscyphus*), which are sheathed in a cone-shaped tube showing well-developed longitudinal folds and horizontal annulations (Chapman, 1966; Werner, 1966, 1973). However, differences between them are also evident. In particular, *Stephanoscyphus* may be either solitary or colonial. The periderm of colonial forms is irregularly branched (Jarms, 1991), in some cases with a tube-in-tube structure (Werner, 1966, fig. 13). By contrast, carinachitid tubes are exclusively solitary. Second, whereas *Stephanoscyphus* has an operculum that is separate from the tube, the tube aperture and lappets of carinachitids constitute a continuous extension of the rest of the tube. Third, the scyphozoan periderm, including the peridermal teeth or cusps inside the tube of *Stephanoscyphus*, is secreted by ectoderm of the lateral body wall. By contrast, the external layer of the carinachitid tube, except for the apex, was generated by epithelium of the oral part, and neither teeth nor cusps are present within the carinachitid tube. Fourth, *Stephanoscyphus* tubes are more or less circular in transverse cross section and uniform in thickness; by contrast, carinachitid tubes are polygonal and exhibit distinct faces and corner sulci. Fifth, an operculum with triangular cusps is absent in *Stephanoscyphus* (Werner, 1966), while oral lobes or lappets are a consistent diagnostic feature of the tube of carinachitids and co-occurring olivooids. Finally, strobilation, a characteristic of *Stephanoscyphus*, has not been observed in carinachitids. In short, these comparisons suggest that carinachitids may only be distantly related to extant scyphozoans.

Comparison with extant hydrothecae.—Extant, colonial thecate hydranths begin and complete their development within a small, capsule-like hydrotheca. The hydrotheca in some species, for example *Sertulariella quadrata* Nutting, 1900a, is square in transverse cross section and exhibits dense transverse striations or longitudinal folds (i.e., *S. rugosa* (Linnaeus, 1758)) similar to those of carinachitid tubes (Nutting, 1900a). The oral end of the hydrotheca has a protective operculum with or without a set of triangular, plate-like teeth or converging cusps capable of opening and closing (Crowell, 1991). Many species of *Sertulariella*, for example *S. quadrata*, *S. rugosa*, and *S. peculiaris* (Leloup, 1935 in Galea, 2008), have an operculum with four triangular cusps (Nutting, 1900a; Chapman, 1966; Galea, 2008) that are somewhat similar to the lobes of *Carinachites spinatus*. *Symplectoscyphus* (Millard, 1975) and *S. rathbuni* (Nutting, 1900a) have three teeth similar to those of *Emeiconularia* (assuming our reconstruction is correct). Notably, the chitinous hydrotheca and operculum are secreted by glandular cells of the epidermis of the hydranth, especially the hypostome (Berrill, 1949), thus supporting the previously inferred oral formation of carinachitid tubes. In rare cases, the apertural teeth of the hydrothecae are folded inward as in solitary carinachitid tubes (Nutting, 1900b, pl. 14, fig. 6). Major differences between hydrothecae and carinachitids include: (1) the colonial habit of hydrothecae; (2) the absence of triangular cusps in the lateral walls of hydrothecae; and (3) the teeth in hydrothecae, which are sheet-like, with a free adaxial end, and thus are quite different from those of carinachitids.

Comparison among carinachitids, olivooids, hexangulaconulariids, and conulariids.—Prior to conducting a cladistic analysis of relationships among extant and fossil taxa within Medusozoa, morphological comparisons among olivooids, carinachitids, hexangulaconulariids, and Paleozoic conulariids are necessary. As noted previously (He, 1987), the similarities among the skeletons of olivooids, carinachitids, hexangulaconulariids, and Paleozoic conulariids are striking (Table 1). They include: (1) possession of a superficially cone-shaped tube that almost completely enveloped the soft tissue (Qian and Bengtson, 1989; Sendino et al., 2011); (2) tube with serially repeated transverse and longitudinal wrinkles (Qian and Bengtson, 1989) representing periodic growth by oral addition (Brood, 1995); (3) fine, regularly spaced longitudinal striations, ~5–10 μm in width, as one of typical features of *Olivooides* tubes (e.g., Yue and Bengtson, 1999, fig. 2D; Steiner et al., 2014, fig. 12.13, 12.14), are present also on the corner surface of *Carinachites tetrasulcatus* (e.g., Conway Morris and Chen, 1992, fig. 9.15, 9.16); (4) tube tapered in the apertural region (Qian and Bengtson, 1989), where the tube aperture is folded inward (e.g., Brood, 1995; Steiner et al., 2014); (5) all tubes exhibit distinct apical and abapical regions (Fig. 1.8) (Van Iten et al., 2010), although the carinachitid apex is unknown yet; and (6) radial symmetry, a characteristic that is a link to the medusozoans, is well represented by all four families.

Apart from the mentioned similarities, additional specific similarities between carinachitids and olivooids are remarkable: (1) The cone-shaped tubes of these two taxa exhibit similar variation in the pattern of radial symmetry. Both of them exhibit rare pentaradial symmetry and dominant tetraradial symmetry. However, triradial symmetry is not known in olivooids. (2) The

Table 1. Morphological comparisons among olivooids, hexangulaconulariids, carinachitids, and conulariids.

Characteristics\taxa	Olivooids	Hexangulaconulariids	Carinachitids	Conulariids
tube shape	cone	cone	cone	cone
longitudinal folds	yes	yes	yes	yes
longitudinal striations	yes	?	yes	no
apical/abapical differentiation	yes	yes	?	yes
periodical growth	yes	yes	yes	yes
radial symmetry	4, 5	3, 4, 5	2	2, 3, 4
oral lobes	yes	no	yes	yes
adradial lobes	yes	no	no	no
thorn-like spines	yes/no	no	yes	no
face/corner	no	yes	yes	yes/no
septa/carina	no	no	no	yes
facial midline	no	no	no/yes	yes
mineralization	no	yes	weak	yes
thickening of tube wall	no	no	yes	yes
displacement	no	yes	yes	yes
apex ornaments	stellae	smooth	?	smooth

tube aperture in both *Carinachites spinatus* and *Olivooides* has four or five prominent plicate apertural lobes (usually termed 'lobate folds' in Yue and Bengtson, 1999; Han et al., 2016a, b; termed 'oral lobes' in Steiner et al., 2014, in *Olivooides multisulcatus* Qian, 1977) (Fig. 5). (3) Lateral ornaments on the tube wall, including plicate thorns (Fig. 5.1) (termed 'plicate cornice' in *O. multisulcatus* [see Han et al., 2016a, fig.2] and 'triangular thickening' by Steiner et al., 2014, fig.10), are derived from the tube aperture (Yasui et al., 2013). (4) As mentioned in the preceding, the soft tissues are always connected to the tube aperture. (5) There are similar patterns of tube formation except for lateral thickening, in both cases with tube formation mediated by soft tissue at the oral end (Yasui et al., 2013; Liu et al., 2014b; Han et al., 2016a, b). (6) Rare preservation of the apertural end in olivooids and carinachitids as well as Paleozoic conulariids probably indicates that the newly secreted tube aperture was predominantly organic or weakly sclerotized and thus less resistant to decay than the lateral ribs.

Differences between carinachitids and olivooids also are evident. Although carinachitid tubes bear regular ribs, they were never compressed during diagenesis along the longitudinal axis as in olivooid tubes. This difference may be partially attributed to the presence in carinachitids of deeply concave corner sulci, outwardly bulging faces, and later ontogenetic thickening, thus providing stronger support for the soft body. The face-corner configuration in carinachitids also reflects an incipient differentiation of the meridian planes. The apertural lobes among different taxa of olivooids vary greatly in morphology. Thus, unlike *Olivooides multisulcatus* (Fig. 5.1–5.3), *Quadrapygites* and *O. mirabilis* Yue, 1984 in Xing et al., 1984 lack clear differentiation in size between the principle apertural lobes and the adradial apertural lobes. By contrast, carinachitids exhibit only the principle apertural lobes. The corner sulci in carinachitids may correspond to the adradial apertural lobes in olivooids. In addition, carinachitids exhibit greater morphological variation on the faces than do olivooids, including variation in rib shape and height, displacement of ribs along the midline, and convergence of the striations. The facial ribs of carinachitids may represent a derived feature in comparison with the continuous transverse crests in olivooids. Finally, it has generally been accepted that the periderm of olivooids was organic and uniform in thickness. By contrast, the tubes of carinachitids, hexangulaconulariids, and conulariids, although showing some degree of flexibility, are relatively thick and slightly mineralized (e.g., Brood, 1995; Qian et al., 1997; Leme et al., 2008; Ford et al., 2016).

Similarities between carinachitids and hexangulaconulariids include: (1) sclerotization of the tube wall, (2) development of faces and corner sulci, (3) transverse ornament showing displacement/offset along the midline of the faces and corner sulci, and (4) sessile benthic mode of life on firm substrates or hard parts (e.g., Van Iten et al., 2016a). The displacement mechanism of carinachitids may have also been present in hexangulaconulariids (Conway Morris and Chen, 1992, fig. 11.12; Van Iten et al., 2010, fig. 2e) and latest Ediacaran *Paraconularia* (e.g., Van Iten et al., 2014, fig. 3c–d; Van Iten et al., 2016b). In this connection, it should be noted that relics of small soft parts extending along the tube axis of conulariids, originally interpreted as remains of an alimentary tract (Babcock, 1989), most likely represent polyps as previously suggested by Van Iten (1991) and supported by currently available material of carinachitids and the internal anatomy of *Olivooides* (e.g., Han et al., 2016a).

Differences between carinachitids and hexangulaconulariids also are evident. In particular, the pseudohexaradial symmetry of hexangulaconulariid tubes, which exhibit a fundamental bimerous tetraradial symmetry, reflects further morphological differentiation of the meridian planes within a framework of tetraradial symmetry. Such meridian plane differentiation, oriented perpendicular to the longitudinal axis, probably indicates unknown differentiation of soft part structures such as gonads, septa, and the vascular system. Finally, the apertural lobes of hexangulaconulariids are not triangular as in carinachitids and olivooids.

Carinachitids share detailed similarities with Paleozoic conulariids (except for Cambrian *Baccaconularia* in Hughes et al., 2000) in face/corner sulcus differentiation and formation of apertural lobes (equivalent to the apertural lappets of Sendino et al., 2011), and both taxa exhibit tri-, tetra- or pentaradial symmetry. However, biradial symmetry, common in conulariids, has not been observed in carinachitids. In addition, the corners of some conulariids, for example *Eoconularia loculata* (Wiman, 1895 in Jerre, 1994), are much thicker than the faces (Jerre, 1994), contrasting with the relatively thickened faces of carinachitid *Emeiconularia trigemme* (Fig. 2.1b). Moreover, in addition to plicate apertural lobes (Ford et al., 2016), conulariids

exhibit two other types of apertural lobes (Sendino et al., 2011). Finally, the internal anatomy of the tube wall of conulariids is much more complex at the corners and midlines than in carinachitids, as summarized by Van Iten (1991, 1992b). For example, there are eight types of internal midline structures (Bischoff, 1978; Van Iten, 1991, 1992b; Jerre, 1994), including: (1) a single continuous (nonseriated) carina, and (2) a pair of continuous carinae (flanking the midline), (3) a pair of seriated carinae, (4) a single seriated carina (subsequently discovered by Hughes et al., 2000 in *Baccaconularia*), and (5) the Y-shaped continuous single carina documented by Jerre (1994) in *Eoconularia loculata* (Wiman). The corners may be: (1) nonthickened, (2) thickened without formation of a clear carina, (3) thickened and bearing a distinct nonseriated carina, or (4) thickened and bearing a seriated distinct carina.

In summary, gross morphological comparisons of the skeletons of olivooids, carinachitids, hexangulaconulariids, and Paleozoic conulariids support the previous hypothesis (He, 1987) that these fossil taxa represent closely related lineages within the Conulata. Since the olivooid soft body exhibits a manubrium within a subumbrellar cavity, tentacles, apertural lappets, and frenula (Han et al., 2016a, b), olivooids and hence all conulatans probably were medusozoans (Van Iten et al., 2006) that were related either to extant cubozoans (Han et al., 2013; Han et al., 2016a,b) or to scyphozoans (Dong et al., 2013; Liu et al., 2014b; Van Iten et al., 2014). The proposal that Conulata constitutes an independent phylum (Babcock et al., 1986; Brood, 1995) or the internal rachis of sea pens (Conway Morris and Chen, 1992) appears unlikely. Carinachitids, originally interpreted as the most primitive taxa within Conulata (He, 1987), are interpreted here as a stock of phylogenetically intermediate forms between olivooids and hexangulaconulariids. The presence of corner sulci and faces with a median line (midline) probably represent synapomorphies of carinachitids, hexangulaconulariids, and conulariids. The general similarities shared by olivooids, hexangulaconulariids, carinachitids, and conulariids (i.e., radial symmetry), probably represent primitive conditions. Finally, the bimerous tetraradial symmetry of hexangulaconulariids may have been independently acquired in this lineage. However, these interpretations await future phylogenetical analysis.

Orientation of the radial symmetry planes in carinachitids.—Similarities in gross morphology between carinachitids, olivooids, and conulariids suggest that their peridermal apertural lobes are homologous structures. If this hypothesis is correct, then the orientation of the meridian planes of olivooids and *Olivooides*-like medusozoans (Han et al., 2013, 2016a, b) may shed new light on the orientation of these planes in carinachitids and conulariids. In the soft body of *Olivooides*, the perradial frenula and apertural lappets, which correspond in position to the perradial pockets (e.g., Han et al., 2013, fig. 3), probably were responsible for the formation and closure of the plicate lobes of the periderm (Han et al., 2016a, figs. 3–5). Apart from the adradial frenulae and apertural lappets, no frenulae or apertural lappets are present in the interradii, where the interradial septa connect the subumbrellar and exumbrellar walls, and there is no interradial apertural lobe on the peridermal tube (Fig. 5). Similarly in carinachitids, the bulging faces and corner sulci may directly reflect the configuration of the tube aperture, and they may correspond in position, respectively, to the perradial pockets and interradial septa of the gastric cavity. This means: (1) that the midline of the facial ribs and the corner sulci were most likely located at the perradii and interradii, respectively; and (2) that the corner sulci may correspond to the former interradial septa/mesenteries (Fig. 3). This orientation may also apply to conulariids if indeed their apertural lobes are homologous with those of carinachitids and olivooids. It should be noted, however, that our suggested orientation of the interradial symmetry planes in conulariids differs from the traditional hypothesis, which is based on similarities between the conulariid and coronate periderms and between the midline carinae of *Eoconularia loculata* Wiman and the gastric septa of stauromedusans (Van Iten et al., 2006). According to this hypothesis, the apertural lobes and facial midlines in conulariids were situated at the interradii (Chapman, 1966; Werner, 1966; Van Iten, 1992a; Jerre, 1994). Confirming or disproving this hypothesis will require the discovery of additional and better-preserved relic soft tissues in conulariids.

Conclusions

A single, exceptionally well-preserved specimen of *Carinachites spinatus*, documented for the first time in the present paper, reveals that the apertural end of the skeletal tube of tetraradial carinachitids exhibits four plicate lobes that are similar to those of co-occurring olivooids and younger conulariids. Similarities between the lateral tube spines and the apertural lobes of carinachitids indicate that all of the transverse ribs on the faces were released adorally and were eventually displaced toward the edges of the tube, a pattern of growth similar to that of co-occurring olivooids. The internal anatomy and symmetry of *Olivooides* suggest a perradial and interradii disposition, respectively, for the four faces and corner sulci of carinachitids. These findings corroborate the previously proposed hypothesis that early Cambrian carinachitids, hexangulaconulariids, olivooids, and conulariids are closed related taxa within the subphylum Medusozoa, although olivooids may have retained certain primitive features.

Acknowledgments

We thank Drs. H. Van Iten (Hanover College, USA), C.B. Skovsted (Swedish Museum of Natural History), and G.A. Brock (Macquarie University) for their suggestions and linguistic improvement of the manuscript. We also thank H.J. Gong, J. Sun, J. Luo, and M.R. Cheng (Northwest University, Xi'an, China) for their assistance in the field and with lab work. X. Han prepared the 3D drawings of the carinachitid specimens, and Y.H. Liu (Chang'an University) provided two carinachitid photos. This work was supported by the Natural Science Foundation of China (NSFC grant 41272019, 41621003, 41372021, 41472015), the '973 project' of the Ministry of Science and Technology of China (grant 2013CB835002, 2013CB837100), the Chinese Academy of Sciences (XDB10010101), and the State Key Laboratory of Palaeobiology and Stratigraphy (No. 163107).

References

Babcock, L., 1989, The enigma of conulariid affinities, *in* Conway Morris, S., and Simonetta, A., eds., The Early Evolution of Metazoa and the Significance of Problematic Taxa: Cambridge, Cambridge University Press, p. 133–143.

Babcock, L., Feldmann, R., Hoffmann, A., and Nitecki, M., 1986, The phylum Conulariida, *in* Hoffman, A., and Nitecki, M.H., eds., Problematic Fossil Taxa: New York, Oxford University Press, p. 135–147.

Bengtson, S., and Yue, Z., 1997, Fossilized metazoan embryos from the earliest Cambrian: Science, v. 277, no. 5332, p. 1645–1648.

Berrill, N., 1949, Developmental analysis of Scyphomedusae: Biological Reviews, v. 24, no. 4, p. 393–409.

Bischoff, G., 1978, Internal structures of conulariid tests and their functional significance, with special reference to Circonulariina n. suborder (Cnidaria, Scyphozoa): Senckenbergiana Lethaia, v. 59, p. 275–327.

Brood, K., 1995, Morphology, structure, and systematics of the conulariids: GFF, v. 117, no. 3, p. 121–137.

Chapman, D., 1966, Evolution of the scyphistoma, *in* Rees, J., ed., The Cnidaria and Their Evolution. Symposia of the Zoological Society of London, No. 16: London, Academic, p. 51–57.

Chen, M.E., 1982, The new knowledge of the fossil assemblages from Maidiping section, Emei County, Sichuan with reference to the Sinian–Cambrian boundary: Chinese Journal of Geology, v. 3, p. 001253–001262.

Conway Morris, S., and Chen, M.E., 1992, Carinachitids, hexaconulariids, and *Punctatus*: Problematic metazoans from the early Cambrian of South China: Journal of Paleontology, v. 66, no. 3, p. 384–406.

Crowell, S., 1991, Regression and replacement of hydranths in thecate hydroids, and the structure of hydrothecae, *in* Wiliams, R.B., Cornelius, P.F.S., Hughes, R.G., and Robson, E.A., eds., Coelenterate Biology: Recent Research on Cnidaria and Ctenophora: Dordrecht, Springer, p. 69–73.

Dong, X.-P., Cunningham, J.A., Bengtson, S., Thomas, C.-W., Liu, J., Stampanoni, M., and Donoghue, P.C., 2013, Embryos, polyps and medusae of the early Cambrian scyphozoan *Olivooides*: Proceedings of the Royal Society B: Biological Sciences, v. 280, no. 1757, p.e20130071

Ford, R.C., Van Iten, H., and Clark, G.R. II, 2016, Microstructure and composition of the periderm of conulariids: Journal of Paleontology, v. 90, no. 3, p. 389–399.

Galea, H.R., 2008, On a collection of shallow-water hydroids (Cnidaria : Hydrozoa) from Guadeloupe and Les Saintes, French Lesser Antilles: Zootaxa, v. 1878, p. 1–54.

Han, J., Kubota, S., Li, G., Yao, X., Yang, X., et al., 2013, Early Cambrian pentamerous cubozoan embryos from South China: PloS One, v. 8, no. 8, p. e70741.

Han, J., Kubota, S., Li, G., Ou, Q., Wang, X., et al., 2016a, Divergent evolution of medusozoan symmetric patterns: Evidence from the microanatomy of Cambrian tetramerous cubozoans from South China: Gondwana Research, v. 31, p. 150–163.

Han, J., Li, G. X., Kubota, S., Ou, Q., Toshino, S., et al., 2016b, Internal microanatomy and zoological affinity of the early Cambrian *Olivooides*: Acta Geologica Sinica (English Edition), v. 90, no. 1, p. 38–65.

He, T., 1987, Early Cambrian conulariids from Yangtze platform and their early evolution: Journal of Chengdu University of Technology (Science and Technology Edition), v. 14, p. 7–18.

He, Y.X, and Yang, X.H., 1986, Early Cambrian coelenterates from Nanjiang, Sichuan: Bulletin of the Chengdu Institute of Geology and Mineral Resources, Chinese Academy of Geological Sciences, v. 7, p. 31–48.

Hughes, N.C., Gunderson, G.O., and Weedon, M.J., 2000, Late Cambrian conulariids from Wisconsin and Minnesota: Journal of Paleontology, v. 74, no. 5, p. 828–838.

Jarms, G., 1991, Taxonomic characters from the polyp tubes of coronate medusae (Scyphozoa, Coronatae): Hydrobiologia, v. 216, no. 1, p. 463–470.

Jerre, F., 1994, Anatomy and phylogenetic significance of *Eoconularia loculata*, a conulariid from the Silurian of Gotland: Lethaia, v. 27, no. 2, p. 97–109.

Leme, J.D.M., Simoes, M.G., Marques, A.C., and Van Iten, H., 2008, Cladistic analysis of the suborder Conulariina Miller and Gurley, 1896 (Cnidaria, Scyphozoa; Vendian-Triassic): Palaeontology, v. 51, p. 649–662.

Li, G., Steiner, M., Zhu, X., Yang, A., Wang, H., and Erdtmann, B.D., 2007, Early Cambrian metazoan fossil record of South China: Generic diversity and radiation patterns: Palaeogeography, Palaeoclimatology, Palaeoecology, v. 254, no. 1, p. 229–249.

Li, P., Hua, H., Zhang, L.Y., Zhang, D.D., Jin, X.B., and Liu, Z., 2007, Lower Cambrian phosphatized *Punctatus* from southern Shaanxi and their ontogeny sequence: Chinese Science Bulletin, v. 52, no. 20, p. 2820–2828.

Linnaeus, C., 1758, Systema naturae, Vol. 1, 10th (Edition): Holmiae, Laurentii Salvii, 824 p.

Liu, Y., Li, Y., Shao, T., Wang, Y.-p., Yu, B., Han, H.-p., and Yang, J., 2005, Two new species of protoconulariids from the early Cambrian in South Shaanxi, China: Acta Micropalaeontologica Sinica, v. 22, no. 3, p. 311–321.

Liu, Y., Li, Y., Shao, T., Zheng, X., Zheng, J., Wang, G., Wang, H., and Wang, K., 2011, A new genus and specie of protoconulariids from the early Cambrian in the south Shaanxi, China: Acta Micropalaeontologica Sinica, v. 28, no. 2, p. 245–249.

Liu, Y.H., Xiao, S.H., Shao, T.Q., Broce, J., and Zhang, H.Q., 2014a, The oldest known priapulid-like scalidophoran animal and its implications for the early evolution of cycloneuralians and ecdysozoans: Evolution & Development, v. 16, no. 3, p. 155–165.

Liu, Y., Li, Y., Shao, T., Zhang, H., Wang, Q., and Qiao, J., 2014b, *Quadrapyrgites* from the lower Cambrian of South China: Growth pattern, post-embryonic development, and affinity: Chinese Science Bulletin, v. 59, no. 31, p. 4086–4095.

Luo, H.L., Jiang, Z.W., Wu, X.C., Song, X.L., Lin, O.Y., and Zhang, S.S., 1982, The Sinian-Cambrian Boundary in Eastern Yunnan: Kinming, People's Publishing House, 265 p.

Maloof, A.C., Porter, S.M., Moore, J.L., Dud, F.Ö., Bowring, S.A., Higgins, J.A., Fike, D.A., and Eddy, M.P., 2010, The earliest Cambrian record of animals and ocean geochemical change: Geological Society of America Bulletin, v. 122, no. 11–12, p. 1731–1774.

Millard, N.A.H., 1975, Monograph on the Hydroida of Southern Africa: Cape Town, Kaapstad, 513 p.

Nutting, C.C., 1900a, American Hydroids (II): Washington, DC, U.S. Government Printing OfficeWashington, DC, 150 p.

Nutting, C.C., 1900b, American Hydroids (III): Washington, DC, US Government Printing Office, 113 p.

Puce, S., Bavestrello, G., Arillo, A., Azzini, F., and Cerrano, C., 2002, Morpho-functional adaptation to suspension feeding in *Eudendrium* (Cnidaria, Hydrozoa): Italian Journal of Zoology, v. 69, no. 4, p. 301–304.

Qian, Y., 1977, Hyolitha and some problematica from the lower Cambrian Meishucun Stage in central and SW China: Acta Palaeontologica Sinica, v. 16, no. 2, p. 255–275.

Qian, Y., and Bengtson, S., 1989, Palaeontology and biostratigraphy of the early Cambrian Meishucunian Stage in Yunnan Province, South China: Fossils and Strata, v. 24, p. 1–156.

Qian, Y., Van Iten, H., Cox, R., Zhu, M., and Zhuo, E., 1997, A brief account of *Emeiconularia trigemme*, a new genus and species of protoconulariid: Acta Micropalaeontologica Sinica, v. 14, no. 4, p. 475–488.

Qian, Y., Chen, M.E., Feng, W., Xu, J., and Liu, D., 1999, Classification and early evolution of different group of SSFS, *in* Qian, Y., ed., Taxonomy and Biostratigraphy of Small Shelly Fossils in China: Beijing, Science Press of China, p. 1–59.

Sendino, C., Zágoršek, K., and Vyhlasová, Z., 2011, The aperture and its closure in an Ordovician conulariid: Acta Palaeontologica Polonica, v. 56, no. 3, p. 659–663.

Steiner, M., Li, G.X., Qian, Y., and Zhu, M.Y., 2004, Lower Cambrian small shelly fossils of northern Sichuan and southern Shaanxi (China), and their biostratigraphic importance: Geobios, v. 37, no. 2, p. 259–275.

Steiner, M., Li, G.X., Qian, Y., Zhu, M.Y., and Erdtmann, B.D., 2007, Neoproterozoic to early Cambrian small shelly fossil assemblages and a revised biostratigraphic correlation of the Yangtze Platform (China): Palaeogeography Palaeoclimatology Palaeoecology, v. 254, no. 1–2, p. 67–99.

Steiner, M., Qian, Y., Li, G., Hagadorn, J.W., and Zhu, M., 2014, The developmental cycles of early Cambrian Olivooidae fam. nov. (?Cycloneuralia) from the Yangtze Platform (China): Palaeogeography, Palaeoclimatology, Palaeoecology, v. 398, p. 97–124.

Van Iten, H., 1991, Evolutionary affinities of conulariids, *in* Conway Morris, S., and Simonetta, A., eds., The Early Evolution of Metazoa and the Significance of Problematic Taxa: Cambridge, Cambridge University Press, p. 145–156.

Van Iten, H., 1992a, Anatomy and phylogenetic significance of the corners and midlines of the conulariid test: Palaeontology, v. 35, no. 2, p. 335–358.

Van Iten, H., 1992b, Microstructure and growth of the conulariid test: Implications for conulariid affinities: Palaeontology, v. 35, no. 2, p. 359–372.

Van Iten, H., de Moraes Leme, J., Simões, M.G., Marques, A.C., and Collins, A.G., 2006, Reassessment of the phylogenetic position of conulariids (?Ediacaran–Triassic) within the subphylum Medusozoa (phylum Cnidaria): Journal of Systematic Palaeontology, v. 4, no. 2, p. 109–118.

Van Iten, H., Zhu, M.Y., and Li, G.X., 2010, Redescription of *Hexaconularia* He and Yang, 1986 (lower Cambrian, South China): Implications for the affinities of conulariid-like small shelly fossils: Palaeontology, v. 53, p. 191–199.

Van Iten, H., Marques, A.C., Leme, J.d.M., Pacheco, M.L., and Simões, M.G., 2014, Origin and early diversification of the phylum Cnidaria Verrill: Major developments in the analysis of the taxon's Proterozoic–Cambrian history: Palaeontology, v. 57, no. 4, p. 1–14.

Van Iten, H., Muir, L., Simões, M.G., Leme, J.M., Marques, A.C., and Yoder, N., 2016a, Palaeobiogeography, palaeoecology and evolution of Lower Ordovician conulariids and *Sphenothallus* (Medusozoa, Cnidaria), with emphasis on the Fezouata Shale of southeastern Morocco: Palaeogeography, Palaeoclimatology, Palaeoecology, v. 460, p. 170–178.

Van Iten, H., Leme, J.M., Pacheco, M.L.A.F., Simões, M.G., Fairchild, T.R., Rodrigues, F., Galante, D., Boggiani, G.C., and Marques, A.C., 2016b, Origin and early diversification of phylum Cnidaria: Key macrofossils from the Ediacaran System of North America, *in* Goffredo, S., and Dubinsky, Z., eds, The Cnidaria, Past, Present and Future: Berlin, Springer, p. 31–40. doi: 10.1007/978-3-319-31305-4_3.

Werner, B., 1966, *Stephanoscyphus* (Scyphozoa, Coronatae) und seine direkte Abstammung von den fossilen Conulata: Helgoländer Wissenschaftliche Meeresuntersuchungen, v. 13, no. 4, p. 317–347.

Werner, B., 1973, New investigations on systematics and evolution of the class Scyphozoa and the phylum Cnidaria: Publications of the Seto Marine Biology Lab, v. 20, p. 35–61.

Xing, Y., Ding, Q., Luo, H., He, T., and Wang, Y., 1984, The Sinian–Cambrian boundary of China: Bulletin of the Institute of Geology, Chinese Academy of Geological Sciences, Special Issue, p. 155–170.

Yasui, K., Reimer, J.D., Liu, Y., Yao, X., Kubo, D., Shu, D., and Li, Y., 2013, A diploblastic radiate animal at the dawn of Cambrian diversification with a simple body plan: Distinct from Cnidaria? PLoS One, v. 8, no. 6, p. e65890.

Yin, G., He, T., Qian, Y., and Xiao, B., 1999, Geological and geographical distribution of SSF, with discussion on early Cambrian geographical provinces, *in* Qian, Y., ed., Taxonomy and Biostratigraphy of Small Shelly Fossils in China: Beijing, Science Press of China, p. 1–59.

Yue, Z., and Bengtson, S., 1999, Embryonic and post-embryonic development of the early Cambrian cnidarian *Olivooides*: Lethaia, v. 32, p. 181–195.

Zhang, H., Xiao, S., Liu, Y., Yuan, X., Wan, B., Muscente, A., Shao, T., Gong, H., and Cao, G., 2015, Armored kinorhynch-like scalidophoran animals from the early Cambrian: Scientific Reports, v. 5, article no. 16521.

Accepted 23 February 2017

5.4 Anatomy and affinities of a new 535-million-year-old medusozoan from the Kuanchuanpu Formation, South China

Most descriptions of *Olivooides* have focused on the external morphology of its globular embryonic stages and more advanced turret-like post-hatching stages known as *Punctatus*. Based on external features such as the annulated ridges, the oral lobes and the radial symmetry, tentative reconstructions of the life cycle of *Olivooides* have been made (Han et al. 2013, Steiner et al. 2014) and hypotheses concerning its affinities have been proposed, including possible phylogenetical relationships with extant groups of Cnidaria. This paper aimed 1) to explore the internal structure of the embryonic stages of *Olivooides* by means of X-Ray microtomographic methods following previous studies that used similar techniques (Dong et al. 2013, Han et al. 2013); 2) to clarify the affinities of these enigmatic fossils and to test hypotheses concerning their possible phylogenetical relationships to extant animal groups, especially within Cnidaria.

We show here the pentamerous internal organization of the larva stage of a new genus *Sinaster*, which relates to the *Olivooides* fossils and clarify the relation between external and internal features. This set on new data obtained via micro tomographic methods is used in this paper to test various hypotheses concerning the affinities of *Olivooides*-like fossils.

The pentamerous symmetry of *Olivooides* had prompted previous authors to consider it as an ancient echinoderm. However, the development of echinoderms starts with a bilaterally symmetrical embryo and larva. When fully developed, the larva undergoes metamorphosis (loss of gut and larval arms). At that stage, the right and left side of the larva becomes the aboral and oral area, respectively, the bilateral symmetry disappears giving rise to a radial pentamerous symmetry (Mooi and David 2008, David and Mooi 2014). Our study and previous works clearly show that *Olivooides* had no comparable development and displayed a pentaradial symmetry from its earliest embryonic stages onwards. Moreover, there is no evidence, in *Olivooides*, of a water cycling system and a calcareous endoskeleton that characterize echinoderms. The echinoderm hypothesis should definitely be rejected (Dong et al. 2016).

We analyzed three other hypotheses which were currently proposed to support the placement of *Olivooides* / *Olivooides*-like fossils within either the ecdysozoans or the cnidarians (scyphozoan or cubozoan). Steiner et al., (2014) considered *Olivooides* as possibly related to ecdysozoans (e.g. priapulid worms). Although bilaterians, priapulid worms display an evident pentaradial symmetry exemplified by the 5-fold arrangement of their pharyngeal teeth (Adrianov and Malakhov 2001). This character led Steiner et al. (2014) to consider *Olivooides* as possibly affiliated to priapulids or more generally to cycloneuralians. However, *Olivooides* has a primary pentamerous symmetry whereas it is secondarily acquired in priapulid worms. Other major

differences such as the absence of a through gut and introvert bearing scalids in *Olivooides* (Han et al. 2013, Dong et al. 2016) do not support the scalidophoran hypothesis.

The radial symmetry of *Olivooides* naturally led authors to draw comparisons with one of the most diverse group of extant radial animals, the cnidarians. Dong et al. (2013; 2016) suggested that *Olivooides* had possible close relationships with scyphozoan coronates whereas Han et al. (2013) instead, proposed phylogenetical links with cubozoans. The new data presented here allow to test these opposing views and more generally to reassess the assumed cnidarian affinities of *Olivooides*.

Interestingly, *Sinaster* displays a combination of morphological features found both in polypoid and medusoid phases and cannot be assigned to any crown group of extant medusozoans. However, its oral lappets and other endodermal lamellae, such as the stronger interradial septa, would suggest possible relationship with the Cubozoa and Scyphozoa. Phylogenetical analysis resolves *Sinaster* as a possible member of the stem group Cubozoa.

Palaeontology The Palaeontological Association www.palass.org

[Palaeontology, 2017, pp. 1–15]

ANATOMY AND AFFINITIES OF A NEW 535-MILLION-YEAR-OLD MEDUSOZOAN FROM THE KUANCHUANPU FORMATION, SOUTH CHINA

by XING WANG[1,2], JIAN HAN[1,*], JEAN VANNIER[2], QIANG OU[3,4], XIAOGUANG YANG[1], KENTARO UESUGI[5], OSAMU SASAKI[6] *and* TSUYOSHI KOMIYA[7]

[1]Early Life Institute & Department of Geology, State Key Laboratory of Continental Dynamics, Northwest University, 229 Taibai Road, Xi'an, 710069, China; elihanj@nwu.edu.cn
[2]UMR 5276 du CNRS, Laboratoire de géologie de Lyon: Terre, Planètes, Environnement, Université Lyon 1, Bâtiment GEODE, 2, rue Raphaël Dubois, Villeurbanne, 69622, France
[3]Early Life Evolution Laboratory, School of Earth Sciences & Resources, University of Geosciences, Beijing, 100083, China
[4]Department of Zoology, University of Kassel, Kassel, 34132, Germany
[5]Japan Synchrotron Radiation Research Institute (JASRI) 1-1-1 Kouto, Sayo-cho, Sayo-gun, Hyogo Japan
[6]Tohoku University Museum, Tohoku University, 6-3 Aoba, Aramaki, Aoba-ku, Sendai, Japan
[7]Department of Earth Science & Astronomy, Graduate School of Arts and Sciences, The University of Tokyo, Tokyo, 153-8902, Japan
*Corresponding author

Typescript received 10 April 2017; accepted in revised form 30 June 2017

Abstract: We describe here *Sinaster petalon* gen. et sp. nov., a new embryonic form from the *c.* 535 million-year-old Kuanchuanpu Formation of South China (Ningqiang, Shaanxi Province). The excellent three-dimensional, phosphatic preservation of these microfossils allowed us to use x-ray microtomographic techniques to make accurate reconstructions of their internal structures and to compare their anatomy point-by-point with that of extant cnidarians and other animal groups. *Sinaster petalon* has anatomical features typical of extant Medusozoa (Cnidaria), such as coronal muscles, perradial and adradial frenula, interradial septa, accessory septa, gonad-lamellae, tentacle buds and perradial pockets. Although *Sinaster* cannot be straightforwardly assigned to any crown-group within Medusozoa, the presence of marginal lappets and endodermal lamellae suggests that it is closer to Cubozoa and Scyphozoa than to any other group of modern cnidarians. The tentative placement of *Sinaster* within the stem-group Cubozoa is justified by the presence of a velarium supported by a frenulum. The cubozoan affinities of *Sinaster* are also supported by cladistic analysis.

Key words: Cnidaria, Cubozoa, Early Cambrian, embryo, Kuanchuanpu Formation, periderm.

THE small shelly fossil (SSF) assemblages of the Kuanchuanpu Formation of South China (Shaanxi Province; Fortunian Stage, Terreneuvian Series, *c.* 535 Ma) contain abundant skeletal elements (He 1987; Qian 1999) but also remarkably preserved soft-bodied organisms such as embryonic and larval stages of cnidarians (Conway Morris & Chen 1992; Bengtson & Yue 1997; Steiner *et al.* 2004; Dong *et al.* 2013, 2016; Han *et al.* 2013, 2016*a*), ecdysozoans (Liu *et al.* 2014; Zhang *et al.* 2015) and also possible meiobenthic deuterostomes (Han *et al.* 2017*a*). These exceptional fossils provide key information on the early stages of animal evolution near the Ediacaran–Cambrian boundary and before the Cambrian Explosion *sensu stricto*.

Recent studies using scanning electron microscopy (SEM) and x-ray microtomography (XTM) provide very detailed morphological information on these early organisms (Chen & Dong 2008; Han *et al.* 2010, 2013, 2016*a*, 2017*b*, *c*; Dong *et al.* 2013). Steiner *et al.* (2004) described a scyphopolyp with many filamentous tentacles, Han *et al.* (2010) the earliest sea-anemone-like cnidarian and Dong *et al.* (2013) a possible ephyra-like medusa with pentaradial symmetry. The oldest representatives of Cubozoa (box jellyfish) were also discovered in the Kuanchuanpu Formation (Han *et al.* 2013). The exquisite preservation of their septal structures allowed unprecedented detailed comparisons with their modern counterparts (Han *et al.* 2013, 2016*a*, *b*; Toshino *et al.* 2015). Liu *et al.* (2014) and Zhang *et al.* (2015) described two minute scalidophoran worms, which provide insight into the early evolution of ecdysozoans, a major animal clade that rapidly became dominant in the later Cambrian marine ecosystems exemplified by the Chengjiang biota.

doi: 10.1111/pala.12320

Although the anatomy of many of these early cnidarians and ecdysozoans has been reconstructed in detail, important aspects of their palaeobiology, taphonomy, systematics and phylogeny remain poorly understood or debated, especially their cycle of development from embryo to adult, their taxonomy and their phylogenetic relationships to extant groups (Dong *et al.* 2013, 2016; Han *et al.* 2013). Numerous forms have been kept in open nomenclature in order to avoid potential problems of synonymy until additional specimens can be obtained.

One of the most studied forms, *Olivooides* Qian, 1977 (see Bengtson & Yue 1997 for a reconstructed developmental cycle), is a spherical organism with an external stellate ornament that is assumed to represent the embryonic stage of a larger tubular animal from the same locality that has been described as *Punctatus* (Bengtson & Yue 1997; Yue & Bengtson 1999*a*, *b*; Yao *et al.* 2011, fig. 3b1). Recent studies (Dong *et al.* 2013; Han *et al.* 2013) have also revealed that *Olivooides*-like fossils had a pentaradial anatomy as evidenced by the connection of the gastric septa (mesenteries) to the double-layered body wall and the arrangement of tentacles and gonad lamellae. As a whole, this body plan is comparable to that of some extant medusozoans such as cubomedusozoans (Han *et al.* 2013) or scyphomedusozoans (Dong *et al.* 2013, 2016). The symmetry of these embryonic fossils is dominantly pentamerous, but some of them are tetraradial (Han *et al.* 2016*b*) as in the vast majority of extant cnidarians. Although the *Olivooides*-like cnidarians from the Kuanchuanpu biota are prehatched embryos with virtually the same overall external morphology as *Olivooides*, they display a greater variety of internal structures. We describe here a new genus and species, *Sinaster petalon* gen. et sp. nov., based on exceptionally well-preserved prehatched embryos from the Kuanchuanpu Formation. Although *Sinaster* resembles *Olivooides*-like fossils in its overall shape, its internal structures clearly distinguish it from other co-occurring embryos.

TERMINOLOGY AND ORIENTATION OF EMBRYONIC MEDUSOZOANS

The terminology used here is that of previous works on Cambrian and extant cnidarians (Hyman 1940; Thiel 1966; Werner 1973; Thomas & Edwards 1990; Gershwin & Alderslade 2006; Han *et al.* 2013, 2016*a*, *b*).

The definition of the meridian plane in these specimens follows Han *et al.* (2013, 2016*a*, *b*). We follow the current classification of Cnidaria into the Class Anthozoa and the Subphylum Medusozoa which encompasses the following classes: Cubozoa (box jellyfish and sea wasps), Hydrozoa (hydroids and hydra-like animals), Scyphozoa (true jellyfish), Staurozoa (stalked jellyfish) (Daly *et al.* 2007). Cubomedusa and Scyphomedusa are used here to designate the medusoid stages of Cubozoa and Scyphozoa.

Abbreviations. aal, adradial apertural lobe; af, adradial furrow; afl, adradial fold lappet; afr, adradial frenulum; as, accessory septum; cg, coronal groove; cl, claustrum; crm, circumferential muscle; cs, coronal stomach; en + pe, egg envelope + periderm; eu, exumbrella; g, gonad; gl, gonad-lamella; go, gastric ostium; icp, interradial corner pillar; if, interradial furrow; is, interradial septum; ln, lappet node; mb, manubrium; ml, marginal lappet; mp, mesogonial pockets; pal, perradial apertural lobe; pfl, perradial fold lappet; pfr, perradial frenulum; ph, phacellus; pp, perradial pocket; rc, radial canal; sf, septal funnel; sn, septal nodes; sp, suspensorium; stl, stellate ornaments; su, subumbrella; tb, tentacular bud; ve, velarium; *, perradius; →, interradius.

MATERIAL AND METHOD

Fossil specimens were obtained by acetic acid maceration of phosphatic limestones from the Kuanchuanpu Formation (Qian 1999) and picked under a binocular microscope. Two specimens (ELISN 89-107 and ELISN 115-39) were examined under SEM and then investigated with computed x-ray microtomography (XTM) at Tohoku University, Japan, and the synchrotron of Spring-8 in Hyogo, Japan. SEM and XTM (Tohoku University, Japan) were both used to image the external and internal features of the best preserved specimens (Wang *et al.* 2017, appendices 1, 2). Selected specimens were further examined using synchrotron radiation at Spring-8 in Hyogo, Japan. Thousands of images of virtual thin-sections (Figs 2, 5) through each specimen were acquired at a resolution of 1004 × 1004 pixels (XTM) and 1920 × 1920 pixels (synchrotron XTM). XTM data were processed using V.G. Studio 2.2 Max in order to enhance contrast between key internal anatomical features by using artificial colours and to generate detailed three-dimensional reconstructions of the microscopic fossils (Figs 3–4, 6–7). Cladistic analysis was carried out using PAUP* v. 4.0 b10 (Swofford 2003). The unweighted analysis of the data matrix (Wang *et al.* 2017, appendix 3) containing 104 unordered characters taken from Marques & Collins (2004), Van Iten *et al.* (2006*a*) and Han *et al.* (2016*c*).

All specimens are deposited at the Early Life Institute (ELI), Northwest University, Xi'an, Shaanxi Province, China. This material and microtomography data are available on request via Prof. Jian Han.

Institutional abbreviations. ELI, Early Life Institute, Northwest University, China. GMPKU, Geological Museum of Peking University, Beijing, China.

SYSTEMATIC PALAEONTOLOGY

Phylum CNIDARIA Verrill, 1865
Subphylum MEDUSOZOA Petersen, 1979
Class uncertain
Family OLIVOOIDAE Steiner *et al*., 2014

Genus SINASTER nov.

LSID. urn:lsid:zoobank.org:act:1BDC6FE9-E8FD-4F93-AE25-ED01169B583C

Derivation of name. From the Latin *Sina* (China) and *aster* (star), alluding to the star-shaped embryo in transverse cross-section and the Chinese origin of the fossil material.

Diagnosis. Ovoid shape with smooth envelope. Single polar aperture. Body with pentaradial symmetry. Periderm with smooth external surface, no stellate ornament; five perradial folded lobes and five pairs of interradial folded lobes equally distributed around the peridermal aperture. Soft-tissues: spacious subumbrella cavity with five pairs of small hollow interradial tentacles inserted on the inner wall of the subumbrella and directed toward the oral-aboral axis of the animal; bell margin with perradial and adradial apertural lappets, each corresponding with overlying folded lobes and underlying frenulae; five spacious perradial pockets, separating subumbrella far from exumbrella; exumbrella and subumbrella connected by long interradial septa with no free ends; two sub-interradial accessory septa, sprouting from the exumbrella wall, relatively close to abaxial root of each interradial septum; one pair of gonad-like lamellae on each side of the middle part of the interradial septum; short cone-shaped manubrium projecting deep into the broad subumbrellar cavity.

Sinaster petalon sp. nov.
Figure 1B, C, E, F

LSID. urn:lsid:zoobank.org:act:FC97933E-D3B0-41C8-8846-191D853C504C

Derivation of name. From *petalo* (Greek), petal.

Holotype. ELISN 89-107; deposited in the collections of the Early Life Institute, Department of Geology, Northwest University, China.

Additional material. ELISN 115-39 as paratype (see Description below).

Diagnosis. As for genus.

Occurrence. Lower Cambrian Kuanchuanpu Formation (equivalent to the Fortunian Stage of the Terreneuvian Series), Ningqiang County, Shaanxi Province, China.

DESCRIPTION

External morphology

The holotype of *S. petalon* (ELISN 89-107) has a spherical bell shape (*c.* 600 μm in diameter) and an inconspicuous, thin egg envelope (Fig. 1B, E). The embryonic periderm is smooth over its entire surface (Figs 1B, 3, 5A) except near the peridermal aperture. The 15 centripetal, tongue-shaped folded lobes around the periderm aperture display a pentamerous symmetry along the oral–aboral axis (Fig. 1B). Five of them are larger and folded and are designated here as perradial folded lobes. They are intercalated with five pairs of smaller, narrower folded lobes designated as adradial folded lobes. The boundary of folded lobes fades away aborally. Each folded lobe shows a set of vaulted shallow wrinkles, variable in number, arching toward the central peridermal aperture (Figs 1B, E; 3A). This pattern of folded lobes (5 + 10) is relatively common in the pentamerous embryos (e.g. ELISN 31-179; Fig. 1A) from the Kuanchuanpu biota.

The paratype of *S. petalon* has the same size and external morphology as the holotype and lacks the typical external ornament of *Olivooides*. Its periderm is damaged and incomplete. It shows a pentaradial symmetry with five perradial triangular blade-like structures located near the aperture, and rooting from the inner layer (Fig. 1C). Two furrows are visible along the perradii and are designated here as an adradial furrow (af) and an interradial furrow (if) (Fig. 1F). Many thin shallow coronal grooves (cg) occur between the two furrows along the perradial on the outer layer (Fig. 5D).

Internal anatomy

XTM of the holotype reveals fine details of the internal features of *S. petalon* (Figs 2, 3). The egg envelope and the periderm seem to be fused with no conspicuous perivitelline space in between. However, there is a larger interspace between the periderm and the enclosed soft-tissue (Fig. 3A), designated here as the peridermal cavity. Transverse cross-sections through the holotype soft tissues show an outer circular thin layer (*c.* 10 μm in thickness) and an inner pentagonal thicker layer (*c.* 15 μm thick). The pentagonal section of the inner layer becomes rounded toward the bell margin. Apart from the medusoid rim, the outer layer is attached to the inner layer via five evenly-spaced interradial septa (Fig. 2F–I), which partition the gastric cavity into five spacious perradial pockets (pp; Han *et al*. 2013). Each interradial septum stretches about one-third of the height of the body (is; Fig. 3B) and lacks a free adaxial end (Fig. 2I). In the holotype, the interradial septum (*c.* 180 μm in maximal length and triangular in cross-section) tapers towards the aboral–oral axis, at the mid-level of the bell. The interradial septum also diminishes towards the bell rim to become invisible near to the aperture.

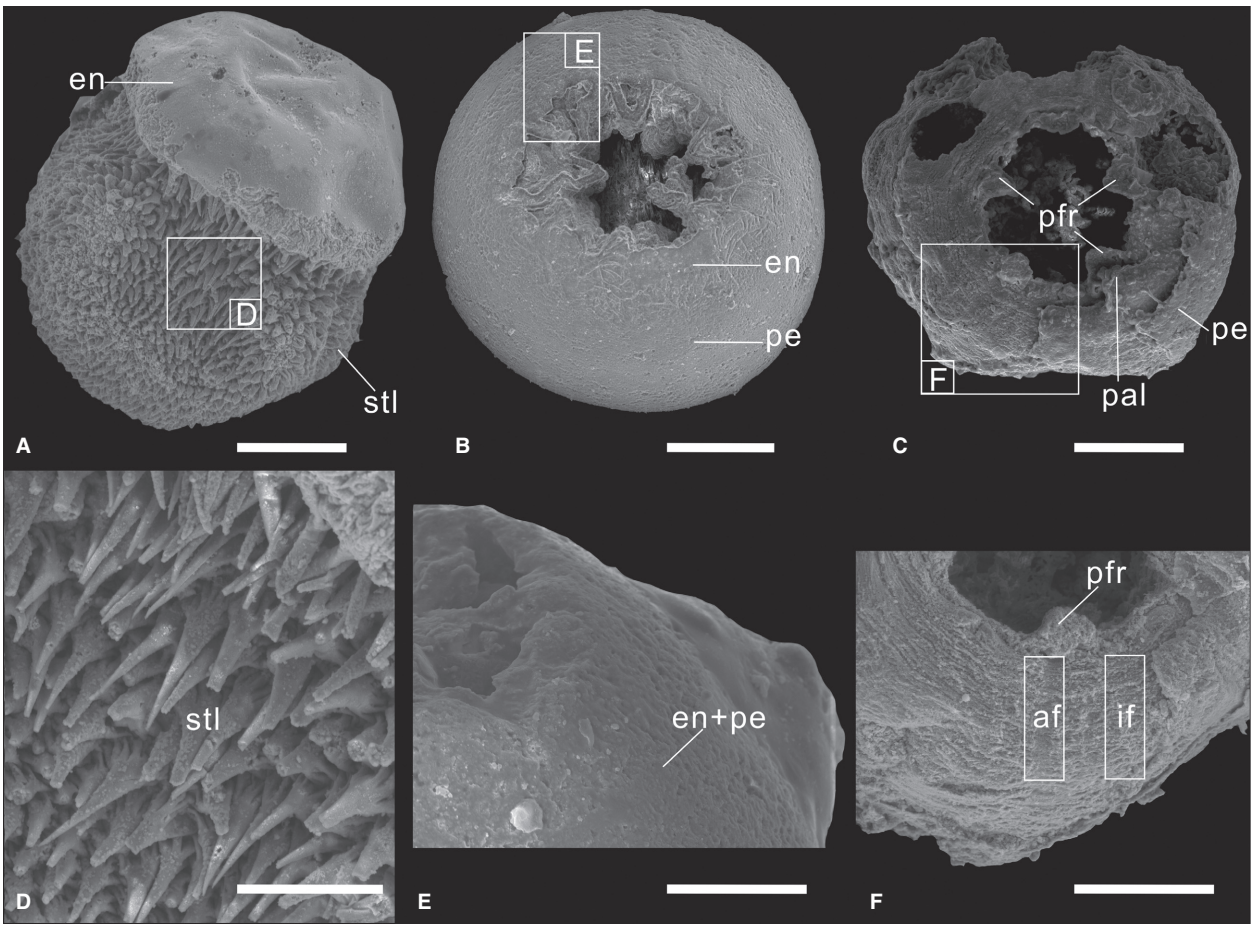

FIG. 1. External morphology of pre-hatched fossil embryos from the lower Cambrian Kuanchuanpu Formation, Shaanxi Province, China. A, D, *Olivooides*, ELISN 31-179 with the periderm bearing stellate ornament, general view and details of ornament. B, E, *Sinaster petalon* gen. et sp. nov., ELISN 89-107, holotype showing the smooth periderm, general view and details of the peridermal aperture. C, F, *S. petalon* gen. et sp. nov., ELISN 115-39, paratype, showing features of the outer layer. All SEM images. *Abbreviations*: af, adradial furrow; en, egg envelope; if, interradial furrow; pal, perradial apertural lobe; pe, periderm; pfr, perradial frenulum; stl, stellate ornaments. Scale bars represent: 200 μm (A, C); 150 μm (B); 50 μm (D); 100 μm (E, F).

Oral views display five large perradial lappets and five pairs of smaller adradial lappets, which are rooted in the margin of the outer layer and seem to correspond to the perradial and adradial folded lobes of the peridermal sheath (Figs 2B–C, 3B). Five pairs of tiny buds occur at about three-quarters of the height of the bell (Fig. 2F). They are superficially rooted in the adaxial side of the inner layer and are directed horizontally toward the oral–aboral axis (Fig. 2F). Each bud is stout, being *c.* 45 μm long and *c.* 30 μm wide. A short cone-like shaft (*c.* 85 μm high and *c.* 35 μm wide) with a rounded base is present within the inner cavity below the level of the paired tiny buds (Fig. 2A, I). Above it, a large dark solid mass with a spiny appearance pierces the inner layer and extends into the perradial pockets (Fig. 2A, F–I; voids filled by minerals). This solid structure may be diagenetic in origin. Five pairs of vertical strip-like curved adradial septa (Fig. 2G) occur in the perradial pockets. They project bilaterally from the inner surface of the outer layer, and stand quite close to the proximal end of the interradial septa (Fig. 2H, I). Each adradial septum is *c.* 90 μm long and curves toward the perradial pockets. Its maximal length occurs at the middle level of the bell (Fig. 2G, H). Five pairs of tiny pisolitic lamellae, merely *c.* 15 μm long, occur in the middle of each interradial septum. They lie closer to the aboral end of the bell than to the adradial septa (Figs 2H; 3B, H). Viewed in oral sections, there are 5 thin, nose-like perradial structures and 10 pairs of tiny adradial structures situated above the paired tiny buds (Fig. 2E). The oral end of these nose-like structures is connected to a distinct skirt-like circular tissue around the cavity margin of the inner layer (Figs 2, 3D). This circular tissue shows a connection with the apertural lappets and its diameter (180 μm) is much less than that of the cavity of the inner layer. Five concentric striated strips occur around the skirt-like circular tissue and are interrupted at each interradius (Figs 2D–E, 3E, G). Each strip consists of four to five bundles of fibres, with each fibre having a maximal diameter of about *c.* 3 μm (Fig. 3E). The same fibres with similar bundles are also present in ELISN 83-66 (Han *et al.* 2016*a*, fig. 3D) and ELISN 35-1 (Han *et al.* 2016*b*, fig. 6K). The paratype specimen (Figs 1C, F; 4; 5) has well-preserved internal

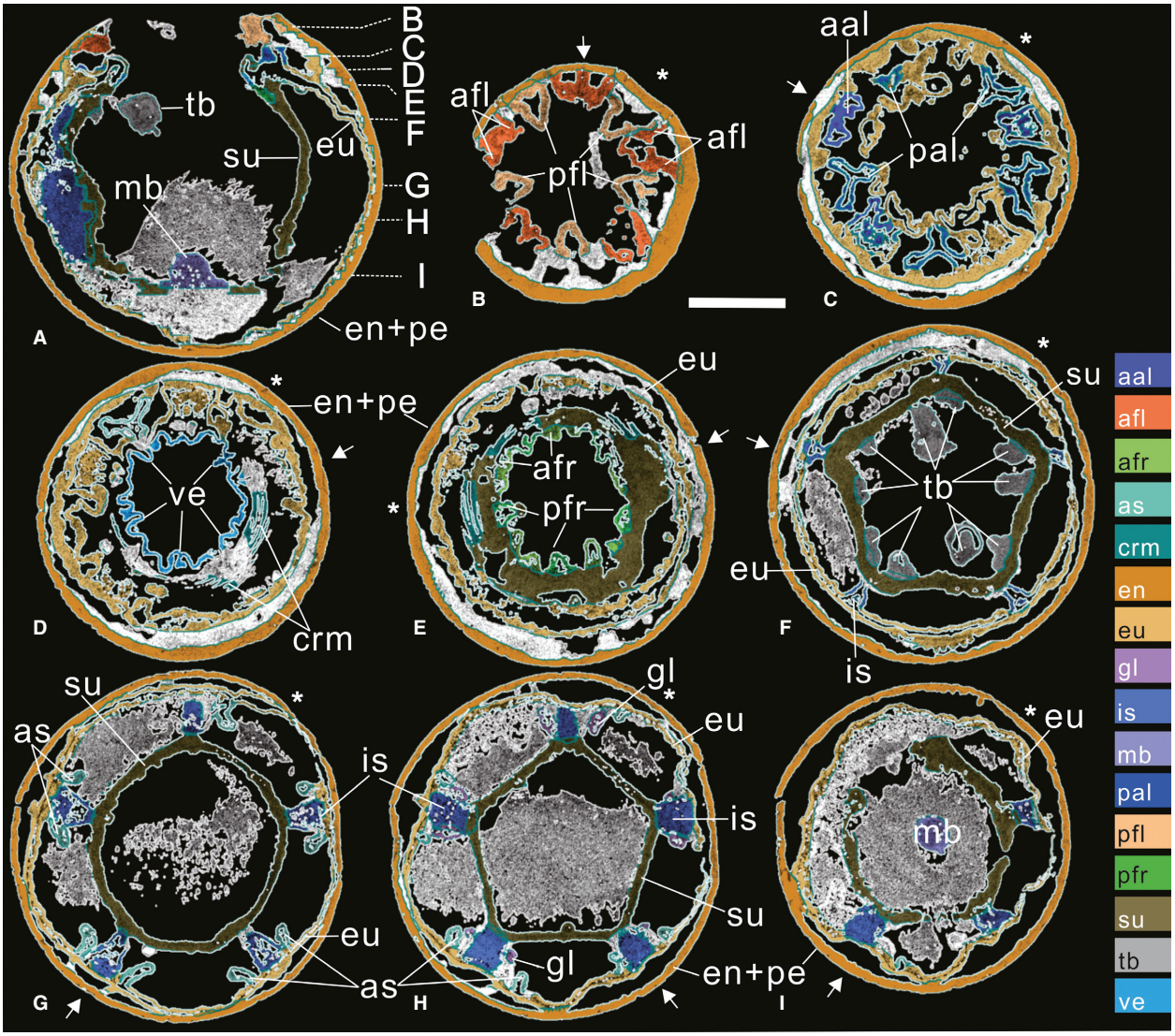

FIG. 2. *Sinaster petalon* gen. et sp. nov. from the lower Cambrian Kuanchuanpu Formation, Shaanxi Province, China; ELISN 89-107, holotype, microtomographic sections. A, axial section through the manubrium; positions of horizontal sections B–I are indicated. B–I, horizontal sections from oral to aboral part; major internal structures identified by colours generated by VG Studio 2.2 MAX. See colourless sections in Wang *et al.* (2017, appendix 1). *Abbreviations*: aal, adradial apertural lobe; afl, adradial fold lappet; afr, adradial frenulum; as, accessory septum; crm, circumferential muscle; en + pe, egg envelope + periderm; eu, exumbrella; gl, gonad-lamella; is, interradial septum; mb, manubrium; pal, perradial apertural lobe; pfl, perradial fold lappet; pfr, perradial frenulum; su, subumbrella; tb, tentacular bud; ve, velarium; *, perradius; →, interradius. Scale bar represents 200 μm.

features but its external ones are severely damaged. It has the same internal morphology and pentaradial symmetry as the holotype, but differs from it in some features. There are fewer void-filling minerals within the cavity of the inner layer (Fig. 4). The skirt-like soft tissue of the paratype looks thinner and smaller than that of the holotype (Fig. 5C). These differences may have a taphonomic origin.

In summary, x-ray microtomography of two specimens provides a detailed picture of the whole internal structure of this new early Cambrian embryonic form. A suite of ectodermic and endodermic features (see Discussion below) is recognized (Figs 2–5). Each interradial septum extends deeply into the bell while the adjacent adradial septum extends over only half of its length. The peridermal apertural lobes, apertural lappets and other structures exhibit a 5 perradial + 10 adradial pattern.

DISCUSSION

Interpretation of Sinaster

Sinaster petalon presents the following suite of morphological characters typical of modern cnidarians:

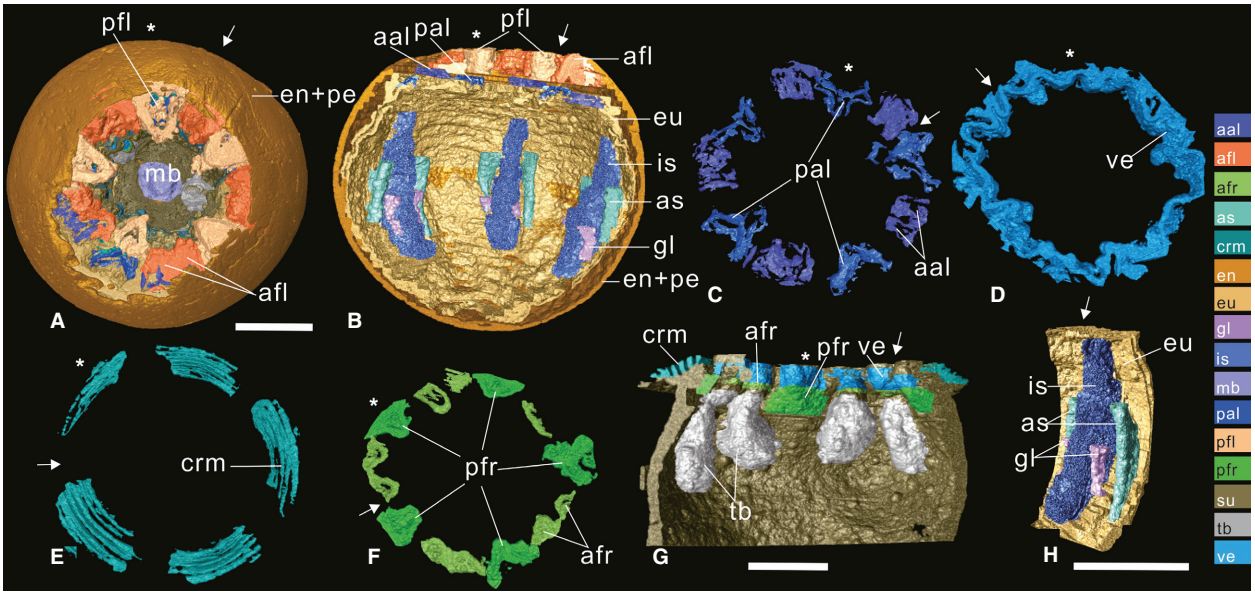

FIG. 3. *Sinaster petalon* gen. et sp. nov. from the lower Cambrian Kuanchuanpu Formation, Shaanxi Province, China; ELISN 89-107, holotype, three-dimensional model obtained using VG Studio 2.2 MAX. Colours identify anatomical structures. A, oral view showing the manubrium and the perradial and adradial apertural folded lobes. B, inner-lateral view of the half body showing the arrangement of the apertural folded lobes of the periderm and the underlying perradial apertural lappets; for clarity, the subumbrellar elements are obscured. C, oral view showing the perradial lappets and the adradial lappets. D, zigzag margin of the velarium. E, five bands of coronal muscles interrupting at the interradii. F, oral view showing the perradial frenula and adradial frenula. G, inner-lateral view of the subumbrella showing the arrangement of the interradial tentacular buds and the perradial and adradial frenula; in a strict sense, each tentacle is located at the adradius. H, one-fifth of the body showing the arrangement of the interradial septum, gonad lamellae and accessory septa. *Abbreviations*: aal, adradial apertural lobe; afl, adradial fold lappet; afr, adradial frenulum; as, accessory septum; crm, circumferential muscle; en + pe, egg envelope + periderm; eu, exumbrella; gl, gonad-lamella; is, interradial septum; mb, manubrium; pal, perradial apertural lobe; pfl, perradial fold lappet; pfr, perradial frenulum; su, subumbrella; tb, tentacular bud; ve, velarium; *, perradius; →, interradius. Scale bars represent: 150 μm (A–F); 75 μm (G); 150 μm (H).

1. The bell is organized in two layers. The inner and outer layers are interpreted here as the subumbrella and the exumbrella, respectively (Figs 2, 4).
2. These two layers are connected by interradial septa (is) which divide the gastric cavity into five spacious perradial pockets (pp, see Han *et al.* 2013; Fig. 3B, H).
3. Each interradial septum lacks a free adaxial end. This general organization is that of typical extant medusae (Hyman 1940). The interior of the interradial septa seems to be solid in the holotype, but has tiny hollows in the paratype (Fig. 4E–G).
4. As seen in oral view, five larger perradial lappets and five pairs of smaller adradial lappets are rooted in the ridge of the exumbrella (Figs 2–4).
5. Five paired tiny buds interpreted here as tentacular buds, are also rooted in the inner layer of the subumbrella (Fig. 3G).
6. The cone-like structure with a rounded base situated within the subumbrellar cavity and below the level of the tentacular buds, is interpreted here as the manubrium. In the holotype, the manubrium appears to be solid, which is most likely to be a diagenetic artefact. The mouth opening is indiscernible, though was probably situated at the free end of the manubrium (Figs 2, 3, 6).
7. Viewed from apertural sections, five thin nose-like structures and five pairs of smaller ones are interpreted as perradial and adradial frenula respectively (Figs 3, 5); these would have strengthened the medusa structure.
8. The circular tissue around the margin of the subumbrellar cavity, above the frenula, is interpreted here as a velarium (Figs 3, 5, 6), which may also have played a role in strengthening the bell of the medusa. The velarium, with the aid of coronal muscles, may conceivably have allowed the bell to contract rhythmically (Han *et al.* 2013).
9. These coronal muscles are represented by five bundles of concentric striated strips around the velarium. These muscles are interrupted at each interradius as in extant cnidarians (Figs 3, 6).
10. Five pairs of accessory septa are rooted in the inner layer of the exumbrella, and project into the perradial pockets (Figs 2–6).

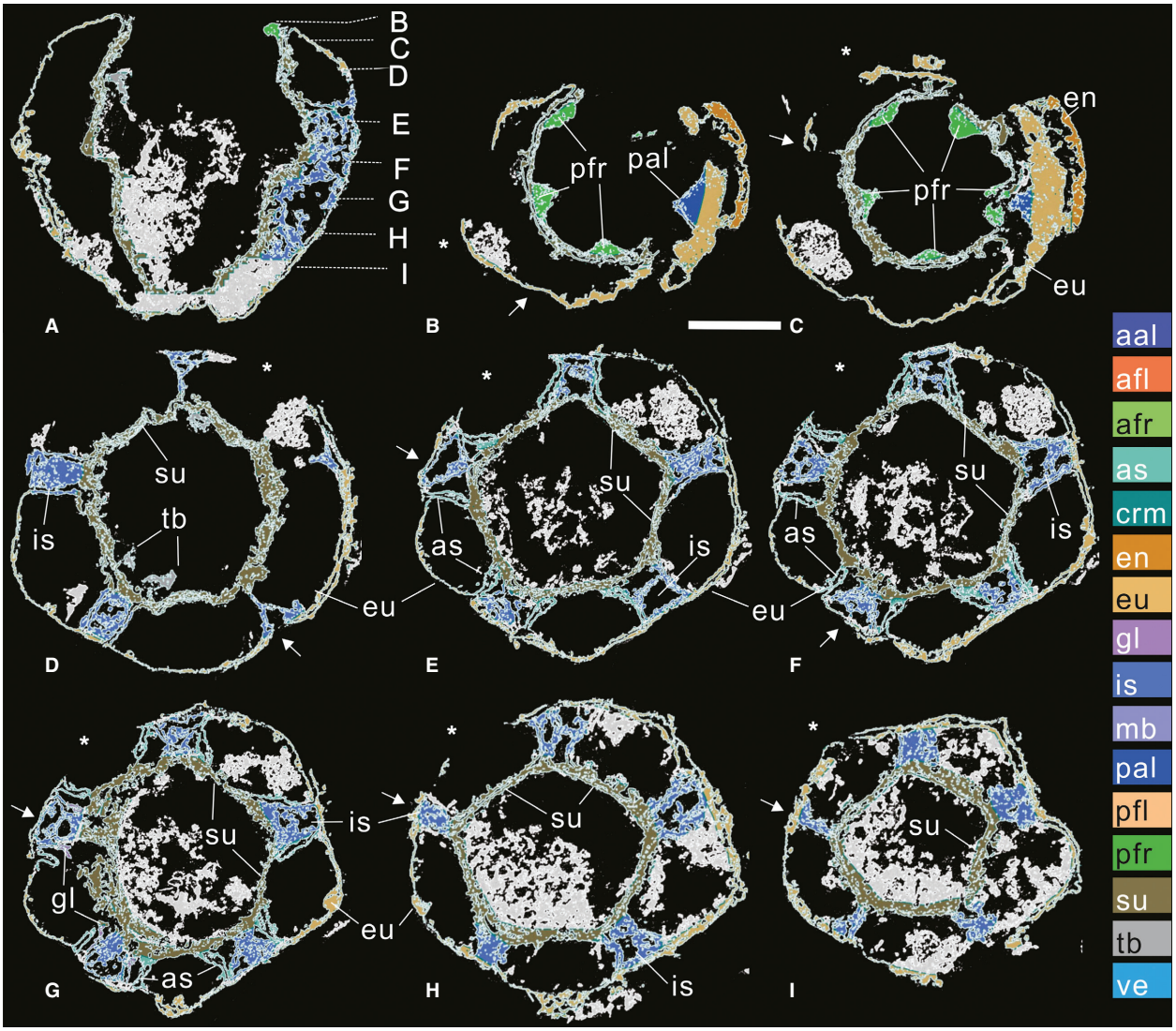

FIG. 4. *Sinaster petalon* gen. et sp. nov. from the lower Cambrian Kuanchuanpu Formation, Shaanxi Province, China; ELISN 115-39, paratype, microtomographic sections. A, axial section through the middle of the aperture; positions of horizontal sections B–I are indicated. B–I, horizontal sections from oral to aboral part. Major internal structures identified by colours generated by VG Studio 2.2 MAX; see colourless sections in Wang *et al.* (2017). *Abbreviations*: aal, adradial apertural lobe; afl, adradial fold lappet; afr, adradial frenulum; as, accessory septum; crm, circumferential muscle; en, egg envelope; eu, exumbrella; gl, gonad-lamella; is, interradial septum; mb, manubrium; pal, perradial apertural lobe; pe, periderm; pfl, perradial fold lappet; pfr, perradial frenulum; su, subumbrella; tb, tentacular bud; ve, velarium; *, perradius; →, interradius. Scale bar represents 150 μm.

11. Five pairs of tiny pisolitic structures occur in the middle of each interradial septum (Figs 2–6) and are interpreted here as gonad lamellae.

These 11 characters indicate that *Sinaster petalon* is most probably a cnidarian.

Tentacular buds

The bud-like structures of *Sinaster* are intepreted here as tentacular buds (tb) (point 5 above and Figs 2–5). Although the embryonic forms described in this paper have no exact equivalent among modern cnidarians, relevant comparisons can be made with the developmental stages of tentacles in extant cubozoans and scyphozoans. In the adult medusae, tentacles generally sprout from both umbrellas, but ontogenetically originate from the subumbrella (Conant 1898; Chapman 2001). They bud from the distal end of the blade-like gelatinous pedalium, which is rooted in the subumbrellar structure (e.g. in the adult stage of the cubozoan *Tripedalia cystophora*). In the younger sessile polyp stages, tentacles occur at the four

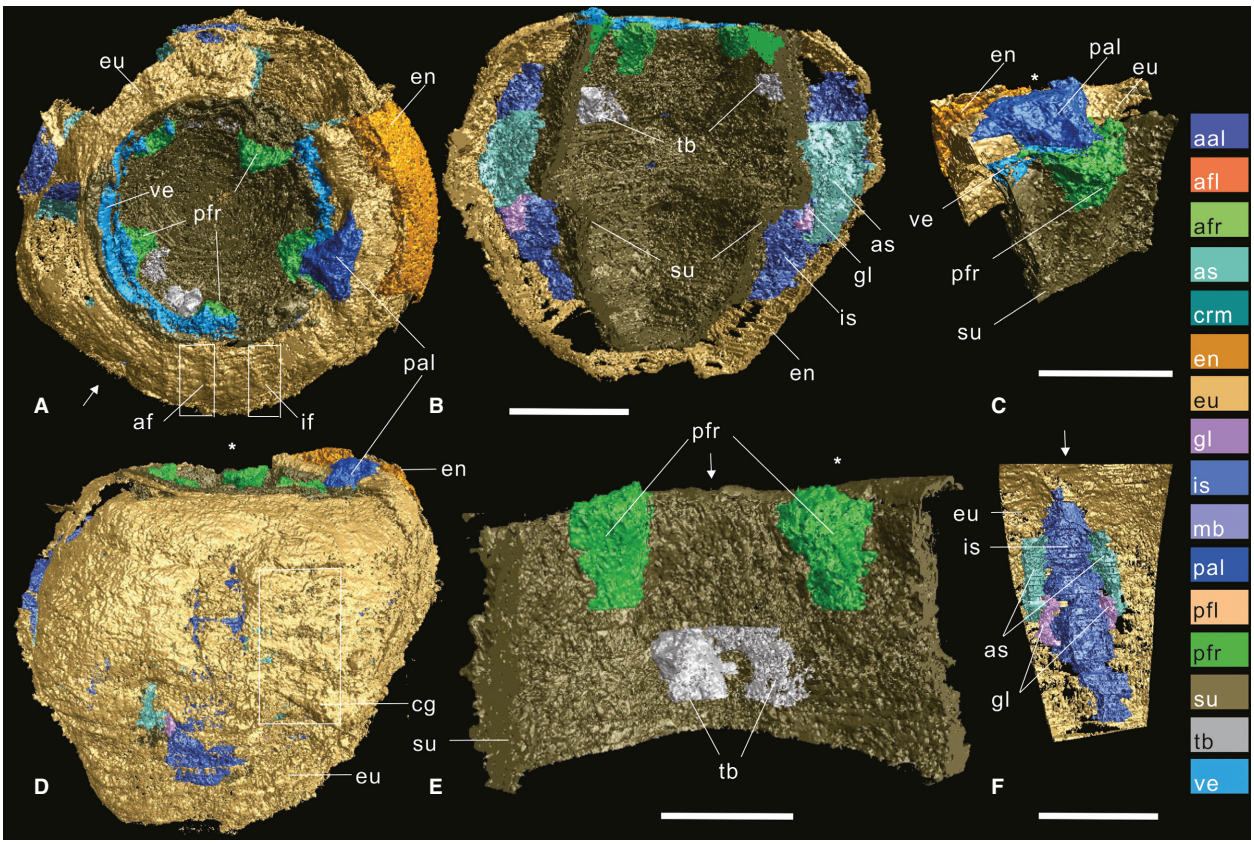

FIG. 5. *Sinaster petalon* gen. et sp. nov. from the lower Cambrian Kuanchuanpu Formation, Shaanxi Province, China; ELISN 115-39, paratype, three-dimensional model obtained using VG Studio 2.2 MAX. Colours identify anatomical structures. A, oral view showing the perradial lappet, velarium, perradial and adradial frenula. B, inner-lateral view of the half body showing the subumbrellar elements and the structures along the interradial septa. C, one-fifth apertural part showing the perradial lappet underlying the velarium and the perradial frenulum. D, surface of the exumbrella showing the shallow coronal grooves. E, one-fifth subumbrella showing the tentacular buds in the interradius and the frenula in the perradius. In a strict sense, each tentacle is located at the adradius. F, one-fifth exumbrella showing the gonad lamellae rooted into the interradial septa, and the accessory septa projecting from the interior layer of the exumbrella. *Abbreviations*: aal, adradial apertural lobe; af, adradial furrow; afl, adradial fold lappet; afr, adradial frenulum; as, accessory septum; cg, coronal groove; crm, circumferential muscle; eu, exumbrella; en, egg envelope; gl, gonad-lamella; if, interradial furrow; is, interradial septum; mb, manubrium; pal, perradial apertural lobe; pfl, perradial fold lappet; pfr, perradial frenulum; su, subumbrella; tb, tentacular bud; ve, velarium; *, perradius; →, interradius. Scale bars represent: 150 μm (A, B, D, F); 50 μm (C); 75 μm (E).

corners of the oral side of the animal (Werner *et al.* 1971). Features interpreted as subumbrellar tentacles also occur in the sea anemone-like cnidarian *Eolympia* and cubozoan-like specimens (Han *et al.* 2010, 2013, 2016*a*, *b*) and an unidentified fossil cnidarian polyp (Steiner *et al.* 2004) from the same horizon (Kuanchuanpu Formation) and locality where *Sinaster* was found. In summary, although we lack information concerning the post-embryonic development of the tentacular buds of *Sinaster*, we find no reason to reject the hypothesis that they originate from the subumbrellar structure and represent the early developmental stages of tentacles which would have developed at a more advanced polyp stage through ontogeny.

Reproductive organs in early and extant cnidarians

Gonads vary widely in shape, size and disposition among the four classes of cnidarians, and thus they are of great significance for the systematics and phylogeny of the group. In anthozoan anemones, the gonads occur within the gastroderm of the septa/mesenteries in the form of longitudinal band-like structures behind the septal filaments (Russell 1970). Gonads tend to be fused within one side of each septum (= mesentery) (Thomas & Edwards 1990). Thus the anthozoan septum is a combined structure with many functions such as support, digestion and body contraction and the production of gametes. The eight gastrodermal gonad bands of

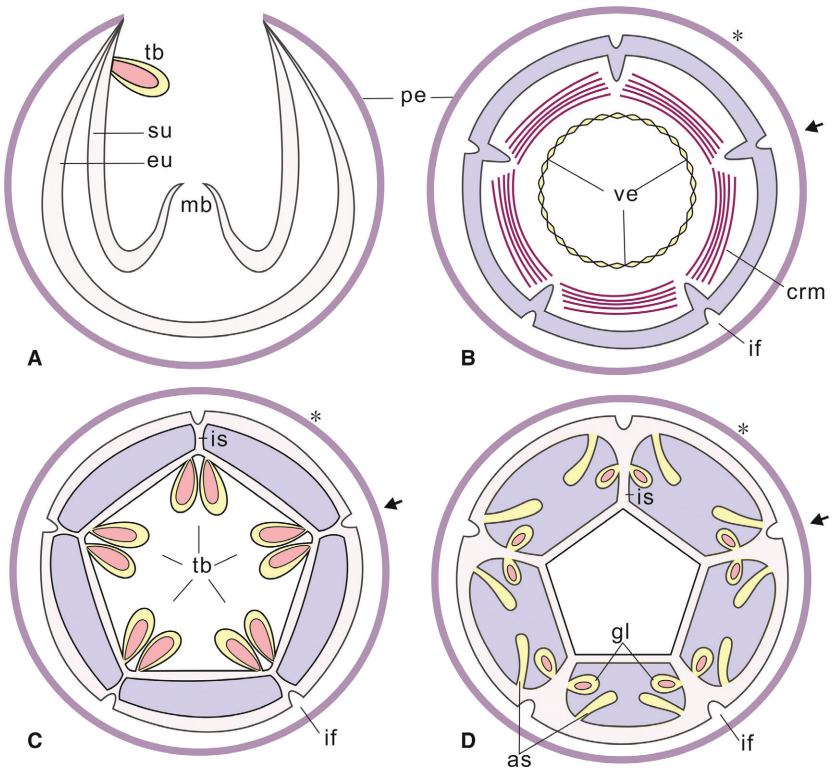

FIG. 6. Simplified cross-sections showing the internal features of *Sinaster* gen. et sp. nov. from the lower Cambrian Kuanchuanpu Formation, Shaanxi Province, China. A, vertical section through the manubrium, tentacle buds. B–D, horizontal sections; exumbrellar surface with the internal furrows; B, section near oral aperture showing the rounded velarium and the coronal muscles interrupted in interradii; C, section under velarium level showing five pairs of tentacular buds; D, section showing five pairs of the accessory septa and five pairs of the gonad lamellae. *Abbreviations*: as, accessory septum; crm, circumferential muscle; eu, exumbrella; gl, gonad lamellae; if, interradial furrow; is, interradial septum; mb, manubrium; pe, periderm; su, subumbrella; tb, tentacular buds; ve, velarium; *, perradius; →, interradius.

stauromedusae are also distributed along each side of the interradial septa, but are located closer to the distal end of the septa. As in anthozoans and staurozoans, the gonads of scyphozoans and cubozoans arise from the gastrodermis, and appear as well-delimited, paired strip-like outgrowths close to or along the interradial septa (Gershwin & Alderslade 2006). The gonad lamellae of *Sinaster* have a smaller size but we have no information concerning their internal complexity. However, scyphozoan gonads exhibit much greater diversity. In coronate medusae, eight gonads are derived from the subumbrellar endoderm; they are situated more or less close to the adradii and their distal end extends toward the perradii (Russell 1970; see also Fig. 8B). In Semaeostome and Rhizostomae medusae, there are only four folded gonads (Russell 1970; Tiemann & Jarms 2010). In hydrozoans, gonads develop from pouches of epidermal epithelium on either side of the manubrium or on the subumbrellar surface along the perradial canals (Thomas & Edwards 1990).

The gonad lamellae and accessory septa of *Sinaster petalon* and other unnamed fossil embryos from the Kuanchuanpu biota (ELISN 31-5 and ELISN 108-343, Han *et al.* 2013; GMPKU 3089, Dong *et al.* 2013) are clearly derived from the exumbrellar endodermis. They closely resemble the interradial gonads of cubozoans and also display important similarities to the reproductive organs of scyphozoans (Stauromedusae, Coronatae). For example, their accessory septa recall the gonads of extant coronates. Both structures are more or less adradial and are derived from the gastric epidermis (Han *et al.* 2013, 2016*a*). The aboral part of the gonad lamellae and accessory septa of ELISN 31-5 and ELISN 108-343 are rooted in the inner layer of the exumbrella, but most of their derived tissues are fused with the exterior subumbrellar layer at the middle level of the bell (Han *et al.* 2013; see Figs 4, 7A). The gonad lamellae and accessory septa, derived from exumbrellar endodermis as illustrated by *Sinaster petalon*, may represent the ancestral condition in cnidarians.

Comparisons with Olivooides

Sinaster petalon resembles *Olivooides multisulcatus* and *O. mirabilis*, two abundant embryonic forms from the Kuanchuanpu Formation (Hua *et al.* 2004; Dong 2009). However, *O. mirabilis* has a distinctive jar-like shape with a cap-like structure covering the aperture (Hua *et al.* 2004). Most of its developmental stages are characterized by a dense spiny external ornament (Steiner *et al.* 2014). Clearly these characteristics are not found in *S. petalon*.

Comparisons with Olivooides*-like embryos*

Sinaster petalon shares important characters with two *Olivooides*-like embryos (e.g. ELISN 31-5 and ELISN 108-343 interpreted as cubozoans by Han *et al.* (2013; see also

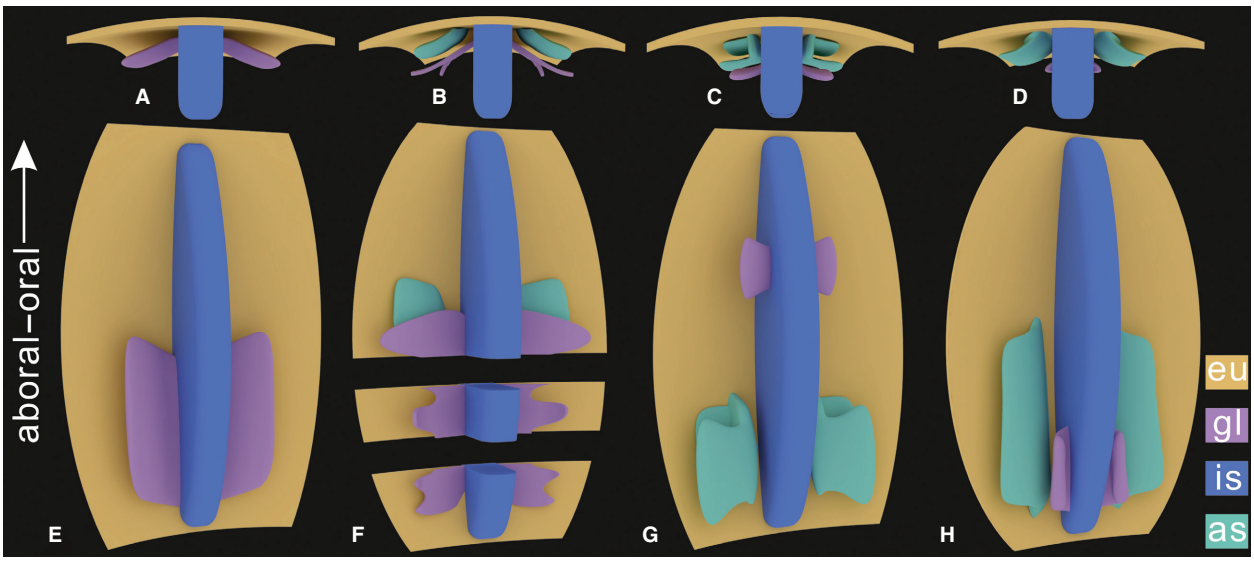

FIG. 7. Simplified reconstructions of the reproductive organs of extant (A, E) and lower Cambrian (B, F; C, G) medusozoans. Each form is represented in lateral and vertical views. Each image represents one-fifth of the animal. A, E, extant cubozoans with no accessory septa (Conant 1898). B, F, unnamed Cambrian form from the Kuanchuanpu biota with gonad lamellae and accessory septa (based on ELISN31-5; Han *et al.* 2013). C, G, unnamed Cambrian form from the Kuanchuanpu biota with gonad lamellae and distally branched accessory septa (based on GMPKU3089; Dong *et al.* 2013). D, H, *Sinaster petalon* gen. et sp. nov. with gonad lamellae and accessory septa (based on ELISN89-107). The subumbrellar wall and other anatomical structures are removed in order to expose the interradial septa, gonad lamellae and accessory lamellae.

Table 1). These are: (1) pentaradial symmetry exemplified by five pairs of tentacular buds; (2) five interradial septa supporting the medusa bell; (3) five pairs of gonad-like lamellae growing bilaterally in the interradial septa; (4) five pairs of accessory lamellae projecting into each perradial pocket; (5) a short manubrium; and (6) '5 + 10 pattern' of frenula and apertural lappets. However, *S. petalon* differs from *Olivooides*-like embryos in several anatomical features: (1) a completely smooth periderm; (2) interradial septa lacking free ends; (3) smaller and shorter gonad-like lamellae without bifurcation (Fig. 7); and (4) less developed endodermic lamellae and gastric pockets. These comparisons indicate that *S. petalon* and the two unnamed cubozoans represented by ELISN 31-5 and ELISN 108-343 are most probably neither conspecific nor congeneric but may belong to the same family.

TABLE. 1. Morphological comparisons between *Sinaster petalon* gen. et sp. nov. and *Olivooides* embryos, all from the lower Cambrian Kuanchuanpu Formation.

	Periderm	Interradial septa / radial wall	Gonad lamellae / unnamed	Accessory septa / recurved wall	Bell texture / unnamed
ELISN 89-107	Complete, smooth	One third of the height of the bell	Near to the aboral section of the bell, continuous	One sixth of the height of the bell	Unknown
ELISN 115-39	Incomplete, smooth	One third of the height of the bell	Near to the aboral section of the bell, continuous	One sixth of the height of the bell	With adradial furrow, interradial furrow and coronal groove
ELISN 31-5	Unknown, with an envelope	Half the height of the bell	Middle of the bell, discontinuous	One sixth of the height of the bell	Same as ELISN 115-39
ELISN 108-343	Incomplete, with an envelope	Half the height of the bell	Middle of the bell, discontinuous	One sixth of the height of the bell	Same as ELISN 115-39
GMPKU 3089	Unknown	Half the height of the bell	Near to the oral section, tiny; unnamed	One eighth of the height of the bell	Same as ELISN115-39; unnamed

Sinaster petalon also shares a series of common features with another unnamed embryo from the Kuanchuanpu Formation (GMPKU 3089, Dong *et al.* 2013; Table 1). These are: (1) interradial and adradial furrows and shallow coronal grooves on the external layer of the exumbrella (see Dong *et al.* 2013, fig. 3a, b); (2) spacious perradial pockets created by the straight and long interradial septa; (3) long curved accessory septa projecting into the perradial pockets (see Dong *et al.* 2013, fig. 3); (4) paired, tiny gonad-like lamellae rooted in the interradial septa (see Dong *et al.* 2013, fig. 3j); and (5) tentacular buds with inner cavity. However, GMPKU 3089 has several features which do not occur in *S. petalon*, such as: (1) the lack of a periderm; (2) gonad-like lamellae in a much higher position (Fig. 7); (3) perradial pockets with a smaller volume; and (4) five pairs of depressions under the tentacular buds and five radial canals. All of these features indicate that GMPKU 3089 differs from *S. petalon* but may belong to *Sinaster*.

Systematic position of Sinaster *and* Olivooides*-like fossils*

Two competing hypotheses have been proposed for the systematic position of *Olivooides*-like fossils: Scalidophora (Ecdysozoa; Steiner *et al.* 2014) or Scyphozoa and Cubozoa (Cnidaria; Dong *et al.* 2013; Han *et al.* 2013; Liu *et al.* 2014; Steiner *et al.* 2014). This debate also concerns *Sinaster* and is summarized below.

The Scalidophora hypothesis

We think that this hypothesis can be rejected on the following grounds:

1. *Olivooides*-like fossils have either pentaradial or tetraradial symmetry (Dong *et al.* 2013; Han *et al.* 2013, 2016a) and thus do not have a bilateral body plan. Modern Scalidophora such as priapulids and their assumed early Cambrian ancestors (e.g. Chengjiang biota; Huang *et al.* 2004; Vannier 2012) are bilaterians with an antero-posterior polarity and a ventral cord (Nielsen 1995; Adrianov & Malakhov 2001). No such bilateral arrangement occurs in *Olivooides*-like fossils.
2. No eubilaterian has a double-layered body wall connected by pentaradial septa.
3. Representatives of *Olivooides*-like fossils lack the annulated trunk and swollen introvert with scalid rows that characterizes extinct and extant scalidophorans. *Eopriapulites sphinx,* which co-occurs with *Olivooides* embryos in the Kuanchuanpu Formation, is the oldest known scalidophoran. Its 18 longitudinal rows of scalids (Ruppert *et al.* 2004; Liu *et al.* 2014) have no equivalent in *Olivooides*.
4. Both extinct (e.g. *Ottoia prolifica*; Vannier 2012) and extant scalidophorans have a cylindrical gut linking the anterior (mouth) and posterior (anus) ends of the body. The single apical aperture of *Olivooides* embryos superficially resembles the mouth opening of scalidophorans (Steiner *et al.* 2014), but it is really just an invagination of the theca. The real 'mouth' is located at the end of the manubrium (Han *et al.* 2013; Figs 2, 3) whereas the 'gut' *sensu* Dong *et al.* (2013) probably starts at the aboral stalk of soft-tissue.
5. The body wall of extant scalidophorans such as priapulids (Vannier 2012) consists of a relatively thin cuticle lined with longitudinal and circular muscles (Ruppert *et al.* 2004) and separates the coelomic cavity from the external medium. The peridermal theca of the *Olivooides* embryos has no such features.

The Cnidaria option

Comparison with anthozoans. Anthozoans are characterized by bilateral symmetry, an actinopharynx, and direct and indirect mesenteries with free ends (Hyman 1940). Both extinct and extant representatives of the group lack paired tentacles, a manubrium and lappets such as those present in *Sinaster petalon* and other *Olivooides*-like embryos.

Comparison with hydrozoans

Sinaster petalon and other *Olivooides*-like embryos differ from hydrozoans (hydropolyps and hydromedusae). Most solitary or colonial hydropolyps are partly or entirely surrounded by a tubulous cuticle or perisac, and they possess numerous circumoral tentacles surrounding a cone-shaped hypostome without oral lips or lappets (Hyman 1940; Thomas & Edwards 1990). The cuticle (or perisac) and hypostome of extant hydrozoans resemble the periderm and manubrium of *S. petalon*. However, the hydrozoan septa are highly reduced or invisible. The gastric cavity of hydropolyps does not partition into several pouches, while the gastric pockets of *S. petalon* are separated by interradial septa. In addition, the manubrium/hypostome of *S. petalon* are located deep within the subumbrellar cavity. Hydromedusae have four perradial canals, four primary tentacles, as well as a very distinctive velum with neither frenula nor lappets (Thiel 1966). In contrast, all known *Olivooides*-like embryos have a circle of tentacles close to the interradii that are derived from the subumbrellar wall.

Comparison with staurozoans

The life cycle of extant staurozoans lacks the alternation of a sessile polyp and a swimming medusa and is commonly interpreted as an attached medusa stage (Collins *et al.* 2006). The external morphology of extant staurozoans is similar to that of naked, juvenile *Olivooides*-like fossils lacking a periderm (see Steiner *et al.* 2014, fig. 12: 7, 8). Their spacious perradial pockets are comparable to those of *S. petalon* and other *Olivooides*-like fossils. Notably, the pedal disk of staurozoans is fastened to the substrate by a chitinous secretion (Hyman 1940) that might represent a vestigial periderm. Longitudinal muscles, usually seen in the extant staurozoans, are not present in *Sinaster* (Miranda *et al.* 2015, 2016). The triangular marginal lappets, strip-shaped gonads and paired tentacles of *Sinaster* have no counterparts in modern staurozoans. For these reasons, *S. petalon* cannot be placed within the staurozoans.

Comparison with scyphozoans

As previously proposed for *Olivooides* (He 1987), *Sinaster petalon* might be placed among scyphozoans and especially scyphopolyps, based on the presence of marginal lappets, paired gonads, coronal muscles and an annulated sessile periderm. However, the periderm is a common feature among anthozoans and all cnidarian polyps except staurozoans (Ruppert *et al.* 2004). In general, the periderm of extant cnidarians does not cover the entire body as it does in the Kuanchuanpu medusozoans. Also, *S. petalon* can hardly been placed within one of the three scyphozoan orders, namely Coronatae, Semaeostomeae and Rhizostomeae. For example, it lacks the rhopalia, complex radial canals and well-developed mouth arms of the Semaeostomeae and Rhizostomeae. Furthermore, the coronal furrow, exumbrellar pedalia, and radial canals typical of Coronatae have no equivalent in *S. petalon*. Marginal lappets and paired gonads are two important characters shared with scyphozoans which might indicate a common ancestry.

Comparison with cubozoans

Sinaster petalon is most similar to extant cubozoan medusae. Specifically, in that the: (1) concentration of subumbrella tentacles in the interradii is a diagnostic feature of extant cubozoans (Conant 1898; Chapman 2001); (2) morphology and arrangement of the gonadal lamellae is similar to those of both cubozoans and scyphozoans (Figs 7, 8); (3) support of the velarium by the perradial frenula is also a distinctive feature of extant cubozoans (Conant 1898); (4) interradial septa, which connect the subumbrellar and exumbrellar walls, lack a free end. In these respects, *S. petalon* more closely resembles present-day cubozoans than do other *Olivooides*-like embryos (e.g. ELISN 31-5). However, *Sinaster* does not possess the typical pedalia and sensory organs seen in modern cubozoans and in fossil jellyfish from the Chengjiang biota (Han *et al.* 2016c). Finally, the marginal lappets and the adradial frenula of *Sinaster* are absent in the modern representatives of the group.

PHYLOGENETIC ANALYSIS

In total, 25 taxa (including *Sinaster petalon*) and 104 characters (see definitions in Marques & Collins 2004 and Han

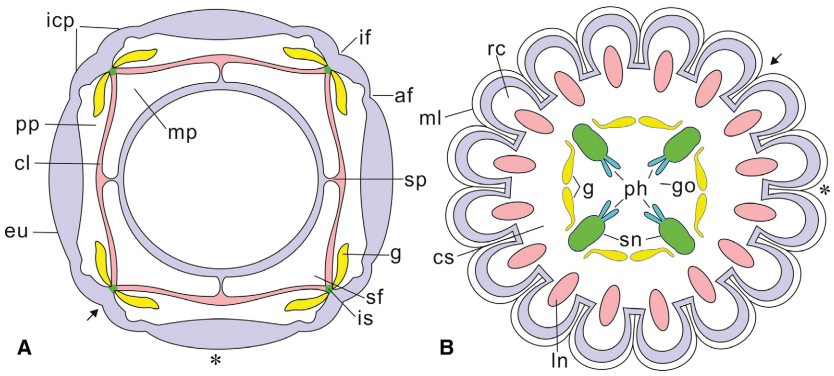

FIG. 8. Simplified horizontal cross-sections through the extant medusae. A, cubozoan. B, scyphozoan (coronate medusa). *Abbreviations*: af, adradial furrow; cl, claustrum; cs, coronal stomach; eu, exumbrella; g, gonad; go, gastric ostium; icp, interradial corner pillar; if, interradial furrow; is, interradial septa; ln, lappet node; ml, marginal lappet; mp, mesogonial pockets; ph, phacellus (gastric filament); pp, perradial pocket; rc, radial canal; sf, septal funnel; sn, septal nodes; sp, suspensorium; *, perradius; →, interradius. Modified from Russell (1970, text-fig. 37) and Tiemann & Jarms (2010).

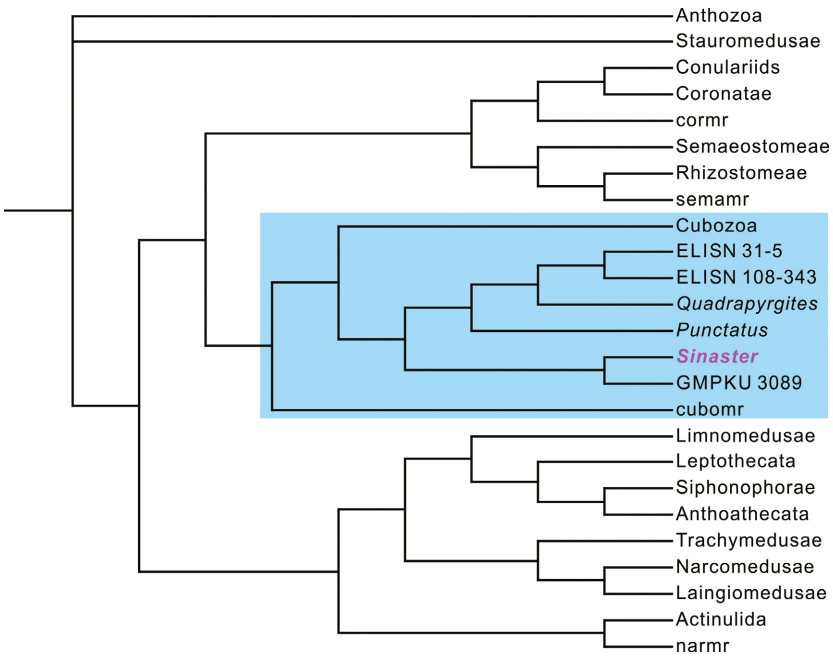

FIG. 9. Consensus tree for Medusozoa acquired using PAUP* v. 4.0 b10. ELISN 31-5, ELISN 108-343 and GMPKU 3089 are uncertain taxa in Han *et al.* (2013) and Dong *et al.* (2013) respectively. The co-occurring *Quadrapyrgites* and *Punctatus* also were found in the Kuanchuanpu Formation. Cormr, semamr, narmr, cubomr represent, respectively, unnamed fossils of the Coronata, Semaestomeae, Narcomedusae and Cubomedusa from the Middle Cambrian Marjum Formation, Utah (Cartwright *et al.* 2007).

et al. 2016c), were considered for analysis using PAUP* v. 4.0 b10, yielding 999 shortest trees (tree length = 177 steps, consistency index = 0.65, rescaled consistency index = 0.50) (Wang *et al.* 2017, appendix 3). All characters have equal weight, 8 of them are constant, and 25 variable characters are parsimony-uninformative. This corroborates the molecular analysis of Collins *et al.* (2006) which found scyphozoans and cubozoans to form a monophyletic group. As shown on the consensus tree (Fig. 9), *Sinaster* and GMPKU 3089 are close to each other. *Sinaster* and other fossil embryos (e.g. GMPKU 3089, ELISN 31-5 and ELISN 108-343) belong to the total group Cubozoa (Fig. 9; highlighted in blue). This tentative phylogenetic analysis suggests that *Sinaster* and its allied embryonic forms may belong to the stem-group Cubozoa.

CONCLUSIONS

Sinaster petalon exhibits a mixture of features typical of polypoid and medusoid phases. Its internal anatomical structure (e.g. gonad lamellae, accessory septa, perradial and adradial frenula) appear to be more complex than those of all extant medusozoan polyps. Although it bears a well-developed subumbrellar cavity and coronal muscles, it lacks sensory organs comparable to those of extant medusae. The presence of a periderm around *Sinaster* and the manifest absence of sensory features would support the view that the adult stage is a sessile medusa.

Sinaster cannot be straightforwardly assigned to any crown group of extant medusozoans. However, the presence of marginal lappets and endodermal lamellae suggest that it is closer to Cubomedusa and Scyphomedusa than to any other group of modern cnidarians. The presence in *Sinaster* of a velarium supported by the frenulum is an important cubozoan character that would support its position in the stem-group Cubomedusae.

The morphological similarity of *Sinaster* with both cubozoans and scyphozoans supports the hypothesis that these fossils represent the common ancestors of Cubozoa + Scyphozoa. However, cladistic analysis suggests closer affinities with Cubozoa than with Scyphozoa. The subsequent reduction of various internal structures and of the external periderm through evolution would have led to the divergence between these two groups.

Although quite similar in their external morphology, the pentamerous embryonic medusae from the early Cambrian Kuanchuanpu biota display considerable anatomical variation, exemplified here by *Sinaster petalon*. Clearly, any future attempt to establish the taxonomy of these fossils should take into consideration not only their external shape and micro-ornament but also and above all their internal structures, which can be easily revealed with microtomographic techniques.

Authors' contributions. JH designed the research; XW and JH developed the interpretation; KU, OS and TK conducted the synchrotron and micro-CT. XW reconstructed the micro-CT data. XW, JH, JV and QO wrote the paper with input with the other authors, all of whom read and approved the final manuscript.

Acknowledgements. We thank Gong, H. J., Sun, J., Luo, J., Han, X. and Cheng M. R. (State Key Laboratory for Continental Dynamics, Northwest University, Xi'an, China) for their

assistance in both field and laboratory work, Yin, Z. J. (Nanjing Institute of Geology and Palaeontology, Chinese Academy of Sciences, Nanjing, China) for technical assistance with 3D-reconstructions. We thank H. Van Iten (Department of Geology, Hanover College, Indiana) and an anonymous referees for correcting and improving our manuscript. Current work is supported by the National Natural Science Foundation of China (NSFC grant 41272019), the '973 project' of the Ministry of Science and Technology of China (2013CB835002, 2013CB837100), the '111 project' of the Programs of Introducing Talents of Discipline to Universities (W20136100061) and the Most Special Fund from the State Key Laboratory of Continental Dynamics, Northwest University, Xi'an, China.

DATA ARCHIVING STATEMENT

This published work and the nomenclatural acts it contains, have been registered in ZooBank: http://zoobank.org/References/3F910127-DEE5-406F-9808-B32C2FB177DB

Data for this study are available in the Dryad Digital Repository: https://doi.org/10.5061/dryad.ng76g

Editor. George Sevastopulo

REFERENCES

ADRIANOV, A. V. and MALAKHOV, V. V. 2001. Symmetry of priapulids (Priapulida). 1. Symmetry of adults. *Journal of Morphology*, **247** (2), 99–110.

BENGTSON, S. and YUE, Z. 1997. Fossilized metazoan embryos from the earliest Cambrian. *Science*, **277**, 1645–1648.

CARTWRIGHT, P., HALGEDAHL, S. L., HENDRICKS, J. R., JARRARD, R. D., MARQUES, A. C., COLLINS, A. G. and LIEBERMAN, B. S. 2007. Exceptionally preserved jellyfishes from the Middle Cambrian. *PLoS One*, **2**, e1121.

CHAPMAN, D. M. 2001. Development of the tentacles and food groove in the jellyfish *Aurelia aurita* (Cnidaria: Scyphozoa). *Canadian Journal of Zoology*, **79** (4), 623–632.

CHEN, F. and DONG, X. P. 2008. The internal structure of Early Cambrian fossil embryo *Olivooides* revealed in the light of synchrotron x-ray tomographic microscopy. *Chinese Science Bulletin*, **53**, 3860–3865.

COLLINS, A. G., SCHUCHERT, P., MARQUES, A. C., JANKOWSKI, T., MEDINA, M. and SCHIERWATER, B. 2006. Medusozoan phylogeny and character evolution clarified by new large and small subunit rDNA data and an assessment of the utility of phylogenetic mixture models. *Systematic Biology*, **55**, 97–115.

CONANT, F. S. 1898. *The Cubomedusae: a memorial volume*. Johns Hopkins Press, Baltimore. https://doi.org/10.5962/bhl.title.1736

CONWAY MORRIS, S. and CHEN, M. E. 1992. Carinachitids, Hexangulaconulariids, and *Punctatus*: problematic metazoans from the Early Cambrian of South China. *Journal of Paleontology*, **66**, 384–406.

DALY, M., BRUGLER, M. R., CARTWRIGHT, P., COLLINS, A. G., DAWSON, M. N., FAUTIN, D. G., GRANCE, S. C., McFADDEN, C. S., OPRESKO, D. M., RODRIGUEZ, E., ROMANO, S. L. and STAKE, J. L. 2007. The phylum Cnidaria: a review of phylogenetic patterns and diversity 300 years after Linnaeus. *Zootaxa*, **1668**, 127–182.

DONG, X.-P. 2009. The anatomy, affinity and developmental sequences of Cambrian fossil embryos (In Chinese). *Acta Palaeontological Sinica*, **48**, 390–401.

—— CUNNINGHAM, J. A., BENGTSON, S., THOMAS, C.-W., LIU, J., STAMPANONI, M. and DONOGHUE, P. C. J. 2013. Embryos, polyps and medusae of the Early Cambrian scyphozoan *Olivooides*. *Proceedings of the Royal Society B*, **280**, 20130071.

—— VARGAS, K., CUNNINGHAM, J. A., ZHANG, H. Q., LIU, T., CHEN, F., LIU, J., BENGTSON, S. and DONOGHUE, P. C. J. 2016. Developmental biology of the early Cambrian cnidarian *Olivooides*. *Palaeontology*, **49**, 387–407.

GERSHWIN, L. A. and ALDERSLADE, P. 2006. *Chiropsella bart* n. sp., a new box jellyfish (Cnidaria: Cubozoa: Chirodropida) from the Northern Territory, Australia. *The Beagle*, **22**, 15–21.

HAN, J., KUBOTA, S., UCHIDA, H., STANLEY, G. D. Jr, YAO, X. Y., SHU, D. G., LI, Y. and YASUI, K. 2010. Tiny sea anemone from the lower Cambrian of China. *PLoS One*, **5**, e13276.

—— —— LI, G. X., YAO, X. Y., SHU, D. G., LI, Y., KINOSHITA, S., SASAKI, O., KOMIYA, T. and YAN, G. 2013. Early Cambrian pentamerous cubozoan embryos from South China. *PLoS One*, **8**, e70741.

—— —— —— OU, Q., WANG, X., YAO, X. Y., SHU, D., LI, Y., UESUGI, K., HOSHINO, M., SASAKI, O., KANO, H. and SATO, T. 2016*a*. Divergent evolution of medusozoan symmetric patterns: evidence from the microanatomy of Cambrian tetramerous cubozoans from South China. *Gondwana Research*, **31**, 150–163.

—— LI, G. X., KUBOTA, S., OU, Q., TOSHINO, S., WANG, X., YANG, X. G., UESUGI, K., MASATO, H., SASAKI, O., KANO, H., SATO, T. and KOMIYA, T. 2016*b*. Internal microanatomy and zoological affinity of the Early Cambrian *Olivooides*. *Acta Geologica Sinica (English Edition)*, **90** (1), 38–65.

—— HU, S. X., CARTWRIGHT, P., ZHAO, F. C., OU, Q., KUBOTA, S., WANG, X. and YANG, X. G. 2016*c*. The earliest pelagic jellyfish with rhopalia from Cambrian Chengjiang Lagerstätte. *Palaeogeography, Palaeoclimatology, Palaeoecology*, **449**, 166–173.

—— CONWAY MORRIS, S., OU, Q., SHU, D. G. and HUANG, H. 2017*a*. Meiofaunal deuterostomes from the basal Cambrian of Shaanxi (China). *Nature*, **542**, 228–231.

—— LI, G. X., WANG, X., YANG, X. G., GUO, J. F., SASAKI, O. and KOMIYA, T. 2017*b*. *Olivooides*-like tube aperture in early Cambrian carinachitids (Medusozoa, Cnidaria). *Journal of Paleontology*, published online 29 June. https://doi.org/10.1017/jpa.2017.10

—— CAI, Y. P., SCHIFFBAUER, J. D., HUA, H., WANG, X., YANG, X. G., UESUGI, K., KOMIYA., T. and SUN,

J. 2017*c*. A *Cloudina*-like fossil with evidence of asexual reproduction from the earliest Cambrian, South China. *Geological Magazine*, published online 9 January. https://doi.org/10.1017/s0016756816001187

HE, T. G. 1987. Early Cambrian conulariids from the Yangtze platform and their early evolution (In Chinese). *Journal of Chengdu College of Geology*, **14**, 7–18.

HUA, H., CHEN, Z. and ZHANG, L. Y. 2004. Early Cambrian phosphatized blastula- and gastrula-stage animal fossils from southern Shaanxi, China. *Chinese Science Bulletin*, **49**, 487–490.

HUANG, D. Y., VANNIER, J. and CHEN, J. Y. 2004. Recent Priapulidae and their Early Cambrian ancestors: comparisons and evolutionary significance. *Geobios*, **37** (2), 217–228.

HYMAN, L. H. 1940. *The invertebrates*. McGraw Hill, 726 pp.

LIU, Y. H., XIAO, S. H., SHAO, T. Q., BROCE, J. and ZHANG, H. Q. 2014. The oldest known priapulid-like scalidophoran animal and its implications for the early evolution of cycloneuralians and ecdysozoans. *Evolution & Development*, **16** (3), 155–165.

MARQUES, A. C. and COLLINS, A. G. 2004. Cladistic analysis of Medusozoa and cnidarian evolution. *Invertebrate Biology*, **123**, 23–42.

MIRANDA, L. S., COLLINS, A. G. and MARQUES, A. C. 2015. Is *Haootia quadriformis* related to extant Staurozoa (Cnidaria)? Evidence from the muscular system reconsidered. *Proceedings of the Royal Society B*, **282** (1803), 20142396.

—— HIRANO, Y. M., MILLS, C. E., FALCONER, A., FENWICK, D., MARQUES, A. C. and COLLINS, A. G. 2016. Systematics of stalked jellyfishes (Cnidaria: Staurozoa). *PeerJ*, **4**, e1951.

NIELSEN, C. 1995. *Animal evolution: interrelationships of the living phyla*. Oxford University Press.

PETERSEN, K. W. 1979. Development of coloniality in Hydrozoa. 105–139. *In* LARWOOD, G. and ROSEN, B. R. (eds). *Biology and systematics of colonial organisms*. Academic Press.

QIAN, Y. 1977. Hyolitha and some problematica from the Lower Cambrain Meishucun Stage in central and S. W. China. *Acta Palaeontologica Sinica*, **16**, 255–275.

—— 1999. *Taxonomy and biostratigraphy of small shelly fossils in China (In Chinese)*. Science Press, Beijing.

RUPPERT, E. E., FOX, R. S. and BARNES, R. D. 2004. *Invertebrate zoology: a functional evolutionary approach*. Brooks Cole Publishing, Belmont, CA.

RUSSELL, F. S. 1970. *The Medusae of the British Isles. 2. Pelagic Scyphozoa with a supplement to the first volume on Hydromedusae*. Cambridge University Press.

STEINER, M., LI, G. X. and QIAN, Y. 2004. Lower Cambrian small shelly fossils of northern Sichuan and southern Shaanxi (China), and their biostratigraphic importance. *Geobios*, **37**, 259–275.

—— QIAN, Y., LI, G. X., HAGADORN, J. W. and ZHU, M. Y. 2014. The developmental cycles of early Cambrian Olivooidae fam. nov. (?Cycloneuralia) from the Yangtze Platform (China). *Palaeogeography, Palaeoclimatology, Palaeoecology*, **398**, 97–124.

SWOFFORD, D. L. 2003. *PAUP*. Phylogenetic Analysis Using Parsimony (and other methods), v. 4*. Sinauer Associates, Sunderland, MA.

THIEL, H. 1966. The evolution of Scyphozoa: a review. 77–117. *In* REES, W. J. (ed.) *The Cnidaria and their evolution*. Symposia of the Zoological Society of London, **16**, Academic Press.

THOMAS, M. B. and EDWARDS, N. C. 1990. Cnidaria: Hydozoa. 91–184. *In* HARRISON, F. W. and WESTFALL, J. A. 1990. *Microscopic anatomy of invertebrates. Vol. 2: Placozoa*, *Porifera*, *Cnidaria*, and *Ctenophora*. Wiley-Liss.

TIEMANN, H. and JARMS, G. 2010. Organ-like gonads, complex oocyte formation, and long-term spawning in *Periphylla periphylla* (Cnidaria, Scyphozoa, Coronatae). *Marine Biology*, **157** (3), 527–535.

TOSHINO, S., MIYAKE, H. and SHIBATA, H. 2015. *Meteorona kishinouyei*, a new family, genus and species (Cnidaria, Cubozoa, Chirodropida) from Japanese Waters. *ZooKeys*, **503**, 1–21.

VAN ITEN, H., LEME, J. M., SIMÕES, M. G., MARQUES, A. and COLLINS, A. G. 2006*a*. Reassessment of the phylogenetic position of conulariids in the subphylum Medusozoa (phylum Cnidaria). *Journal of Systematic Palaeontology*, **4**, 109–118.

VANNIER, J. 2012. Gut contents as direct indicators for trophic relationships in the Cambrian marine ecosystem. *PLoS One*, **7** (12), e52200.

VERRILL, A. E. 1865. Classification of polyps (extract condensed from Synopsis of the Polyps and Corals of the North Pacific Exploring Expedition under Commodore C. Ringgold and Captain John Rodgers, U.S.N.). *Communications of the Essex Institute*, **4**, 145–152.

WANG, X., HAN, J., VANNIER, J., OU, Q., YANG, X., UESUGI, K., SASAKI, O. and KOMIYA, T. 2017. Data from: Anatomy and affinities of a new 535-million-year-old medusozoan from the Kuanchuanpu Formation, South China. *Dryad Digital Repository*. https://doi.org/10.5061/dryad.ng76g

WERNER, B. 1973. New investigations on systematics and evolution of the class Scyphozoa and the phylum Cnidaria. *Publications of the Seto Marine Biological Laboratory*, **20**, 35–61.

—— CUTRESS, C. E. and STUDEBAKER, J. P. 1971. Life cycle of *Tripedalia cystophora* Conant (Cubomedusae). *Nature*, **232**, 582–583.

YAO, X. Y., HAN, J. and JIAO, G. X. 2011. Early Cambrian epibolic gastrulation: a perspective from the Kuanchuanpu Member, Dengying Formation, Ningqiang, Shaanxi, South China. *Gondwana Research*, **20**, 844–851.

YUE, Z. and BENGTSON, S. 1999*a*. Phosphatized embryo fossils from the Cambrian explosion. *Chinese Science Bulletin*, **44**, 842–845.

—— —— 1999*b*. Embryonic and post-embryonic development of the Early Cambrian cnidarian *Olivooides*. *Lethaia*, **32**, 181–195.

ZHANG, H. Q., XIAO, S. H., LIU, Y. H., YUAN, X. L., WAN, B., MUSCENTE, A. D., SHAO, T., GONG, H. and CAO, G. 2015. Armored kinorhynch-like scalidophoran animals from the early Cambrian. *Scientific Reports*, **5**, 16521.

5.5 A coronate-like medusa from the early Cambrian Kuanchuanpu Formation, south China

The description of *Hanagyroia orientalis*, a new globular embryonic fossil from the lowermost Cambrian Kuanchuanpu Formation gives the opportunity to test hypotheses concerning the affinities of *Olivooides* and *Olivooides*-like fossils (Dong et al. 2016, Han et al. 2013, Liu et al. 2014b, Liu et al. 2017, Wang et al. 2017) and more precisely to which group of extant cnidarians they might belong. Recent papers suggest that these fossils share numerous morphological traits with scyphozoans and cubozoans and might be affiliated to one of these two groups. We also keep in mind that *Olivooides* and *Olivooides*-like fossils may belong to an earlier off-shot of the cnidarian evolutionary tree and have therefore no direct relationships with modern lineages.

A microtomographic exploration of *Hanagyroia orientalis* gen. and sp. nov. allows us to describe its internal microstructures in details and to compare them with those of Olivooides other *Olivooides*-like forms (e.g. *Sinaster*; see Wang et al., 2017). *Hanagyroia* is interpreted as a new pentamerous medusozoan, characterized by five well-developed perradial oral lips around a remarkably large manubrium, a conspicuous equatorial groove, and five short, interradial pairs of extensile tentacles at the bell margin. Internally, five broad and stout interradial septa join horizontally to form the claustra. The most remarkable feature of *Hanagyroia orientalis* gen. and sp. nov. is its lobed mouth (manubrium consisting of five large perradial lobes) and its equatorial groove reminiscent of that of extant scyphozoan coronates. However, the cladistic analysis suggests that *Hanagyroia* has closer affinities with cubozoans than with scyphozoans and may represent an intermediate morphological type between scyphozoans and cubozoans. The well-developed oral lips and paired short strong tentacles of *Hanagyroia* suggest a direct development.

A Coronate-like medusa from the early Cambrian Kuanchuanpu Formation, south China

Xing Wang[a, b], Jean Vannier[b], Xiaoguang Yang[a], Shin Kubota[c], Qiang Ou[d], Xiaoyong Yao[e], Kentaro Uesugi[f], Osamu Sasaki[g], Tsuyoshi Komiya[h], Jian Han[a, *]

[a]State Key Laboratory of Continental Dynamics, Shaanxi Key laboratory of Early Life and Environment, Department of Geology, Northwest University, Xi'an, 710069, P.R. China

[b]Université Lyon 1, UMR 5276 du CNRS, Laboratoire de géologie de Lyon: Terre, Planètes, Environnement, bâtiment GEODE, 2, rue Raphaël Dubois, Villeurbanne 69622, France

[c]Seto Marine Biological Laboratory, Field Science Education and Research Center, Kyoto University, Shirahama, Wakayama 649-2211, Japan

[d]Early Life Evolution Laboratory, School of Earth Sciences and Resources, China University of Geosciences, Beijing 100083, P.R. China

[e]School of Earth Science and Land Resources, Key Laboratory of Western China's Mineral Resources and Geological Engineering, Ministry of Education, Chang'an University, Xi'an 710054, P.R. China

[f]Japan Synchrotron Radiation Research Institute (JASRI) 1-1-1 Kouto, Sayo-cho, Sayo-gun, Hyogo, Japan

[g]Tohoku University Museum, Tohoku University, 6-3 Aoba, Aramaki, Aoba-ku, Sendai, Japan

[h]Department of Earth Science and Astronomy, Graduate School of Arts and Sciences, The University of Tokyo, Tokyo 153-8902, Japan

* To whom correspondence should be addressed. E-mail: elihanj@nwu.edu.cn (H.J.)

Abstract

The tetra- or pentaradial fossil embryos and related hatched individuals from the early Cambrian Kuanchuanpu Formation are of great significance for understanding the early evolution of medusozoans. Whether the precise divergence of these early Cambrian fossil medusozoans corresponds to external morphology of periderm or involves detail correlations of the internal anatomic structures (i.e. manubrium, tentacles, septa, claustra, suspensorium, frenula and velarium), still remains in hot debate. Here we describe a new pentamerous medusozoan, *Hanagyroia orientalis* gen. et sp. nov., characterized by five well-developed perradial oral lips around a remarkably large manubrium, a conspicuous equatorial groove, and five short, interradial pairs of extensile tentacles at the bell margin. Internally, five broad and stout interradial septa join horizontally to form the claustra. *Hanagyroia orientalis* gen. et sp. nov. lacks frenula, apertural lappets and velarium that are seen in coeval micro fossils and extant cubozoans. Although *Hanagyroia orientalis* gen. et sp. nov. resembles extant coronate scyphozoans by its round medusa-like bell margin and equatorial groove, cladistic analysis suggests its close affinity with cubozoans. *Hanagyroia* may represent the intermediate morphological type between scyphozoans and cubozoans. The well-developed oral lips and paired short strong tentacles of *Hanagyroia* suggest a direct development.

Key words: Cnidarian, cubozoan, oral lip, Kuanchuanpu Formation, early Cambrian

1. Introduction

The *ca.* 3, 700 species of extant medusozoans (Daly et al., 2007) are grouped into four major classes (Staurozoa, Hydrozoa, Scyphozoa, and Cubozoa) that can be distinguished by the morphology and arrangement of various external and internal features (e.g. gonads, interradial canals, apertural lappets, tentacles, etc.) and their lifecycle.

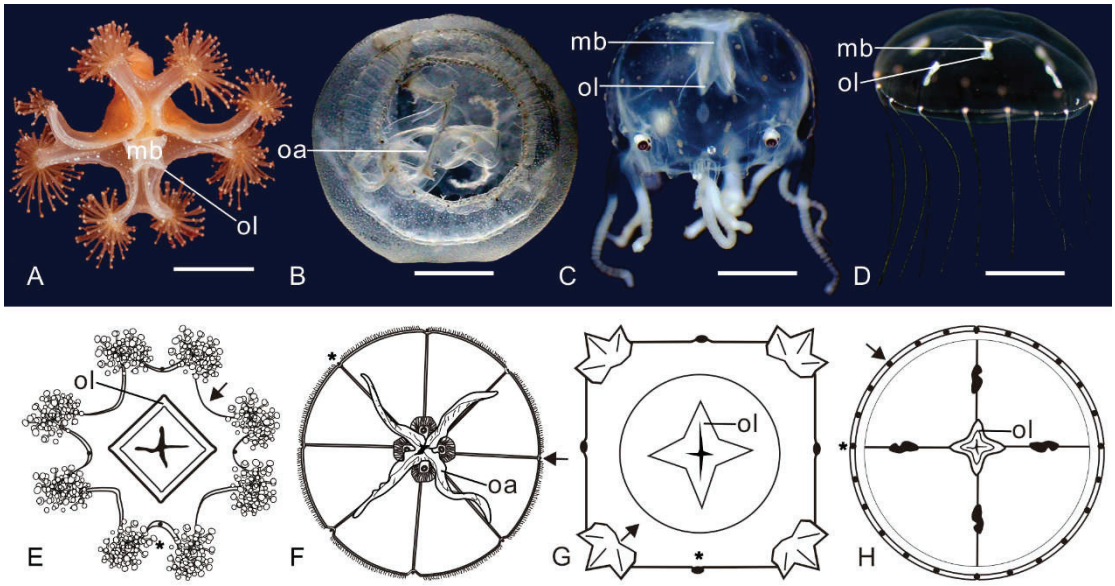

Fig. 1. Photographs and diagrams in oral view showing the tetraradial symmetry, oral lips and manubrium of typical extant medusae. A, E. Staurozoa exemplified by *Haliclystus.* B, F. Scyphozoa exemplified by *Aurelia aurita.* C, G. Cubozoa exemplified by *Tripedalia cystophora* Conant, 1898 (*Charybdeida*). D, H. Hydrozoa exemplified by *Clytia hemisphaerica.* Abbreviations: mb, manubrium; oa, oral arm; ol, oral lip; *, perradii; →, interradii. Scale bars: 5 mm in A, B; 2mm in C; 5mm in D. A, D. Courtesy of K. Telnes and T. Momose, respectively.

The bodyplan of most medusae is characterized by a tetraradial symmetry, also with exceptions (pentaradial symmetry seen in Burkenroad (1931) and Lin et al., (2013)), expressed by the extension of oral lips / arms, which are used traditionally to define the meridian planes of the medusozoans (Fig. 1; Conant, 1898; Haeckel, 1879; Hyman, 1940; Mayer, 1910; Meglitsch, 1967; Lesh Laurie and Suchy, 1991). But the substantial reason for this definition has never been mentioned.

The earliest known unambiguous jellyfish from the Chengjiang biota (*ca.* 520 Ma; Han et al., 2016c) and the jellyfish fossils documented from the middle Cambrian, Utah (Cartwright et al., 2007), which are preserved as impression fossils, and display a clear tetraradial symmetry. Phosphatized microfossils from the Kuanchuanpu Formation (*ca.* 535 Ma) often display exceptionally well-preserved three-dimensional external and internal features (Briggs et al., 1993; Xiao et al., 1998), that make it possible to study their external morphology and internal anatomy. Some tetra- or pentaradial symmetric embryos and juveniles were mostly interpreted as medusozoans (Dong et al., 2013; 2016; Han et al., 2013; 2016b; Liu et al., 2014; 2017; Wang et al., 2017; Zhang

et al., 2015; Steiner, et al., 2014). The fossil medusozoans are with many characteristic features of extant medusae (e.g. double-wall system, manubrium, interradial septa, claustra, gonad-lamellae) and have either a pentaradial or, more rarely, a tetraradial symmetry. Like in the extant medusozoans, their body is subdivided by meridian planes in interradial or perradial position. However, the existence of the manubrium and the tentacles of coeval micro fossils is still doubtful.

Here we describe a new pre-hatched pentamerous medusozoan fossil, *Hanagyroia orientalis* gen. et sp. nov. which had a whorl of five pairs of subumbrellar tentacles near the outermost margin of the bell-shaped body. Its equatorial groove is reminiscent of the coronal groove of coronate scyphozoans (Hyman, 1940; Russel, 1970; Mayer, 1910). More importantly, *Hanagyroia orientalis* gen. et sp. nov had a conspicuous manubrium and a large mouth fringed with well-developed oral lips in perradial position. In addition, *Hanagyroia* gives clues on better understanding the lifecycle and median orientation of the early Cambrian fossil medusozoans.

2. Material and method

Three specimens were collected from the Lower Cambrian Kuanchuanpu Formation at the Shizhonggou section, Ningqiang County, Shaanxi Province, China (Qian, 1977). Fossils were recovered by dissolution of limestone in a 10% acetic acid. Specimens were analyzed by the scanning electron microscopy (SEM) at Northwest University, China and the X-ray micro tomography (XTM) at Tohoku University, Japan. Thousands of images of virtual sections (Fig. 3, Appendix 2) through the specimen ELISN107-470 were acquired at a resolution of 1004 * 1004 pixels (XTM). XTM data were processed using V.G. Studio 2.2 Max in order to enhance contrast between key internal anatomical features by using artificial colours and to generate detailed three-dimensional reconstructions of the microscopic fossil (Figs. 3–4). Cladistic analysis was carried out using PAUP* v. 4.0 b10 (Swofford, 2003). The unweighted analysis of the data matrix (Appendix 3; Table 1) contain 22 groups and 105 unordered characters taken from Marques & Collins (2004), Dong et al. (2013), Van Iten et al. (2006), Han et

al. (2013; 2016c) and Wang et al. (2017). All specimens are deposited at the Early Life Institute, Northwest University, China.

3. Systematic Paleontology

Phylum Cnidaria Verrill, 1865

Subphylum Medusozoa Peterson, 1979

Class, Order uncertain

Family Olivooidae Steiner et al., 2014

Genus Hanagyroia nov.

Etymology: derived from *Hana*, flower in Japanese; *gyro*, literally 'turn' in Greek.

Diagnosis: Bell-shaped body divided into a wide oral unit and a low cone-shaped aboral unit separated by a deep equatorial groove. Deep and narrow subumbrellar cavity. Central flaring, large manubrium topped with a pentagon-shaped mouth with five perradial slit-like oral lips. Circular subumbrellar rim margined with a circle of five interradial pairs of short tentacular buds. No frenulae and velarium near by the bell margin. No apertrual lappets around the bell margin. Aboral end with five short round-cornered perradial ridges; oral end of each perradial ridge with a triangular cornice. Internally, five broad and stout interradial septa horizontally connected to form the claustra. Exumbrellar and subumbrellar walls fused together near the oral margin.

Remarks: The most striking differences between this new genus and other previously described medusozoans from the Kuanchuanpu Formation are the absence of the frenula, apertural lappets and velarium. The new genus has a conspicuous manubrium with well-developed oral lips and a narrow sunbumbrellar cavity which is surrounded by five paired stout tentacles. The oral lips of the three fossils are located on the perradii.

***Hanagyroia orientalis* gen. et sp. nov.**

(Fig. 2 A-C, Figs. 3-5; Appendices 1 C; 2; 5)

Etymology： *orientalis* refers to China, an oriental country, and Asia.

Diagnosis: As for genus.

Holotype: ELISN107-470; deposited at the Early Life Institute, Department of Geology, Northwest University, China.

Other material: ELISN66-15 and ELISN96-77 as paratype (see description below).

Occurrence: Lower Cambrian Kuanchuanpu Formation (equivalent to the Fortunian Stage of the Terreneuvian Series), Ningqiang, Shaanxi, China.

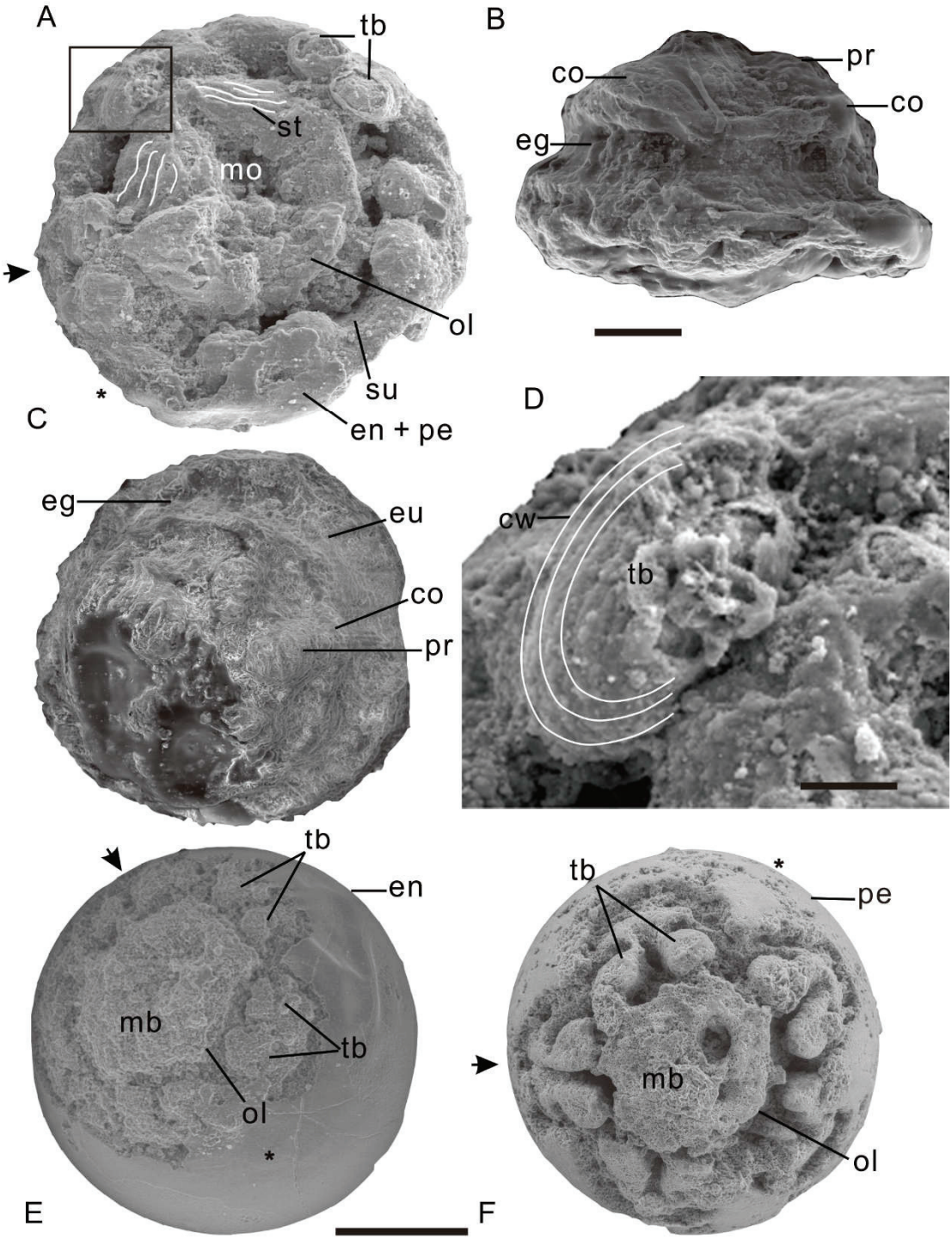

Fig. 2. Prehatched medusae from the Lower Cambrian Kuanchuanpu Formation, south China. A–D, *Hanagyroia orientalis* gen. et sp. nov., ELISN107-470, holotype. A. Oral view showing paired tentacular buds, and manubrium with perradial oral lips. B. Lateral view showing equatorial groove and triangular cornice. C. Aboral view showing perradial ridge. D. Detailed view (see rectangular area in A) showing the circular wrinkles on tentacular buds. E. ELISN96-77, oral view showing tentacles and manubrium with perradial oral lips (Appendix 1 A). F. ELISN66-15 (Appendix 1 B) oral view showing perradial oral lips. Abbreviations: co, cornice; cw, circular wrinkles; eg, equatorial groove; en, egg envelope; eu, exumbrella; mb, manubrium; mbc, manubrial cavity (esophagus); mo, mouth; ol, oral lip; pe, periderm; pr, perradial ridge; st, stripe; su, subumbrella; tb, tentacular bud. *, perradii; →, interradii. Scale bars: 200μm in E, F, 100μm in A–C, 25 μm in D.

4. Description and interpretation

H. orientalis gen. et sp. nov., as shown by the holotype specimen ELISN107-470, appears as a hat-shaped bell associated by a small vestigial egg envelope. The bell is *ca.* 450 μm wide and 300 μm high (Fig. 2 A-B). The low conical apical (aboral) region forms a five-folded pyramid that is delimited from the rest oral unit by a deep circumferential equatorial groove at the sub-middle height of the bell (Fig. 2 B-C). Micro-CT data reveal more detailed anatomic structures that are strictly arranged in a perfect pentamerous pattern (Figs 2-5; Appendices 1-2, 5).

Tentacles: The bell margin bears a circle of five pairs of short capitate projections of uniform size, *ca.* 50 μm in length and height and with an elliptic cross-section. (Figs. 2 A; 6 A-B). The projections in each pair are close to each other lo*ca*ting on the interradii. The surface of the projections bears fine circular wrinkles (cw) (Figs. 2 D; 6 A-B), indicating possible transverse muscular fibers. These projections are interpreted here as tentacle buds. Small lumens occur in each pair of tentacular buds, and are named here tentacular bud funnel (tbf, Figs. 3 G; 4 B).

Manubrium: The central area of the bell is occupied by a rather large, flaring-shaped structure, approximately three-fifth the diameter and height of the bell. It is interpreted here as manubrium (mb). Its distal opening, the mouth (mo), is rounded

in oral view and pentagon in cross section (Figs. 2 A, E-F; 4 A-D; Appendices 1-2, 4). The mouth bears five well-developed centripetal strips interpreted here as oral lips (ol) which direct inwardly to the mouth opening (Figs. 2 A; 3 H; 4 A, D; Appendices 1 C, 4). The strips are highly reminiscent of the oral lips of the medusa manubrium (Fig. 1). The surface of each strip are covered with 3-5 fine stripes (Fig. 2 A). The interradii of the median plane of the holotype specimen ELISN107-470 is defined by paired tentacles as the living medusozoans. And the oral lips of the specimen ELISN107-470 are located on the perradii, thus 72° offsetting in disposition from those of extant medusae in a case of pentaradial pattern (Fig. 1; Appendix 1 C). The manubrium is separated from the peripheral bell margin by a deep but narrow subumbrellar cavity (Figs. 2 A; 4 A-B, D).

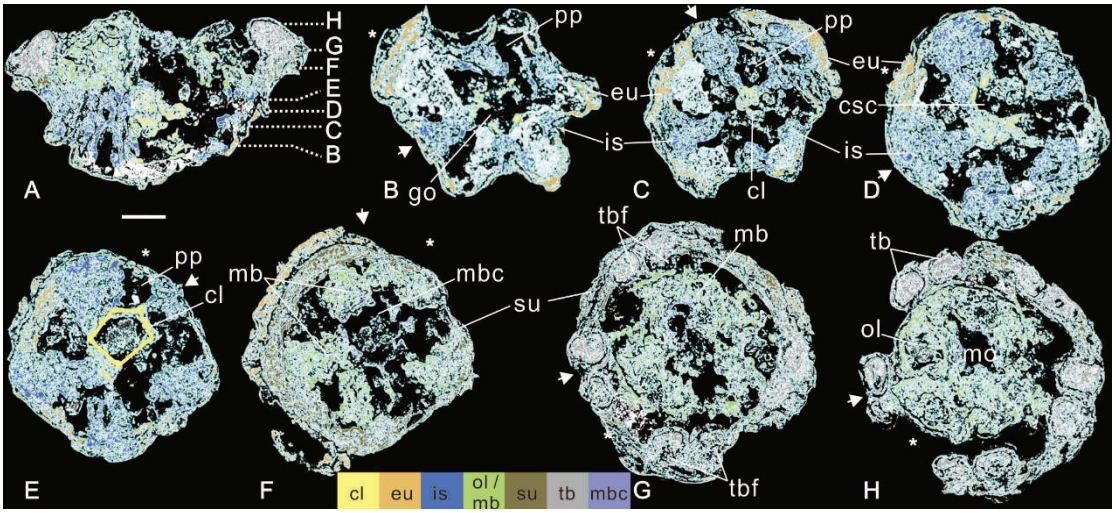

Fig. 3. *Hanagyroia orientalis* gen. et sp. nov. from the early Cambrian Kuanchuanpu Formation, south China; microtomographic sections through the holotype specimen (ELISN107-470). A. Lateral section through the manubrium of the holotype specimen (ELISN107-470), indicating the position of transverse sections B-H. B-H. Transverse sections perpendicular to the aboral-oral axis. Major external and internal structures represented by colours generated by VG Studio 2.2 MAX (colourless sections in Appendix 2). Abbreviations: cl, claustra (yellow pentagon in E); csc, central stomach cavity; eu, exumbrella; go, gastric ostium; is, interradial septum; mb, manubrium; mbc, manubrial cavity (esophagus); mo, mouth; ol, oral lip; pp, perradial pocket; su, subumbrella; tb, tentacular bud; tbf, tentacular bud funnel; *, perradii; →, interradii. Scale bar: 100 µm in A-H.

Aboral ridges and furrows: The aboral unit exhibits five evenly spaced and notably broadly arched perradial ridges (pr) which are intercalated by a series of five triangular concaved interradial depressions that are interpreted here as interradial furrows (if, Figs. 2 C; 4 C, F; 6 D; Appendix 5). The other end of each ridge ends as a prominent triangular cornice (co) above the equatorial groove (Fig. 2 B-C; 4 C; 6 C). The perradial ridges and interradial furrows form a corrugated external structure and converge towards the aboral apex (Figs. 4 C, F; 6 C-D; Appendix 5).

Interradial septa and claustra: The aboral end of *Hanagyroia orientalis* gen. et sp. nov.is pentagonal in transverse section (Fig. 3 B; Appendix 2 B) which has a central chamber and five uniform septal structures arising from the endodermic side of each interradial depression of the exumbrella, interpreted here as the central gastric cavity and interradial septa, respectively (Fig. 3 B-E). These septa, triangular in cross section near the gastric floor (Figs. 3 B-E; 4 D-E), direct inwardly and orally. Each interradial septum has an apparently expanded proximal end with an inner hollow cavity. These cavities are named the interradial septal funnels (isf, Figs. 4 E; 5).

At the level of the equatorial groove, the distal ends of the septa reach the central part of gastric cavity (csc, Figs. 4 E; 5), and subdivide it into five perradial pockets (pp, Fig. 3 B-E). More orally below this level, five vertical, axial walls (almost in perradial position) bridge the neighboring interradial septa (Figs. 3 C-E; 5), that are interpreted as the claustra (cl) which could partition the whole gastric cavity into the five perradial pockets and the central gastric cavity. Among the bridge of the claustra in perradii, there are several tiny funnels connecting the central stomach cavity to the perradial pockets, interpreted here as gastric ostia (go, Figs. 3 B; 5).

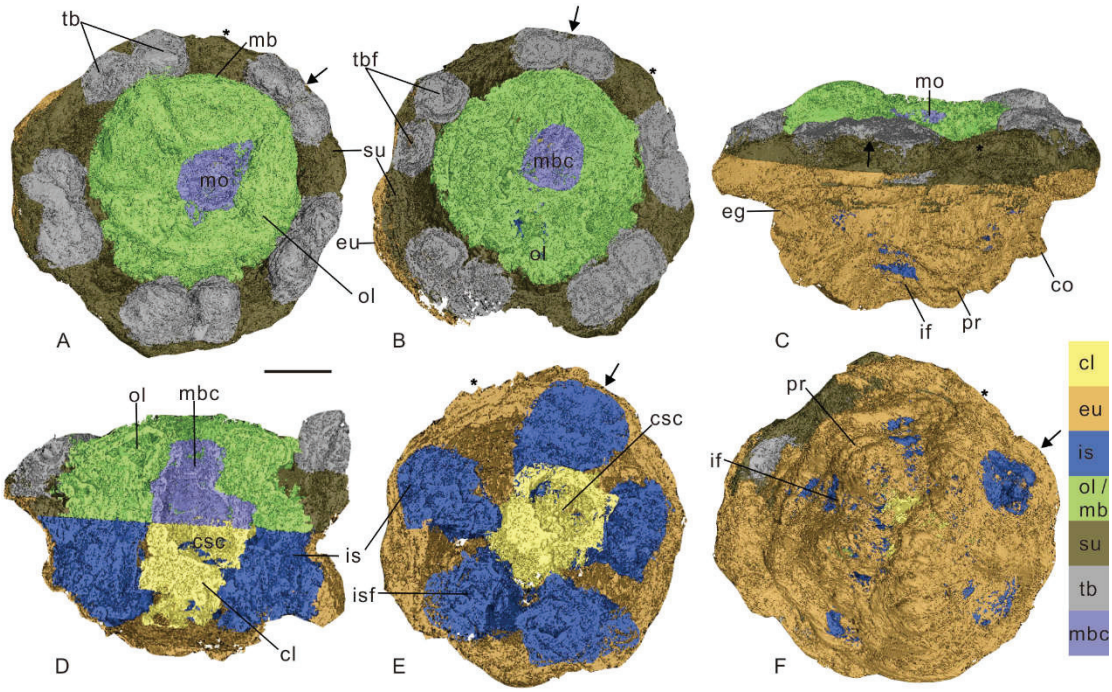

Fig. 4. *Hanagyroia orientalis* gen. et sp. nov. from the lower Cambrian Kuanchuangpu Formation, Shaanxi Province, China; holotype specimen (ELISN107-470), three-dimensional model generated by VG Studio 2.2 MAX. Colours indicate distinct anatomical structures. Abbreviations: cl, claustra; co, cornice; csc, central stomach cavity; eg, equatorial groove; eu, exumbrella; if, interradial furrow; is, interradial septum; isf, interradial septal funnel; mb, manubrium; mbc, manubrial cavity (esophagus); mo, mouth; ol, oral lip; pr, perradial radge; su, subumbrella; tb, tentacular bud; tbf, tentacular bud funnel; *, perradii; →, interradii. Scale bar: 100 µm in A-F.

Umbrellar fusion: The transverse outline of the exumbrella varies according to its position along the oral-aboral axis. Apically it appears as a five-pointed star (Figs. 3 B; 4 F; Appendices 2 B; 4); below the equatorial groove, it transforms into a round-cornered pentagon because of the thickening the interradial septa (Fig. 3 C-D; Appendix 2 C-D); orally the pentagon plumps into a circular structure representing the bell rim (Figs. 3 E-H; 4 A; Appendix 2 E-H). The body wall at the equatorial groove is thinner than anywhere else. The subumbrella (su), which is thinner than the exumbrella (eu), can be traced aborally deep into the equatorial groove (eg). Immediately below the equatorial groove, the subumbrella is separated from the exumbrellar wall by a narrow ring cleft between them at the one-third height of the bell (Figs. 3 F; 4 D; Appendix 2 F). More orally, the two umbrellar walls fuse together, making the interradial septa (is) disappear almost completely and reducing the subumbrellar cavity (Figs. 3 E-G; 4 E; 6 A-B; Appendices 2 E-G; 4).

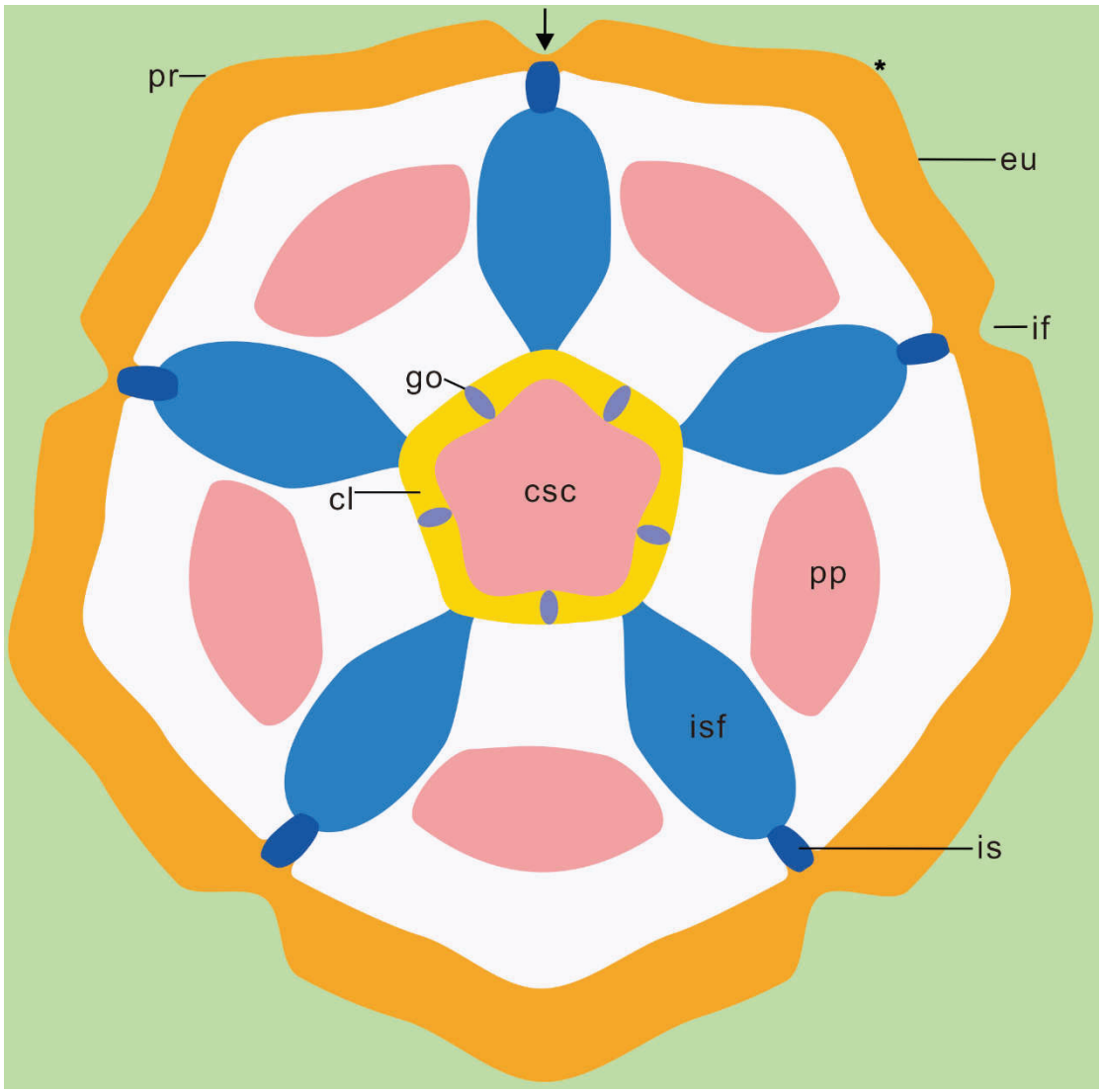

Fig. 5. Simplified transverse section through the middle part of the *Hanagyroia orientalis* gen. et sp. nov. from the lower Cambrian Kuanchuangpu Formation, Shaanxi Province, China. Abbreviations: cl, claustra; csc, central stomach cavity; eu, exumbrella; go, gastric ostium; if, interradial furrow; is interradial septum; isf, interradial septal funnel; pp, perradial pocket; pr, perradial ridge. *, perradii; →, interradii.

The paratype specimens (ELISN66-15 and ELISN96-77) have the same size. Both show a well-developed manubrium with lobed edges, surrounded by five paired stout tentacles that are smaller than those of the holotype, *ca.* 20-40 µm in length and height. A relatively thick periderm adheres to a thinner smooth layer interpreted as the egg membrane (Fig. 2 E-F).

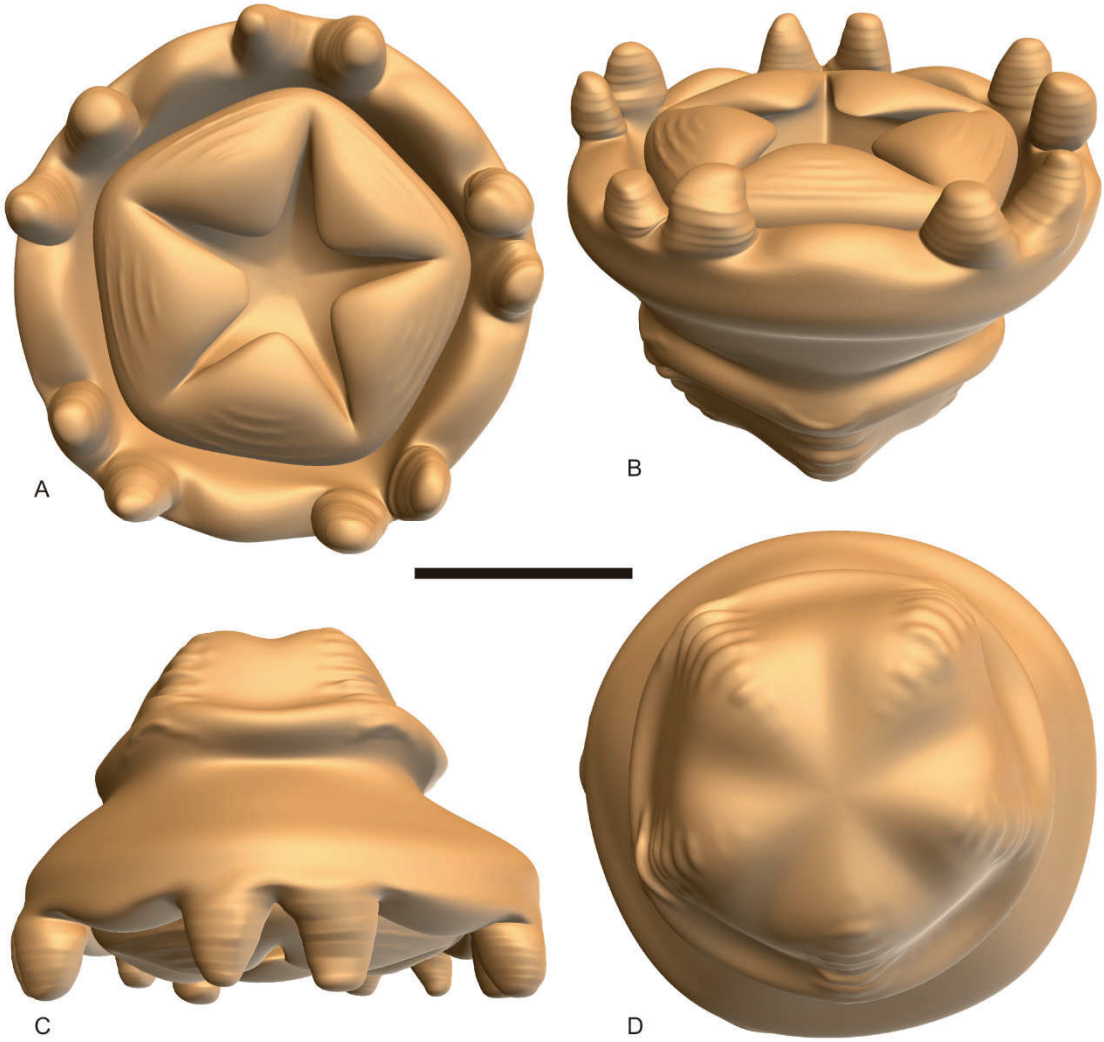

Fig. 6. Reconstructions of Hanagyroia orientalis gen. et sp. nov. from the lower Cambrian Kuanchuangpu Formation, Shaanxi Province, China. A. oral view. B-C. Lateral view. D. Aboral view. Artistic 3D reconstruction by Xi Liu, Northwest University, Xi'an, China. Scale bar: 150 μm (A-D).

5. Affinities of *Hanagyroia*

Hanagyroia can be confidently interpreted as a cnidarian based on its radial symmetry, two body layers and single body opening. Both tetraradial and pentaradial cnidarians (Han et al., 2013; 2016a; 2016b; Dong et al., 2013; 2016; Liu et al., 2014; 2016; Wang et al., 2017) are represented in the lower Cambrian Kuanchuanpu biota. Extant representatives of the medusozoans are overwhelmingly tetraradial and can easily be compared with their Cambrian counterparts. However, the assignment of *Hanagyroia* to any order of extant medusozoans is more difficult to establish. Hypotheses need to be tested.

Staurozoa option

H. orientalis gen. et sp. nov. strongly differs from extant stauromedusans (Hyman, 1940; Miranda et al., 2016) in having a fusion of sub- and exumbrella, a coronal (equatorial) groove, a large manubrium, but lack any sign of secondary tentacle clusters. However, *H. orientalis* gen. et sp. nov. has a claustra comparable with that of living staurozoans (Miranda et al., 2017). This feature has the function to partition the gastric cavity into the central stomach cavity and the perradial pockets (Berrill, 1963). This would indicate that the claustra may have evolved independently in each order of extant medusozoans possibly for improving digestion efficiency.

Hydrozoa option

In extant hydrozoans (e. g. *Clytia hemisphaerica*, Houliston et al., 2010), the radial canals are usually reduced or weakly developed. In contrast, the interradial septa of *H. orientalis* gen. et sp. nov. are well-developed and have a triangular shape. Moreover diagnostic features of hydrozoans such as the frenula, marginal lappets and velum (Thiel, 1966), cannot be found in *H. orientalis* gen. et sp. nov. The hydrozoan hypothesis can be rejected on the basis of these major differences.

Scyphozoa and Cubozoa options

Typical scyphozoan features such as clear interradial septa, round medusa bell margin, exumbrella, subumbrella, oral lips occur in *Hanagyroia* (Hyman, 1940). Scyphozoa includes three Orders: Semaeostomeae, Rhizostomeae and Coronatae (Daly et al., 2007). However, *H. orientalis* gen. et sp. nov. lacks rhopalia, ring canals, and developed folded oral arms which characterize extant semaeostomes (e.g. *Aurelia aurita* in Fig. 1 B, F). Rhizostomes and semaeostomes have the same overall morphology, except that they bear distinctive marginal tentacles and a large manubrium with numerous tiny sucker (Mayer, 1910). By contrast with *Hanagyroia orientalis* gen. et sp. nov., extant rhizostomes lack interradial furrows and perradial ridges and possess well-developed oral lips. Accordingly *H. orientalis* gen. et sp. nov. could be hardly placed into Semaeostomeae or Rizostomeae. *Hanagyroia* is reminiscent of extant coronates in

that its conspicuous equatorial (coronal) groove which separates the medusa bell into two parts. However, the apertural lappets and coronate-type pedalia which are diagnostic characters in extant coronates (Marques and Collins, 2004), could not be seen in *Hanagyroia*.

Hanagyroia also shows traits reminiscent of extant cubozoans. Its primary paired tentacles, which are located on interradii and directed inward to the medusa bell without the second tentacular clusters, are exclusively found in extant cubozoans (e.g. *Tripedalia cystophora*, that have only one tentacle per pedalium (Coates et al., 2006; Werner et al., 1971). The claustra of *Hanagyroia* obviously plays the role on partitioning the gastric cavity into the central gastric cavity and the five perradial pockets as those in extant medusozoans. It may strengthen medusa digestion by increasing the surface of gastric cavities. However, the marked anatomical characters of the extant cubozoans, such as the frenula, the velarium and the pedalia (Conant, 1898) could not be seen in *Hanagyroia*.

6. Phylogeny

To clarify the phylogenetic placement of H. orientalis in the total-group medusozoans, we carried out a preliminary cladistic analysis on the basis of 22 taxa and 104 characters by using PAUP* 4.0 b10 (Fig. 7; Appendices 3-4; Table 1). The data matrix is combined with the previous works (Dong et al., 2016; Han et al., 2013; 2016a; Margue and Collins, 2004; Van Iten et al., 2006; Wang et al., 2017). A total of 104 characters have equal weight, with 9 of them constant, 28 variable characters parsimony-uninformative, and 67 characters parsimony-informative. One strict consensus tree is acquired, with tree length (TL) = 90, consistency index (CI) = 0.8484, and rescaled consistency index (RC) = 0.7618.

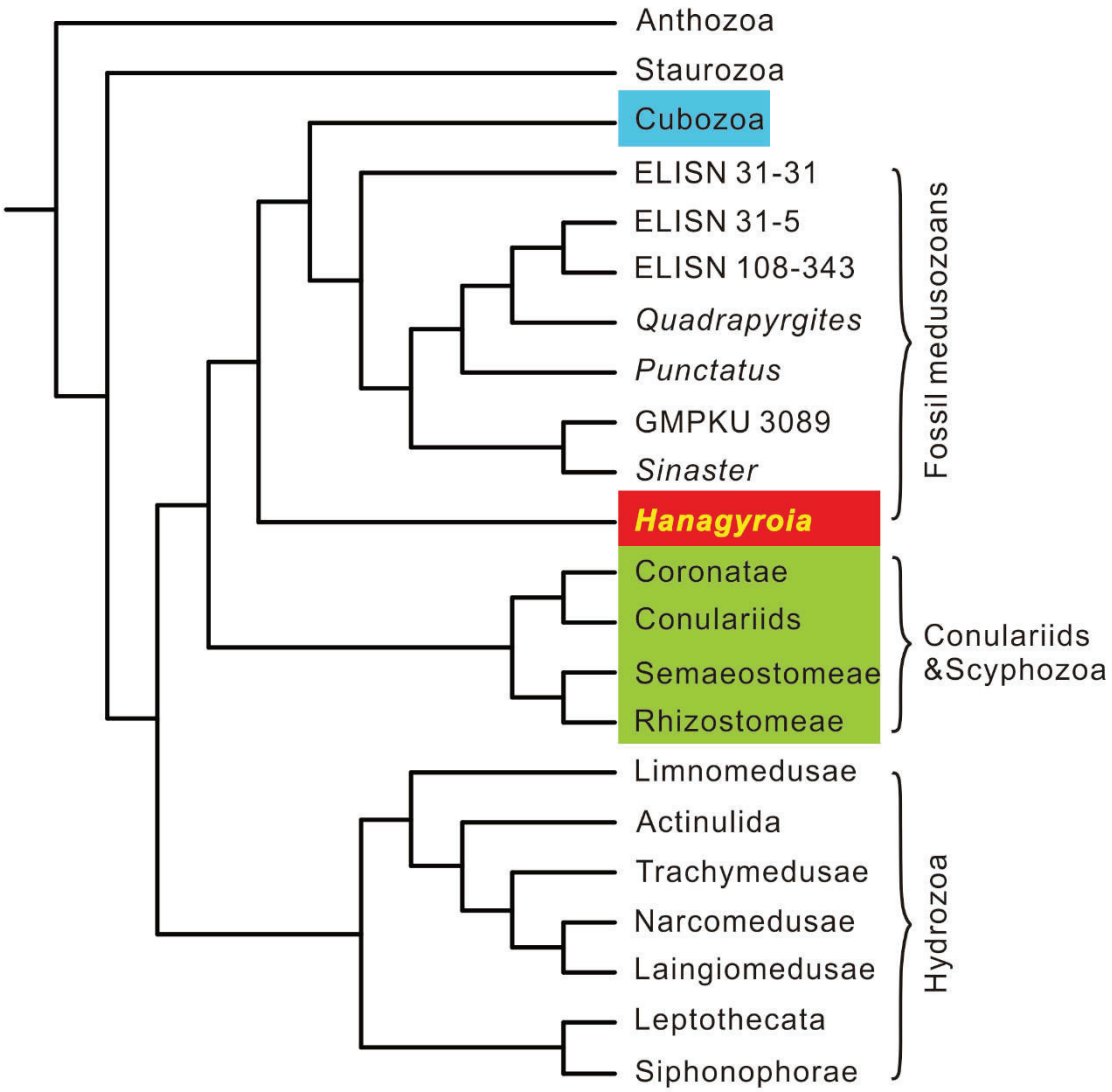

Fig. 7. Strict consensus tree of cnidarians using PAUP* 4.0 b10. ELISN31-5, ELISN108-343, GMPKU3089 are in uncertain taxonomy in Han et al. (2013; 2016b), Dong et al. (2013) and *Sinaster* was from Wang et al. (2017) respectively. The co-occurring *Quadrapyrgites* and *Punctatus* were also found in the Kuanchuanpu Formation.

Our cladistic results (Fig. 7) are largely consistent with the phylogenies obtained by previous authors (Van Iten et al., 2006; Marques et al., 2004; Collins et al., 2006). A monophyletic group with *H. orientalis* gen. et sp. nov., extant cubozoans, as well as a sub-clade with *H. orientalis* gen. et sp. nov. and other coeval fossil medusozoans are well supported. Hence, *H. orientalis* gen. et sp. nov. is more closely related to cubozoans than to hydrozoans. The placement of *Hanagyroia* in the stem group of Cubozoa is supported by our cladistic analysis although its remarkable equatorial

groove suggests affinities with coronate scyphozoans.

7. Development

H. orientalis gen. et sp. nov. has a sperical shape and smooth periderm that are comparable with *Olivooides* which was named by its olive-shaped gross morphology (Qian, 1977). However, the taxonomy of *Olivooides* still remain in controversial. The developmental lifecycle of *Olivooides*-like fossil medusozoans was first depicted by Bengtson and Yue (1997), and was further described in other previous work to confirm its direct development (Han et al., 2013; Steiner et al., 2014).

The three specimens discussed herein can supply the sequence of the developmental lifecycle of *H. orientalis* gen. et sp. nov. The paratype specimens (ELISN96-77 and ELISN66-15) and holotype specimen (ELISN107-470) may represent three developmental stages respectively (Appendix 1). The complete periderm adhering to the egg membrane of the specimen ELISN96-77 could be assumed to be the pre-hatching stage. A series of anatomical characters of the holotype specimen (ELISN107-470) may indicate its hatching stage, including (1) comparatively large size, (2) a conspicuous lobed manubrium with an opened mouth opening, (3) well-developed oral lips located in perradii and (4) paired short but strong tentacles locating in interradii. The rest paratype specimen (ELISN66-15) may be intermediator. These three fossils are *ca.* 450-500 μm wide and 300-350 μm high that may indicate their directly lecithotrophic development which is comparable with extant medusozoans (Berrill, 1949; Han et al., 2013). The large mouth opening indubitably indicates that *H. orientalis* gen. et sp. nov. could feed once hatched. The well-developed oral lips in the conspicuous manubrium and retractile tentacles may give a clue on its carnivores nature.

8. Conclusion

H. orientalis gen. et sp. nov. supplies considerable anatomical variations compared with coeval fossil medusozoans from the Kuanchuanpu biota and extant medusozoans. *Hanagyroia* provides sufficient evidence for the presence of a conspicuous

manubrium and paired tentacles in the fossil medusozoans from the Kuanchuanpu Formation. Although *Hanagyroia* resembles coronate scyphozoans (e.g. the equatorial groove), our cladistic analysis based on morphological characters suggests an affinity with cubozoans. Our available material of this early Cambrian medusozoan suggests a sequence of direct development, which somehow enlightens the evolution of ontogeny in coeval fossil medusozoans.

Authors' contributions

JH designed the research; XW, JH and JV interpreted the fossil material; KU, OS and TK conducted the synchrotron and micro-CT. XW reconstructed the micro-CT analyses. XW, JH, JV and QO wrote the paper with input from the other authors. All authors read and approved the final manuscript.

Competing interests statement

The authors have no competing interests to declare.

Acknowledgments

This work was supported by Natural Science Foundation of China (Nos. 41621003, 41772010, 41572017, 41672009, 41720104002), the "111 project" of Ministry of Education of China (No. D17013) and the Most Special Fund from the State Key Laboratory of Continental Dynamics, Northwest University, China (BJ11060). We thank H. Van Iten (Department of Geology, Hanover College, Indiana) for correcting and improving our manuscript. We also thank H.J. Gong, X. Liu, J. Sun and M.R. Cheng (State Key Laboratory for Continental Dynamics, Northwest University, Xi'an, China) for their assistance in both field and lab work.

References

Bengtson, S., Yue, Z., 1997. Fossilized Metazoan embryos from the earliest Cambrian. Science, 277, 1645–1648. doi: 10.1126/science.277.5332.1645

Berrill, M., 1963. Comparative functional morphology of the Stauromedusae. Canadian Journal of Zoology, 41, 741–752. doi.org/10.1139/z63-046

Berrill, N.J., 1949. Developmental analysis of Scyphomedusae. Biological Reviews, 24, 393–409. https://doi.org/10.1111/j.1469-185X.1949.tb00581.x

Briggs, D.E.G., Kear, A.J., Martill, D.M. and Wilby, P.R., 1993. Phosphatization of soft-tissue in experiments and fossils. Journal of the Geological Society, 150, 1035–1038. https://doi.org/10.1144/gsjgs.150.6.1035

Brusca, R.C. and Brusca G.J., 2003. Invertebrates. 2nd edition. Sinauer Associates, Sunderland, MA. 936 pp.

Burkenroad, M.D., 1931. A new pentamerous Hydromedusa from the Tortugas. The Biological Bulletin, 61, 115–119. https://doi.org/10.2307/1537049

Cartwright, P., Halgedahl, S.L., Hendricks, J.R., Jarrard, R.D., Marques, A.C., Collins, A.G. and Lieberman, B.S., 2007. Exceptionally preserved jellyfishes from the Middle Cambrian. PLoS One, 2, e1121. https://doi.org/10.1371/journal.pone.0001121

Coates, M.M., Garm, A., Theobald, J.C., Thompson, S.H. and Nilsson, D., 2006. The spectral sensitivity of the lens eyes of a box jellyfish, *Tripedalia cystophora* (Conant). The Journal of Experimental Biology, 209, 3758–3765. doi: 10.1242/jeb.02431

Collins, A.G., Schuchert, P., Marques, A.C., Jankowski, T., Medina, M. and Schierwater, B., 2006. Medusozoan phylogeny and character evolution clarified by new large and small subunit rDNA data and an assessment of the utility of phylogenetic mixture models. Systematic Biology, 55, 97–115. doi: 10.1080/10635150500433615

Conant, F.S., 1898. The Cubomedusae: a memorial volume. Johns Hopkins Press, Baltimore. https://doi.org/10.5962/bhl. title.1736

Daly, M., Brugler, M., Cartwright, P., Collins, A., Dawson, M., Fautin, D., France, S., McFadden, C., Opresko, D. and Rodrigues, E., 2007. The phylum Cnidaria: a review of phylogenetic patterns and diversity 300 years after Linnaeus. Zootaxa, 1668, 127–182. doi: http://dx.doi.org/10.11646/zootaxa.1668.1.11

Dong, X.P., Cunningham, J.A., Bengtson, B., Thomas, C.W., Liu, J., Stampanoni, M. and Donoghue, P.C.J., 2013. Embryos, polyps and medusae of the Early Cambrian scyphozoan *Olivooides*. Proceedings of the Royal Society B, 280, 20130071. doi: 10.1098/rspb.2013.0071

— Vargas, K., Cunningham, J.A., Zhang, H.Q., Liu, T., Chen, F., Liu, J., Bengtson, S. and Donoghue, P.C.J., 2016. Developmental biology of the early Cambrian cnidarian *Olivooides*. Palaeontology, 49, 387–407. https://doi.org/10.1111/pala.12231

Gershwin, L., 1999. Clonal and population variation in jellyfish symmetry. Journal of the Marine Biological Association of the United Kingdom, 79 (6), 993–1000. doi: 10.1017/S0025315499001228

Haeckel, E., 1879. Das system der medusen: erster theil einer monographie der medusen. , vol. 1: G. Fischer.

Han, J., Kubota, S., Li, G.X., Yao, X.Y., Shu, D.G., Li, Y., Kinoshita, S., Sasaki, O., Komiya, T. and Yan, G. 2013. Early Cambrian pentamerous cubozoan embryos from South China. PLoS One, 8, e70741. https://doi.org/10.1371/journal.pone.0070741

— — — Ou, Q., Wang, X., Yao, X. Y., Shu, D., Li, Y., Uesugi, K., Hoshino, M., Sasaki, O., Kano, H. and Sato, T., 2016a. Divergent evolution of medusozoan symmetric patterns: evidence from the microanatomy of Cambrian tetramerous cubozoans from South China. Gondwana Research, 31, 150–163. https://doi.org/10.1016/j.gr.2015.01.003

— — — — Toshino, S., Wang, X., Yang, X.G., Uesugi, K., Masato, H., Sasaki, O., Kano, H., Sato, T. and Komiya, T., 2016b. Internal microanatomy and zoological affinity of the Early Cambrian *Olivooides*. Acta Geologica Sinica (English Edition), 90 (1), 38–65. https://doi.org/10.1111/1755-6724.12641

— Hu, S.X., Cartright, P., Zhao, F.C., Ou, Q., Kubota, S., Wang, X. and Yang, X.G., 2016c. The earliest pelagic jellyfish with rhopalia from Cambrian Chengjiang

Lagerstätte. Palaeogeography, Palaeoclimatology, Palaeoecology, 449, 166–173. https://doi.org/10.1016/j.palaeo.2016.02.025

Houliston, E., Momose, T. and Manuel, M., 2010. *Clytia hemisphaerica*: a jellyfish cousin joins the laboratory. Trends in Genetic, 26 (4), 159–167. doi:10.1016/j.tig.2010.01.008

Hyman, L.H., 1940. The invertebrates. McGraw Hill, 726 pp.

Lesh-Laurie, G.E. and Suchy, P.E., 1991. Cnidaria: Scyphozoa and Cubozoa. In: Microscopic Anatomy of the Invertebrates, Vol. 2. Harrison FW & Westfall JA, eds. Wiley-Liss, New York, 185-266.

Lin, M., Xu, Z.Z., Huang, J.Q., Guo, D.H.,Wang, C.G., Xiang, P. and Dirhamsyah, 2013. Two new species of Leptomedusae from the Bitung Strait, Indonesia (Cnidaria). Acta Zootaxonomica Sinica, 38 (4), 756–761.

Liu, Y.H., Li, Y., Shao, T.Q., Zhang, H.Q., Wang, Q., and Qiao, J.P., 2014. *Quadrapyrgites* from the lower Cambrian of South China: growth pattern, post-embryonic development, and affinity. Chinese Science Bulletin, 59 (31), 4086–4095. doi:10.1007/s11434-014-0481-5

— Shao, T.Q., Zhang, H.Q., Wang, Q., Zhang, Y.N., Chen, C., Liang, Y.C., and Xue, J.Q., 2017. A new scyphozoan from the Cambrian Fortunian Stage of South China. Palaeontology, 60 (4), 511–518. doi: 10.1111/pala.12306

Margues, A.C. and Collins, A.G., 2004. Cladistic analysis of Medusozoa and cnidarian evolution. Invertebrate Biology, 123, 23–42. https://doi.org/10.1111/j.1744-7410.2004.tb00139.x

Mayer, A.G., 1910. Medusae of the world: the Scyphomedusae, Volume III. Carnegie Institution of Washington, Washington.

Meglitsch, P.A., 1967. Invertebrate zoology. Oxford Univ. Press, New York, 961 pp.

Miranda, L.S., Hirano, Y.M., Mills, C.E., Falconer, A., Fenwick, D., Marques, A.C. and Collins, A.G., 2016. Systematics of stalked jellyfishes (Cnidaria: Staurozoa). PeerJ, 4, e1951. doi: 10.7717/peerj.1951

— García-Rodríguez, J., Collins, A.G., André C. Morandini, A. C. and Marques, A.C., 2017. Evolution of the claustrum in Cnidaria: comparative anatomy reveals that it is exclusive to some species of Staurozoa and absent in Cubozoa. Organisms Diversity & Evolution, 17 (4), 753–766. https://doi.org/10.1007/s13127-017-0342-6

Qian, Y., 1977. Hyolitha and some problematica from the Lower Cambrain Meishucun Stage in central and S. W. China. Acta Palaeontologica Sinica, 16, 255–275.

Russell, F.S., 1970. The Medusae of the British Isles. 2. Pelagic Scyphozoa with a supplement to the first volume on Hydromedusae. Cambridge University Press.

Steiner, M., Qian, Y., Li, G.X., Hagadorn, J.W. and Zhu, M.Y., 2014. The developmental cycles of early Cambrian Olivooidae fam. nov. (?Cycloneuralia) from the Yangtze Platform (China). Palaeogeography, Palaeoclimatology, Palaeoecology, 398, 97–124. https://doi.org/10.1016/j.palaeo.2013.08.016

Swofford, D.L., 2003. PAUP*. Phylogenetic Analysis Using Parsimony (and other methods), v. 4. Sinauer Associates, Sunderland, MA.

Thiel, H., 1966. The evolution of the Scyphozoa, a review. In: Rees, W.J. (Ed), Cnidaria and their Evolution. Academic Press, London, 77–117.

Van Iten, H., Leme, J.M., Simoes, M.G., Marques, A. and Collins, A.G., 2006. Reassessment of the phylogenetic position of conulariids in the subphylum Medusozoa (phylum Cnidaria). Journal of Systematic Palaeontology, 4, 109–118. https://doi.org/10.1017/S1477201905001793

Verrill, A.E., 1865. Classification of polyps (extract condensed from Synopsis of the Polyps and Corals of the North Pacific Exploring Expedition under Commodore C. Ringgold and Captain John Rodgers, U.S.N.). Communications of the Essex Institute, 4, 145–152.

Wang, X., Han, J., Vannier, J., Ou, Q., Yang, X.G., Uesugi, K., Sasaki, O. and Komiya, T., 2017. Anatomy and affinities of a new 535-million-year-old medusozoan from

the Kuanchuanpu Formation, South China. Palaeontology, 60 (6), 853–867. doi: 10.1111/pala.12320

Werner, B., Cutress, C.E. and Studebaker, J.P., 1971. Life cycle of *Tripedalia cystophora* Conant (Cubomedusae). Nature, 232, 582–583. doi:10.1038/232582a0

Xiao, S.H., Zhang, Y. and Knoll, A.H., 1998. Three-dimensional preservation of algae and animal embryos in a Neoproterozoic phosphorite. Nature, 391, 553–558. doi:10.1038/35318

Zhang, H.Q., Xiao, S.H., Liu, Y.H., Yuan, X.L., Wan, B., Muscente, A.D., Shao, T.Q., Gong, H. and Cao, G., 2015. Armored kinorhynch-like scalidophoran animals from the early Cambrian. Scientific Reports, 5, 16521. doi:10.1038/srep16521

Chapter 6: Discussions

Chapter 6: Discussions

6.1 Affinities of *Olivooides* and related forms with a radial symmetry

At least three different hypotheses regarding the affinities of *Olivooides* and its related forms need to be discussed and tested in light of current knowledge.

6.1.1 The echinoderm hypothesis

The pentamerous symmetry of *Olivooides* makes us immediately think of echinoderms. However, the development of extant echinoderms starts with a bilaterally symmetrical embryo and larva (Lowe and Wray 1997) (Fig. 72). When fully developed, the larvae undergo metamorphosis (loss of gut and larval arms). At that stage, the right and left sides of the larva become the aboral and oral area, respectively. The bilateral symmetry disappears giving rise to a radial pentamerous symmetry (Mooi and David 2008, David and Mooi 2014). *Olivooides* has no comparable development and displays a pentaradial symmetry from its earliest embryonic stages onwards. Moreover, there is no evidence, in *Olivooides*, of a water cycling system and a calcareous endoskeleton that characterize echinoderms. The echinoderm hypothesis seems implausible to us and should be rejected.

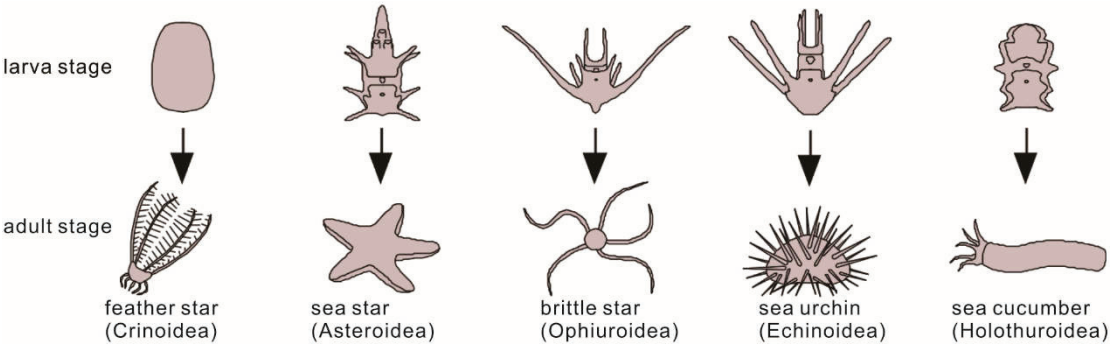

Fig. 72. Body symmetry in both larva and adult stage of extant echinoderms. Modified from Lowe and Wray, 1997.

6.1.2 The scalidophoran hypothesis

Steiner et al. (2014) suggested that *Olivooides* / *Punctatus* may represent the larval stages of scalidophoran worms because of its pentamerous body symmetry and its tube-like feature (post hatching stage of *Olivooides*) recalling the protective outer case (lorica) secreted by loriciferans. Extant scalidophorans are marine pseudocoelomate protostomes that were proposed on morphological grounds to unite three phyla: the Kinorhyncha, the Priapulida and the Loricifera, which are worm-shaped bodies with

the anterior proboscis or introvert (Telford et al. 2008). Scalidophorans moult their chitinous cuticle and have rings of cuticular spiny outgrowths (scalids) on their introvert (Wennberg, Janssen and Budd 2009). Undoubted fossil representatives of Scalidophora have been reported in the Cambrian (e.g. *Eolorica deadwoodensis* (Harvey, Butterfield and evolution 2017), *Ottoia guizhouensis* (Yang, Zhao and Zhang 2016) *Ottoia* (Vannier 2012), *Markuelia* (Dong 2007)), including the Kuanchuanpu biota (*Eopriapulites sphinx*, (Liu et al. 2014c)).

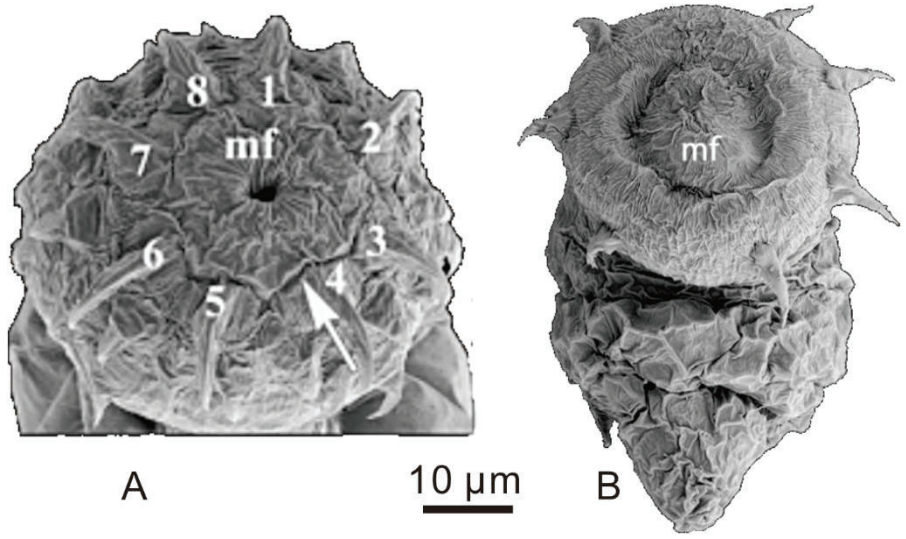

Fig. 73. Scalid pattern and morphology of hatching larvae of priapulids. A. *Priapulus caudatus*, apical anterior with eight first-ring scalids; the arrow points to the connection field between mouth field (mf) and the scalid area. B. *Halicryptus spinulosus* with everted introvert bearing a ring of scalids around the mouth field (mf). A from (Wennberg et al. 2009); B from Janssen et al. 2009.

The scalidophoran contains several flaws: 1) modern scalidophorans such as priapulids and their assumed early Cambrian ancestors (e.g. those from the Chengjiang and Burgess Shale biota); see (Huang, Vannier and Chen 2004, Vannier 2012) are bilaterians with an anterior-posterior polarity and a ventral cord (Nielsen 2012, Adrianov and Malakhov 2001). No such bilateral symmetry is found in *Olivooides* which has either a pentaradial or tetraradial symmetry (Dong et al. 2013, Han et al. 2013, Han et al. 2016b) well expressed in its oral region. *Olivooides* has a primary pentamerous symmetry whereas it is secondarily acquired in priapulid worms (Dong et al. 2016). The most evident and major difference with scalidophorans is that *Olivooides* lacks a through gut and has no introvert bearing scalids (Han et al. 2013, Dong et al. 2016, Wennberg et al. 2009, Janssen, Wennberg and Budd 2009) (Fig. 73). Larval stages of *Priapulus caudatus* and *Halicryptus spinulosus* are crowned with a swollen ring armed with well-developed hook-like scalids (Fig. 73). No such scalids occur around the mouth of *Olivooides*. *Eopriapulites sphinx* Liu et al. (2014c) co-occurs with *Olivooides* embryos in the Kuanchuanpu Formation and is the oldest known

scalidophoran worm. It has a cylindrical body with 18 longitudinal rows of scalids (Ruppert, Barnes and Fox 2004, Liu et al. 2014c). No such cuticular outgrowths are found in any developmental stage of *Olivooides* / *Punctatus*. There is therefore every reason to reject the scalidophoran hypothesis.

6.1.3 The cnidarian hypothesis

This hypothesis is supported by the following arguments: 1) *Olivooides* / *Punctatus* consists of two body layers (exumbrella and subumbrella) (Han et al. 2013, Wang et al. 2017) which are connected by interradial septa comparable with those of extant medusozoans (Hyman 1940);
2) These fossils have a single opening (mouth) with no through gut connecting the mouth to the anus, both in embryonic and more advanced stages (Han et al. 2013, Dong et al. 2016);
3) Paired features recalling tentacular buds occur in *Olivooides* fossils, which can be best compared with equivalent features in extant cubozoans (Han et al. 2013, Wang et al. 2017);
4) Specialized features comparable with the velarium and frenula of extant cubozoans (e.g. *Meteorona kishinouyei* see in (Toshino, Miyake and Shibata 2015)) occur in *Olivooides*-like forms such as *Sinaster* (Wang et al. 2017). Detailed descriptions these features are given in
Chapter 5.4.

6.1.4 The atypical pentaradial symmetry of *Olivooides* and its related forms

1) The vast majority of modern medusozoans are characterized by a tetradial symmetry, although several exceptions are worth being noted here. For example, *Eirene pentanemalis* is a hydrozoan (Leptomedusae, Eirenidae, (Lin et al. 2013)) with a remarkable pentamerous symmetry exemplified by five radial canals, five gonads near the middle part of the radial canals and five lip-like features around the mouth (Fig. 74).

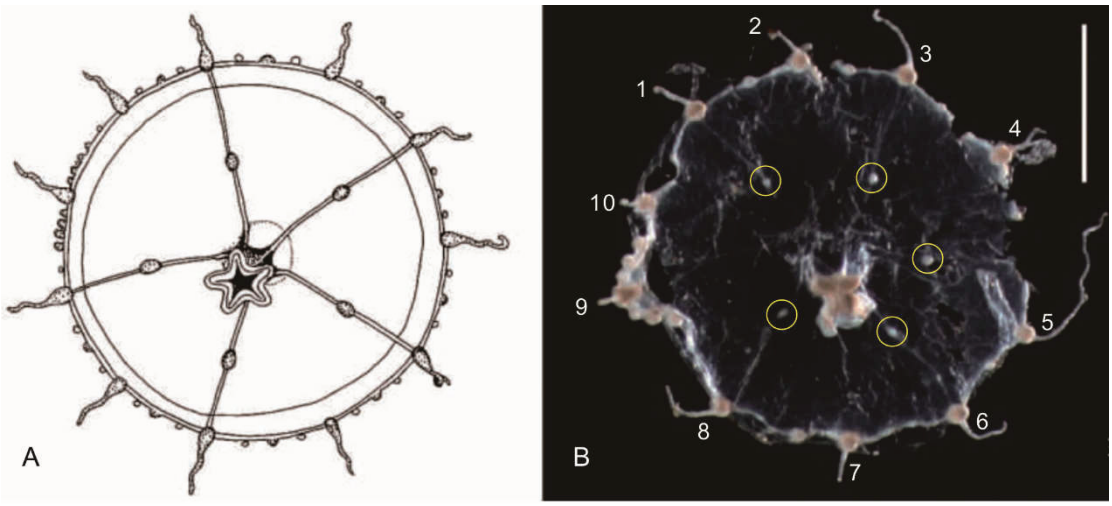

Fig. 74. The pentamerous hydrozoan, *Eirene pentanemalis* Lin et al. (2013), from Indonesia. A. Reconstruction. B. Specimen showing ten tentacles (N. 1-10) surrounding the bell margin. Yellow circles indicate tiny ovoid-shaped gonads. Scale bar: 1 mm. Modified from Lin et al., 2013.

As most scyphozoans, *Aurelia* reproduces asexually via a polypoid form (scyphostoma) by repeated transverse fission which generates and eventually releases immature medusae called ephyrae. Ephyrae have a very small size and are characterized by an incised bell margin, radial arms or primary tentacles with a radial configuration. Although most scyphozoan ephyrae are tetramerous, other symmetry patterns have been reported in *Aurelia* (Gershwin 1999) (Fig. 75). Thus, a single polyp can generate tri, tetra, penta, or hexaradial ephyrae which conserve their respective symmetry pattern as they develop into free-swimming medusae (see gonad arrangement; Fig. 75).

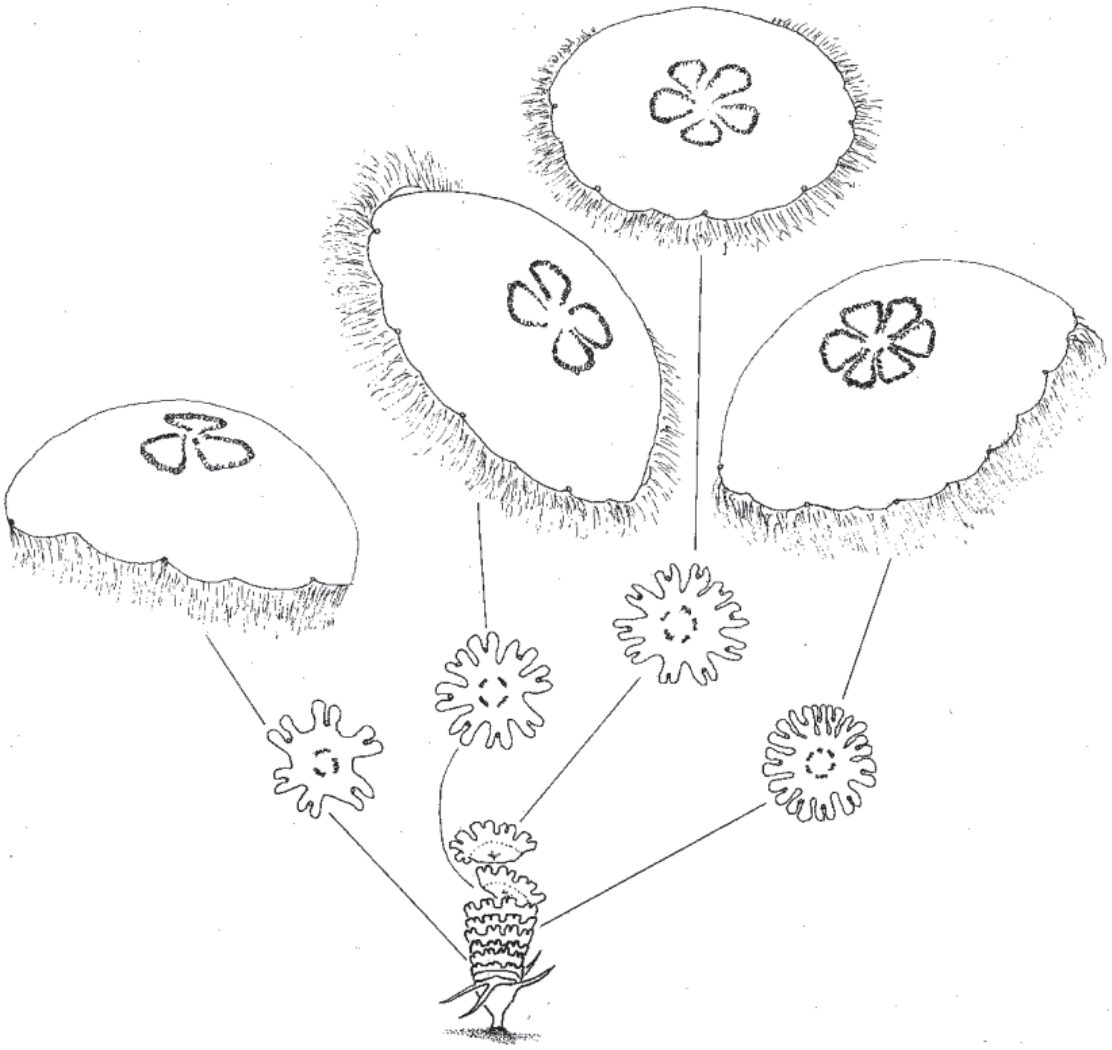

Fig. 75. Diagram showing various symmetry patterns in the ephyrae of *Aurelia* produced during a single strobilation. From Gershwin, 1999.

The symmetric variation happens frequently, even in one lineage, however, the factors that trigger these variations are not well constrained. They may have a genetic, environmental or developmental origin (Gershwin 1999).

2) No fossil jellyfish from the early Cambrian Chengjiang biota (*ca.* 521 Ma) (Han et al. 2016a) and middle Cambrian Marjum Formation of Utah (*ca.* 505 Ma) (Cartwright et al. 2007) show indication of a pentaradial symmetry. Instead these remarkably preserved fossils exhibit consistent tetramerous morphological features (e.g. the four radial canals and the tentacles equaling to multiple 4).

3) It has often been argued that *Olivooides* and its related forms could hardly be considered as cnidarians because of their atypical pentaradial symmetry (Han et al. 2013, Han et al. 2016b, Dong et al. 2013, Dong et al. 2016, Wang et al. 2017). Although tetraradial symmetry is indeed prevalent among modern cnidarians and their early and middle Cambrian ancestors, a variety of symmetry patterns seems to have co-existed in the early stages of the evolution of medusozoans, exemplified by co-occurring

pentaradial and tetraradial cnidarian embryos from the Kuanchuanpu biota (Han et al. 2016b) (Fig. 49). We hypothesize here that the tetraradial symmetry has become prevalent in a relatively early stage of the cnidarian evolution (early Cambrian) but co-existed with other symmetry modes in the lowermost Cambrian (e.g. pentaradial). The problem remains how and why the pentaradial symmetry disappeared for the benefit of the tetraradial one. Tetraradial symmetry might have selected through the evolution of the cnidarian because of some adaptive value.

The intriguing example of *Aurelia* which has the capacity to generate various symmetry patterns at the ephyra and more advanced stages of its development raises the question of the importance of symmetry in cnidarians. Pentaradial and tetraradial ephyrae and young medusae of *Aurelia* although different in their body symmetry have exactly the same body plan in terms of overall external shape, external and internal organs. Whether pentaradial or tetraradial, they have the same mode of locomotion, feeding and reproduction (Gershwin 1999). This questions the overemphasis sometimes given to symmetry patterns in the debate concerning the phylogenetic affinities of ancestral cnidarians.

6.1.5 The atypical developmental cycle of *Olivooides* and its related forms

The first unanimous fossil jellyfish is found in Chengjiang biota (*ca.* 521 Ma) which is proposed developing the same lifestyle as modern medusae based on its overall morphology such as the broad medusa bell, the sixteenth rhopalia locating evenly on the bell margin (Han et al. 2016a). However, the developmental cycle of *Olivooides* and its related fossils from the Kuanchuanpu biota is probably complex that maybe different to that of the fossil medusae found in Chengjiang biota.

Attempts (Chapter 3) have been made to reconstruct the life cycle of *Olivooides* and its allied forms (Han et al. 2013, Steiner et al. 2014). Although fragmentary and lacking adult forms, these assumed cycles differ markedly from those of modern cnidarians in many aspects. One of the major differences seems to be the absence of a planula stage which characterizes all extant cnidarians. As for the symmetry patterns (see above) these differences have been used to question and even to reject the cnidarian affinities of these ancient organisms. We are testing and discussing here two hypotheses concerning the possible developmental process of *Olivooides* and its allied forms.

The development of *Olivooides* and its related fossils was compared (Bengtson and Zhao 1997) with the scyphozoan coronates (Chapman and Werner 1972, Jarms, Morandini and Silveira 2002) which has the sessile polyp stage (stephanoscyphistomae) releasing the younger medusa into the water column once metamorphosed from the planula.

The studied fossils may develop directly which can be identified by several aspects: large body size; the absence of planula and ephyra stages; the remarkable tentacles

and mouth once hatched.

Body size

Extant scyphozoan eggs, diameter of ranging from 30 – 300 μm, develop indirectly which have the planula and ephyra stages through metamorphosis (Berrill 1949, Han et al. 2013). All studied fossil embryos of Olivooides and its related fossils are statistically between 450 – 800 μm that may indicate the adequate nutrition supporting their directly lecithotrophic development which is comparable with extant medusozoans.

Egg envelope

The remained fragments of egg envelope can be observed in the latest gastrulation stage assumes that the whole embryonic process happened within the egg envelope. And the stellate ornaments cover on the periderm can be seen from the embryonic stage to larva stage that suggests no sign of metamorphosis from zygotes to planula (Yao et al. 2011).

Planula and ephyra

Olivooides and its allied forms have a well-documented continuous development from early dividing embryos to post-hatching larvae (Hua et al. 2004, Steiner et al. 2014, Dong et al. 2013, Han et al. 2013) with no gap that would imply the existence of a planula larva. Taphonomy can hardly explain the absence of a planula stage. Very fragile tissues prone to decay such as gonads, tentacles and interradial septa, are preserved in many specimens from the Kuanchuanpu biota. If the planula larva had really existed it would have a strong probability to be found among the SSFs assemblages.

Dong et al. (2013) described tiny compressed star-like microfossils from the Kuanchuanpu biota which superficially resemble the ephyrae of modern cnidarians. However, their size (200 μm) is much smaller than that of extant ephyra (2 – 10 mm in *Aurelia aurita*, see in (Båmstedt, Lane and Martinussen 1999)). These fossils provide no strong evidence that the cnidarians from the Kuanchuanpu biota developed via strobilation and the emission of ephyrae into the water column. The probable absence of ephyra stage is another original feature of these early cnidarians.

However, the existence of ephyra and planula needs to be further tested.

Tentacles and mouth

As depicted in Chapter 5.5, three specimens of the new found *Olivooides*-like fossils (Wang et al., unpublished) are with five paired interradial tentacles and a remarkable mouth with the well-developed oral lips also indicate that they can feed once hatched which supposes a direct development.

Hypothesis A

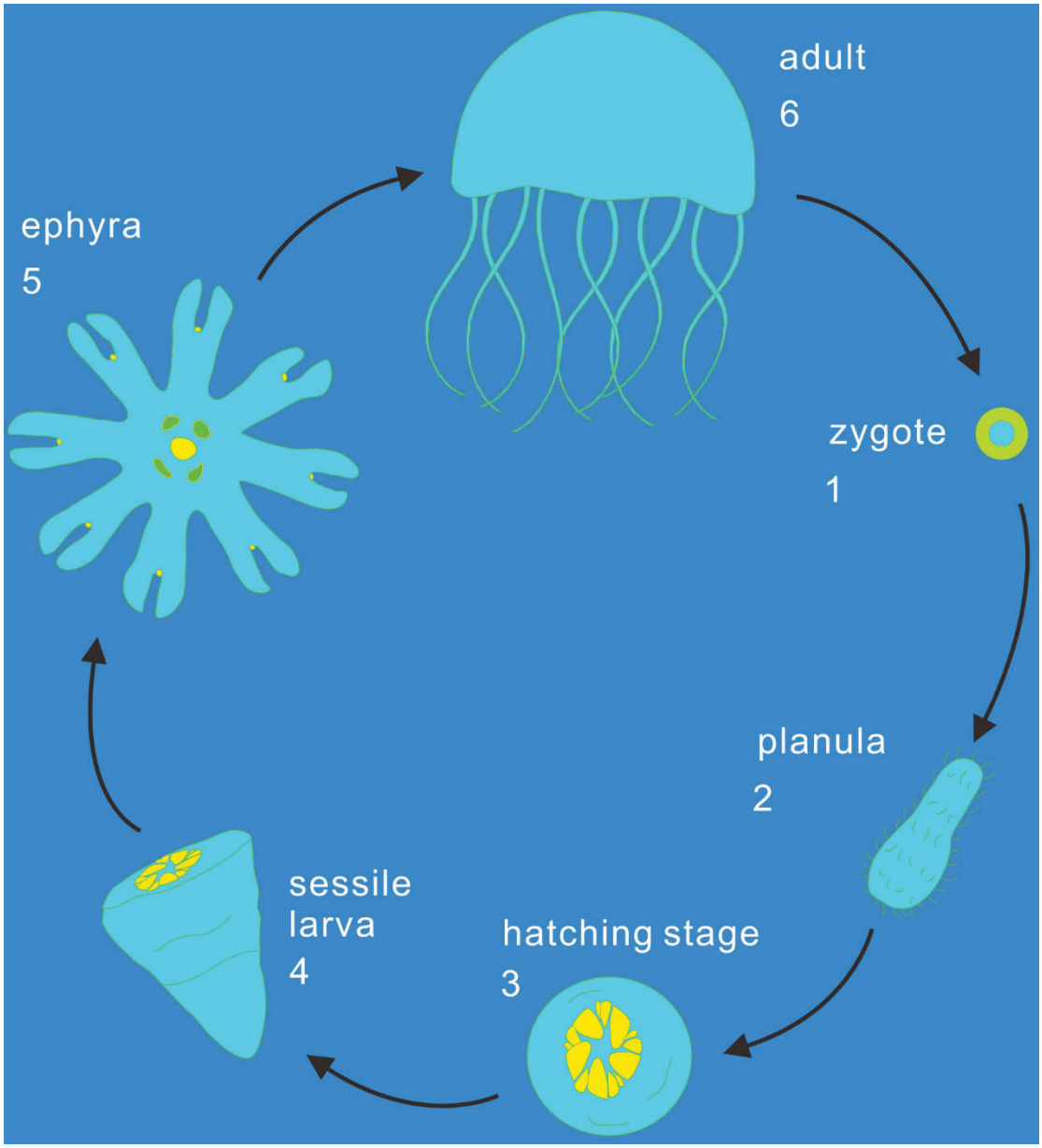

Fig. 76. Developmental cycle of *Olivooides* and its related fossils: hypothesis A. The developmental cycle is comparable with that extant medusozoans (scyphozoans + cubozoans) with a supposed planula stage followed by a polyp stage, ephyra stage and medusa stage. Modified from Han et al., 2013; Steiner et al., 2014.

According to this hypothesis (A, Fig. 76), the lifecycle of *Olivooides* would be comparable with that of extant scyphozoans and cubozoans and would require a planula stage after the hatching stage. The planula would develop into a larva through metamorphosis that cannot be observed in light of the fossil record. The conical sessile larva would release young ephyra-type medusae, later growing into adult free-swimming medusae (Fig. 76). However, it is important to note here that the sessile larva of Olivooides differs markedly from the sessile polyp of extant medusozoan (e.g. important microstructures such as the perradial teeth cannot be seen in *Olivooides*).

More importantly, this hypothesis is severely undermined by the fact that the supposed existence of a planula larva, ephyra stage and the medusa stage is supported by no fossil evidence. The absence of these three major elements is unlikely to result from taphonomy bias.

Hypothesis B

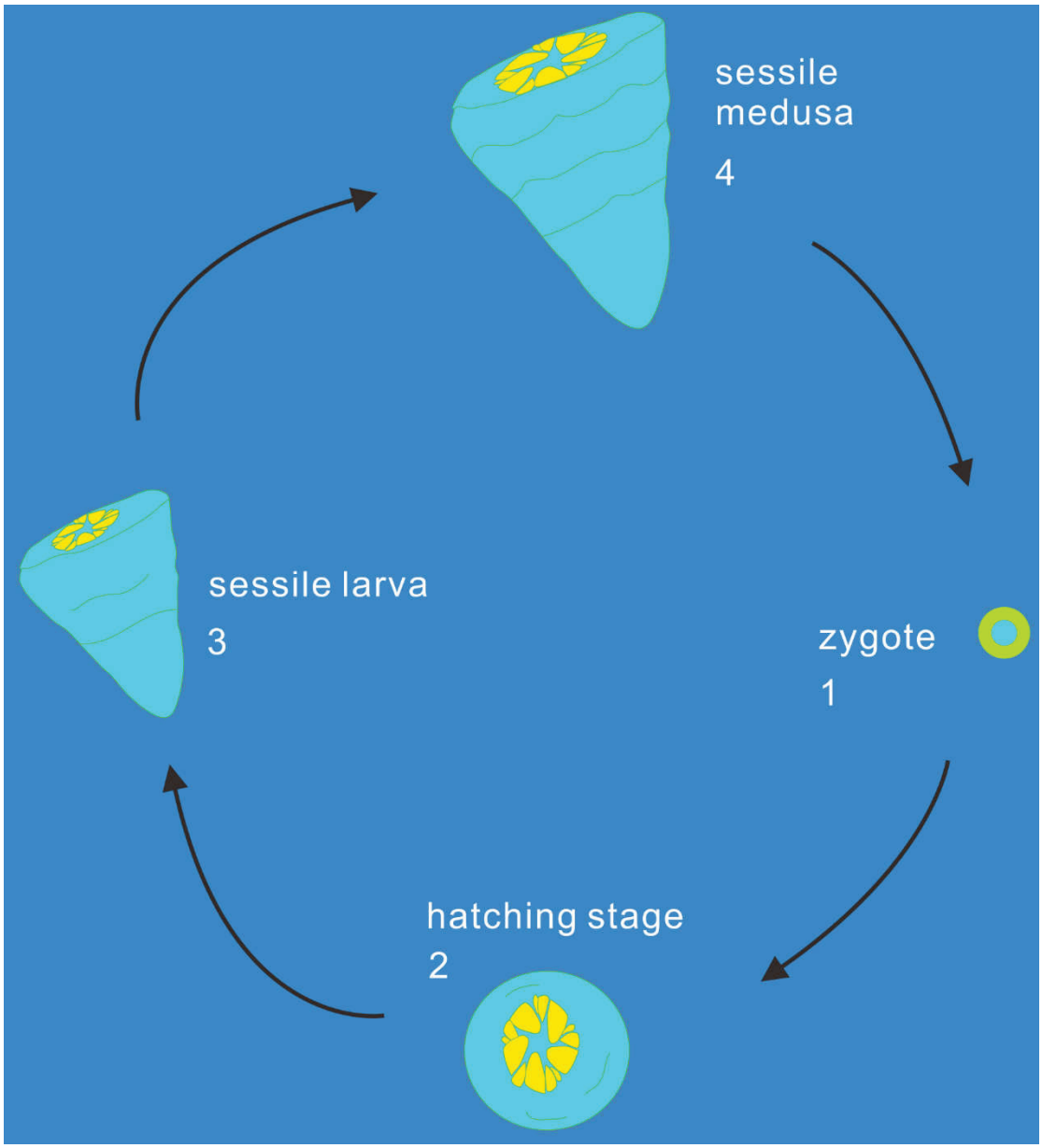

Fig. 77. Developmental cycle of *Olivooides* and its related fossils with no planula stage. Zygotes develop directly into a spherical embryo which transforms into a conical larva and eventually a sessile medusa. Modified from Han et al., 2013; Steiner et al., 2014.

Olivooides and its allied forms would develop as follows (Fig. 77): Fertilized eggs would develop directly into a spherical embryo without a planula stage. This embryo would

give rise to a sessile conical larva which would grow into a sessile adult medusa. We hypothesize that *Olivooides* had no planula stage because no gap can be found in its embryonic development (the transition between the dividing embryo and the post-hatching larva seems to be continuous) that would suggest an intermediate larval stage (Wang et al., under review). According to this hypothesis, the development of *Olivooides* would be direct, relatively "simplified" when compared with that of extant medusozoans and in no way incompatible with cnidarian affinities. It would correspond to an extinct mode of development with unique characteristics (e.g. sessile polyp medusa) which has no direct counterpart in modern cnidarians. There remains the problem of how these polyp medusae developed into adults and engage into a new reproductive cycle. Unfortunately, the Kuanchuanpu biota consists of mainly microscopic organisms and fails to provide information on assumed adult stages. Until now, no medusae (or fragments of them) comparable to extant ones or those from the Chengjiang biota (Han et al. 2016a) has been found in our SSFs assemblages.

As for the atypical symmetry, there is no reason to reject the cnidarian affinities of Olivooides on the basis of its atypical mode of development. Simply we should admit to think that the ancestors of cnidarians may have developed directly and not in the same way as do modern representatives of the group. The shift from a direct development to an indirect development with a planula larva and free-swimming adult may have been induced by environmental changes and may have presented evolutionary advantages. However, when and how this shift occurred remains hypothetical.

6.2 Cambrian cnidarians: possible placement and relation to modern lineages

Fossils with assumed cnidarian affinities comprise the Olivooidae, *Eolympia*, hexaconulariids and *Carinachites* (see Table in Chapter 3). The family Olivooidae erected by Steiner et al. (2014) contains *Olivooides* and *Quadrapyrgites*, *Sinaster*, *Qinscyphus* and several unnamed specimens described in previous work. Olivooidae are defined by Steiner et al. (2014) as organisms forming tubes with a circular to oval cross-section in the post-embryonic part, with a tetraradial or pentaradial conical apex made of embryonic tissue, whose external ornamentation is different from that of the post-embryonic tissue. The main part of their tube is formed by steep crests of post-embryonic tissue, which is abapically closed by terminal folds of the same tissue.

As indicated before (Chapters 3.2; 5; 6.1), two hypotheses on the affinity of Olivooidae (*Olivooides* and related forms) have been proposed that would place this family either in the stem group Scyphozoa (Dong et al. 2013, Liu et al. 2014b) or the stem group Cubozoa (Han et al. 2013, Wang et al. 2017). Our purpose here is to replace Olivooidae in the cnidarian tree and to reassess its phylogenetic relations to other Kuanchuanpu cnidarians (e.g. *Eolympia*) or cnidarian candidates (hexaconulariids and *Carinachites*),

and to modern representatives of the group (Fig. 78).

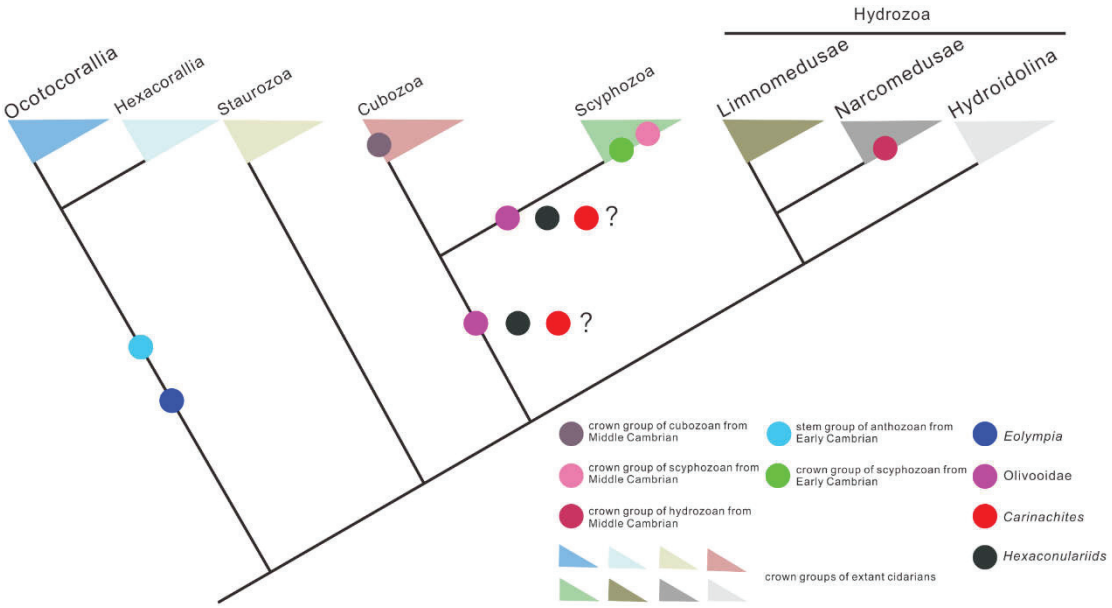

Fig. 78. Tentative phylogenetic placement of Cambrian cnidarians and possible relation to modern cnidarian lineages. The divergence between main cnidarian lineages is based on current molecular data (Collins et al. 2006a).

Eolympia pediculata Han et al., 2010 is a minute (size *ca.* 450 µm) pedunculate form with a cylindrical upper part crowned by a ring of evenly spaced bud-like features interpreted as a tentacle crown (multiple of 6). Eighteen (multiple of 6) mesenteries occur within its inner cylindrical cavity. Han et al. (2010) considered *E. pediculata* as possibly belonging to the sister group of extant anthozoans based on its 18 (multiple of 6) complete and incomplete mesenteries (Han et al. 2010) (Chapter 3; Fig. 56).

Hexaconulariids still remain an enigmatic group. Its assumed affinities with scyphozoans are based on a very limited number of morphological resemblances with modern scyphozoans (e.g. external ornament resembling the segmented pattern of the stephanoscyphistoma of coronate polyps (Van Iten et al. 2014) (Chapter 3; Fig. 59)).

Similarly, the phylogenetic affinities of *Carinachites* are uncertain because the lack of information concerning its inner anatomy.

Although very limited information is available concerning the internal structure and soft anatomy of *Carinachites*, some important resemblances between *Olivooides* and *Carinachites* are worth to be noted here. They concern their oral part, and more precisely, the presence, in the two forms, of four oral apertural lobes surrounding the mouth opening (Han et al. 2018).

Xianguangia sinica Chen and Erdtmann, 1991 from the early Cambrian Chengjiang biota (*ca.* 521 Ma) recently revised by Ou et al., (2017) is interpreted as a member of the sister group of extant anthozoans based detailed morphological evidence (e.g. sophisticated, feather-like tentacles surrounding the oral part, columnar body lined with external ridges, ring-like constriction and holdfast; (Ou et al. 2017, Hou et al.

2017, Chen 1991) (Chapter 3; Fig. 35).
Archisaccophyllia kunmingensis Hou et al., 2005 from the same biota is another sessile fossil organisms which seems to be close to Anthozoa. Its diagnostic features are a cylindrical body with longitudinal ridges, possible tentacles surrounding the oral disc, and a pedal disc (Hou et al. 2005, Hou et al. 2017) (Chapter 3; Fig. 36). However, its status among or outside the cnidarian tree remains controvertial (see phoronid hypothesis; (Zhang and Holmer 2014)).
Yunnanoascus haikouensis Hu et al., 2007 from the Chengjiang biota is convincingly reinterpreted by Han et al. (2016a) as a crown group scyphozoans based on the presence of rhopalia, possible radial canals and marginal tentacles (Hu et al. 2007, Han et al. 2016a).
Although the placement of the middle Cambrian jellyfish from the Marjum biota within cnidarians is not open to question (see Chapter 2), their precise assignment to the crown groups Cubozoa, Scyphozoa and Hydrozoa would benefit from more detailed analysis. The revision of this important fossil material may help clarify this issue.

6.3 Early evolution of symmetry in cnidarians

The fossil jellyfish (*Yunnanoascus haikouensis* Hu et al., 2007) and anthozoans (*Xianguangia sinica* Chen and Erdtmann, 1991) from the early Cambrian Chengjiang biota (*ca.* 521 Ma) (Han et al. 2016a, Ou et al. 2017) display a clear tetraradial and bilateral symmetry, respectively, both typical of modern cnidarians. Similarly, the assumed crown group cnidarians from the younger middle Cambrian Marjum biota (*ca.* 505 Ma) (Cartwright et al. 2007) are all tetraradial (Cubozoa, Scyphozoa, Hydrozoa). Therefore an important evolutionary gap seems to exist between the lowermost Cambrian cnidarians characterized by diverse symmetry patterns, a small body size and a thick periderm, and the early and middle Cambrian ones dominated by tetraradial symmetry and much larger in size.
How the last common ancestor of metazoan looked like remains open to speculation cause of the lack of fossil evidence concerning their Precambrian evolutionary history. Some authors (e.g. (Nielsen 2012)) suggested that the first metazoan had a spherical body and was holopelagic. *Nematostella vectensis* is a model organism for the study of evolution. Recent genomic studies of this anthozoan animal suggest that that the oral-aboral axis of anthozoans is homologous with the dorsal-ventral axis of bilaterains (Matus et al. 2006, Finnerty et al. 2004) and that the evolution of bilateral symmetry predates the emergence of anthozoans and the diversification of cnidarians into various symmetry patterns. The remote (Precambrian) ancestry of animal bilaterality is attested by *Dickinsonia*, an Ediacaran flat organism with an anterior-posterior axis and modules organized in an alternating pattern according to glide reflection symmetry rather than true bilateral symmetry. Steroid biomarkers show that *Dickinsonia* was an animal, and the earliest animal to date (Bobrovskiy et al. 2018b).

Current phylogenies based on molecular and morphological data designate anthozoans as the most basal cnidarian group which effectively retains bilateral symmetry, and the sister group of medusozoans (Collins 2002, Collins et al. 2006b). In this context, the very first ancestors of cnidarians might have been bilateral organisms which adopted radial symmetry later on in the course of evolution (Brasier and Antcliffe 2008, Bobrovskiy et al. 2018b). However, this major shift in the body plan remains to be explained at the genetic level (Ryan et al. 2007).

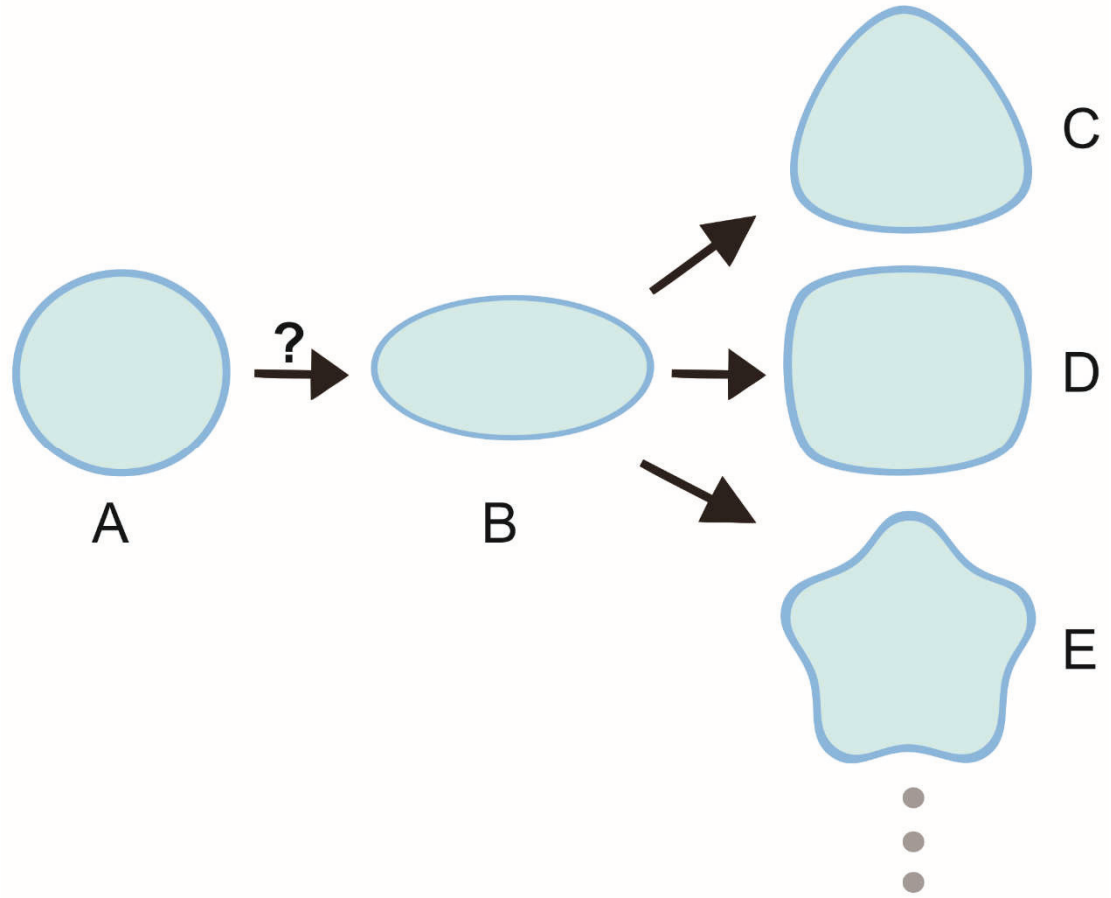

Fig. 79. Possible evolution of cnidarian symmetry from hypothetical bilateral ancestors to various radial forms. A. The hypothetical last common ancestor of cnidarian may have had a spherical symmetry (Nielsen 2012). B. We assume that a radiation of symmetry patterns occurred in the early evolution of cnidarians (possibly across the Precambrian-Cambrian boundary) from a bilateral ancestor. C-E. Tri, tetra and pentaradial symmetries, respectively. The grey solid dots represent other possible symmetry patterns.

We suggest that various types of symmetry patterns (tri, tetra, penta, etc.) may have arisen from a hypothetical bilateral cnidarian ancestor and that the Kuanchuanpu biota brings evidence of this 'symmetry radiation' exemplified by the tetraradial and pentaradial Olivooidae, the tri-, tetra- or pentaradial carinachitids, and the bi, tetra / hexaradial hexaconularids. The pentaradial symmetry, although dominant in this biota, co-existed with the tetraradial symmetry that characterizes a huge percentage of

present-day cnidarians. Rather than being 'atypical', the pentaradial symmetry is one expression among others of the early diversification of cnidarians, that probably has an evolutionary advantage at the time of this event (Fig. 79).

6.4 Lifestyles and environments of early cnidarians

6.4.1 The meiofauna hypothesis

The organisms from Kuanchuanpu biota are remarkable by their very small size (400 – 1000 µm, rarely larger than 2 mm). Cnidarians are no exception which raises the question of their habitat, within the water column, at the water-sediment interface or deeper into the sediment.

Rhopalia are sensory organs essential to numerous modern medusozoans living within the water column. They act as gravity sensors and keep the medusa bell in the upright position during swimming. Remains of rhopalia occur in a jellyfish species from the Chengjiang biota (Han et al. 2016a) suggesting evident adaptation of these animals to an active planktonic lifestyle. In contrast, the "sessile medusa" stage of *Olivooides* and its allied (Figs. 45-51; 53-63) show no trace of such sophisticated sensory organs. The absence of rhopalia cannot be simply explained by taphonomic and diagenetic factors and more likely suggest that *Olivooides* and allied forms were non-swimming sessile organisms and indeed best defined as sessile medusae. This interpretation is also supported by the overall morphology of *Olivooides* and related forms (e.g. conical shape and apical polarity). Their conical apexes seem to be consistent with a sessile mode of life and a larval settlement on the substrate after the hatching process (Bengtson and Yue 1997, Han et al. 2013, Steiner et al. 2014). If the planktonic option is to be ruled out, then how can we characterize more precisely the habitat of these early cnidarians.

Olivooides and related forms fall within the size range of modern meiobenthic animals. The present-day meiofauna consists of a great variety of tiny invertebrates ranging from 40 to 1000 µm (rarely up to 2 mm) which live and shelter in sediment, typically within the interstices formed between the sand grains. It is dominated by tiny arthropods and larval stages of various animal groups. Although rare, cnidarians occur in the present-day meiofauna, for example the hydromedusa *Halammohydra* (300 – 1200 µm) from the littoral sands of the North Sea (Remane 1927) and the scyphomedusa *Stylocoronella riedli* (less than 500 µm) from the Adriatic Sea. The extant meiobenthic organisms show various adaptations to living within this interstitial network, the sediment grain size being critical to their settlement (Giere 2008). As noted in Chapter 3, the sediment of the Kuanchuanpu Formation, contains between 35% – 55% of sand grains with a grain size of 50 to 1000 µm (Wang et al. 2010a). Although its original composition and depositional setting are still awaiting to be studied in details, the relatively high proportion of sand grains seems to be

consistent with the presence of a meiofaunal habitat potentially sheltering various meiobenthic animal groups (Hypothesis 1; Fig. 80).

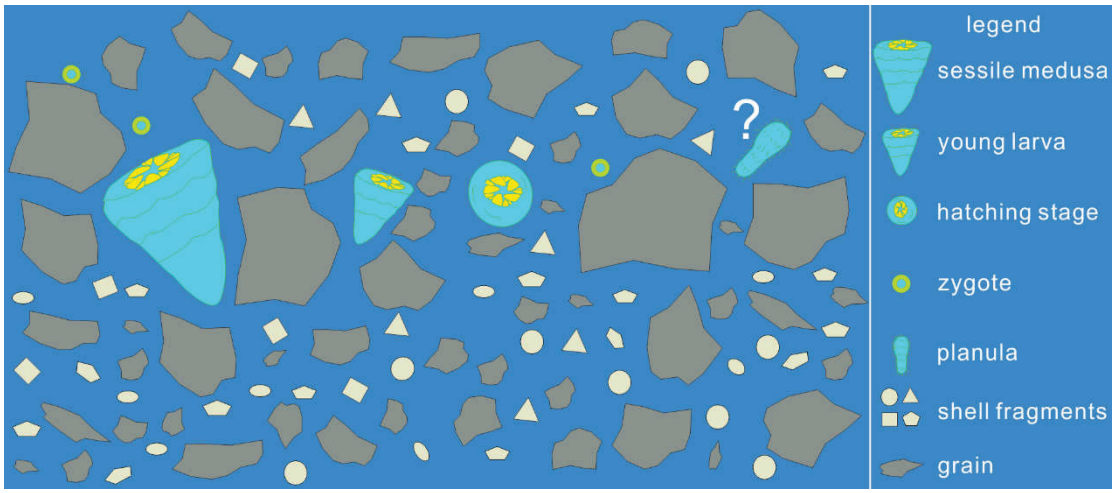

Fig. 80. Hypothesis 1: *Olivooides* and its related forms from Kuanchuanpu biota are considered as interstitial meiobenthic organisms. Planula stage is hypothetical.

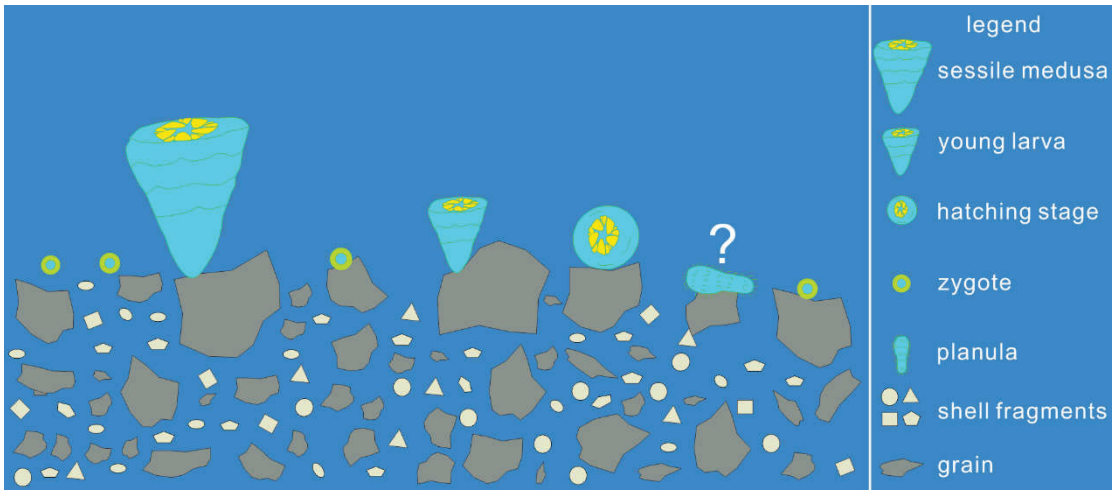

Fig. 81. Hypothesis 2: *Olivooides* and its related forms from Kuanchuanpu biota are considered as sessile epibenthic organisms living at the water-sediment interface. Planula stage is hypothetical.

Another option (Hypothesis 2; Fig. 81) is to consider that *Olivooides* and related forms lived at the water-sediment interface as sessile epibenthic animals attached to sedimentary particles. This would suppose that organisms were attached to a micro-substrate via for example mucous substances. Comparable attachment processes are known to occur in the planula larvae of modern cnidarians which settle down on the sea bottom before continuing their developmental cycle. However, no trace of any sticky substance or attachment feature can be seen near the conical apex of the larval stages of *Olivooides*.

Beyond these interpretations, we should not forget that the very specific size range of the fossil organisms from the Kuanchuanpu biota might reflect a taphonomic bias - i.e. that only small animals were phosphatized shortly after death within the water-sediment interface and that adult epibenthic organisms and those living within the water column (e.g. swimming medusa) could not be preserved and left no trace. If this scenario was correct, then our view of the diversity, lifestyle, and developmental cycle of the Kuanchuanpu animals would be severely altered and distorted. However, no fragments of large organisms which in theory have the potential for being mineralized, are found in the Kuanchuanpu biota. This would reinforce our idea that the original animal communities of Kuanchuanpu indeed consisted of very small organisms that fell within the range of modern meiobenthos (Fig. 80) or were tiny sessile organisms at the water-sediment interface (Fig. 81). The absence of planktonic organisms such as medusae may have a different cause, if we suppose that they decayed extremely rapidly within the column where the concentration of phosphate was most probably much less than at the water-sediment interface.

Some extant marine animals have a temporary meiobenthic lifestyle during the early stages of their development and shift to a different habitat when they grow in size to become adults (Giere 2008). This may be the case of the cnidarians from the Kuanchuanpu biota as well.

A meiofaunal lifestyle has been recently proposed for *Saccorhytus*, a tiny primitive deuterostome from the Kuanchuanpu Formation (Han et al. 2017). The co-occurrence of kinorhynch-like worms in the same biota (Zhang et al. 2015), which are represented in the modern meiofauna also support the hypothesis that the Kuanchuanpu biota may represent a meiobenthic ecosystem a key importance in the early diversification of animal life.

Conclusions

Recent detailed studies of the SSFs assemblages from the Kuanchuanpu Formation have casted light on marine biodiversity at a critical time in the early evolution of animal life, before the “Cambrian Explosion“ reaches its peak. These 535 million-year-old assemblages contain not only the exoskeletal remains of tiny biomineralizing animals but also remarkably well-preserved soft-bodied invertebrates such as worms, deuterostomes and embryonic and larval stages of cnidarians. The purpose of this thesis was to study the cnidarian component of this remarkable fauna and to test whether the assumed cnidarian affinities of these tiny animals are valid or not. We also studied younger early Cambrian jellyfish from the Chengjiang biota (*ca.* 521 Ma) in order to understand how cnidarians evolved and diversified through the early stages of their evolutionary history. Our work is mainly based on the three-dimensional exploration of the internal anatomy of the microfossils from the Kuanchuanpu Formation by using Scanning Electron Microscopy (SEM) and Computed X-ray Microtomography (XTM). We found strong additional evidence that some of these fossils such as *Olivooides* and its allied forms had close relationships with cnidarians. Indeed important features of their internal and external anatomy identify them as cnidarians and invalidate other hypotheses proposed by previous authors, such as the ecdysozoan or echinoderm options. However, the cnidarians from the Kuanchuanpu Formation differ from modern representatives of the group in their “atypical” symmetry patterns (e.g. pentaradiality is prevalent), developmental mode and possibly ecology (e.g. habitat). For example, no planula and ephyra stages seem to occur through their development. The lack of these features typical of modern cnidarians does not seem to result from taphonomy bias but more likely suggest a direct and “simplified” mode of development. The dominant pentaradial symmetry of the Kuanchuanpu cnidarians (e.g. *Olivooides*) cannot be used as a solid argument against their cnidarian affinities. A more realistic view may be to consider that the lowermost Cambrian cnidarians had distinct developmental processes and that the indirect developmental mode which characterizes modern cnidarians appeared later in the evolution of the group. Our study and those of previous authors indicate that several symmetry patterns co-existed within the early cnidarian stock exemplified by tetraradial and pentaradial forms. The reason why tetraradial symmetry became overwhelmingly dominant among modern cnidarians remains unknown. Because of their “atypical” features, the early cnidarians from the Kuanchuanpu biota cannot be straightforwardly assigned to any crown group but may find their place with the stem groups scyphozoan and cubozoans. Crown-group scyphozoans, cubozoans and hydrozoans do not seem to present before Stage 2 of the early Cambrian and the Middle Cambrian. The consistent very small size of the Kuanchuanpu organisms should be interpreted with caution. Secondary phosphatization may have favored the preservation of very small organisms within a narrow infra-millimetric range (taphonomic window), allowing no larger forms to be mineralized and eventually

fossilized. However, the lack of cuticular and body fragments of adult animals prompt us to consider that the Kuanchuanpu fauna may be comparable with the modern meiobenthos. Whether these tiny organisms colonized interstitial environments or had a sessile lifestyle at the water-sediment interface cannot be resolved until detailed information concerning their natural and depositional environment and habit can be obtained. Although our study is based on different taphonomic windows (3D-preserved phosphatized microfossils and Burgess Shale-type macrofossils preserved in compression) and therefore calls for cautiousness, we hypothesize that cnidarians may have undergone major evolutionary changes during the early Cambrian, a shift from strictly microbenthic to pelagic or mixed lifestyles, the replacement of a dominant pentaradial symmetry by a tetraradial one and the adoption of indirect development, which altogether laid the foundations of modern cnidarian diversity.

References

Adrianov, A. V. & V. V. J. J. o. M. Malakhov (2001) Symmetry of priapulids (Priapulida). 1. Symmetry of adults. 247**,** 99-110.

Aguinaldo, A. M. A., J. M. Turbeville, L. S. Linford, M. C. Rivera, J. R. Garey, R. A. Raff & J. A. J. N. Lake (1997) Evidence for a clade of nematodes, arthropods and other moulting animals. 387**,** 489-493.

Amelin, Y., A. N. Krot, I. D. Hutcheon & A. A. Ulyanov (2002) Lead Isotopic Ages of Chondrules and Calcium-Aluminum-Rich Inclusions. *Science,* 297**,** 1678-1683.

Arai, M. N. 1997. *A functional biology of Scyphozoa*. Springer Science & Business Media.

Babcock, L. E. & R. M. Feldmann. 1986. *Devonian and Mississippian Conulariids of North America: General Description and Conularia. A*.

Babcock, L. E., A. M. Grunow, G. R. Sadowski & S. A. J. P. Leslie, Palaeoclimatology, Palaeoecology (2005) Corumbella, an Ediacaran-grade organism from the Late Neoproterozoic of Brazil. 220**,** 7-18.

Baldauf, S. (2003) The deep roots of eukaryotes. *Science,* 300**,** 1703-1706.

Båmstedt, U., J. Lane & M. J. M. B. Martinussen (1999) Bioenergetics of ephyra larvae of the scyphozoan jellyfish Aurelia aurita in relation to temperature and salinity. 135**,** 89-98.

Bengtson, S., S. Conway Morris & B. Cooper. 1990. *Early Cambrian fossils from south Australia*.

Bengtson, S. & Z. Yue (1997) Fossilized metazoan embryos from the earliest Cambrian. *Science,* 277**,** 1645-1648.

Bengtson, S. & Y. Zhao (1997) Fossilized metazoan embryos from the earliest Cambrian. *Science,* 277**,** 1645.

Berrill, N. J. B. R. (1949) Developmental analysis of scyphomedusae. 24**,** 393-409.

Bobrovskiy, I., J. M. Hope, A. Ivantsov, B. J. Nettersheim, C. Hallmann & J. J. Brocks (2018a) Ancient steroids establish the Ediacaran fossil Dickinsonia as one of the earliest animals. *Science,* 361**,** 1246-1249.

Bobrovskiy, I., J. M. Hope, A. Ivantsov, B. J. Nettersheim, C. Hallmann & J. J. J. S. Brocks (2018b) Ancient steroids establish the Ediacaran fossil Dickinsonia as one of the earliest animals. 361**,** 1246-1249.

Brasier, M. & J. Lindsay (1998) A billion years of environmental stability and the emergence of eukaryotes: new data from northern Australia. *Geology,* 26**,** 555-558.

Brasier, M. D. & J. B. J. P. Antcliffe, Palaeoclimatology, Palaeoecology (2008) Dickinsonia from Ediacara: a new look at morphology and body construction. 270**,** 311-323.

Briggs, D. E., F. J. Collier & D. H. Erwin. 1994. *The fossils of the Burgess Shale*.

Briggs, D. E. & C. Nedin (1997) The taphonomy and affinities of the problematic fossil Myoscolex from the Lower Cambrian Emu Bay Shale of South Australia. *Journal of Paleontology,* 71**,** 22-32.

Brusca, R. & G. Brusca (2003) Invertebrates 2nd Eds. *Sunderland, UK: Sinauer Associates*.

Budd, G. E. 1998. Stem group arthropods from the Lower Cambrian Sirius Passet fauna of north Greenland. In *Arthropod relationships*, 125-138. Springer.

Butterfield, N. J. (2000) Bangiomorpha pubescens n. gen., n. sp.: implications for the evolution of sex, multicellularity, and the Mesoproterozoic/Neoproterozoic radiation of eukaryotes. *Paleobiology,* 26**,** 386-404.

--- (2011) Animals and the invention of the Phanerozoic Earth system. *Trends in ecology & evolution,* 26**,** 81-87.

Cai, Y., H. Hua, J. D. Schiffbauer, B. Sun & X. J. G. R. Yuan (2014) Tube growth patterns and microbial mat-related lifestyles in the Ediacaran fossil Cloudina, Gaojiashan Lagerstätte, South China. 25**,** 1008-1018.

Cai, Y., J. D. Schiffbauer, H. Hua & S. J. P. R. Xiao (2011) Morphology and paleoecology of the late Ediacaran tubular fossil Conotubus hemiannulatus from the Gaojiashan Lagerstätte of southern Shaanxi Province, South China. 191**,** 46-57.

Canfield, D. E., S. W. Poulton & G. M. Narbonne (2007) Late-Neoproterozoic deep-ocean oxygenation and the rise of animal life. *Science,* 315**,** 92-95.

Caron, J.-B. & J. Vannier (2016) Waptia and the diversification of brood care in early arthropods. *Current Biology,* 26**,** 69-74.

Carr, M., B. S. Leadbeater, R. Hassan, M. Nelson & S. L. Baldauf (2008) Molecular phylogeny of choanoflagellates, the sister group to Metazoa. *Proceedings of the National Academy of Sciences*.

Cartwright, P., S. L. Halgedahl, J. R. Hendricks, R. D. Jarrard, A. C. Marques, A. G. Collins & B. S. J. P. o. Lieberman (2007) Exceptionally preserved jellyfishes from the Middle Cambrian. 2**,** e1121.

Cavalier-Smith, T. (1987) The simultaneous symbiotic origin of mitochondria, chloroplasts, and microbodies. *Annals of the New York Academy of Sciences,* 503**,** 55-71.

Chapman, D. & B. J. H. w. M. Werner (1972) Structure of a solitary and a colonial species of Stephanoscyphus (Scyphozoa, Coronatae) with observations on periderm repair. 23**,** 393.

Chen, J. J. B. o. t. N. M. o. N. s. (1997) Biology of the Chengjiang fauna. 10**,** 11-106.

Chen, J. Y. E., B.D. 1991. *Lower Cambrian fossil Lagerstatte from Chengjiang, Yunnan, China: insights for reconstructing early metazoan life*.

Chen, M., Y. Chen, Y. J. B. Qian, Tianjin Institute of Geology & M. Resources (1981) Some tubular fossils from Sinian-Lower Cambrian boundary sequences, Yangtze Gorge. 3**,** 117-124.

Coates, M. M., A. Garm, J. C. Theobald, S. H. Thompson & D.-E. Nilsson (2006) The spectral sensitivity of the lens eyes of a box jellyfish, Tripedalia cystophora (Conant). *Journal of Experimental Biology,* 209**,** 3758-3765.

Collins, A. G. (2002) Phylogeny of Medusozoa and the evolution of cnidarian life cycles. *Journal of Evolutionary Biology,* 15**,** 418-432.

Collins, A. G., P. Schuchert, A. C. Marques, T. Jankowski, M. Medina & B. Schierwater (2006a) Medusozoan phylogeny and character evolution clarified by new large and small subunit rDNA data and an assessment of the utility of phylogenetic mixture models. *Systematic Biology,* 55**,** 97-115.

Collins, A. G., P. Schuchert, A. C. Marques, T. Jankowski, M. Medina & B. Schierwater (2006b) Medusozoan phylogeny and character evolution clarified by new large and small subunit rDNA data and an assessment of the utility of phylogenetic mixture models. *Systematic Biology,* 55**,** 97.

Conant, F. S. 1898. *The Cubomedusæ: a memorial volume*. Johns Hopkins Press.

Conway Morris, S. (1989) Burgess Shale faunas and the Cambrian explosion. *Science,* 246**,** 339-346.

Conway Morris, S. (2000) The Cambrian "explosion": slow-fuse or megatonnage? *Proceedings of the National Academy of Sciences,* 97**,** 4426-4429.

Conway Morris, S. & M. J. J. o. P. Chen (1992) Carinachitids, hexangulaconulariids, and Punctatus: problematic metazoans from the Early Cambrian of South China. 384-406.

Cook, P. J. & J. H. Shergold (1984) Phosphorus, phosphorites and skeletal evolution at the Precambrian—Cambrian boundary. *Nature,* 308**,** 231.

Cuthill, J. F. H. & S. Conway Morris (2014) Fractal branching organizations of Ediacaran rangeomorph fronds reveal a lost Proterozoic body plan. *Proceedings of the National Academy of Sciences,* 111**,** 13122-13126.

Daly, M., M. R. Brugler, P. Cartwright, A. G. Collins, M. N. Dawson, D. G. Fautin, S. C. France, C. S. McFadden, D. M. Opresko & E. Rodriguez (2007) The phylum Cnidaria: a review of phylogenetic patterns and diversity 300 years after Linnaeus.

David, B. & R. J. E. Mooi (2014) How Hox genes can shed light on the place of echinoderms among the deuterostomes. 5**,** 22.

Dodd, M. S., D. Papineau, T. Grenne, J. F. Slack, M. Rittner, F. Pirajno, J. O'neil & C. T. Little (2017) Evidence for early life in Earth's oldest hydrothermal vent precipitates. *Nature,* 543**,** 60.

Dong, X.-P., J. A. Cunningham, S. Bengtson, C.-W. Thomas, J. Liu, M. Stampanoni & P. C. Donoghue (2013) Embryos, polyps and medusae of the Early Cambrian scyphozoan Olivooides. *Proc. R. Soc. B,* 280**,** 20130071.

Dong, X. J. C. S. B. (2007) Developmental sequence of Cambrian embryo Markuelia. 52**,** 929.

Dong, X. P., K. Vargas, J. A. Cunningham, H. Zhang, T. Liu, F. Chen, J. Liu, S. Bengtson & P. C. Donoghue (2016) Developmental biology of the early Cambrian cnidarian Olivooides. *Palaeontology,* 59**,** 387-407.

Donoghue, P. C. & J. B. Antcliffe (2010) Early life: Origins of multicellularity. *Nature,* 466**,** 41.

Droser, M. L., L. G. Tarhan & J. G. Gehling (2017) The rise of animals in a changing environment: global ecological innovation in the late Ediacaran. *Annual Review of Earth and Planetary Sciences,* 45**,** 593-617.

Dunn, C. W., G. Giribet, G. D. Edgecombe & A. Hejnol (2014) Animal phylogeny and its evolutionary implications. *Annual review of ecology, evolution, and systematics,* 45**,** 371-395.

Dunn, C. W., A. Hejnol, D. Q. Matus, K. Pang, W. E. Browne, S. A. Smith, E. Seaver, G. W. Rouse, M. Obst & G. D. J. N. Edgecombe (2008) Broad phylogenomic sampling improves resolution of the animal tree of life. 452**,** 745.

El Albani, A., S. Bengtson, D. E. Canfield, A. Bekker, R. Macchiarelli, A. Mazurier, E. U. Hammarlund, P. Boulvais, J.-J. Dupuy & C. Fontaine (2010) Large colonial organisms with coordinated growth in oxygenated environments 2.1 Gyr ago. *Nature,* 466**,** 100.

Elicki, O. (2006) Microbiofacies analysis of Cambrian offshore carbonates from Sardinia (Italy): environment reconstruction and development of a drowning carbonate platform.

Erwin, D. H., M. Laflamme, S. M. Tweedt, E. A. Sperling, D. Pisani & K. J. Peterson (2011) The Cambrian conundrum: early divergence and later ecological success in the early history of animals. *science,* 334**,** 1091-1097.

Evans, N. M., A. Lindner, E. V. Raikova, A. G. Collins & P. Cartwright (2008) Phylogenetic placement of the enigmatic parasite, Polypodium hydriforme, within the Phylum Cnidaria. *BMC evolutionary biology,* 8**,** 139.

Fairchild, T. R., E. A. Sanchez, M. L. A. Pacheco & J. J. I. J. o. A. de Moraes Leme (2012) Evolution of Precambrian life in the Brazilian geological record. 11**,** 309-323.

Feldmann, R. & L. J. N. G. R. Babcock (1986) Exceptionally preserved conulariids from Ohio-reinterpretation of their anatomy. 2**,** 464-472.

Finnerty, J. R., K. Pang, P. Burton, D. Paulson & M. Q. J. S. Martindale (2004) Origins of bilateral symmetry: Hox and dpp expression in a sea anemone. 304**,** 1335-1337.

Ford, T. D. J. G. T. (1999) Topics The Precambrian fossils of Charnwood Forest. 15**,** 230-234.

Ford, T. D. J. P. o. t. Y. G. S. (1958) Pre-Cambrian fossils from Charnwood forest. 31**,** 211-217.

Forterre, P. (2005) The two ages of the RNA world, and the transition to the DNA world: a story of viruses and cells. *Biochimie,* 87**,** 793-803.

Gaillard, C., J. Goy, P. Bernier, J. P. Bourseau, J. C. Gall, G. Barale, E. Buffetaut & S. J. P. Wenz (2006) New jellyfish taxa from the upper Jurassic lithographic limestones of Cerin (France): Taphonomy and ecology. 49**,** 1287-1302.

Germs, G. J. J. A. J. o. S. (1972) New shelly fossils from Nama Group, south west Africa. 272**,** 752-761.

Gershwin, L.-a. J. J. o. t. M. B. A. o. t. U. K. (1999) Clonal and population variation in jellyfish symmetry. 79**,** 993-1000.

Gershwin, L. A. & P. Alderslade (2006) Chiropsella bart n. sp., a new box jellyfish (cnidaria: cubozoa: chirodropida) from the Northern Territory, Australia. *The Beagle,* 22**,** 15-21.

Giere, O. 2008. *Meiobenthology: the microscopic motile fauna of aquatic sediments*. Springer Science & Business Media.

Glaessner, M. F. & M. J. P. Wade (1966) The late Precambrian fossils from Ediacara, South Australia. 9**,** 599-628.

Goloboff, P. A., J. S. Farris & K. C. J. C. Nixon (2008) TNT, a free program for phylogenetic analysis. 24**,** 774-786.

Grotzinger, J. P. & D. H. Rothman (1996) An abiotic model for stromatolite morphogenesis. *Nature,* 383**,** 423.

Hadzi, H. (1944) Slovenska Akad. Znanosti Umetnosti, Ljubl. Turbellarijska teorija knidarijev (Turbellarien-Theorie der Knidarien).

Hadži, J. J. S. Z. (1953) An attempt to reconstruct the system of animal classification. 2**,** 145-154.

Hagadorn, J. W. & B. J. J. o. P. Waggoner (2000) Ediacaran fossils from the southwestern Great Basin, United States. 74**,** 349-359.

Hahn, G., R. Hahn, O. Leonardos, H. Pflug & D. J. G. e. P. Walde (1982) Körperlich erhaltene Scyphozoen-Reste aus dem Jungpräkambrium Brasiliens. 16**,** 1-18.

Han, J., S. Hu, P. Cartwright, F. Zhao, Q. Ou, S. Kubota, X. Wang & X. J. P. Yang, Palaeoclimatology, Palaeoecology (2016a) The earliest pelagic jellyfish with rhopalia from Cambrian Chengjiang Lagerstätte. 449**,** 166-173.

Han, J., S. Kubota, G. Li, Q. Ou, X. Wang, X. Yao, D. Shu, Y. Li, K. Uesugi & M. J. G. R. Hoshino (2016b) Divergent evolution of medusozoan symmetric patterns: Evidence from the microanatomy of Cambrian tetramerous cubozoans from South China. 31**,** 150-163.

Han, J., S. Kubota, G. Li, X. Yao, X. Yang, D. Shu, Y. Li, S. Kinoshita, O. Sasaki & T. Komiya (2013) Early Cambrian pentamerous cubozoan embryos from South China. *PLoS One,* 8**,** e70741.

Han, J., S. Kubota, H.-o. Uchida, G. D. Stanley Jr, X. Yao, D. Shu, Y. Li & K. Yasui (2010) Tiny sea anemone from the Lower Cambrian of China. *PLoS One,* 5**,** e13276.

Han, J., G. Li, S. Kubota, Q. Ou, S. Toshino, X. Wang, X. Yang, K. UESUGI, H. MASATO & O. Sasaki (2016c) Internal microanatomy and zoological affinity

of the early Cambrian Olivooides. *Acta Geologica Sinica-English Edition,* 90**,** 38-65.

Han, J., G. Li, X. Wang, X. Yang, J. Guo, O. Sasaki & T. J. J. o. P. Komiya (2018) Olivooides-like tube aperture in early Cambrian carinachitids (Medusozoa, Cnidaria). 92**,** 3-13.

Han, J., S. C. Morris, Q. Ou, D. Shu & H. Huang (2017) Meiofaunal deuterostomes from the basal Cambrian of Shaanxi (China). *Nature,* 542**,** 228-231.

Hand, C. J. S. Z. (1959) On the origin and phylogeny of the coelenterates. 8**,** 191-202.

Harbison, G., L. Madin & N. J. D. S. R. Swanberg (1978) On the natural history and distribution of oceanic ctenophores. 25**,** 233-256.

Harrison, F. W. 1991. *Microscopic anatomy of invertebrates*. Wiley-Liss.

Harvey, T. H., N. J. J. N. e. Butterfield & evolution (2017) Exceptionally preserved Cambrian loriciferans and the early animal invasion of the meiobenthos. 1**,** 0022.

He, T. G. (1987) Early Cambrian conulariids from the Yangtze platform and their early evolution (In Chinese). *Journal of Chengdu College of Geology,* 14**,** 7-18.

Hou, X.-G., A. Richard J., P.-Y. Cong, S. David J., S. Derek J., G. Sarah E., X.-Y. Ma, P. Mark A. & W. Mark. 2017. *The Cambrian fossils of Chengjiang, China: the flowering of early animal life*. John Wiley & Sons.

Hou, X. g., G. Stanley, J. Zhao & X. y. J. L. Ma (2005) Cambrian anemones with preserved soft tissue from the Chengjiang biota, China. 38**,** 193-203.

Hu, S., M. Steiner, M. Zhu, B.-D. Erdtmann, H. Luo, L. Chen & B. J. P. Weber, Palaeoclimatology, Palaeoecology (2007) Diverse pelagic predators from the Chengjiang Lagerstätte and the establishment of modern-style pelagic ecosystems in the early Cambrian. 254**,** 307-316.

Hua, H., Z. Chen, X. Yuan, L. Zhang & S. J. G. Xiao (2005) Skeletogenesis and asexual reproduction in the earliest biomineralizing animal Cloudina. 33**,** 277-280.

Hua, H., Z. Chen & L. J. C. S. B. Zhang (2004) Early Cambrian phosphatized blastula-and gastrula-stage animal fossils from southern Shaanxi. 49**,** 487.

Huang, D., J. Vannier & J. J. G. Chen (2004) Recent Priapulidae and their Early Cambrian ancestors: comparisons and evolutionary significance. 37**,** 217-228.

Hyman, L. H. 1940. *The invertebrates*. McGraw Hill.

Ivantsov, A. Y. (2009) New reconstruction of Kimberella, problematic Vendian metazoan. *Paleontological Journal,* 43**,** 601.

--- (2010) Paleontological evidence for the supposed Precambrian occurrence of mollusks. *Paleontological Journal,* 44**,** 1552-1559.

--- (2013) Trace fossils of Precambrian metazoans “Vendobionta” and “Mollusks”. *Stratigraphy and Geological Correlation,* 21**,** 252-264.

Ivantsov, A. Y. J. I. Z. (2017) The most probable Eumetazoa among late Precambrian macrofossils. 14**,** 127-133.

Janssen, R., S. A. Wennberg & G. E. J. F. i. Z. Budd (2009) The hatching larva of the priapulid worm Halicryptus spinulosus. 6**,** 8.

Jarms, G. 1991. Taxonomic characters from the polyp tubes of coronate medusae (Scyphozoa, Coronatae). In *Hydrobiologia*, 463-470. Springer.

Jarms, G., A. C. Morandini & F. L. Silveira (2002) Cultivation of polyps and medusae of Coronatae (Cnidaria, Scyphozoa) with a brief review of important characters. *Helgol. Mar. Res.,* 56**,** 203-210.

Javaux, E. J., C. P. Marshall & A. Bekker (2010) Organic-walled microfossils in 3.2-billion-year-old shallow-marine siliciclastic deposits. *Nature,* 463**,** 934.

Jiang, Z. W. (1980) The Meishucun stage and fauna of the Jinning County, Yunnan. *Bulletin of the Chinese Academy of Geological Science,* 1**,** 75-92.

Joyce, G. F. (2002) The antiquity of RNA-based evolution. *Nature,* 418**,** 214.

Laflamme, M. & G. M. Narbonne (2008) Ediacaran fronds. *Palaeogeography, Palaeoclimatology, Palaeoecology,* 258**,** 162-179.

Li, P., H. Hua, L. Zhang, D. Zhang, X. Jin & Z. J. C. S. B. Liu (2007) Lower Cambrian phosphatized Punctatus from southern Shaanxi and their ontogeny sequence. 52**,** 2820-2828.

Li, X.-H. (1999) U–Pb zircon ages of granites from the southern margin of the Yangtze Block: timing of Neoproterozoic Jinning: Orogeny in SE China and implications for Rodinia Assembly. *Precambrian Research,* 97**,** 43-57.

Li, Z.-X., X. Li, P. Kinny, J. Wang, S. Zhang & H. J. P. R. Zhou (2003) Geochronology of Neoproterozoic syn-rift magmatism in the Yangtze Craton, South China and correlations with other continents: evidence for a mantle superplume that broke up Rodinia. 122**,** 85-109.

Li, Z. & C. M. J. E.-S. R. Powell (2001) An outline of the palaeogeographic evolution of the Australasian region since the beginning of the Neoproterozoic. 53**,** 237-277.

Li, Z. P. (1984) The discovery and its significance of small shelly fossils in Hexi area, Xixiang, Shaanxi. *Geol. Shaanxi,* 2**,** 73-77.

Lin, M., Z. Z. Xu, J. Q. Huang, D. H. Guo, C. C. Wang, P. Xiang & Dirhamsyah (2013) Two new species of Leptomedusae from the Bitung Strait, Indonesia (Cnidaria) (in Chinese). *Acta Zootaxonomica Sinica,* 38**,** 756-761.

Liu, A. G., J. J. Matthews, L. R. Menon, D. McIlroy & M. D. J. P. o. t. R. S. o. L. B. B. S. Brasier (2015) The arrangement of possible muscle fibres in the Ediacaran taxon Haootia quadriformis. 282**,** 20142949.

Liu, A. G., J. J. Matthews, L. R. Menon, D. McIlroy & M. D. J. P. R. S. B. Brasier (2014a) Haootia quadriformis n. gen., n. sp., interpreted as a muscular cnidarian impression from the Late Ediacaran period (approx. 560 Ma). 281**,** 20141202.

Liu, Y., Y. Li, T. Shao, H. Zhang, Q. Wang & J. Qiao (2014b) Quadrapyrgites from the lower Cambrian of South China: growth pattern, post-embryonic development, and affinity. *Chinese science bulletin,* 59**,** 4086-4095.

Liu, Y., T. Shao, H. Zhang, Q. Wang, Y. Zhang, C. Chen, Y. Liang & J. Xue (2017) A new scyphozoan from the Cambrian Fortunian Stage of South China. *Palaeontology,* 60**,** 511-518.

Liu, Y., S. Xiao, T. Shao, J. Broce & H. Zhang (2014c) The oldest known priapulid-like scalidophoran animal and its implications for the early evolution of cycloneuralians and ecdysozoans. *Evolution & Development,* 16**,** 155-165.

Liu, Y. H., Y. Li, T. Q. Shao, Y. P. Wang, B. Yu, H. P. Han & J. Yang (2005) Two nes species of protoconulariids from the early Cambrian in south Shaaxi, China. *Micropaleontology,* 22**,** 311-321.

Liu, Y. H., Y. li, T. Q. Shao, X. Zheng, J. Zheng, G. Wang, H. Q. Wang & K. Wang (2011) A new genus and species of protoconulariids from early Cambrian in the southern Shaaxi, China. *Micropaleontology,* 28**,** 244-249.

Logan, G. A., J. Hayes, G. B. Hieshima & R. E. Summons (1995) Terminal Proterozoic reorganization of biogeochemical cycles. *Nature,* 376**,** 53.

Lowe, C. J. & G. A. J. N. Wray (1997) Radical alterations in the roles of homeobox genes during echinoderm evolution. 389**,** 718.

Luo, H. L., Jiang, Z.W., Tang, L.D. (1994) Stratotype sections for Lower Cambrian stages in China (in Chinese). *Yunnan Science and Technology Press, Kunming***,** 183.

Marques, A. C. & A. G. Collins (2004) Cladistic analysis of Medusozoa and cnidarian evolution. *Invertebrate Biology,* 123**,** 23-42.

Martin, E. L. O. 2016. Animal communities of the Early Ordovician (~ 480 Ma): qualitative and quantitative studies from the exceptionally preserved fossils of the Fezouata Shale (Morocco). Université de Lyon.

Matus, D. Q., K. Pang, H. Marlow, C. W. Dunn, G. H. Thomsen & M. Q. J. P. o. t. N. A. o. S. Martindale (2006) Molecular evidence for deep evolutionary roots of bilaterality in animal development. 103**,** 11195-11200.

Mayer, A. G. 1910. *Medusae of the world: The Hydromedusae*. Carnegie institution of Washington.

Miranda, L. S., Collins, A.G., Marques, A.C. (2015) Is Haootia quadriformis related to extant Staurozoa (Cnidaria)? Evidence from the muscular system reconsidered. *Proceedings of the Royal Society of London B: Biological Sciences,* 282**,** 20142396.

Mooi, R. & B. David (2008) Radial symmetry, the anterior/posterior axis, and echinoderm Hox genes. *Annual Review of Ecology, Evolution, Systematics,* 39**,** 43-62.

Morris, S. C. (1989) Burgess Shale faunas and the Cambrian explosion. *Science,* 246**,** 339-346.

Morris, S. C. & J. S. Peel (2008) The earliest annelids: Lower Cambrian polychaetes from the Sirius Passet Lagerstätte, Peary Land, North Greenland. *Acta Palaeontologica Polonica,* 53**,** 137-148.

Narbonne, G. M. (2004) Modular construction of early Ediacaran complex life forms. *Science,* 305**,** 1141-1144.

--- (2005) The Ediacara biota: Neoproterozoic origin of animals and their ecosystems. *Annu. Rev. Earth Planet. Sci.,* 33**,** 421-442.

Narbonne, G. M., M. Laflamme, C. Greentree & P. Trusler (2009) Reconstructing a lost world: Ediacaran rangeomorphs from Spaniard's Bay, Newfoundland. *Journal of Paleontology,* 83**,** 503-523.

Narbonne, G. M., P. M. Myrow, E. Landing & M. M. J. C. J. o. E. S. Anderson (1987) A candidate stratotype for the Precambrian–Cambrian boundary, Fortune head, Burin Peninsula, southeastern Newfoundland. 24**,** 1277-1293.

Nielsen, C. 2012. *Animal evolution: interrelationships of the living phyla*. Oxford University Press on Demand.

Otto, J. J. 1976. Early development and planula movement in Haliclystus (Scyphozoa: Stauromedusae). In *Coelenterate ecology and behavior*, 319-329. Springer.

Ou, Q., J. Han, Z. Zhang, D. Shu, G. Sun & G. J. P. o. t. N. A. o. S. Mayer (2017) Three Cambrian fossils assembled into an extinct body plan of cnidarian affinity. 114**,** 8835-8840.

Ou, Q., S. C. Morris, J. Han, Z. Zhang, J. Liu, A. Chen, X. Zhang & D. J. B. b. Shu (2012) Evidence for gill slits and a pharynx in Cambrian vetulicolians: implications for the early evolution of deuterostomes. 10**,** 81.

Park, E., D.-S. Hwang, J.-S. Lee, J.-I. Song, T.-K. Seo, Y.-J. J. M. p. Won & evolution (2012) Estimation of divergence times in cnidarian evolution based on mitochondrial protein-coding genes and the fossil record. 62**,** 329-345.

Paterson, J. R., G. D. Edgecombe, D. C. GARCÍA-BELLIDO, J. B. Jago & J. G. Gehling (2010) Nektaspid arthropods from the lower Cambrian Emu Bay Shale Lagerstätte, South Australia, with a reassessment of lamellipedian relationships. *Palaeontology,* 53**,** 377-402.

Peng, S. H., L. E. Babcock & R. A. Cooper. 2012. The Cambrian Period. In *The geologic time scale*, 437-488. Elsevier.

Peng, S. J. G. A. (2003) Chronostratigraphic subdivision of the Cambrian of China. 1**,** 135.

Pernet, B. J. T. B. B. (2001) Escape hatches for the clonal offspring of serpulid polychaetes. 200**,** 107-117.

Peters, S. E. & R. R. Gaines (2012) Formation of the 'Great Unconformity'as a trigger for the Cambrian explosion. *Nature,* 484**,** 363.

Peterson, K. J. (2005) Macroevolutionary interplay between planktic larvae and benthic predators. *Geology,* 33**,** 929-932.

Philippe, H., R. Derelle, P. Lopez, K. Pick, C. Borchiellini, N. Boury-Esnault, J. Vacelet, E. Renard, E. Houliston & E. Quéinnec (2009) Phylogenomics revives traditional views on deep animal relationships. *Current Biology,* 19**,** 706-712.

Planavsky, N. J., D. Asael, A. Hofmann, C. T. Reinhard, S. V. Lalonde, A. Knudsen, X. Wang, F. O. Ossa, E. Pecoits & A. J. Smith (2014) Evidence for oxygenic photosynthesis half a billion years before the Great Oxidation Event. *Nature Geoscience,* 7**,** 283.

Powell, C. M., Z. Li, M. McElhinny, J. Meert & J. J. G. Park (1993) Paleomagnetic constraints on timing of the Neoproterozoic breakup of Rodinia and the Cambrian formation of Gondwana. 21**,** 889-892.

Qian, Y. (1977) Hyolitha and some problematica from the Lower Cambrian Meishucun Stage in central and S. W. China (in Chinese). *Acta Palaeontol Sin,* 16**,** 255–275.

Qian, Y. 1999. *Taxonomy and biostratigraphy of small shelly fossils in China*. Science Press, Beijing.

Qian, Y., H. Vaniten, R. S. Cox, M. Y. Zhu & E. J. Zhou (1997) A brief account of Emeiconularia Trigemme, a new genus and species of protoconulariid. *Acta Micropaleontology Sinica,* 14**,** 475-488.

Raikova, E. (1988) On the systematic position of Polypodium hydriforme Ussov (Coelenterata). *Sponges and Cnidaria. Contemporary State and Perspectives of Investigations. Zoological Institute of the USSR Academy of Sciences, Leningrad***,** 116-122.

--- (2008) Cytomorphological peculiarities of Polypodium hydriforme (Cnidaria). *Journal of the Marine Biological Association of the United Kingdom,* 88**,** 1695-1702.

Remane, A. J. Z. f. M. u. Ö. d. T. (1927) Halammohydra, ein eigenartiges Hydrozoon der Nord-und Ostsee. 7**,** 643-677.

Runnegar, B. J. A. (1985) Shell microstructures of Cambrian molluscs replicated by phosphate. 9**,** 245-257.

Ruppert, E. E., R. D. Barnes & R. S. Fox. 2004. *Invertebrate zoology: a functional evolutionary approach*.

Ryan, J. F., M. E. Mazza, K. Pang, D. Q. Matus, A. D. Baxevanis, M. Q. Martindale & J. R. J. P. o. Finnerty (2007) Pre-bilaterian origins of the Hox cluster and the Hox code: evidence from the sea anemone, Nematostella vectensis. 2**,** e153.

Ryan, J. F., K. Pang, C. E. Schnitzler, A.-D. Nguyen, R. T. Moreland, D. K. Simmons, B. J. Koch, W. R. Francis, P. Havlak & S. A. Smith (2013) The genome of the ctenophore Mnemiopsis leidyi and its implications for cell type evolution. *Science,* 342**,** 1242592.

Schopf, J. & A. Kudryavtsev (2005) Three-dimensional Raman imagery of precambrian microscopic organisms. *Geobiology,* 3**,** 1-12.

Schuchert, P. J. R. S. Z. (2009) The European athecate hydroids and their medusae (Hydrozoa, Cnidaria): Filifera part 5. 116**,** 441-507.

Seilacher, A. 2007. *Trace fossil analysis*. Springer Science & Business Media.

Shao, T.-Q., Y.-H. Liu, Q. Wang, H.-Q. Zhang, H.-H. Tang & Y. J. P. Li (2016) New material of the oldest known scalidophoran animal Eopriapulites sphinx. 25**,** 1-11.

Shu, D.-G., S. C. Morris, J. Han, Z.-F. Zhang & J.-N. J. N. Liu (2004) Ancestral echinoderms from the Chengjiang deposits of China. 430**,** 422.

Shu, D.-G., S. C. Morris, J. Han, Z.-F. Zhang, K. Yasui, P. Janvier, L. Chen, X.-L. Zhang, J.-N. Liu & Y. Li (2003a) Head and backbone of the Early Cambrian vertebrate Haikouichthys. *Nature,* 421**,** 526.

Shu, D.-G., S. C. Morris, J. Han, Z.-F. Zhang, K. Yasui, P. Janvier, L. Chen, X.-L. Zhang, J.-N. Liu & Y. J. N. Li (2003b) Head and backbone of the Early Cambrian vertebrate Haikouichthys. 421**,** 526.

Shu, D.-G., S. C. Morris, Z.-F. Zhang & J. J. P. o. t. R. S. o. L. B. B. S. Han (2010) The earliest history of the deuterostomes: the importance of the Chengjiang Fossil-Lagerstätte. 277**,** 165-174.

Shu, D. (2003) A paleontological perspective of vertebrate origin. *Chinese Science Bulletin,* 48**,** 725-735.

Shu, D. g., S. C. Morris, X.-L. Zhang, L. Chen, Y. Li & J. J. N. Han (1999) A pipiscid-like fossil from the Lower Cambrian of South China. 400**,** 746.

Silveira, F. J., G. Morandini, A. (2002) Experiments in nature and laboratory observations with Nausithoe aurea (Scyphozoa: Coronatae) support the concept of perennation by tissue saving and confirm dormancy. 2**,** 1-25.

Skovsted, C. B., B. Pan, T. P. Topper, M. J. Betts, G. Li & G. A. J. P. Brock, palaeoclimatology, palaeoecology (2016) The operculum and mode of life of the lower Cambrian hyolith Cupitheca from South Australia and North China. 443**,** 123-130.

Smith, M. P. & D. A. Harper (2013) Causes of the Cambrian explosion. *Science,* 341**,** 1355-1356.

Smith, M. R. & J.-B. Caron (2015) Hallucigenia's head and the pharyngeal armature of early ecdysozoans. *Nature,* 523**,** 75.

Smith, M. R. & J. Ortega-Hernández (2014) Hallucigenia's onychophoran-like claws and the case for Tactopoda. *Nature,* 514**,** 363.

Steiner, M., G. Li, Y. Qian & M. Zhu (2004) Lower Cambrian small shelly fossils of northern Sichuan and southern Shaanxi (China), and their biostratigraphic importance. *Geobios,* 37**,** 259-275.

Steiner, M., G. Li, Y. Qian, M. Zhu & B.-D. J. P. Erdtmann, Palaeoclimatology, Palaeoecology (2007) Neoproterozoic to early Cambrian small shelly fossil assemblages and a revised biostratigraphic correlation of the Yangtze Platform (China). 254**,** 67-99.

Steiner, M., Y. Qian, G. Li, J. W. Hagadorn & M. Zhu (2014) The developmental cycles of early Cambrian Olivooidae fam. nov.(? Cycloneuralia) from the Yangtze Platform (China). *Palaeogeography, Palaeoclimatology, Palaeoecology,* 398**,** 97-124.

Summons, R. E., L. L. Jahnke, J. M. Hope & G. A. Logan (1999) 2-Methylhopanoids as biomarkers for cyanobacterial oxygenic photosynthesis. *Nature,* 400**,** 554.

Swofford, D. L. (2003) PAUP*: phylogenetic analysis using parsimony, version 4.0 b10.

Taylor, P. D. & O. J. J. o. t. G. S. Vinn (2006) Convergent morphology in small spiral worm tubes ('Spirorbis') and its palaeoenvironmental implications. 163**,** 225-228.

Telford, M. J., S. J. Bourlat, A. Economou, D. Papillon & O. J. P. T. o. t. R. S. o. L. B. B. S. Rota-Stabelli (2008) The evolution of the Ecdysozoa. 363**,** 1529-1537.

Thiel, H. (1966) The evolution of Scyphozoa: A review. 77-117.

Toshino, S., H. Miyake & H. J. Z. Shibata (2015) Meteorona kishinouyei, a new family, genus and species (Cnidaria, Cubozoa, Chirodropida) from Japanese Waters. 1.

Van Iten, H. (1991a) Anatomy, patterns of occurrence, and nature of the conulariid schott. *Palaeontology,* 34**,** 939-954.

Van Iten, H. 1991b. *Evolutionary affinities of conulariids*. Cambridge University Press, Cambridge.

Van Iten, H., M. Burkey, J. D. M. Leme & A. C. J. G. Marques (2014) Cladistics and mass extinctions: the example of conulariids (Scyphozoa, Cnidaria) and the End Ordovician Extinction Event. 136**,** 275-280.

Van Iten, H., J. de Moraes Leme, S. Coelho Rodrigues & M. J. P. Guimaraes Simoes (2005a) Reinterpretation of a conulariid-like fossil from the Vendian of Russia. 48**,** 619-622.

Van Iten, H., J. de Moraes Leme, M. G. Simões, A. C. Marques & A. G. J. J. o. S. P. Collins (2006) Reassessment of the phylogenetic position of conulariids (? Ediacaran-Triassic) within the subphylum medusozoa (phylum cnidaria). 4**,** 109-118.

Van Iten, H., Z. Maoyan & G. Li (2010) Redescription of Hexaconularia He and Yang, 1986 (Lower Cambrian, South China): implications for the affinities of conulariid-like small shelly fossils. *Palaeontology,* 53**,** 191-199.

Van Iten, H., Z. Vyhlasova, M.-Y. Zhu & Q. J. J. o. P. Yi (2005b) Widespread occurrence of microscopic pores in conulariids. 79**,** 400-407.

Van Iten, H. J. P. (1992a) Microstructure and growth of the conulariid test: implications for conulariid affinities. 35**,** 359-372.

--- (1992b) Morphology and phylogenetic significance of the corners and midlines of the conulariid test. 35**,** 335-358.

Vannier, J. (2012) Gut contents as direct indicators for trophic relationships in the Cambrian marine ecosystem. *PloS one,* 7**,** e52200.

Vannier, J., C. Aria, R. S. Taylor & J.-B. Caron (2018) Waptia fieldensis Walcott, a mandibulate arthropod from the middle Cambrian Burgess Shale. *Royal Society Open Science,* 5**,** 172206.

Vannier, J., I. Calandra, C. Gaillard & A. Żylińska (2010) Priapulid worms: Pioneer horizontal burrowers at the Precambrian-Cambrian boundary. *Geology,* 38**,** 711-714.

Vannier, J., M. Steiner, E. Renvoisé, S.-X. Hu & J.-P. J. P. o. t. R. S. o. L. B. B. S. Casanova (2007) Early Cambrian origin of modern food webs: evidence from predator arrow worms. 274**,** 627-633.

Vinn, O. & M. Zaton (2012) Inconsistencies in proposed annelid affinities of early biomineralized organism Cloudina (Ediacaran): structural and ontogenetic evidences.

Wade, M. J. P. (1972) Hydrozoa and Scyphozoa and other medusoids from the Precambrian Ediacara fauna, South Australia. 15**,** 197-225.

Wang, X., J. Han, J. Vannier, Q. Ou, X. Yang, K. Uesugi, O. Sasaki & T. Komiya (2017) Anatomy and affinities of a new 535-million-year-old medusozoan from the Kuanchuanpu Formation, South China. *Palaeontology,* 60**,** 853-867.

Wang, X., H. Hua, P. Li & W. Han (2010a) Depositional environment and biostratinomic model of the early Cambrian Kuanchuanpu Biota fron southern Shaanxi (English abstract). *Paleontology,* 49**,** 125-132.

Wang, Y., F. Zhang, W. Fan, G. Zhang, S. Chen, P. A. Cawood & A. J. T. Zhang (2010b) Tectonic setting of the South China Block in the early Paleozoic: Resolving intracontinental and ocean closure models from detrital zircon U-Pb geochronology. 29.

Warren, L., M. Pacheco, T. R. Fairchild, M. Simões, C. Riccomini, P. C. Boggiani & A. J. G. Cáceres (2012) The dawn of animal skeletogenesis: ultrastructural analysis of the Ediacaran metazoan Corumbella werneri. 40**,** 691-694.

Wennberg, S. A., R. Janssen & G. E. J. I. B. Budd (2009) Hatching and earliest larval stages of the priapulid worm Priapulus caudatus. 128**,** 157-171.

Werner, B. (1973) New investigations on systematics and evolution of the class Scyphozoa and the phylum Cnidaria. *Publ. Seto Mar. Biol. Lab,* 20**,** 35-61.

Widder, E. A. J. S. (2010) Bioluminescence in the ocean: origins of biological, chemical, and ecological diversity. 328**,** 704-708.

Williams, G. C. J. P. o. (2011) The global diversity of sea pens (Cnidaria: Octocorallia: Pennatulacea). 6**,** e22747.

Wood, R. A. J. E.-S. R. (2011) Paleoecology of the earliest skeletal metazoan communities: Implications for early biomineralization. 106**,** 184-190.

Xiao, S. & A. H. J. L. Knoll (1999) Fossil preservation in the Neoproterozoic Doushantuo phosphorite lagerstätte, South China. 32**,** 219-238.

Xiao, S. & M. Laflamme (2009) On the eve of animal radiation: phylogeny, ecology and evolution of the Ediacara biota. *Trends in Ecology & Evolution,* 24**,** 31-40.

Xiao, S., Y. Zhang & A. H. Knoll (1998) Three-dimensional preservation of algae and animal embryos in a Neoproterozoic phosphorite. *Nature,* 391**,** 553.

Yang, X.-g., J. Han, X. Wang, J. D. Schiffbauer, K. Uesugi, O. Sasaki & T. J. P. Komiya, Palaeoclimatology, Palaeoecology (2017) Euendoliths versus

ambient inclusion trails from early Cambrian Kuanchuanpu Formation, South China. 476**,** 147-157.

Yang, Y., Y. Zhao & X. J. J. o. S. P. Zhang (2016) Fossil priapulid Ottoia from the Kaili biota (Cambrian Series 3) of South China. 14**,** 527-543.

Yao, X., J. Han & G. J. G. R. Jiao (2011) Early Cambrian epibolic gastrulation: A perspective from the Kuanchuanpu Member, Dengying Formation, Ningqiang, Shaanxi, South China. 20**,** 844-851.

Yin, J. C., Ding, L.F., He, T.G., et al. (1980) The Palaeontology and Sedimentary Environment of the Sinian System in Emei-Ganluo Area. *1980***,** 231.

Yin, Z., M. Zhu, E. H. Davidson, D. J. Bottjer, F. Zhao & P. Tafforeau (2015) Sponge grade body fossil with cellular resolution dating 60 Myr before the Cambrian. *Proceedings of the National Academy of Sciences,* 112**,** E1453-E1460.

Young, G. A. & J. W. J. P. Hagadorn (2010) The fossil record of cnidarian medusae. 19**,** 212-221.

Young, G. A., D. M. Rudkin, E. P. Dobrzanski, S. P. Robson & G. S. J. G. Nowlan (2007) Exceptionally preserved Late Ordovician biotas from Manitoba, Canada. 35**,** 883-886.

Yue, Z. & S. Bengtson (1999) Embryonic and post-embryonic development of the Early Cambrian cnidarian *Olivooides*. *Lethaia,* 32**,** 181-195.

Yue, Z. J. B. o. t. I. o. G., Chinese Academy of Geological Sciences (1986) Microstructure and systematic position of Olivooides (Porifera). 14**,** 147-152.

Zacaï, A., J. Vannier & R. Lerosey-Aubril (2016) Reconstructing the diet of a 505-million-year-old arthropod: Sidneyia inexpectans from the Burgess Shale fauna. *Arthropod Structure & Development,* 45**,** 200-220.

Zapata, F., F. E. Goetz, S. A. Smith, M. Howison, S. Siebert, S. H. Church, S. M. Sanders, C. L. Ames, C. S. McFadden & S. C. J. P. O. France (2015) Phylogenomic analyses support traditional relationships within Cnidaria. 10**,** e0139068.

Zhang, H. & X.-P. Dong (2015) The oldest known larva and its implications for the plesiomorphy of metazoan development. *Science bulletin,* 60**,** 1947-1953.

Zhang, H., A. Maas & D. J. J. o. P. Waloszek (2018) New material of scalidophoran worms in Orsten-type preservation from the Cambrian Fortunian Stage of South China. 92**,** 14-25.

Zhang, H., S. Xiao, Y. Liu, X. Yuan, B. Wan, A. Muscente, T. Shao, H. Gong & G. Cao (2015) Armored kinorhynch-like scalidophoran animals from the early Cambrian. *Scientific Reports,* 5**,** 16521.

Zhang, X., D. Shu, J. Han, Z. Zhang, J. Liu & D. Fu (2014) Triggers for the Cambrian explosion: hypotheses and problems. *Gondwana Research,* 25**,** 896-909.

Zhang, Z.-F. & L. E. Holmer. 2014. An agglutinated early Cambrian actinotroch-like phoronid from the Chengjiang Lagerstätten and its implications. In *Palaeontological Association Annual Meeting*, 53.